TECHNISCHE UNIVERSITÄT MÜNCHEN

Lehrstuhl für Experimentelle Genetik

Catabolism of glucocorticoids – novel pathways for stress reduction in zebrafish

Janina J. Tokarz

Vollständiger Abdruck der von der Fakultät Wissenschaftszentrum Weihenstephan für Ernährung, Landnutzung und Umwelt der Technischen Universität München zur Erlangung des akademischen Grades eines

Doktors der Naturwissenschaften

genehmigten Dissertation.

Vorsitzender:		Univ.-Prof. Dr. E. Grill
Prüfer der Dissertation:	1.	apl. Prof. Dr. J. Adamski
	2.	Univ.-Prof. Dr. J. Buchner
	3.	Univ.-Prof. Dr. J. Durner

Die Dissertation wurde am 24.05.2012 bei der Technischen Universität München eingereicht und durch die Fakultät Wissenschaftszentrum Weihenstephan für Ernährung, Landnutzung und Umwelt am 08.08.2012 angenommen.

Table of contents

Abstract

Stress is the physiological response to stressors occurring in the environment of each organism. In teleost fish, stressors are perceived in the hypothalamus and transmitted along the hypothalamus-pituitary-interrenal (HPI) axis leading to the release of cortisol to the circulation. Cortisol acts as major stress hormone and contributes to the appropriate stress response by regulating metabolic, reproductive, and immune functions. Since the effects of cortisol can become maladaptive, catabolism and excretion of the potent hormone are vitally important. Steroid hormone biosynthesis, metabolism, and pre-receptor regulation of their activity are regulated by enzymes of the hydroxysteroid dehydrogenase family (HSD). While HSDs in mammals are extensively studied, only few orthologs are characterized in fish.

In zebrafish (*Danio rerio*), an emerging model for endocrine research, an orphan HSD was discovered, functionally characterized, annotated, and its physiological function elucidated. In this work, it was found that this HSD candidate was closely related to 17β-HSD types 3 and 12 and had orthologs in other species. The enzyme catalyzed the efficient conversion of cortisone to 4-pregnen-17,20β,21-triol-3,11-dione (20β-hydroxycortisone), which was identified by LC-MS/MS. The orphan HSD was annotated as zebrafish 20β-HSD type 2. During embryonic development as well as in adult tissues, 20β-HSD type 2 was co-expressed with 11β-HSD type 2 known to inactivate cortisol by oxidation to cortisone. Upon cortisol treatment of zebrafish embryos, transcripts of both genes were up-regulated accompanied by increased protein amounts of 20β-HSD type 2. The latter was demonstrated by a polyclonal antibody against zebrafish 20β-HSD type 2, which was developed and optimized in this work. However, cortisol treatment significantly decreased the activity of 20β-HSD type 2. This observation was addicted to the inhibitory effect of cortisol on 20β-HSD type 2 in high concentrations far above physiological levels. Application of a cortisol independent, short-term physical stressor to wild-type zebrafish larvae resulted in up-regulation of both 11β-HSD type 2 and 20β-HSD type 2 along with up-regulation of HPI axis genes.

To determine the impact of a transient knock-down of 20β-HSD type 2 in zebrafish development, morpholino antisense technology was employed. No developmental changes appeared under normal culturing conditions, but prominent effects were observed upon cortisol challenge. The reaction product of 20β-HSD type 2, 20β-hydroxycortisone, was not a physiological ligand for zebrafish glucocorticoid or mineralocorticoid receptor. Instead of being involved in steroid signaling, 20β-hydroxycortisone was found to be excreted into fish holding water after conjugation with glucuronic acid and sulfates. Using wild-type embryo homogenates, 11β-HSD type 2 and 20β-HSD type 2 were found to act concertedly in converting cortisol to 20β-hydroxycortisone.

The results demonstrate clearly that 20β-HSD type 2 is involved in cortisol catabolism, excretion, and stress reduction and represents together with 11β-HSD type 2 a novel pathway for rapid cortisol inactivation and excretion in zebrafish. A role for 20β-HSD type 2 in reproduction related processes like oocyte maturation or sex pheromone synthesis is unlikely. A human ortholog of zebrafish 20β-HSD type 2 was not identified in this work, although 20β-hydroxycortisone was detected in human urine. Increasing evidence for a human 20β-HSD and its family affiliation are discussed.

This work describes the discovery of a novel pathway for cortisol catabolism and excretion in teleost fish and contributes to the understanding of biochemical stress reduction. Furthermore, the starting point for a deeper exploration of the human glucocorticoid catabolism pathways is provided.

Zusammenfassung

Stress ist die physiologische Antwort auf Stressreize, die in der Umgebung jedes Lebewesens auftreten. Knochenfische nehmen Stressreize im Hypothalamus wahr und leiten sie entlang der Hypothalamus-Hypophyse-Interrenalorgan-Achse (HPI-Achse) weiter, woraufhin die Zellen des Interrenalorgans Cortisol produzieren und in den Blutkreislauf sekretieren. Cortisol fungiert als Stresshormon, das durch Regulation von Stoffwechsel, Fortpflanzung und Immunsystem die angemessene Stressantwort einleitet. Da sich die Effekte von Cortisol auch negativ auswirken können, kommt dem Abbau und der Exkretion des Hormons eine große Bedeutung zu. Biosynthese, Inaktivierung und Regulation der Aktivität von Steroidhormonen auf Prä-Rezeptor-Ebene werden durch Enzyme aus der Familie der Hydroxysteroid Dehydrogenasen (HSDs) reguliert. Während HSDs in Säugetieren umfangreich beschrieben worden sind, sind in Fischen nur wenige Orthologe charakterisiert.
Der Zebrafisch (*Danio rerio*) gewinnt als Modellorganismus für endokrinologische Forschung zunehmend an Popularität. In dieser Arbeit wurde im Genom des Zebrafisches eine unbekannte HSD identifiziert, funktionell charakterisiert, annotiert und ihre physiologische Funktion bestimmt. Der Kandidat zeigte sich eng verwandt mit 17β-HSD3 und 17β-HSD12 und Orthologe in anderen Spezies konnten auch gefunden werden. Da die neue HSD den Umsatz von Cortison zu 4-Pregnen-17,20β,21-triol-3,11-dion (20β-Hydroxycortison; identifiziert mittels LC-MS/MS) katalysierte, wurde das Enzym als 20β-HSD2 annotiert. Sowohl in der Embryonalentwicklung des Zebrafisches als auch in adulten Geweben wurden 20β-HSD2 und 11β-HSD2 ähnlich exprimiert. 11β-HSD2 ist für die Oxidation von Cortisol zu Cortison verantwortlich. Die Transkripte beider Gene wurden bei Behandlung von Zebrafischembryonen mit Cortisol verstärkt exprimiert. Darüberhinaus konnte mittels eines selbst entwickelten und optimierten polyklonalen Antikörpers gezeigt werden, dass auch die Menge an 20β-HSD2 Protein erhöht war. Die Cortisolbehandlung führte zu einer signifikanten Reduktion der 20β-HSD2 Aktivität, die jedoch allein dem inhibierenden Effekt von Cortisol in Konzentrationen weit über den physiologischen Werten auf die 20β-HSD2 zugeschrieben werden konnten. Wurden Wildtyp Larven einem kurzzeitigen, physikalischen Stressreiz ausgesetzt, konnte eine erhöhte Expression von 11β-HSD2 und 20β-HSD2 sowie von einigen Genen der HPI-Achse nachgewiesen werden.
Ein Knock-down der 20β-HSD2 in Zebrafischembryonen mittels Morpholino Antisense Technologie hatte unter Normalbedingungen keine Entwicklungsstörungen zur Folge, jedoch konnten deutliche morphologische Änderungen nach Cortisolgabe beobachtet werden. Das Reaktionsprodukt der 20β-HSD2, 20β-Hydroxycortison, war kein physiologischer Ligand für Glucocorticoid- oder Mineralocorticoidrezeptor. 20β-Hydroxycortison wurde als Exkretionsprodukt in Fischwasser gefunden, wo es sowohl mit Glucuronsäure als auch mit Sulfaten konjugiert vorlag. Enzymatische Untersuchungen von Wildtyp Embryohomogenaten zeigten, dass 11β-HSD2 und 20β-HSD2 gemeinsam Cortisol zu 20β-Hydroxycortison umsetzten.
Die erhaltenen Ergebnisse zeigen, dass 20β-HSD2 im Abbau und der Ausscheidung von Cortisol sowie der Reduktion von Stress eine Rolle spielt und gemeinsam mit 11β-HSD2 einen neuen Stoffwechselweg zur effizienten Inaktivierung und Ausscheidung von Cortisol im Zebrafisch darstellt. Eine Beteiligung der 20β-HSD2 in der Fortpflanzung, d.h. der Reifung von Ooycten bzw. der Synthese von Geschlechtspheromonen, kann ausgeschlossen werden. Das humane Ortholog der 20β-HSD2 aus Zebrafisch konnte in dieser Arbeit nicht gefunden werden, jedoch wurde 20β-Hydroxycortison in menschlichem Urin nachgewiesen. Die sich verdichtenden Hinweise auf eine humane 20β-HSD und ihre Familienzugehörigkeit werden diskutiert.
Diese Arbeit beschreibt die Entdeckung eines neuen Stoffwechselweges zum Abbau und zur Ausscheidung von Cortisol in Knochenfischen und leistet einen Beitrag zum Verständnis des biochemischen Stressabbaus. Darüber hinaus wird der Ausgangspunkt für eine vertiefende Untersuchung des Glucocorticoidkatabolismus im Menschen geschaffen.

Abbreviations

17α,20β-DP	17α,20β-dihydroxy-4-pregnen-3-one
20β-S	17α,20β,21-trihydroxy-4-pregnen-3-one
ABCG	ATP-binding cassette sub-family G
ACTH	adrenocorticotropic hormone
AKR	aldo-keto reductase
APCI	atmospheric pressure chemical ionization
APS	ammonium peroxodisulfate
ATP	adenosine triphosphate
BCIP	5-bromo-4-chloro-3-indolyl phosphate
BLAST	basic local alignment search tool
bp	base pair
BSA	bovine serum albumin
cDNA	complementary DNA
cps	counts per second
CR	carbonyl reductase
CRF-R	CRH receptor
CRH	corticotropin releasing hormone
DMEM	Dulbecco's modified eagle medium
DMF	dimethylformamide
DNA	deoxyribonucleic acid
dNTP	deoxy nucleotides
dpf	days post fertilization
ECL	enzymatic chemiluminescence
EPI	enhanced product ion
ER	endoplasmic reticulum
EST	expressed sequence tag
FBS	fetal bovine serum
FITC	fluorescein isothiocyanate
GFP	green-fluorescent protein
GRE	glucocorticoid response element
GRα	glucocorticoid receptor isoform α
GST	glutathione S-transferase
GTH	gonadotropin
HPA axis	hypothalamus-pituitary-adrenal axis
hpf	hours post fertilization
HPI axis	hypothalamus-pituitary-interrenal axis
HPLC	high performance liquid chromatography
HRP	horseradish peroxidase
HSD	hydroxysteroid dehydrogenase
IPTG	isopropyl-β-D-thiogalactopyranoside
kb	kilo bases
kDa	kilo Dalton
KLH	keyhole limpet haemocyanin
LB	Luria-Bertani
LC-MS/MS	liquid chromatography coupled to tandem mass spectrometry
MC2R	melanocortin 2 receptor
MDR1/P	multidrug resistance protein
MEM	Minimum essential medium
MIH	maturation-inducing hormone
MMTV	mouse mammary tumor virus

MR	mineralocorticoid receptor
MRM	multiple reaction monitoring
mRNA	messenger RNA
NAD^+	β-nicotinamide adenosine dinucleotide
$NADH + H^+$	β-nicotinamide adenosine dinucleotide, reduced form
$NADPH + H^+$	β-nicotinamide adenosine dinucleotide 3'-phosphate, reduced form
$NADPH^+$	β-nicotinamide adenosine dinucleotide 3'-phosphate
NaP_i	sodium phosphate
NBT	4-nitroblue tetrazolium chloride
NJ	Neighbor-Joining
OATP	organic anion-transporting polypeptide
OD	optical density
PBS	phosphate buffered saline
PCR	polymerase chain reaction
PLB	passive lysis buffer
PVDF	polyvinylidene fluoride
qPCR	quantitative real-time polymerase chain reaction
RNA	ribonucleic acid
rpm	rotations per minute
RT-PCR	reverse transcription polymerase chain reaction
SDR	short-chain dehydrogenase/reductase
SDS-PAGE	sodium dodecyl sulfate polyacrylamide gel electrophoresis
SPE	solid phase extraction
StAR	steroidogenic acute regulatory protein
TEMED	tetramethylethylenediamine
UV	ultra violet
X-Gal	5-bromo-4-chloro-3-indolyl-β-D-galactopyranoside

1 Introduction

Organisms strive to maintain homeostasis, which is a stable condition characterized by dynamic equilibrium reactions and regulatory processes. However, environmental conditions as well as interactions with other organisms can disrupt homeostasis and are therefore considered to be stressful. Stress is an evolutionary old system that allows an organism to perceive a challenging situation and to react appropriately. In a life-threatening situation (e.g., facing a predator), an organism has to be ready to act, so that schematic reactions (fight-or-flight decisions) are preferred over a precise but tedious evaluation of the situation. In today's civilized society, facing a predator is a rare event, which led to a different definition of stress in humans. Generally, stress in humans is understood as exposure to demands, which can be either objective, external factors (e.g., heat, cold, toxic substances, injury) or emotional factors (e.g., expectations, apprehensions, conflicts).
Perception and response to a stressor are divided into three phases. In the alarm phase, the stressor is perceived in the hypothalamus and transmitted via hormone cascades along the hypothalamus-pituitary-adrenal (HPA) axis to the adrenal glands. These glands release the catecholamine epinephrine and the steroid cortisol. Both hormones participate in the activation of the whole organism allowing for a fast and if necessary reflexive stress response, while only cortisol is considered being the "stress hormone". The second phase is called resistance and characterized by accomplishing the appropriate response to the stressor. The last phase is the exhaustion phase, where the organism recovers from the stress and regains homeostasis. In today's working life, chronic stress is getting more and more common resulting in long-term health impairment [1]. Chronic stress increases the risk for cardiovascular diseases [2], anxiety and depression [3], and contributes to altered immune system reactivity [4].

1.1 Stress and glucocorticoids in teleost fish

1.1.1 Stress as a part of natural environment

Naturally, the quality of a stressor for humans deviates from a stressor for fish, as both vertebrate families have adapted to different environments. However, apart from facing different stressors, the hypothalamus-pituitary-adrenal axis is conserved among vertebrates allowing for good comparability of the physiological stress responses between different taxa.
Stress was once defined as "the non-specific response of the body to any demand placed on it" [5]. This definition was recently refined by Barton as stress being a state of threatened homeostasis, which is reestablished by a complex suite of adaptive responses [6]. The energy demanding process of regaining and stabilizing homeostasis imposes an allostatic load onto the organism, which is generally denoted by the physiological response to stressors [7].
The nature of stressors for teleost fish is variable and thereby complicates a categorization. Nevertheless, stressors can be classified according to their origin or their duration. Regarding the origin, stressors can be divided into being physical and environmental or social and symbolic [8]. Physical stressors include injuries, manipulations, or handling, as well as environmental variables like temperature, oxygen content, salinity, pH, or the presence of toxicants or pathogens. Social stressors are characterized by interactions with conspecifics including hierarchy, crowding, or aggressiveness, but also by interactions with different species, e.g., predators [8]. Another classification can be built regarding the duration and intensity of the stressor distinguishing acute and chronic stressors. Acute stressors are more common in nature, show a high intensity for a short time, and consist of a challenging situation like predation or fighting conspecifics. On the other hand, chronic stressors are mostly environmental in nature, having a low intensity but persist for a long time. Nowadays, chronic stressors are predominantly of anthropogenic influence on ecosystems, e.g., pollution or aquaculture [8].

1.1.2 The stress response

The interaction of an organism with its environment is not schematic but rather depending on a complex regulatory network. The same holds true for stress responses, where the magnitude is dependent on the type, intensity, and duration of the stressor as well as the history of the animal [6, 8, 9]. The magnitude of stress response to a similar stressor can vary significantly between species and sexes [10, 11]. Generally, the stress response is considered to be adaptive and allows the fish to cope with the disturbance [6], which is widely accepted especially regarding acute stressors [8]. However, when a stressor is chronic or extremely severe, the response becomes maladaptive and threatens the health, the well-being, and the survival of the fish [6, 8].
The stress response affects a variety of physiological mechanisms ranging from gene and protein changes, differentially regulated metabolism and energy balance, to immune, endocrine, neuronal, and behavioral changes. These changes are firstly important to overcome the stressful situation and secondly involved in compensation of the imbalances produced by either the stressor or the stress response [8]. The physiological stress response is divided into three phases. Primary responses are occurring fast and modulate endocrine changes like cortisol and epinephrine secretion as well as alterations in neurotransmitter activities [6]. Secondary responses are regulated by hormones released in the first phase and are characterized by metabolic, cellular, hematological, respiratory, and immune changes as well as osmoregulatory disturbances [6]. Tertiary responses affect the whole animal and include changes in growth, reproduction, disease resistance, swimming capacity, and modified behavioral patterns like feeding or aggression [6].
The stress perception and transmission system is highly conserved in all vertebrates [10] utilizing the same tissues as well as the same transmitters. In humans, the hypothalamus-pituitary-adrenal (HPA) axis is used for stress transmission, but teleost fish do not possess a discrete adrenal gland. The adrenal function is fulfilled by homologous interrenal cells embedded in the head kidney [12], and thus, stress transmission occurs via the hypothalamus-pituitary-interrenal (HPI) axis (Figure 1.1). The hypothalamus perceives the stressor due to input from the central and peripheral nervous system [13, 14] and secretes corticotropin releasing hormone (CRH). CRH signals via specific G-protein coupled receptors (CRF-R1 and CRF-R2) [15] and stimulates the corticotropic and melanotropic cells of the pituitary [16] to cleave the large precursor protein proopiomelanocortin [17]. This cleavage allows for secretion of adrenocorticotropic hormone (ACTH) to the circulation and its binding to melanocortin 2 receptor (MC2R) on the surface of the interrenal cells [15]. Upon this stimulus, the interrenal cells initiate cortisol biosynthesis and release cortisol to the circulation [18].
De novo biosynthesis of cortisol (Figure 1.1) in teleost fish starts with the transport of cholesterol into the mitochondria mediated by steroidogenic acute regulatory protein (StAR) [19]. Subsequently, the side chain is cleaved. This reaction is catalyzed by monooxygenase P450scc (Cyp11a1) yielding pregnenolone. In the next steps, 17α-hydroxylation and 3β-hydroxysteroid dehydrogenation occur mediated by steroid 17α-hydroxylase/17,20-lyase (Cyp17) and 3β-hydroxysteroid dehydrogenase (Hsd3b), respectively. 17α-hydroxyprogesterone is then hydroxylated at position C21 by 21-hydroxylase (Cyp21a2), and the resulting 11-deoxycortisol is finally converted to cortisol catalyzed by 11-hydroxylase (Cyp11b2) [20].

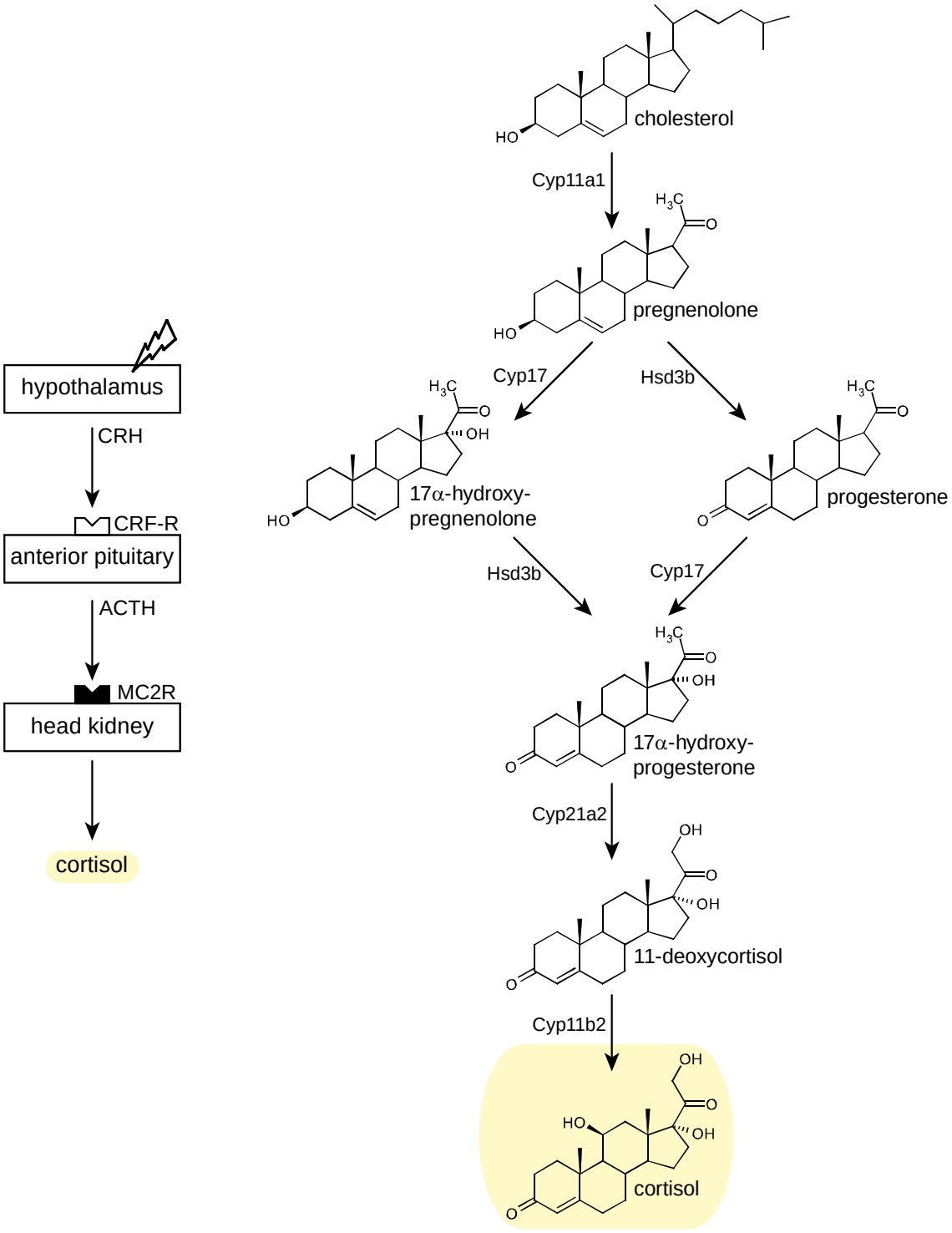

Figure 1.1: Signaling cascade of the hypothalamus-pituitary-interrenal axis and the processes involved in cortisol biosynthesis. The hypothalamus perceives the stressor and releases CRH, which binds to its receptor (CRF-R) and stimulates the pituitary to secrete ACTH into the circulation. ACTH binds to MC2R on the surface of the interrenal cells, which initiate cortisol synthesis and release to the circulation. The right part of the figure depicts the cortisol biosynthesis pathway from cholesterol. The respective enzymes are denoted. Modified from Alsop & Vijayan 2009 [13].

The ontogeny of the HPI axis in developing fish is not yet completely understood. In common carp, *Cyprinus carpio*, the HPI axis was found to be functional at the time of hatching [21]. These results slightly deviate from findings in zebrafish, *Danio rerio*. Transcripts of HPI axis relevant genes (*Crh, Pomc, Mc2r, Star, Cyp11b2, Crf-R1* and *Crf-R2*) were detected prior to hatch in zebrafish [13, 15]. Hatching of zebrafish embryos occurs between 48 and 72 hours post fertilization (hpf) [22], while a

stressor induced cortisol response was not evident until 97 hpf [13]. The delay between all HPI axis components being in place and their functionality in stress transmission was explained by a slower development of peripheral and central neurons, which relay stressor stimuli to the hypothalamus [13]. Nevertheless, the HPI axis is generally considered to be functional around the time of hatch of fish embryos from different species [20].

1.1.3 Effects of cortisol on fish physiology

Cortisol mediates its plethora of effects via binding to members of the nuclear hormone receptor family (glucocorticoid and mineralocorticoid receptor), an important class of ligand-binding transcription factors [23, 24]. Upon ligand binding, the receptor translocates into the nucleus and is able to bind to response elements (e.g., glucocorticoid response elements, GRE), thereby enhancing or repressing transcription of target genes. In both humans and teleost fish, cortisol is the unique ligand for the glucocorticoid receptor (GR) displaying binding affinities in the low nanomolar range [20, 25, 26]. Furthermore, cortisol binds to the mineralocorticoid receptor (MR); a receptor that regulates ionic and water transport processes. The affinity of cortisol to the MR is even higher than the affinity of aldosterone, the native MR ligand in humans [26]. A similar observation has been reported for rainbow trout (*Oncorhynchus mykiss*) MR [27]. Since in the human circulation cortisol is more abundant than aldosterone, constant MR activation by cortisol is avoided by expression of the cortisol-inactivating enzyme 11β-HSD type 2 in mineralocorticoid sensitive tissues [28-30]. In teleost fish, the native ligand for the MR is not yet known. Fish lack the capability of aldosterone biosynthesis due to absence of the respective enzyme [27, 31]. This entailed the speculation of cortisol exerting both glucocorticoid and mineralocorticoid activity in teleost fish [32, 33]. Recently, *in vitro* transactivation assays provided evidence that 11-dehydrocorticosterone might be the physiological ligand for teleostean MR [27, 34].

Despite the described mechanism of action by binding to a receptor and regulating gene expression, cortisol can also stimulate non-genomic effects, which are generally faster. Although evidence on a non-genomic action of cortisol is accumulating, the underlying molecular mechanisms are far from clear [20, 35].

As already indicated above, cortisol as major stress hormone contributes to the regulation of a variety of physiological processes. The influence of cortisol on metabolism, immune system, and reproduction has been the focus of many studies, while other aspects of cortisol involvement in fish physiology remain only partially elucidated.

An important function of cortisol in the stress response is the activation of catabolic processes to meet the energy demand necessary for appropriate stress response and regain of homeostasis [9]. Upon stress, plasma concentrations of glucose, lactate, and free amino acids are found to be increased in tilapia (*Oreochromis niloticus*) along with elevated hepatic enzyme activities [36]. In peripheral tissues, e.g., white muscle and adipose tissue, and in liver proteolysis and lipolysis are enhanced resulting in increased plasma concentrations of free amino acids and un-esterified fatty acids [20]. Cortisol also stimulates gluconeogenesis and glucose *de novo* synthesis in liver [9, 20]. Especially free amino acids are used as substrates to fuel gluconeogenesis in liver.

The influence of cortisol on the immune system can either be stimulatory as well as adverse depending on the intensity and the duration of the stressor. Generally, coping with stress imposes an allostatic load that is interfering with the needs of appropriate immune response [8]. An acute, short-term stressor induces a stimulatory response pattern including the activation of an immune response (adaptive), while a chronic stressor has a suppressive effect on the immune system enhancing the chances for infections (maladaptive) [8]. Stress-induced enhanced vulnerability increased the mortality of brown trout (*Salmo trutta*) and rainbow trout due to common bacterial and fungal diseases [37]. Thus, stress-immune system interactions are responsible for the susceptibility of fish to pathogens entailing serious consequences for the fish's health, although the precise molecular mechanisms are not clear up to now and need further investigation [9].

Comparable to the immune system, stress affects reproduction differently, depending on when in the life cycle it is encountered and the severity and duration of the stressor [7]. In general, the maturation and spawning physiology is tightly connected with stress responses [11]. While disturbances or handling affect the timing of rainbow trout reproduction (either accelerating or delaying), the same

stressor causes tilapia to respond with acceleration or complete inhibition of reproduction [11]. Additionally, the stress coping strategies affect reproductive fitness and gamete and progeny quality adversely [7, 11]. Cortisol was found to interact with both estradiol and 11-ketotestosterone [11], and both reproductive hormones can influence the HPI axis vice versa [10], although the molecular mechanisms underlying this hormone cross-talk are not elucidated until now.

Cortisol influences osmoregulatory processes not only in the response to a stressor, but is also involved in acclimation of euryhaline fish to either sea water or fresh water. In zebrafish, cortisol stimulated the uptake of calcium ions [38]. In Mozambique tilapia (*Oreochromis mossambicus*), it helps to adapt the fish to abrupt sea water exposure and decreases the mortality rate usually associated with hyperosmotic shock [39]. For several fish species, it is generally accepted that cortisol acts synergistic with the growth hormone to increase sea water tolerance by enhancing ion release from the gills. On the other hand, cortisol interacts with prolactin and may thereby promote ion uptake during fresh water acclimation [40]. While the actions of growth hormone and prolactin are antagonistic, cortisol interacts with both hormones displaying a dual role in osmoregulation of fish [40].

Like in terrestrial vertebrates, cortisol is considered to be involved in embryonic development of fish [20]. Evidence for this hypothesis is accumulating, though the precise responsible mechanisms are not yet elucidated. Many studies have quantified cortisol in zygotes of different fish species and in subsequent embryonic development, demonstrating that cortisol is provided maternally to the zygote [13, 41, 42]. Rainbow trout embryos treated with a high concentration of cortisol displayed a delayed hatching, while juveniles treated with a low concentration of cortisol exhibited enhanced growth [43]. On the other hand, excess cortisol causes increased mortality and severe developmental abnormalities in zebrafish embryos, which were characterized by abnormal craniofacial cartilage development, altered somitogenesis, blood pooling, and pericardial and yolk edema [44]. The cortisol-stimulated aberrant development was addicted to matrix metalloproteinases, which are central enzymes for remodeling the extracellular matrix and play important roles in development, reproduction, tissue resorption, wound healing, and apoptosis [44, 45]. Not only excess cortisol entails developmental abnormalities, but also the disruption of cortisol signaling by knock-down of the glucocorticoid receptor in zebrafish embryos [41]. In knock-down animals, increased apoptosis and subsequent craniofacial deformities were observed. In 5 dpf larvae, the GR knock-down resulted in severe malformations of neural, vascular, and visceral organs [41].

Recently, cortisol was also identified to be a component of a systemic signaling pathway that is required for the circadian cell cycle rhythmicity [46].

Since cortisol is the major hormone stimulating the stress response, quantification of cortisol in fish plasma was long used to determine the intensity of the stressor. Already in 1989 Pickering & Pottinger [37] showed that plasma cortisol is higher upon an acute stressor (1 hour of handling and confinement) than after a chronic stress situation (prolonged confinement and crowding) for both brown trout and rainbow trout, resulting in consequences for aquaculture [47]. Analysis of cortisol in plasma requires a fish large enough to draw blood from it and is therefore not applicable to small fish, e.g., zebrafish. Cortisol in zebrafish is consequently determined for the whole body, sacrificing the entire study population [10, 48, 49]. However, it has long been known from pheromone analyses that fish release steroids into the water including cortisol (see [50, 51] and references therein). The development of methods for steroid extraction from large water samples and quantification of cortisol in these extracts demonstrated that stress of a fish can be determined by analyzing the cortisol content of the medium [52, 53]. This approach has several advantages: firstly, it is a non-invasive approach rendering fish handling and bleeding unnecessary; secondly, sampling stress confounding the results is mostly avoided; thirdly, repeated measurements on the same fish are enabled; and fourthly, this approach allows for non-lethal measurements on small fish like zebrafish [51].

Up to now, most studies employed immunoassays for the quantification of cortisol (and other steroids, e.g., estradiol or 11-ketotestosterone) using either radioimmunoassay or enzyme-linked immunosorbent assay. Both methods are commercially available and easy to handle, however, they are impaired by inadequate specificity and sensitivity. Both disadvantages can be conquered by applying mass spectrometry based assays, either following gas chromatography or liquid chromatography [54].

Being a potent hormone, the level of cortisol has to be tightly controlled by regulating the ratio of biosynthesis (controlled by the HPI axis) and catabolism as well as clearance. The metabolic clearance of cortisol from plasma is affected by stress, salinity, maturity, toxicants, and nutritional state of the fish [20] and is conducted by tissue uptake and catabolism. The liver is the key organ for cortisol

catabolism and the hepato-biliary system is the main route of cortisol excretion, although renal and branchial paths also play a role [20, 55]. In humans, cortisol is primarily inactivated by 11β-HSD type 2 yielding cortisone [56], followed by reduction steps at positions C4-C5, C3, and C20. The obtained dihydro- and tetrahydro-derivatives of both cortisol and cortisone are subsequently either glucuronidated or sulfated to increase water solubility or excreted without conjugation via the urine. Teleost fish are generally considered to catabolize cortisol along similar pathways [20], but only few studies have investigated glucocorticoid excretion in fish so far. Vermeirssen & Scott [55] demonstrated that glucuronidated steroids are predominantly released via the bile, sulfated steroids are excreted with urine, and unconjugated steroids are removed by diffusion from the gills. Analysis of conjugated steroids derived from bile identified both tetrahydro-derivatives of cortisol and cortisone, beside 20β-cortolone, 5β-dihydrocortisone, cortisol, and cortisone as major excretion products of rainbow trout [57, 58], thus underlining similar catabolic pathways to humans.

1.2 Zebrafish: an emerging model not only for developmental biology

Zebrafish, *Danio rerio*, are small and robust tropical freshwater fish that can be maintained in relatively small facilities causing only little husbandry costs. The fish are asynchronous spawners that breed well under laboratory conditions and can provide a constant supply of fertilized eggs. The fertilization occurs externally as well as the rapid embryonic development [59-61]. The principal body plan is established 24 hours post fertilization and most organs are fully developed 4 days post fertilization [22, 60]. In addition, zebrafish embryos are optically transparent enabling microscopic observations and monitoring of developmental processes in a living animal [59-62]. The external development of zebrafish embryos facilitated the design and development of a variety of tools for genetic manipulations, e.g., microinjection of nucleic acids or antisense oligonucleotides, but also adult fish are amenable to genetic modifications like chemically induced mutagenesis or transgenesis [59, 63, 64]. The rapid increase of transgenic zebrafish lines demonstrates the value of this model for *in vivo* analysis of all aspects of developmental biology [65]. A valuable tool for accuracy in developmental biology is the staging series in development of zebrafish embryos as well as from juveniles to adults [22, 66]. Further advantages of zebrafish as model organism are the completely sequenced genome, a database providing virtually every information around zebrafish [67], and the availability of zebrafish cell lines [68]. Recently, zebrafish were also proposed to be a good model for behavioral studies [69]. An excellent overview of the history of zebrafish progression from an unknown fish to a widely used model organism can be found in Grunwald & Eiser 2002 [70].

Zebrafish is widely used as model in developmental biology, but the fish shares further physiological aspects with mammalian species. The endocrine system, e.g., the involved hormones, receptors, and signaling cascades are strikingly conserved between zebrafish and its mammalian counterparts [71, 72]. Most receptors are expressed before birth, which imposes difficulties for investigation of the developmental role in mammals – a challenge that is easily overcome using zebrafish [71]. Additionally, zebrafish are useful in studies concerning endocrine-disrupting chemicals, which are rampant not only in aquatic environments but can also cause alterations in development, homeostasis, and health of vertebrates [60]. The above mentioned advantages of the zebrafish are beneficial for assessing the effects, targets, and mechanisms of action of these chemicals [60, 73].

In recent years, zebrafish turned out to be an excellent model especially in stress research. While most other teleost fish have duplicated HPI axis genes due to a teleost-specific genome duplication event 350 million years ago, zebrafish contains only one gene for each component of the HPI axis [13, 18]. Furthermore, the glucocorticoid signaling mediated by the glucocorticoid receptor displays a convergent evolution between zebrafish and human, as both species contain only one gene for the GR that is alternatively spliced in a similar manner [62]. Both human and zebrafish GRα act as ligand-activated transcription factor, whereas the splice-variant GRβ does not bind glucocorticoid agonists, lacks the transactivation activity, and acts as dominant-negative inhibitor of the canonical GRα [25, 62]. Recently, zebrafish was also introduced as model for investigating glucocorticoid resistance [74].

1.3 The SDR superfamily

Short-chain dehydrogenases/reductases (SDRs) represent one of the largest enzyme families with currently 46000 known members and over 300 deposited crystal structures [75]. The family continues to grow in number of known structures and functional diversity [76]. SDR enzymes are also one of the evolutionary oldest superfamilies, since they are present in all domains of life (bacteria, fungi, plants, animals), which emphasizes their versatility and fundamental importance [75, 76]. In humans alone, over 70 SDR genes exist, and a variety of inherited diseases have genetic defects in SDR genes as their underlying cause [75, 77]. SDRs catalyze NAD(P)(H)-dependent oxidation or reduction reactions using a wide range of substrates (alcohols, sugars, steroids, aromatic compounds, fatty acids, retinols, prostaglandins, and xenobiotics) [76, 78, 79], reflecting their large functional diversity. Enzymes consist typically of 250-350 amino acids. The variation in chain length is addicted to either multi-domain enzymes comprising a SDR domain or SDR enzymes including N- or C-terminal hydrophobic extensions for membrane insertions [77]. SDR enzymes show only low pairwise sequence identities of approximately 15-30 %. However, the family is characterized by specific and highly conserved sequence motifs (see Table 1.1) allowing for functional assignment, family allocation, and predictions of cofactor preferences [76].

Table 1.1: Conserved sequence motifs in the classical SDR family.

SDR motif (classical)	suggested function
TGxxxGhG	structural role in coenzyme binding region
Dhx[cp]	adenine ring binding of coenzyme
GxhDhhhNNAGh	structural role in stabilizing the central β-sheet
hNhxG	part of active site
GxhhxhSSh	part of active site
Yx[AS][ST]K	part of active site
h[KR]h[NS]xhxPGxxxT	structural role, reaction direction

Amino acids are given in single letter code. ‘c’ denotes a charged residue, ‘h’ a hydrophobic residue, ‘p’ a polar residue and ‘x’ any residue. Alternative amino acids at a motif position are given in brackets. Adapted from Kallberg *et al*. 2002 [76].

The N-terminal region of SDRs binds the cofactor and is thus slightly higher conserved than the substrate-binding C-terminal part [76, 80]. Based on the characteristic sequence motifs and the observed variations, SDR enzymes are classified into five subfamilies: classical, extended, intermediate, divergent, and complex [76, 79]. The two largest and best characterized subfamilies of classical and extended SDRs are further divided into seven and three subfamilies, respectively. Classical SDRs are mostly oxidoreductases and prefer NADP(H) as cofactor, while extended SDRs contain isomerases, lyases, and a few oxidoreductases preferring NAD(H) [76].
The increasing number of SDR family members initiated in 2009 the reassignment of presently known SDR sequences and resulted in a novel nomenclature system [75] based on the previously published subfamily classification [76]. Every SDR gene is now annotated with SDR in its name followed by a number. SDRs from human and the most common ones were attributed with the lower numbers from 1-48. The SDR subfamilies are now called ‘types’ and the type is also added to the candidate’s name (C, classical; E, extended; I, intermediate; D, diverse; X, complex; A, atypical (containing proteins with SDR topology but lack of enzymatic activity)). If necessary, this annotation is followed by the numbering of family members and splice variants. The above mentioned 11β-HSD type 2 catalyzing the inactivation of cortisol to cortisone is now annotated as SDR9C3, to give an example of the nomenclature system [75]. The SDR nomenclature system is in accordance with the established nomenclature of aldo-keto reductases [81].
Despite sharing low primary sequence identity, the three-dimensional structures of SDR enzymes are clearly homologous displaying a common α/β-folding pattern [77-79]. The structure is characterized by a central β-sheet typical of a Rossmann fold with α-helices on either side [75]. Furthermore, SDR enzymes form homodimers or homotetramers for being enzymatically active [82, 83].

1.4 HSDs as regulators of hormone action

Hydroxysteroid dehydrogenases (HSDs) form an important subfamily of SDR enzymes [84]. HSDs catalyze the reduction or oxidation of carbonyl or hydroxyl groups on the steroid backbone, respectively, thereby playing a pivotal role in both activation and inactivation of all steroid hormones [85, 86]. Additionally, HSDs are responsible for the regulation of the binding affinity of steroid hormones to their receptors and constitute a pre-receptor mechanism of hormone regulation, as steroids have higher affinity to their respective receptor in the hydroxyl form [87-89]. HSDs accept different positions on the steroid backbone for conversion (3, 5, 11, 17, and 20), which is incorporated in the name of the respective enzyme [86, 89]. Being members of the SDR superfamily, also HSD enzymes catalyze their reactions in dependency of NAD(H) or NADP(H) as cofactor. While the HSD reactions *in vitro* are reversible [88], the enzymes show strong directional preferences *in vivo* driven by cofactor affinities and the existing cofactor gradients [90].

17β-HSDs control the last step in biosynthesis and the activation and inactivation of androgens and estrogens [91, 92]. In humans, up to now 14 different 17β-HSDs were identified [93], that were numbered in the order of their cloning [88]. In recent years it was shown that the substrate preference of 17β-HSDs is diverse and not restricted to steroids and that evidence for physiological roles of these enzymes in other pathways than steroid metabolism is accumulating [92]. However, 17β-HSD types 1, 2, and 3 were considered to be key enzymes in steroid hormone regulation with a restricted expression pattern thus designated ‘classical’ 17β-HSDs [72, 92]. Contrary, ‘multifunctional’ 17β-HSD types 4, 6-10, and 12 show a widespread tissue distribution pattern and broader substrate specificity accepting fatty acids, bile acids, retinoids, and sterols [72, 92, 93]. Recent evidence of 17β-HSD type 1 catalyzing the efficient conversion of not only steroids but also retinoids [94], calls the classification of 17β-HSD enzymes described above into question.

Beside 17β-HSDs, 11β-HSDs play a crucial role exclusively in steroid metabolism regulating tissue specific glucocorticoid effects. As already mentioned, 11β-HSD type 2 acts protectively on both GR and MR by inactivating cortisol to cortisone, while 11β-HSD type 1 is a local enhancer of glucocorticoid action by converting cortisone to the active form cortisol [56, 95, 96].

Being essential for steroid hormone homeostasis and other metabolic pathways, mutations and polymorphisms in genes of 17β-HSD and 11β-HSD family members are involved in pathogenesis of a variety of diseases [93, 97-101], including disorders of reproduction, neural diseases, pathogenesis of cancers, and metabolic diseases like obesity.

Since teleost fish, especially zebrafish, are emerging models for studying endocrinology, the number of both annotated and characterized HSDs from fish is increasing. In zebrafish, out of 14 mammalian 17β-HSDs nine were identified as sequence homologs [72] and types 1, 2, and 3 were cloned and functionally characterized [94, 102-105]. Such systematic approaches have so far not been conducted for other teleosts, but in Japanese eel and tilapia 17β-HSD type 1 was characterized [106, 107]. In tilapia, 17β-HSD types 8 and 12 have been additionally described [107], along with 17β-HSD type 4 from brown trout [108]. 11β-HSD type 2 enzymes from teleost fish are described in more detail, as they were found to catalyze not only the conversion of cortisol to cortisone but also the conversion of 11-hydroxytestosterone to 11-ketotestosterone. Thus, it is accepted that 11β-HSD type 2 regulates cortisol action and provides the active androgen 11-ketotestosterone in several fish species for reproduction [109-112]. The enzyme supposed to catalyze the conversion of cortisone to cortisol, 11β-HSD type 1, is annotated in several fish species [113, 114], but is so far not functionally characterized.

1.5 The aim of this study

A protein family of the size of the SDR superfamily contains many 'orphan' members – enzymes which are annotated to be SDRs but are not functionally characterized. The same holds true for the significantly smaller family of HSDs, since many candidate sequences in a wide range of species are annotated as HSD based on sequence similarities alone.
In 2004, several new 17β-HSD candidates were identified in the zebrafish genome based on sequence homology to human 17β-HSD type 3 [103]. Two of the 17β-HSD type 3 homologs in zebrafish were described to be 17β-HSD type 12 enzymes. The third HSD homolog identified by Mindnich *et al.* [103] was named zf3.2 and considered to be a novel, yet unknown steroid dehydrogenase. The identification of a steroidal substrate for zf3.2 but not its product [115] was the starting point for an in-depth functional characterization of the enzyme in this work.
The aim of this thesis was to annotate zf3.2 according to its function and to determine the physiological role of the enzyme in zebrafish development and adult homeostasis. To this end, the reaction product of zf3.2 needed to be identified by a LC-MS/MS method especially developed for this purpose. Knowledge of the reaction product would allow for determination of the catalyzed reaction of the enzyme. Furthermore, the kinetic parameters of zf3.2 were to be determined and the expression of the gene analyzed in adult zebrafish and developing embryos. Obtained results were to be evaluated in the light of known physiological processes and the resulting hypotheses of a physiological role of zf3.2 experimentally verified. Therefore, functional assays including knock-down of zf3.2 in zebrafish embryos and challenge experiments were to be performed.

2 Methods, material, and equipment

2.1 Handling of bacteria

2.1.1 Cultivation

For plasmid preparation or recombinant protein production, *Escherichia coli* were cultivated in liquid LB medium containing the appropriate selective antibiotic. The antibiotic was chosen depending on the resistance gene encoded on the bacteria's plasmid(s). The bacteria were cultivated with gentle agitation (180-200 rpm) at 37 °C for several hours up to overnight.
For selection of transformed *E. coli* or isolation of single colonies from agar stabs, bacteria were cultivated at 37 °C overnight on LB agar plates containing the appropriate antibiotic. If plasmids allowing for Blue-White Screening were used, plates were modified by streaking out 40 µl X-Gal (20 mg/ml in DMF) and 8 µl 0.5 M IPTG. Vectors for Blue-White Screening carry the gene for β-galactosidase which is synthesized upon IPTG induction and converts X-Gal. As a result, the respective colony is stained blue and denotes a colony transformed with a vector without insert, as the β-galactosidase gene will be disrupted by successful cloning of an insert into the multiple cloning site.
For long-term storage of *E. coli*, equal amounts of liquid culture and sterile 80 % glycerol were mixed and frozen at -80 °C.

LB medium	10 g BACTO Pepton 5 g yeast extract 10 g NaCl ad 1 l H_2O, autoclave
LB agar	LB medium 10 g/l Bacto-agar autoclave
antibiotics (final concentrations)	Ampicillin (50 µg/ml) Kanamycin (50 µg/ml) Chloramphenicol (30 µg/ml) added after cooling of the solution to at least 50 °C

2.1.2 Transformation of chemocompetent *E. coli*

For transformations, 1-10 µl of plasmid, ligation reaction, or Gateway recombination reaction was added to 50 µl of chemocompetent *E. coli* cells (Invitrogen). The *E. coli* strain used for transformation was chosen depending on the downstream application. The mixture was incubated on ice for 20 min and heat-shocked at 42 °C in a water bath for 45 sec. After a short incubation on ice, 500 µl of LB medium without antibiotics was added and the cells were incubated at 37 °C and 750 rpm for 1 h. 50-200 µl of the suspension was plated on pre-warmed LB agar plates containing the appropriate selective antibiotic and incubated overnight at 37 °C. Obtained colonies were screened for the desired insert (see 2.6). Glycerol stocks were prepared from single colonies after thorough insert verification.

2.1.3 Expression of recombinant proteins

For production of recombinant proteins in *E. coli*, expression plasmids were transformed into the Rosetta 2 (DE3) pLysS strain. Single colonies were stored as glycerol stocks. From this stock, a 5 ml pre-culture was grown overnight in the appropriate selective LB medium. 1 ml of this culture was transferred to 50 ml fresh medium and bacteria were grown at 37 °C and 200 rpm until $OD_{600\,nm}$ reached 0.8. For induction of protein expression, the culture was split evenly and IPTG was added at a final concentration of 0.5 mM to one of the aliquots. Both cultures were further grown for 4 h and then harvested by centrifugation at 21900 x g and 4 °C for 10 min. Pellets were stored at -80 °C until use.

2.2 Mammalian cell lines

2.2.1 Cultivation and storage

In this work, different cell lines were cultivated for diverse purposes. HEK293 cells were used for recombinant expression of proteins and subsequent enzymatic analysis, as these cells show only minor endogenous activity with steroids. Since HeLa cells grow epithelial-like, they were mostly used for subcellular localization studies of recombinant enzymes. For reporter gene experiments, COS-1 cells were employed. All cell lines were cultivated at 37 °C and 5 % CO_2 in a humidified atmosphere.
Cryo-conserved cells were thawed rapidly in a water bath at 37 °C and transferred to 10-15 ml pre-warmed supplemented medium. Subsequently, cells were centrifuged at 1000 x g for 5 min, the medium removed and the cells resuspended in 6 ml supplemented medium. Cells were then transferred to a culture flask and incubated under growth conditions.
HeLa cells were maintained in MEM medium (PAA Laboratories) supplemented with 10 % FBS (PAA Laboratories), 100 U/ml penicillin, and 100 µg/ml streptomycin (Invitrogen). HEK293 and COS-1 cells were maintained in DMEM medium containing the same supplements. When cells reached confluence, they were washed once with PBS and split at an appropriate ratio using trypsine-EDTA (GibcoBRL).
For cryo-conservation, cells were washed with PBS, detached with trypsine-EDTA and resuspended in 10 ml supplemented medium. After pelleting the cells by centrifugation at 1000 x g for 5 min, the medium was removed and the cells resuspended in supplemented medium containing 10 % DMSO. 1-2 x 10^6 cells were transferred into cryo tubes (Nunc) and placed in a freezing container (Nalgene) at -80 °C, allowing for progressive freezing at -1 °C/min. For long-term storage, cells were stored in liquid nitrogen.

PBS	10 mM NaP_i, pH 7.4 150 mM NaCl

2.2.2 Transient transfection

Cells were transfected with expression plasmids at a confluence of 30-40 %. Using FuGENE 6 (Roche), the appropriate amount of serum-free medium was mixed with the transfection reagent and incubated at room temperature for 5 min. DNA was added and the mixture incubated for 15 min prior to drop wise addition to the cells. In case of X-tremeGENE 9 (Roche), the same protocol was followed, but the final incubation step was elongated to 30 min. Transfections using X-tremeGENE HP (Roche) followed a different protocol. Here, DNA and serum-free medium were mixed prior to addition of transfection reagent. The mixture was then incubated at room temperature for 30 min and applied drop wise to the cells. HeLa cells were transfected with FuGENE 6, HEK293 cells with X-tremeGENE 9, and COS-1 cells with X-tremeGENE HP. Table 2.1 shows the composition of transfection mixtures for different cell culture formats. Following transfection, cells were further cultivated for 24-48 h.

Table 2.1: Composition of transfection mixtures using different transfection reagents.

culture vessel	volume transfection mixture (µl)	volume transfection reagent (µl)	amount of DNA (µg)
FuGENE 6			
6 well plate	100	3	1
T-75 flask	800	24	8
X-tremeGENE 9			
6 well plate	100	3	1
T-75 flask	1000	30	10
X-tremeGENE HP			
12 well plate	100	4	1

2.2.3 Harvesting of cells

48 h post transfection, cells were harvested. Cells were washed with PBS, detached with trypsine-EDTA, and resuspended in supplemented medium. After pelleting the cells by centrifugation at 1000 x g, the medium was removed and the cells were resuspended in 10 ml PBS per harvested T-75 flask. 20 µl of the cell suspension was subjected to lysis and quantification of total protein (see chapters 2.8.1 and 2.8.3). Cell aliquots containing 300-1000 µg of total protein were centrifuged at 21900 x g and 4 °C for 15 min, the supernatants were removed, and the cell pellets were stored at -80 °C until use.

2.2.4 Subcellular localization analyses

About 5 x 10^4 HeLa cells were seeded per well in 6-well plates containing glass coverslips, transiently transfected as described above, and stained after an incubation time of 24 h. For counterstaining of the endoplasmic reticulum, the plasmid pDsRed2-ER (Clontech) was cotransfected with the plasmid coding for the respective enzyme of interest. Cells were washed twice with PBS and fixed for fluorescence microscopy by incubation for 10 min at 37 °C and 5 % CO_2 in fixation solution. To detect myc-tagged recombinant proteins, cells were permeabilized with permeabilization solution for 5 min at room temperature. After washing the cells twice with PBS unspecific binding sites were blocked by incubation of cells in blocking solution for 30 min at room temperature. Immunochemical detection of the myc tag was conducted by incubating a FITC-coupled myc antibody (Sigma) diluted 1:1000 in blocking solution for 1 h at room temperature. Cells were again washed twice with PBS and incubated in PBS containing Hoechst 33342 (Invitrogen) diluted 1:5000 for 2 min at room temperature for counterstaining of the nuclei. After washing the cells twice in PBS, the coverslips were mounted on slides with VectaShield mounting medium (VectorLabs) and examined with an Axiophot epifluorescence microscope (Zeiss) using a 40x oil immersion objective. Three channel optical data were collected with AxioVision Rel. 4.6 (Zeiss). Pearson's coefficient of colocalization was determined by using the Colocalization Finder plug-in for ImageJ software.

Fixation Solution	3.7 % formaldehyde in PBS
Permeabilization Solution	0.5 % Triton X-100 in PBS
Blocking Solution	3 % BSA in PBS

2.2.5 Reporter gene experiments

For the purpose of analyzing the capability of different steroids to activate zebrafish glucocorticoid and mineralocorticoid receptor, COS-1 cells were employed. Since COS-1 cells lack an endogenous glucocorticoid receptor, they are frequently used to study interactions of human and zebrafish glucocorticoid receptor [25]. About 5 x 10^4 cells were seeded per well in 12-well plates and incubated for 24 h. Cells were transfected with expression plasmids using X-tremeGENE HP transfection reagent as described (see chapter 2.2.2). Plasmids coding for receptors (pCS2+_zGRα and pCS2+_zfMR) were transfected together with the reporter plasmid pMMTV-*luc* and the plasmid pGL4.74[*hRluc*/TK] for normalization at the ratio pGL4.74 : pCS2+ : pMMTV-*luc* 1 : 10 : 50. Cells were further incubated for 24 h, the growth medium was replaced by 2 ml fresh medium, and a steroid in methanol (cortisol, cortisone, 20β-hydroxycortisone, 11-dehydrocorticosterone, or aldosterone) was added in final concentrations of 0.1, 1, 10, 100, and 1000 nM. After incubation of cells for another 24 h, the cells were lysed with 1x Passive Lysis Buffer (PLB) provided by the Dual-Luciferase Reporter Assay System (Promega). The manufacturer's lysis protocol was modified by shaking the cells in 1x PLB for 30 min and freezing them at -80 °C for at least 30 min prior to determination of firefly and renilla luciferase activity. Cell lysates were thawed on ice and three times 20 µl (technical replicates) were transferred into an opaque 96-well plate (Nunc). Determination of firefly and renilla luciferase activity was carried out using the Dual-Luciferase Reporter Assay System according to the manufacturer's instructions with the modification of reducing the amount of sample and reagents by 50 %. The bioluminescence was measured with a GloMax Multi Detection System (Promega).
Firefly luciferase signals were normalized to renilla luciferase and the background of methanol treated cells subtracted from steroid treated cells. Averages were taken from technical replicates and mean values calculated from three biological replicates. Data were plotted and fitted according to simple ligand binding model by SigmaPlot 12.0 (Systat Software).

2.3 Working with zebrafish

All experiments were performed on zebrafish (*Danio rerio*) AB/EK wild-type strain. Fish were kept according to standard protocols [59] at the zebrafish facility of the Institute of Developmental Genetics at the Helmholtz Zentrum München – German Research Center for Environmental Health. Adult fish for breeding were a kind gift from Dr. Laure Bally-Cuif, Dr. William Norton, and Dr. Prisca Chapouton.

2.3.1 Embryo production, maintenance, and collection

Zebrafish embryos were obtained by natural spawning and staged according to Kimmel *et al.* [22]. They were kept at 28.5 °C in petri dishes containing embryo water, which was daily replaced by fresh embryo water also removing dead embryos and chorion debris.
For RNA isolation or enzymatic assays, embryos at the desired stage were collected in 1.5 ml tubes, the medium was removed and the embryos immediately snap-frozen in liquid nitrogen. For RNA isolation, 20-30 embryos were collected, while for enzymatic assays 10-20 embryos were sufficient.
Embryos had to be dechorionated prior to whole mount *in situ* hybridizations and protein extractions. To this end, the chorion of living embryos was ripped open using two sharp forceps under a pair of binoculars. Fixation for whole mount *in situ* hybridization is described in the following chapter. Dechorionated fish embryos for protein extraction were snap-frozen in liquid nitrogen after removal of embryo water.
To reduce the amount of yolk proteins especially for Western blot purposes, collected embryos had to be deyolked prior to homogenization. Therefore, the embryos were thawed in 10 ml Deyolking Buffer and placed in a sterile petri dish. The yolk was removed as good as possible without damaging the embryos using two preparation needles under a pair of binoculars. Embryos were carefully collected in a fresh 1.5 ml tube, the remaining buffer removed, and snap-frozen in liquid nitrogen.

All collected samples were stored at -80 °C for further usage.

Embryo water	60 µg/l sea salt
Deyolking Buffer	1x proteinase inhibitor in PBS

2.3.2 Whole mount *in situ* hybridization

Embryos dedicated for whole mount *in situ* hybridizations were kept in embryo water containing 0.003 % 1-phenyl-2-thiourea (Sigma) to prevent pigmentation. Embryos at the desired stage were dechorionated and fixed overnight in fixation solution at 4 °C. After washing twice for 5 min in PBS-T, embryos were dehydrated by 25 %, 50 %, 75 %, and 100 % methanol in PBS-T for 3 min each at room temperature for storage at -20 °C.
For whole mount *in situ* hybridization, embryos were rehydrated through a reversed methanol in PBS-T series. All further steps were carried out at room temperature, unless stated otherwise. Embryos were treated with proteinase K solution for 20 min (30 hpf embryos) or 35-45 min (2-4 dpf larvae). After washing twice carefully with PBS-T for 2 min each, embryos were refixed in fixation solution for 20 min and subsequently rinsed four times 5 min in PBS-T. Prehybridization was carried out by incubating the embryos for 90 min in hybridization buffer at 70 °C. Hybridization was performed overnight in fresh hybridization buffer containing 200 ng digoxygenin labeled RNA probe at 70 °C. Following hybridization, embryos were rinsed for 10 min at 70 °C in 75 % hybridization buffer, 25 % 2x SSC, 10 min at 70 °C in 50 % hybridization buffer, 50 % 2x SSC, 10 min at 70 °C in 25 % hybridization buffer, 75 % 2x SSC, 10 min at 70 °C in 2x SSC and afterwards twice 30 min at 70 °C in 0.05x SSC. Embryos were then washed 5 min at room temperature in 50 % 0.05x SSC, 50 % PBS-T followed by washing twice 5 min in PBS-T. After incubation for 1 h in blocking buffer, embryos were incubated with anti-DIG-AP antibody (Roche) diluted 1:5000 in blocking buffer for 2 h. Following antibody reaction, embryos were rinsed three times for 5 min in PBS-T and afterwards six times for 10 min in PBS-T. Washing was continued thrice for 10 min each in NTMT buffer. Colorimetric signal detection was carried out by incubation of embryos in staining solution. When color had developed to the desired extent, the reaction was stopped by washing the embryos four times for 5 min in PBS-T, and finally in 80 % glycerol in PBS-T for storage at 4 °C. Embryos were mounted in 3 % methylcellulose and photographed with an Axioplan2 stereomicroscope (Zeiss) using AxioVision software (Zeiss).
Embryos for cryosection were rinsed in PBS and then equilibrated in 15 % sucrose in PBS at 4 °C for more than 48 h. Afterwards, the embryos were embedded in 7.5 % gelatine/15 % sucrose solution and frozen in liquid nitrogen before being stored at -80 °C. Sections of frozen embryos were cut serially at 20 µm using a cryostat (CM1950, Leica). Obtained sections were collected on Superfrost slides (ThermoScientific) and dehydrated by heating for 15 min at 70 °C. Sections were mounted in Aqua Poly/Mount (Polysciences) before being photographed with an Axioplan2 stereomicroscope (Zeiss) using AxioVision software (Zeiss).

Fixation Solution	4 % paraformaldehyde	in PBS
PBS-T	0.1 % Tween-20	in PBS
Proteinase K Solution	10 µg/ml Proteinase K	in PBS-T
Hybridization Buffer	50 % formamide 5x SSC, pH 6.0 (adjusted with 1 M citric acid) 50 µg/ml yeast tRNA 50 µg/ml heparin 0.1 % Tween-20	

20x SSC	3 M NaCl 0.3 M Na_3 citrate, pH 7.0	
Blocking Buffer	2 mg/ml BSA 2 % normal goat serum	in PBS-T
NTMT Buffer	0.1 M Tris-HCl, pH 9.5 50 mM $MgCl_2$ 0.1 M NaCl 0.1 % Tween-20	
Staining Solution	225 µg/ml NBT 175 µg/ml BCIP	in NTMT Buffer

2.3.3 Challenging with steroids

Zebrafish embryos were treated with different steroids to analyze their impact on 20β-HSD type 2 expression. According to Hillegass *et al.* [44], treatment started at 3 hpf by replacing normal embryo water with embryo water containing the respective treatment regimen. Fish embryos were continuously exposed through 72 hpf. Samples for RNA isolation and enzyme assays were collected at 24 hpf, 48 hpf, and 72 hpf and snap-frozen in liquid nitrogen. At each sampling point water was exchanged for fresh embryo water containing the respective treatment regimen. Zebrafish embryos were challenged with cortisol (final concentrations 10 mg/l, 25 mg/l, 50 mg/l, 75 mg/l, and 100 mg/l), corticosterone (final concentrations 10 mg/l and 25 mg/l), progesterone, 11-ketotestosterone, and estradiol (final concentrations 1 mg/l and 5 mg/l). Steroids were dissolved in DMF prior to addition into embryo water. Controls, including a no treatment control with embryo water alone and a solvent control consisting of DMF, were run concurrently with each experiment. Embryos were monitored throughout the experiments for viability and developmental abnormalities.
For short-time exposure of zebrafish embryos to cortisol, embryo water was exchanged at 3 hpf to water containing 50 mg/l cortisol in DMF. At 24 hpf, samples were collected for RNA isolation and enzyme assays and the water exchanged to normal embryo water. Additional samples were taken at 48 hpf and 72 hpf, always replacing the water with fresh embryo water. A no treatment control and a control treated with DMF (vehicle) for the same times were included.

2.3.4 Challenging with physical stressor

For subjection of zebrafish larvae to a stressor independent of artificial cortisol treatment, an experimental set-up using a physical stressor consisting of swirling fish was designed. Larvae used for analyses of stress response were 5 dpf old, as Alsop & Vijayan [42] have shown that the stress axis is fully functional by this age. At 3 dpf, pools of 50 larvae were placed in 25 ml glass beakers with 20 ml fresh embryo water and kept further at 28.5 °C until 5 dpf. Prior to challenging by swirling, the water was carefully reduced to 5 ml. Each pool was subjected to a stressor regimen consisting of swirling for 30 sec. After the stress, fish were kept at 28.5 °C and sampled at different time points (5 min, 10 min, 20 min, 30 min, and 60 min). Control samples were collected before applying the stressor. For sample collection, each pool was rapidly divided into two samples and snap-frozen in liquid nitrogen after water removal. To reduce fish handling time which is in itself stressful to the fish, the described approach was used for sampling instead of counting precisely how many fish were placed in each sample. All collected samples were stored at -80 °C for subsequent RNA isolation or enzyme assay.

2.3.5 Microinjection of morpholinos

For transient knock-down of 20β-HSD type 2 in developing zebrafish embryos, microinjection of morpholinos was performed. Morpholino antisense nucleotides are stable molecules that bind to complementary sequences of RNA and can thereby inhibit splicing of mRNA precursors or translation of mRNA [116, 117]. In this work, morpholinos were designed to target the donor splice site of exon 2 of *Hsd20b2* mRNA and were synthesized by Genetools. The splicing morpholino had the following sequence (5'-GAATAAAATACTGACCTCTTCAGCA-3'), while the control morpholino contained five mismatches (5'-GAATAAAATAgTcAgCTCTTgAcCA-3'). Morpholinos were dissolved in water at a concentration of 1 mM and the stock solution stored at room temperature. Prior to injection, working solutions with final concentrations of 125 µM, 250 µM, 375 µM, and 500 µM were prepared. A microinjection tray was prepared by placing a plastic piece carrying six small rods in warm 1.5 % agarose in embryo water forming cavities with 1 mm in depth and 1 mm in width. Embryos at 1 cell stage were placed with the animal pole upside in a microinjection tray and injected into the yolk with approximately 4 nl of morpholino using a FemtoJet injector equipped with a micromanipulator (Eppendorf). Embryos were kept in embryo water at 28.5 °C and were frequently monitored for viability and developmental phenotypes.
At 48 hpf, embryos were collected and snap-frozen in liquid nitrogen for analyses of knock-down efficiency. To verify *Hsd20b2* mis-splicing, RNA was isolated (see 2.5.1) and cDNA synthesized as described in chapter 2.5.3 followed by RT-PCR (see 2.6.1).
For confirmation of diminished 20β-HSD type 2 activity, collected samples were subjected to enzyme assays as well. Assay composition and detection is described in chapter 2.9.1.
Challenging experiments of morpholino-injected embryos were basically performed as described above (2.3.3) using only 10 mg/l cortisol and a solvent control consisting of 0.1 % DMF. Challenged embryos at 48 hpf and 72 hpf were dechorionated and fixed overnight in fixation solution, washed and dehydrated as described for whole mount *in situ* hybridizations (see 2.3.2). Embryos were stored in 100 % methanol at -20 °C. Prior to microscopy, embryos were rehydrated through a reversed methanol in PBS-T series and mounted in 3 % methylcellulose. For microscopy and photography, an Axioplan2 stereomicroscope (Zeiss) with AxioVision software (Zeiss) was used.

2.3.6 Steroid extraction from adult fish holding water

Six adult zebrafish aged between 1.5 and 2 years were placed in a sterile 2 l glass beaker containing 800 ml of freshly prepared fish water. Either mixed gender groups composed of three females and three males or all-female and all-male groups were used. Fish were kept in the beaker for 16 h at 26 °C (room temperature in the fish facility) before they were placed with clean nets back into their aquaria. The water was left to stand 30 min at room temperature to allow for sedimentation of faeces, scales and other particles. Solid phase extraction cartridges (Strata C18-E, 200 mg/6 ml, Phenomenex) were equilibrated with twice 2 ml methanol followed by twice 2 ml water. Afterwards, 750 ml of fish holding water was extracted using a vacuum manifold (Visiprep 24DL, Supelco). To separate conjugated from free steroids, differential elution was carried out by first eluting conjugated steroids with three times 300 µl 47 % methanol in water (v/v). Afterwards, free steroids were eluted with three times 300 µl 100 % methanol. Both eluates were dried using a speed-vac centrifuge (Uniequip, Laborgerätebau Martinsried) at 39 °C. The fraction containing free steroids was reconstituted in 300 µl methanol and stored at -20 °C for LC-MS/MS analyses. The fraction containing conjugated steroids was reconstituted in 500 µl β-glucuronidase buffer, 41 U β-glucuronidase (purified from *E. coli*, Sigma) was added, and the mixture was incubated overnight at 37 °C with shaking. After digestion of steroid-glucuronide conjugates as described, the mixture was extracted by solid phase extraction. Therefore, Strata C18-E, 100 mg/1 ml (Phenomenex) cartridges were equilibrated with twice 1 ml methanol followed by twice 1 ml water. The sample was applied to the cartridge and the glass vial was washed with 500 µl water, which was subsequently applied to the cartridge as well. Conjugated steroids were eluted with twice 200 µl 47 % methanol in water (v/v) followed by elution of free steroids (former glucuronidated steroids now digested) with twice 200 µl 100 % methanol. Both

obtained fractions were again evaporated to dryness using a speed-vac centrifuge at 39 °C. Afterwards, the free steroid fraction was reconstituted in 300 µl methanol and stored at -20 °C until LC-MS/MS analyses. The fraction containing conjugated steroids was reconstituted in 500 µl sulfatase buffer, 7 U sulfatase (crude extract) of *Helix pomatia* was added, and the mixture was incubated with shaking for 4 h at 37 °C. After digestion of steroids conjugated with sulfates, again solid phase extraction using Strata C18-E, 100 mg/1 ml cartridges (Phenomenex) was performed as described in the previous step, but omitting the elution step with 47 % methanol. The solvent was evaporated to dryness in a speed-vac centrifuge at 39 °C, steroids were reconstituted in 300 µl methanol and stored at -20 °C until LC-MS/MS analyses. For details of steroid analyses in all obtained fractions, refer to chapter 2.10.2.2.

Fish water	0.15 g $NaHCO_3$ 0.036 g sea salt 0.0168 g $CaSO_4$ ad 2 l H_2O, pH 6.5-7.0
β-Glucuronidase Buffer	75 mM NaP_i, pH 6.8
Sulfatase Buffer	75 mM NaP_i, pH 5.1

2.4 Methods using DNA

2.4.1 Isolation of plasmids from bacteria

Isolation of plasmid DNA from *E. coli* was carried out in two different scales using either 5 ml or 50-100 ml of an overnight culture. For small-scale preparations the NucleoSpin Plasmid Kit (Macherey-Nagel) was used, while for large-scale preparations the NucleoBond PC100 Kit (Macherey-Nagel) was applied. Bacteria were harvested by centrifugation at 4 °C and 2260 x g for 15 min and the pellet was resuspended in the appropriate buffer of the kit. Further purification was carried out according to the manufacturer's protocol. DNA was eluted in 50 µl of Ampuwa water instead of the supplied buffer in small-scale preparations. In large-scale preparations, DNA was reconstituted in 120 µl of Ampuwa water.

2.4.2 Separation of DNA in agarose gels

For monitoring DNA purity and PCR amplifications, or for subsequent purification, DNA fragments were separated using agarose gel electrophoresis. Different w/v percentages of agarose in 1x TBE were chosen depending on the size of fragments analyzed (0.8-1 % for fragments > 2 kb and 2 % for fragments of 0.3-2 kb). Prior to gel electrophoresis, Loading Dye was added to the DNA, mixed and loaded on a gel containing 0.5 µg/ml ethidium bromide. DNA was separated in a constant electric field (80-180 V) and detected under UV illumination (λ = 254 nm).

10x TBE	108 g Tris 55 g boric acid 9.3 g EDTA ad 1 l H_2O
6x Loading Dye	15 % Ficoll 400 0.25 % bromophenol blue 0.25 % xylene cyanol FF

2.4.3 Purification of DNA from solutions and agarose gels

DNA from solutions containing enzymes, dNTPs, and buffers was purified using the PCR purification kit (SeqLab) according to the manufacturer's instructions. DNA was eluted in 30 µl of Ampuwa water. DNA fragments analyzed by agarose gel electrophoresis were purified using two different methods. After cutting the DNA containing slice out of the gel with a scalpel, the gel piece was transferred to a reaction tube and further processed using the Wizard SV Gel and PCR Clean-Up System (Promega). In contrast to the manufacturer's protocol, elution of DNA was carried out by applying two times 20 µl of Ampuwa water to the column. In case this kit did not elute sufficient DNA, a different approach was used. The gel slice containing the DNA was transferred to a specially prepared 0.5 ml tube. This tube was perforated at the bottom and equipped with some silanized glass wool. The tube was then placed into a 1.5 ml tube and centrifuged for 5 min at room temperature and 6000 x g. The eluate contained the desired DNA fragment.

2.4.4 Determination of DNA concentrations using spectrophotometry

To determine the concentration and quality of purified DNA, the optical density was measured using a NanoDrop ND-1000 spectrophotometer at $\lambda = 260$ nm (for quantity) and $\lambda = 280$ nm (for quality). The concentration of DNA was calculated using the following formula:

$$c\ [ng/\mu l] = OD_{260\ nm} * 50\ ng/\mu l$$

The ratio $OD_{260\ nm}/OD_{280\ nm}$ was used for assessing purity of DNA and is 1.8 in an optimal case.

2.5 Methods using RNA

2.5.1 Isolation of RNA

RNA was isolated from different matrices like frozen cell culture pellets (1-2 x 10^6 cells), dissected tissues conserved in RNAlater, or 10-30 frozen zebrafish embryos. The sample was placed in 1 ml TRIzol reagent per mg of tissue or 1 ml TRIzol reagent per 5-10 x 10^6 cells, respectively. Homogenization was carried out depending on the matrix: harvested cells and zebrafish embryos were homogenized using syringe and 20G needle, while tissues were homogenized with a rotor-stator. RNA was extracted by addition of 2/10 volumes chloroform, vortexing for 15 sec, incubation at room temperature for 3 min, and centrifugation at 4 °C and 21900 x g for 15 min. 0.53 volumes of 100 % ethanol were added to the supernatant while slowly vortexing. This solution was applied to a column of the RNeasy Mini Kit (Qiagen) and RNA was further purified including DNase I digestion according to the manufacturer's protocol. Amount and quality of isolated RNA was assessed using spectrophotometry prior to addition of 40 U RNase inhibitor (Invitrogen). RNA was stored at -80 °C until use.

2.5.2 Determination of RNA concentrations using spectrophotometry

To determine the concentration and quality of purified RNA, the optical density was measured using a NanoDrop ND-1000 spectrophotometer at $\lambda = 260$ nm (for quantity) and $\lambda = 280$ nm (for quality). The concentration of RNA was calculated using the following formula:

$$c\ [ng/\mu l] = OD_{260\ nm} * 40\ ng/\mu l$$

The ratio $OD_{260\ nm}/OD_{280\ nm}$ was used for assessing purity of RNA and is 2.0 in an optimal case.

2.5.3 Reverse transcription into cDNA

1 µg of total RNA was employed for cDNA synthesis using the RevertAid First Strand cDNA Synthesis Kit (Fermentas) according to the manufacturer's instructions. Instead of the supplied Oligo-dT_{18} primer an anchored Oligo-dT_{18} primer (5'-TTTTTTTTTTTTTTTTTTVN-3') in a final concentration of 0.5 µM was used for priming cDNA synthesis. This primer is binding at the junction of the poly-A-tail with the mRNA avoiding reverse transcription of unnecessary adenosides from the tail.

2.5.4 Hybridization probe synthesis and labeling with digoxygenin

For whole mount *in situ* hybridizations, RNA probes were transcribed *in vitro*. Therefore, the coding sequence for 20β-HSD type 2 was subcloned into pBluescript SK+ vector using restriction endonucleases *Bam*H I and *Xba* I (see chapter 2.7.1). After verification of the insert by sequencing, 900 µg of plasmid was linearized separately by digestion with *Kpn* I and *Not* I. The plasmid was then purified using QIAquick PCR purification Kit (Qiagen) and its concentration determined by spectrophotometry. For synthesis of digoxygenin labeled RNA probes the DIG RNA labeling Kit (Roche) was used according to the manufacturer's protocol. RNA was subsequently purified using RNeasy Mini Kit (Qiagen) and the concentration determined by spectrophotometry.

2.6 Polymerase chain reaction (PCR) based methods

Routine PCR amplifications from different templates were performed in 20 µl reactions containing 0.2 mM dNTP mixture, 0.5 µM forward and reverse primer each, and 0.5-2.5 U lab-made *Taq* polymerase in 1x PCR buffer. For improved accuracy in cloning amplifications, proof-reading polymerases like *Pfx* polymerase (Invitrogen) were used. Templates varied from bacterial cultures, plasmid DNA to cDNA.
The standard amplification program run on a Robocycler PCR machine (Stratagene) implied an initial denaturing for 5 min at 95 °C followed by 35 cycles with 30 sec at 95 °C, 30 sec at T_a, and 1 min per kb at 72 °C for elongation. The annealing temperature T_a was determined by T_m - 5 °C, where T_m is the melting temperature specific for the primer pair used. In case of amplifications for Gateway Cloning, annealing temperatures were further reduced due to T_a above the temperature optimum for polymerases. The temperature for elongation was adjusted to the temperature optimum of the used polymerase. The initial denaturing step was elongated to 10 min if PCR were performed on bacteria culture.

10x PCR buffer	100 mM Tris-HCl, pH 9.0
	500 mM KCl
	15 mM $MgCl_2$

2.6.1 Reverse transcription polymerase chain reaction (RT-PCR)

0.5 µl of reverse transcribed cDNA were used as template in RT-PCR reactions containing 0.2 mM dNTP mixture, 0.5 µM forward and reverse primer each, and 0.3 µl lab-made *Taq* polymerase in 1x PCR buffer in a total volume of 20 µl. For routine RT-PCR reactions the amplification program described above was applied. If the amplified fragments were subjected to subcloning, a final elongation step of 5 min at 72 °C was added. For expression analysis and normalization to a reference gene, cycle number was decreased to 28. Aliquots of the PCR products were subsequently separated by agarose gel electrophoresis (see 2.4.2).

2.6.2 Quantitative real-time PCR (qPCR)

Primers for quantitative real-time PCR were designed to span at least one exon-intron boundary to avoid falsified amplification results due to contamination by genomic DNA. The free accessible tool Primer3 software was used to design appropriate primer pairs (http://biotools.umassmed.edu/bioapps/primer3_www.cgi) [118]. Table 2.2 shows the parameters applied for primer design.

Table 2.2: Parameters for primer design using Primer3 tool.

parameter	chosen range
target	X,20*
product size	120-220
max 3' stability	7
max mispriming	10
pair max mispriming	20
length of primer	18-22 bp
melting temperature of primer (T_m)	58-61 °C
max T_m difference	1.5
GC content	45-56 %
max self complementarity	6
max 3' self complementarity	2

* X was denoting the position of the target exon-intron-boundary; the number 20 implied that 20 base pairs around X had to be included into the amplification product.

Obtained primers were tested for specificity prior to expression analyses in preliminary experiments using a cDNA dilution series. Amplified products were separated by agarose gel electrophoresis to ensure a single PCR product and sequenced to confirm identity with the intended target gene.
Real-time PCR amplifications were performed in triplicates using Power SYBR Green PCR Mastermix with ROX as passive reference (Applied Biosystems). Assays consisted of 10 µl Mastermix, 6 µl of water, 1 µl of each primer in a final concentration of 0.5 µM, and 2 µl cDNA diluted 1:20 in water. Reactions were carried out in 384-well plates on a TaqMan 7900HT cycler equipped with SDS2.3 software (Applied Biosystems). The following amplification protocol was applied: denaturation at 95 °C for 10 min, amplification and quantification repeated 39 times at 95 °C for 15 sec and 60 °C for 1 min, and melting curve program (95 °C for 15 sec, 60-95 °C with a heating rate of 0.1 °C/sec and continuous fluorescence measurement). Cycle threshold (C_T) values were determined by SDS2.3 software as the cycle where the fluorescence rises markedly above background fluorescence.
Usually, fold changes of target genes were calculated according to Pfaffl [119] with normalization to one reference gene and to wild-type expression levels. For calculation of fold changes of target genes in stress challenged zebrafish embryos, normalization was performed by using the BestKeeper software tool developed by Pfaffl *et al*. [120]. To this end, up to three reference genes were included for normalization.

2.6.3 PCR-based mutagenesis

For generation of site-directed mutations, two complementary primers carrying the desired mutation in the core region flanked by 15-20 bp to both sides were designed. PCR reactions were performed using mutagenesis and cloning primers to generate two products that overlap in the region of mutation. In a second PCR, equal molar amounts of both purified fragments were employed as template for amplification with cloning primers alone resulting in a fusion of both fragments to a single full-length product. Annealing time was elongated to 1 min to allow for hybridization of DNA template strands in the region of desired mutation. If it was not possible to obtain a full-length open reading frame for

subcloning from cDNA, the approach of fusion by PCR was also used. For PCR-based mutagenesis and fusion PCRs, proofreading polymerases were preferably employed.

2.6.4 Sequencing

The accuracy of cloned inserts or PCR products was verified using the Sanger dideoxy method. A typical sequencing reaction consisted of 1 µl each of 5x buffer and BigDye 3.1 (BigDye Terminator v3.1 Cycle Sequencing Kit, Applied Biosystems), 1 µl primer in a final concentration of 2 µM, 1-2 µl template DNA (50-150 ng), and water in a final reaction volume of 5 µl. Amplification was performed after an initial denaturing step for 5 min at 95 °C in 36 cycles with 30 sec at 95 °C, 45 sec at 53 °C, and 4 min at 60 °C. Sequencing reactions were purified using the Montage Seq_{96} Sequencing Reaction Clean-Up Kit (Millipore) according to manufacturer's instructions and analyzed on an ABI 3730 DNA Analyzer (Applied Biosystems).

2.7 Molecular cloning strategies

2.7.1 Restriction digestion

Digestion of DNA fragments (inserts) and vectors with restriction enzymes yields complementary DNA ends that can be used for ligation. Using two different restriction sites allow for a site-directed insertion of the insert into the vector. 0.1-10 µg of DNA were digested in a total volume of 20-50 µl containing the appropriate buffer, BSA if recommended by the manufacturer, and the respective enzyme. Digestions were incubated at the appropriate temperature for 2 to up to 16 h. The adequate amount of enzyme was calculated according to the assumption that 1 U of enzyme digests 1 µg DNA in 1 h under optimal conditions. Following restriction, the reaction was either stopped by heat inactivation of the enzyme or purification using the PCR Purification Kit (SeqLab) as described in section 2.4.3.

2.7.2 Ligation

For ligation reactions 100-150 ng of digested vector was mixed with a 5-10 times molar excess of digested insert. This mixture was heated at 80 °C for 5 min and chilled on ice to ensure dissociation of secondary structures. T4 DNA ligase and ligation buffer (Fermentas) were added and the total volume was adjusted with water to 10 µl. The reaction was incubated for 3 to up to 16 h at room temperature.
If insertion of blunt-end DNA fragments led to a destruction of the restriction site, an aliquot of the ligation mixture was subjected to a second restriction digestion with a suitable restriction endonuclease. Using this approach, re-ligated vectors were again linearized and the number of false-positive transformants was significantly reduced.

2.7.3 TOPO-TA cloning

TOPO-TA cloning was applied to clone DNA fragments obtained by PCR reactions with *Taq* polymerase. *Taq* polymerase produces A-overhangs in the PCR, which can be ligated to corresponding T-overhangs in the respective vector (TA cloning). The yield of ligation products is increased by the topoisomerase attached to the vectors' cloning sites (TOPO cloning).
In this work, TOPO-TA Cloning Kit comprising the vector pCSII (Invitrogen) was used according to manufacturer's instructions.

2.7.4 Gateway cloning

For fast and convenient subcloning of coding sequences in different expression vectors, the Gateway Cloning System (Invitrogen) based on the recombination of the phage λ DNA into the host *E. coli* chromosome was used. The initial amplification of coding sequences by PCR was carried out using primers containing *attB* sites and a proofreading polymerase. To generate the entry clone, the purified PCR product was recombined into pDONR201 vector using the Gateway BP Clonase Enzyme Mix (Invitrogen). Differing from the manufacturer's protocol, the reaction consisted of 150 ng pDONR201, 50-150 ng of *attB* PCR product, and 1 µl BP Clonase in a total volume of 5 µl. The reaction was incubated for 2 h at room temperature followed by addition of 0.5 µl Proteinase K for termination of the reaction. The mixture was incubated at 37 °C for 10 min and then transformed into chemocompetent *E. coli* (see chapter 2.1.2).
After sequencing of the entry clone to ensure accuracy, a second recombination was carried out to subclone the insert from the donor vector into the destination vector using the Gateway LR Clonase Enzyme Mix (Invitrogen). Deviating from the manufacturer's recommendations, LR reactions consisted of 150-300 ng entry vector, 150 ng destination vector, 2 µl LR reaction buffer, and 2 µl LR Clonase in a total volume of 10 µl. The reaction was incubated for 2 h at room temperature, 0.5 µl Proteinase K were added and incubated for 10 min at 37 °C. Resulting plasmids were transformed into chemocompetent *E. coli*, sequenced to ensure correct insertion, and further used for downstream applications.

2.8 Protein chemistry

2.8.1 Cell lysis and tissue homogenization

Harvested and frozen bacteria pellets after recombinant protein expression in *E. coli* (see 2.1.3) were resuspended in 250 µl lysis buffer and lysed by five freeze/thaw cycles using liquid nitrogen and hot water. The genomic DNA was digested by addition of 2 U endonuclease and $MgCl_2$ (final concentration 30 mM), and incubation for at least 10 min at room temperature. Samples were centrifuged at 21900 x g and 4 °C for 15 min to separate soluble from insoluble proteins. Supernatants were transferred to fresh tubes and the pellet fraction was resuspended in an equal amount of lysis buffer. Protein concentrations were determined for all obtained fractions (see 2.8.3).
Frozen pellets collected after overexpression of recombinant proteins in mammalian cell lines were resuspended in an appropriate amount of reaction buffer (0.5-2 µl/µg). Cells were lysed by six cycles of sonication for 15 sec alternating to incubation on ice for 15 sec. This lysate was either used directly for protein determination or further fractionated by ultracentrifugation (see 2.8.2).
200-400 dechorionated and yolk-reduced zebrafish embryos (see chapter 2.3.1 for details) were thawed on ice, briefly centrifuged and the remaining water removed, before 1 µl ice-cold PBS or reaction buffer per embryo were added. Fish embryos were homogenized on ice using a rotor-stator, which was rinsed with 0.5 µl buffer per embryo after homogenization and the rinsing volume also collected in the lysate. The lysate was either used directly for protein determination, or further fractionated using ultracentrifugation.

Lysis Buffer	0.1 mg/ml lysozyme 1x proteinase inhibitor	in PBS
Reaction Buffer	100 mM NaP_i, pH 7.3 1 mM EDTA 0.05 % BSA	
PBS	10 mM NaP_i, pH 7.4 150 mM NaCl	

2.8.2 Fractionation using ultracentrifugation

For some downstream applications, lysates derived from cell culture or zebrafish embryos were fractionated using ultracentrifugation to enrich membrane-bound proteins. This goal was reached by using either a two-step centrifugation or a three-step centrifugation protocol. In both protocols, the lysates were first centrifuged at 700 x g and 4 °C for 10 min to remove cell debris and the supernatants were transferred to Microfuge Tubes (Beckman). The pellets were resuspended in 300-600 µl reaction buffer or PBS.
In the two-step protocol, the supernatants were centrifuged in a TLA-55 rotor (Beckman) at 55000 x g and 4 °C for 1 h using OptimaMAX ultracentrifuge (Beckman). The resulting supernatants were separated from the respective pellets, which were resuspended in 50 µl reaction buffer or PBS.
In the three-step protocol, the supernatants obtained after centrifugation at 700 x g as described were centrifuged at 18000 x g and 4 °C for 10 min. After separation of supernatants from pellets, the supernatants were subsequently centrifuged at 55000 x g and 4 °C for 1 h, and the resulting supernatants again transferred into fresh tubes. Both obtained pellets after ultracentrifugation were resuspended in 50 µl reaction buffer or PBS.
All obtained fractions were used for enzymatic activity analyses and the protein concentration was determined as described in the following chapter.

2.8.3 Determination of protein concentrations

The determination of total protein concentrations in aliquots of different origin was performed by mixing 20 µl of protein solution with Bradford reagent (BioRad) according to the manufacturer's instructions. After 10 min of incubation at room temperature, the absorption was measured at a wavelength of 595 nm using UV/Vis spectrophotometer DU530 (Beckman Coulter). Serial dilutions of bovine serum albumin were used to generate a standard curve for estimation of total protein content in the sample.

2.8.4 SDS-Polyacrylamide gel electrophoresis (SDS-PAGE)

Prior to separation, protein samples were denatured by addition of equal amounts of 4x Laemmli buffer and heating at 95 °C for 5-10 min. Samples were separated under denaturing conditions using either pre-cast 4-15 % TGX gels (BioRad) or self-made Tris-Glycine gels with different percentages in the resolving gel. Resolving and stacking gels were prepared as denoted in Table 2.3. Separation of proteins was achieved by application of a constant electric field in running buffer at 4 °C. Following electrophoresis, gels were either subjected to Western Blot (see 2.8.5) or stained with Coomassie Brilliant Blue. Therefore, gels were immersed in Coomassie Staining Solution for 4 h and destained by rinsing with 10 % acetic acid at room temperature until background staining was removed. For documentation, stained gels were equilibrated in H_2O, scanned, and dried between two sheets of cellophane.

Table 2.3: Composition of Tris-Glycine gels.

reagent	resolving gel (10 %) (ml)	resolving gel (8 %) (ml)	stacking gel (4 %) (ml)
Acrylamid/bisacrylamid (37.5:1)	1.67	1.2	0.335
Gel Buffer*	1.25	1.25	0.625
MilliQ H_2O	1.455	1.92	1.51
10 % APS	0.02	0.02	0.02
TEMED	0.01	0.01	0.01

* Gel Buffer denotes Separation Gel Buffer in case of resolving gels and Stacking Gel Buffer in case of stacking gels.

4x Laemmli Buffer	200 mM Tris-HCl, pH 6.8 10 % β-mercaptoethanol 10 % SDS 40 % glycerol 0.02 % bromophenol blue
Separation Gel Buffer	1.5 M Tris-HCl, pH 8.8 0.4 % SDS
Stacking Gel Buffer	0.5 M Tris-HCl, pH 6.8 0.4 % SDS
Running Buffer	25 mM Tris-HCl 192 mM glycine 0.1 % SDS
Coomassie Staining Solution	500 mg Coomassie Brilliant Blue G250 200 ml methanol 5 ml acetic acid 295 ml H_2O

2.8.5 Western Blot

For detection of proteins with antibodies, proteins were first separated by SDS-PAGE and then transferred from the gel onto Immobilon FL PVDF membrane (Millipore) by semi-dry blotting. Therefore, the PVDF membrane was wetted with methanol prior to immersion in blotting buffer alongside six pieces of filter paper (Whatman). The gel was incubated separately in blotting buffer for 10 min. A stack of three pieces of filter paper were placed onto the anode of the Trans-Blot SD – Semi Dry Transfer Cell (BioRad), followed by the membrane, the gel, and another three pieces of filter paper. The cathode was placed on top and the proteins transferred to the membrane by application of 20 V for 40 min.
Depending on the label of the secondary antibodies and the detection method, two different protocols were applied. For use of HRP-conjugated secondary antibodies and chemiluminescence detection, the membrane was incubated in 5 % milk powder in PBS for 1 h at room temperature with gentle agitation to saturate unspecific binding sites. Following removal of blocking solution, the membrane was incubated with the primary antibody diluted in 0.5 % milk powder in PBS overnight at 4 °C with gentle rocking. After washing three times with PBS, the membrane was incubated with the secondary antibody diluted in 0.5 % milk powder in PBS for 2 h at room temperature with gentle shaking. The membrane was again washed three times with PBS and the detection was performed using the Western Lightning Chemiluminescence ECL Kit (Perkin Elmer) according to the manufacturer's

instructions. Light signals were either detected by exposing films (Kodak) and developing them in a developer (Curix 60, Agfa), or by recording light signals with the Fusion FX7 (VilberLourmat).
If the secondary antibodies were labeled with near-infrared dyes, a different protocol for detection was carried out. For blocking unspecific binding sites, the membrane was incubated 1 h in Odyssey Blocking Buffer (Li-Cor) at room temperature with gentle agitation. The primary antibodies were diluted in Odyssey Blocking Buffer and incubated with the membrane overnight at 4 °C with gentle shaking. After rinsing three times with PBS-T, the membrane was incubated with IRDye-labeled secondary antibodies (Li-Cor) diluted in Odyssey Blocking Buffer for 1 h at room temperature with gentle rocking. Since the dyes were light-sensitive, the membrane was kept in the dark from now on. After washing the membrane three times with PBS-T and a final washing step with PBS, signal detection was performed using the Odyssey Infrared Imager (Li-Cor).

Blotting Buffer	48 mM Tris-HCl, pH 9.2 33 mM glycine 1.3 mM SDS 20 % methanol
PBS	10 mM NaP_i, pH 7.4 150 mM NaCl
PBS-T	0.05 % Tween-20 in PBS

2.9 Enzyme assays

2.9.1 Enzyme assays with cell pellets, cell fractions, or zebrafish homogenates

For determination of enzymatic activity in protein samples of different origin, two approaches were chosen depending on the desired method of detection. Using tritiated steroids, detection was done by HPLC coupled to a scintillation counter, while addition of unlabeled steroids to the reaction mixture allowed for detection via mass spectrometry. Protein samples were cell lysates (as described in chapter 2.8.1) and fractions from ultracentrifugation (see chapter 2.8.2). Zebrafish embryos collected for enzyme assays were homogenized in an appropriate amount of reaction buffer using syringe and needle (20 G). The composition of standard enzyme assays is depicted in Table 2.4.

Table 2.4: Composition of standard enzyme assays.

component	assay with ^{3}H-labeled substrate	assay with unlabeled substrate
cell lysate, cell fraction aliquot or zebrafish homogenate in reaction buffer	450 µl	440-445 µl
substrate	0.5 µl*	5-10 µl*
cofactor (5 mg/ml in reaction buffer)	50 µl	50 µl

* Final concentrations were depending on the substrate used.

Reactions were initiated by addition of the appropriate cofactor for the enzymatic reaction of interest ($NAD(P)^+$ for oxidations and $NAD(P)H + H^+$ for reductions). After varying incubation times (from 15 min to 24 h; depending on the amount of input material and the expected conversion) at the appropriate temperature (28 °C for fish enzymes and 37 °C for mammalian enzymes) with shaking, reactions were terminated by addition of 100 µl stop solution. Steroids were extracted from the reaction mixture using solid phase extraction cartridges Strata C18-E, 100 mg/1 ml (Phenomenex), which had been prepared by washing twice with 1 ml methanol and equilibrated with twice 1 ml

water. Samples were then applied to the cartridge and the reaction tubes were washed with 500 µl of water, which was subsequently also applied to the SPE cartridge. Elution was performed with twice 200 µl methanol. In case of analyzing the samples with LC-MS/MS, the eluates were evaporated to dryness using a speed-vac centrifuge (Uniequip, Laborgerätebau Martinsried) at 39 °C, followed by reconstitution with 300 µl methanol. Eluates were stored at -20 °C until measurement (for details on separation and steroid analyses refer to chapter 2.10).

Reaction Buffer	100 mM NaP_i, pH 7.3 1 mM EDTA 0.05 % BSA	
Stop Solution	0.21 M ascorbic acid 1 % acetic acid (v/v)	 in methanol

2.9.2 Determination of steady-state kinetic parameters

Steady-state kinetic parameters were elucidated using HEK293 cells which had been transfected with expression plasmids and harvested as described in chapters 2.2.2 and 2.2.3. The total protein concentration per aliquot was determined by Bradford assay using BSA as standard (see chapter 2.8.3). For enzymatic assays, aliquots containing 60-750 µg total protein were resuspended in 240 µl reaction buffer, substrate was added in different concentrations ranging from 0.04-1.02 µM, and reactions were started by addition of 250 µl cofactor (1 mg/ml in reaction buffer) in a total reaction volume of 500 µl. To monitor steroid conversion, 20 nM tritiated substrate was added to each reaction. Steroids were dissolved in methanol and the methanol concentration in the reaction mixture did not exceed 1 %. Samples in triplicates were incubated at 28 °C with shaking for 15 min and reactions were terminated by addition of 100 µl stop solution. Steroids were extracted as described in the previous section and analyzed with HPLC coupled to a scintillation counter (see 2.10.1). For the calculation of kinetic parameters, initial velocities were determined. Michaelis-Menten kinetics were calculated by non-linear fitting using the Enzyme Kinetics 1.3 add-on for SigmaPlot 12.0 (Systat).

2.9.3 Inhibition analyses

The composition of inhibitor analyses was very similar to the determination of steady-state kinetic parameters. As only zebrafish 20β-HSD type 2 was subjected to inhibition analyses, transfected and harvested HEK293 pellets were resuspended in reaction buffer and 80 µg total protein in 240 µl were used per reaction. Cortisone as substrate for 20β-HSD type 2 was added in final concentrations ranging from 0.04-0.52 µM, while cortisol as inhibitor was used in a final concentration of 1 µM and 2 µM. Steroids were dissolved in methanol and the methanol concentration in the reaction mixture did not exceed 2 %. To monitor cortisone conversion, 20 nM tritiated cortisone was added to each sample. Reactions were performed in triplicates, started by addition of 250 µl cofactor NADPH + H^+ (1 mg/ml in reaction buffer), and incubated with shaking at 28 °C for 15 min. Upon addition of 100 µl stop solution the reactions were terminated and the steroids were purified as described in chapter 2.9.1. Analysis of cortisone conversion was carried out using HPLC coupled to a scintillation counter (see 2.10.1). Initial velocities were determined and obtained data was fitted according to Michaelis-Menten and Lineweaver-Burk using the Enzyme Kinetics 1.3 add-on for SigmaPlot 12.0 (Systat).

2.10 Analytical chemistry

2.10.1 HPLC methods for separation of tritiated steroids

Tritiated steroids were separated using two different HPLC columns with different solvent compositions depending on the steroids of interest to be detected. This approach was necessary since the glucocorticoids analyzed in this work had similar chemical properties and proved difficult to separate from each other.
The HPLC System Gold (BeckmanCoulter) consisted of an autosampler LC 502-E, a 125 Solvent Module, and an UV-VIS detector 166. After mixing the HPLC eluate 1:1 with scintillation cocktail (Ready Flow III), the tritium signals were detected using the scintillation counter LB 506 D (Berthold). The HPLC system was controlled by 32Karat software Version 3.0 (BeckmanCoulter).
Cortisol and cortisone were separated on a reversed phase LUNA 5 µm C18(2) 125 x 4 mm column (Phenomenex) using an isocratic mixture of 57 % water and 43 % methanol at a flow rate of 1 ml/min. Under these conditions, retention times for cortisol and cortisone were 17.4 min and 13.6 min, respectively.
To separate cortisone and 20β-hydroxycortisone by baseline, the Allure Biphenyl column (50 x 2.1 mm, 3 µm, Restek) was used with an isocratic mixture of 23 % acetonitrile and 77 % water at a flow rate of 200 µl/min. Retention times were 18.5 min and 13.6 min for cortisone and 20β-hydroxycortisone, respectively.
The separation of cortisol, cortisone, and 20β-hydroxycortisone in one method was achieved by using the reversed phase LUNA 5 µm C18(2) column with 40 % methanol and 60 % water at a flow rate of 1 ml/min. Under these conditions, cortisol eluted after 21.4 min, cortisone at 17.5 min, and 20β-hydroxycortisone at 15.6 min. Unfortunately, the resolution of cortisone and 20β-hydroxycortisone could not be optimized to full base line separation.
Obtained chromatograms were evaluated regarding substrate conversion by integration of peak areas using 32Karat software.

2.10.2 LC-MS/MS methods for analyses of unlabeled steroids

Unlabeled steroids were separated using different HPLC conditions and detected by mass spectrometry (MS). The HPLC system (Shimadzu) consisted of a controller, two pumps LC-20AB and LC-20AD with adjoined degassers, a column oven CTO-20AC with an integrated 6-way switching valve, and an autosampler SIL-20A. For enrichment of sample and additional purification, an online-Solid Phase Extraction was included in the set-up. Therefore, after application of the sample to the online-SPE column (Oasis HLB, 20 x 2.1 mm, particle size 20 µm, Waters) the valve was switched and the analytes were eluted in back-flush to the analytical column. The analytical column was chosen depending on the desired separation conditions as described below. Steroids eluting from the analytical column were ionized and detected using an API4000 QTrap mass spectrometer (Applied Biosystems) equipped with atmospherical pressure chemical ionization (APCI) source. Details on detection parameters are given below. Control of the LC-MS/MS system and recording of chromatograms was achieved with Analyst 1.5.1 software (Applied Biosystems).

2.10.2.1 Method for product identification

This method was designed to achieve baseline separation of a variety of glucocorticoids to identify the reaction product of 20β-HSD type 2. Therefore, the Allure Biphenyl column (50 x 2.1 mm, 3 µm, Restek) was used as analytical column. 20 µl of sample was loaded onto the online-SPE column with 5 % methanol in water (v/v) at a flow rate of 3 ml/min. After switching the valve, the analytes were eluted in back-flush using 20 % solvent A and 80 % solvent B at a flow rate of 0.4 ml/min. Solvent A consisted of a mixture of 90 % water and 10 % acetonitrile with 0.1 % formic acid (v/v), while

solvent B was composed of 90 % acetonitrile and 10 % water with 0.1 % formic acid (v/v). After 1 min, a gradient of 20 % B to 30 % B in 7 min was applied followed by a wash gradient for cleaning of both columns by increasing the acetonitrile content to 90 %. Details on HPLC chromatography are shown in Table 2.5. The oven temperature was set to 30 °C.

Table 2.5: Description of HPLC program used for product identification.

time (min)	module	event	parameter
0.01	Controller	Start	
0.01	Pumps	Pump B Flow	3 ml
0.01	Pumps	Total A Flow	0.4 ml
0.01	Pumps	Pump A B Conc.	20 % B
1.00	Oven	Right Valve	0
1.00	Pumps	Pump A B Conc.	20 % B
8.00	Pumps	Pump A B Conc.	30 % B
10.00	Pumps	Pump A B Conc.	100 % B
10.00	Oven	Right Valve	1
10.01	Pumps	Pump A B Conc.	100 % B
11.00	Pumps	Pump A B Conc.	100 % B
12.00	Pumps	Pump A B Conc.	20 % B
14.00	Pumps	Pump A B Conc.	20 % B
14.01	Controller	Stop	

The mass spectrometer was equipped with an APCI ion source and set to scan in Enhanced Product Ion Scan (EPI) using positive mode for 14.006 min with 1353 cycles. The source parameters were set as follows: Curtain Gas 10.0 psi, Collision Gas high, Nebulizer Current 3.0 psi, Temperature 600 °C, Ion Source Gas 1 40.0 psi, Declustering Potential 71.0 V, Collision Energy 33.0 V, and Collision Energy Spread 10.0 V. Recorded total ion chromatograms were analyzed regarding steroid retention times and fragmentation patterns underlying peaks of interest.

2.10.2.2 Routine method for detection of four glucocorticoids

In this method, cortisone, cortisol, 20β-hydroxycortisone, and 20α-hydroxycortisone were robustly separated by baseline from each other using reversed phase Synergi Fusion RP18 150 x 3 mm, 4 µm column (Phenomenex) as analytical column. 20 µl of the sample was loaded onto the online-SPE column with 5 % methanol in water (v/v) at a flow rate of 3 ml/min. After switching the valve, the analytes were eluted in back-flush using 28 % acetonitrile and 0.1 % formic acid in water (v/v; solvent A) at a flow rate of 0.45 ml/min to the analytical column and separated under isocratic conditions. Following chromatography, a wash gradient was included to clean both online-SPE and analytical column from residual analytes by increasing the acetonitrile content of running solvent to 80 %. Therefore, solvent B consisting of acetonitrile acidulated with 0.1 % formic acid (v/v) was used. Prior to next sample injection, a pre-equilibration step of 5 min was performed to ensure proper equilibration of the analytical column. Details on HPLC configuration are shown in Table 2.6. The oven temperature was set to 30 °C.

Table 2.6: Description of HPLC program used for routine glucocorticoid analyses.

time (min)	module	event	parameter
0.01	Controller	Start	
0.01	Pumps	Pump B Flow	3 ml
0.01	Pumps	Total A Flow	0.45 ml
0.01	Pumps	Pump A B Conc.	0 % B
1.00	Oven	Right Valve	0
12.00	Pumps	Pump A B Conc.	0 % B
13.00	Pumps	Pump A B Conc.	80 % B
14.00	Pumps	Pump A B Conc.	80 % B
15.00	Pumps	Pump A B Conc.	0 % B
15.00	Oven	Right Valve	1
15.01	Pumps	Pump A B Conc.	0 % B
15.01	Controller	Stop	

The mass spectrometer was equipped with an APCI ion source and set to scan in Multiple Reaction Monitoring (MRM) positive mode for 15.005 min with 1936 cycles. The source parameters were set as follows: Curtain Gas 20.0 psi, Collision Gas 5 psi, Nebulizer Current 3.0 psi, Temperature 600 °C, Ion Source Gas 1 40.0 psi, Entrance Potential 10.0 V, and Collision Energy 33.0 V. Detected mass transitions are shown in Table 2.7.

Table 2.7: Parameters for Multiple Reaction Monitoring.

analyte	Q1 mass (Da)	Q3 mass (Da)	Declustering Potential (V)	Collision Energy Spread (V)
cortisone	361.210	163.2	76.0	10.0
cortisol	363.224	121.1	86.0	6.0
20α/20β-hydroxycortisone*	363.200	163.2	80.0	8.0

* Isomers were distinguished by different retention times.

As this method was not optimized for absolute quantification, obtained chromatograms were evaluated regarding signal intensities of each analyte. Frequent injections of standard substances were performed to monitor similar sensitivity throughout the sequential sample analyses.

2.11 Bioinformatic methods

2.11.1 Sequence comparisons and BLAST analyses

To evaluate obtained sequences from wet-lab for accuracy, they were compared to *in silico* constructed reference sequences. For construction of reference sequences and comparison by alignments, the software VectorNTI (Invitrogen) was used. Sequence variants were clarified by inspecting raw sequencing data in BioEdit [121]. Variants were analyzed using different BLAST algorithms and different databases at NCBI (http://blast.ncbi.nlm.nih.gov/), whether they were naturally occurring polymorphisms.
For identification of novel 20β-HSD type 2 candidates in different species, two alternative approaches were applied. One method used the tblastn algorithm at NCBI searching expressed sequence tags, nucleotide collection, and NCBI genomes databases. The other method retrieved related sequences from the BLink link at zebrafish 20β-HSD type 2 entry (CAM14225). Obtained candidates were

carefully chosen according to the quality of alignment with the query sequence and strongly truncated sequences were removed from further analyses.

2.11.2 Alignments and phylogenetic analyses

The direct comparison of protein or DNA sequences to determine their identities was performed using the Alignment Tool ClustalW2 (http://www.ebi.ac.uk/Tools/msa/clustalw2/). In this program, penalty gaps, word size, and substitution matrix were kept at default values.
Phylogenetic analyses were used in this work not only for determination of evolutionary relationships, but also for evaluation of enzyme family affiliations for novel candidate sequences. Since 20β-HSD type 2 enzymes are closely related to 17β-HSD types 3 and 12, simple sequence alignment was not sufficient to reveal family memberships and phylogenetic analyses were therefore recommended. To this end, a multiple alignment of a set of sequences was achieved using Blosum matrix and calculation of phylogenetic trees was conducted with the MEGA v4.1 software [122] applying the Neighbor-Joining (NJ) method. For test of inferred phylogeny a bootstrapping with 1000 replications was performed. The obtained tree was critically inspected for redundant and truncated sequences, which were removed from the analyses. Afterwards, the tree was routed to a distantly related group.

2.12 Materials, equipment, programs

2.12.1 Antibodies

Primary antibodies	Final dilution	Provider
Anti c-Myc 9B11, mouse monoclonal IgG2α	1:200	Cell Signaling
Anti c-Myc 9E10, mouse monoclonal IgG1κ	1:500 (Western Blot); 1:1000 (Immunochemistry)	Roche
Anti actin (20-33), rabbit IgG	1:500	SigmaAldrich
Anti c-Myc 9E10, mouse monoclonal IgG1, FITC-coupled	1:1000	SigmaAldrich
Anti Digoxygenin-AP, sheep polyclonal Fab fragments	1:5000	Roche
Anti-GST 3-4C, mouse monoclonal IgG2bκ	1:8000	Zymed

Secondary antibodies	Final dilution	Provider
HRP-conjugated goat anti mouse IgG + IgM (H+L)	1:8000	Dianova
HRP-conjugated goat anti rabbit IgG	1:5000	Sigma Aldrich
Goat anti mouse IRDye800CW	1:20000	Li-Cor
Goat anti rabbit IRDye680	1:20000	Li-Cor
Goat anti mouse IgG AlexaFluor 488	1:2000	Molecular Probes

2.12.2 Bacteria strains

Escherichia coli DH5α (Life Technologies)
F' φ80d*lac*ZΔM15 Δ(*lac*ZYA-*arg*F)U169 *deo*R *rec*A1 *end*A1 *hsd*R17(rk^-, mk^+) *pho*A *sup*E44 λ^- *thi*-1 *gyr*A96 *rel*A1
Escherichia coli TOP10 (Invitrogen)
F^- *mcr*A (*mrr-hsd*RMS-*mcr*BC) φ80*lac*ZΔM15 Δ*lac*X74 *rec*A1 *ara*D139 Δ(*ara-leu*)7697 *gal*U *gal*K *rps*L (Str^R) *end*A1 *nup*G
Escherichia coli Rosetta 2 (DE3) pLysS (Novagen)
F^- *omp*T *hsd*S_B(r_B^- rn_B^-) *gal dcm* (DE3) pLysSRARE2 (Cam^R)

2.12.3 Cell lines

COS-1 (African green monkey kidney)	ATCC (CRL-1650)
HEK293 (human embryonic kidney)	ATCC (CRL-1573)
HeLa (human cervix carcinoma)	DSMZ (ACC57)

2.12.4 Chemicals, media, and steroids

11-Dehydrocorticosterone	SigmaAldrich
11-Ketotestosterone (4-Androsten-17β-ol-3,11-dione)	SigmaAldrich
1-Phenyl-2-thiourea (PITC)	SigmaAldrich
20α-Hydroxycortisone (4-Pregnen-17,20α,21-triol-3,11-dione)	Steraloids
20β-Hydroxycortisone (4-Pregnen-17,20β,21-triol-3,11-dione)	Steraloids
4-Nitroblue tetrazolium chloride (NBT)	Merck
5-Bromo-4-chloro-3-indolyl phosphate (BCIP)	Merck
5α-Pregnanediol (5α-Pregnan-17,21-diol-3,11,20-trione)	Steraloids
5β-Pregnanediol (5β-Pregnan-17,21-diol-3,11,20-dione)	Steraloids
Acetic acid	Fluka
Acrylamid/bisacrylamid (37.5:1)	Roth
Agarose	Bio&Sell
Aldosterone	SigmaAldrich
Ammonium peroxodisulfate (APS)	Merck
Ampicillin	SigmaAldrich
Ampuwa water	Fresenius Kabi
Aqua Poly/Mount	Polysciences
Bacto agar	Difco
BACTO Pepton	Difco
Boric acid	Merck
Bovine serum albumin	Roth
Bradford Reagent (BioRad Protein Assay)	BioRad
Bromophenol blue	Biomol
Calcium sulfate ($CaSO_4$)	SigmaAldrich
Chloramphenicol	SigmaAldrich
Chloroform (pro analysi)	Merck
Coomassie Brilliant Blue G250	Biomol
Corticosterone	SigmaAldrich
Cortisol (hydrocortisone)	SigmaAldrich
Cortisol-21-glucuronide (4-Pregnen-11β,17,21-triol-3,20-dione-21-glucosiduronate)	Steraloids
Cortisone	SigmaAldrich

Cortisone-21-sulfate sodium salt (4-Pregnen-17,21-diol-3,11,20-trione 21 sulfate, sodium salt)	Steraloids
Dimethyl sulfoxide (DMSO, pro analysi)	Roth
Dimethylformamide (DMF, pro analysi)	Merck
Disodium hydrogen phosphate (Na_2HPO_4)	Merck
dNTP mixture	Fermentas
Dulbecco's Modified Eagle Medium (DMEM)	PAA Laboratories
Estradiol	SigmaAldrich
Ethanol (pro analysi)	Merck
Ethidiume bromide	SigmaAldrich
Ethylenediaminetetraacetate (EDTA)	Merck
Fetal bovine serum (FBS)	GibcoBRL
Ficoll 400	Pharmacia
Formamide	SigmaAldrich
FuGENE 6 transfection reagent	Roche
Gelatine	SigmaAldrich
Glycine	Biomol
Heparin	SigmaAldrich
Hoechst 33342	Invitrogen
Kanamycin	SigmaAldrich
Magnesium chloride ($MgCl_2$)	Roth
Methanol (gradient grade)	Merck
Methylcellulose	Roth
Minimum Essential Medium (MEM)	PAA Laboratories
Monosodium phosphate (NaH_2PO_4)	Merck
N,N,N',N'-Tetramethylethylenediamine (TEMED)	SigmaAldrich
Normal goat serum	SigmaAldrich
Paraformaldehyde (PFA)	SigmaAldrich
Penicillin/Streptomycin	Invitrogen
Power SYBR Green PCR Mastermix	Applied Biosystems
Progesterone	SigmaAldrich
Proteinase inhibitor cocktail tablets	Roche
Proteinase K	SigmaAldrich
RNAlater	Qiagen
RNaseOUT recombinant RNase inhibitor	Invitrogen
Sea salt	Instant Ocean
Silanized glass wool	Fluka
Sodium bicarbonate ($NaHCO_3$)	Merck
Sodium chloride (NaCl)	Merck
Sodium dodecylsulfate (SDS)	Merck
Sucrose	Merck
Tricine	Roth
Tris	Roth
Trisodium citrate (Na_3 citrate)	Merck
Triton X-100	SigmaAldrich
TRIzol reagent	Invitrogen
Tween-20	SigmaAldrich
VectaShield Mounting Medium	VectorLabs
X-tremeGENE 9 DNA Transfection Reagent	Roche
X-tremeGENE HP DNA Transfection Reagent	Roche
Xylene cyanol	Serva
Yeast extract	Nordwald
Yeast tRNA	SigmaAldrich

2.12.5 Enzymes

*Bam*H I	Fermentas
Endonuclease (Benzonase)	SigmaAldrich
Kpn I	Fermentas
Lysozyme	Merck
Not I	Fermentas
Pfx polymerase	Invitrogen
T4 DNA ligase	Fermentas
Taq polymerase	lab-made
Trypsine-EDTA	Gibco-BRL
Xba I	Fermentas
β-Glucuronidase, from *E. coli*, highly purified	SigmaAldrich
β-Glucuronidase, Type 2, from *Helix pomatia*, crude extract (sulfatase)	SigmaAldrich

2.12.6 Kits

BigDye Terminator v3.1 Cycle Sequencing Kit	Applied Biosystems
DIG RNA Labeling Kit	Roche
Dual-Luciferase Reporter Assay System	Promega
Gateway BP Clonase Enzyme Mix	Invitrogen
Gateway LR Clonase Enzyme Mix	Invitrogen
Montage Seq_{96} Sequencing Reaction Clean-Up Kit	Millipore
NucleoBond PC100	Macherey-Nagel
NucleoSpin Plasmid Kit	Macherey-Nagel
PCR Purification Kit	SeqLab
QIAquick PCR Purification Kit	Qiagen
RevertAid First Strand cDNA Synthesis Kit	Fermentas
RNeasy Mini Kit	Qiagen
TOPO-TA Cloning Kit	Invitrogen
Western Lightning Chemiluminescence Reagent Plus	PerkinElmer
Wizard SV PCR and Gel Clean-Up Kit	Promega

2.12.7 Other material

Immobilon FL PVDF membrane	Millipore
Ready Flow III scintillation cocktail	BeckmanCoulter
Strata C18-E, 100 mg/1 ml	Phenomenex
Strata C18-E, 200 mg/6 ml	Phenomenex

2.12.8 Steroids labeled with radionuclides

Cortisone, [1,2-^{3}H(N)] (37 MBq, 60 Ci/mmol)	American Radiolabeled Chemicals
Hydrocortisone, [1,2,6,7-^{3}H(N)] (9.25 MBq, 50 Ci/mmol)	Perkin Elmer

2.12.9 Plasmids

pDONR201	Invitrogen	entry vector (Gateway Cloning System)
pCSII	Invitrogen	TOPO-TA cloning vector
pGEM 3 Zf+	Promega	vector for subcloning
pDsRed2-ER	Clontech	Expression of a marker for endoplasmic reticulum
pCS2+_zGRα	M. J. M. Schaaf (University Leiden, Netherlands) [25]	Expression plasmid coding for zebrafish glucocorticoid receptor isoform α
pMMTV-*luc*	M. J. M. Schaaf (University Leiden, Netherlands) [25]	Containing four glucocorticoid response elements in the promoter (mouse mammary tumor virus promoter) in front of firefly luciferase gene
pGL4.74[*hRluc*/TK]	Promega	Constitutive expression of renilla luciferase (*Renilla reniformes*)
pCS2+_zfMR	GeneArt	Subcloning of zfMR_pUC57 (gene synthesis by GeneScript) into pCS2+ vector to obtain expression plasmid coding for zebrafish mineralocorticoid receptor
pBluescript SK+	Stratagene	Vector allowing for *in vitro* RNA synthesis
pDEST-530	J. Glöckner (IHG)	Modified destination vector (Gateway Cloning System) for mammalian expression; includes C-terminal myc tag
pcDNA3myc/DEST	J. Glöckner (IHG)	Modified destination vector (Gateway Cloning System) for mammalian expression; includes N-terminal myc tag
pDNR-Lib_Blu_Testis_7_D09	M. Hoffmann (MPI Tübingen, Germany)	vector containing open reading frame of *Poecilia reticulata* 20β-HSD type 2 gene
pT7T3D-Pac I_tcbk0068 c.21	D. Esquerré (INRA France)	vector containing open reading frame of *Oncorhynchus mykiss* 20β-HSD type 2 gene
pcDNA3.1 V5-His TOPO_tilapia 17β-HSD type 12	L. Zhou (NIBB, Japan)	vector containing open reading frame of *Oreochromis niloticus* 20β-HSD type 2 gene
pcDNA4/*myc*-His B_zf11β-HSD2	F. Haller (IEG)	expression plasmid coding for zebrafish 11β-HSD type 2
pcDNA4/*myc*-His B_zf11β-HSD3	F. Haller (IEG)	expression plasmid coding for zebrafish 11β-HSD type 3

2.12.10 Equipment

ABI 3730 DNA Analyzer	Applied Biosystems
Allure Biphenyl column 50 x 2.1 mm, 3 µm	Restek
API4000 Qtrap	Applied Biosystems
BioVision gel documentation system	PeqLab
CBM-20A controller	Shimadzu
Cryostat CM1950	Leica
CTO-20AC column oven	Shimadzu
DGU-20A3 degasser	Shimadzu
DGU-20A5 degasser	Shimadzu
FCV-12AH switching valve	Shimadzu
Fusion FX7	VilberLourmat
GloMax Multi Detection System	Promega
HPLC Radioactivity Monitor LB 506 D	Berthold
LC 502-E autosampler	BeckmanCoulter
LC-20AB liquid chromatograph	Shimadzu
LC-20AD liquid chromatograph	Shimadzu
LUNA 5 µm C18(2) 125 x 4 mm column	Phenomenex
Mini PROTEAN IV electrophoresis cell	BioRad
Mini PROTEAN III electrophoresis cell	BioRad
NanoDrop ND-1000 spectrophotometer	PeqLab
Optima MAX Ultracentrifuge	Beckman Coulter
RoboCycler 96 PCR machine	Stratagene
SIL-20AC autosampler	Shimadzu
Synergi Fusion RP18 150 x 3 mm, 4 µm	Phenomenex
System Gold 125 Solvent Module	BeckmanCoulter
System Gold 166 Detector	BeckmanCoulter
TaqMan 7900HT cycler	Applied Biosystems
TLA-55 rotor	Beckman Coulter
Trans-Blot SD - Semi Dry Transfer Cell	BioRad
Ultra-Turrax T8	IKA Labortechnik
Uniequip speed-vac	Laborgerätebau Martinsried
UV/Vis spectrophotometer DU530	Beckman Coulter
Visiprep 24DL vacuum manifold	Supelco

2.12.11 Programs

32Karat	BeckmanCoulter
Analyst 1.5.1	Applied Biosystems
AxioVision Rel. 4.6	Zeiss
Bio-1D	VilberLourmat
BioEdit	http://www.mbio.ncsu.edu/bioedit/bioedit.html
BioVision	PeqLab
BLAST algorithms	http://blast.ncbi.nlm.nih.gov/
ClustalW2	http://www.ebi.ac.uk/Tools/msa/clustalw2/
Fusion	VilberLourmat
ImageJ	http://rsbweb.nih.gov/ij/index.html
MEGA v4.1	htpp://megasoftware.net
ND-1000 V3.1.0	PeqLab
Primer3	http://biotools.umassmed.edu/bioapps/primer3_www.cgi
SDS2.3	Applied Biosystems
SigmaPlot 12.0	Systat Software
VectorNTI	Invitrogen

3 Results

The aim of this work was to achieve the functional characterization, annotation, and elucidation of the biological role of a novel member of the SDR enzyme family. Therefore, several diverse methods ranging from bioinformatics, biochemistry, molecular biology, and analytical chemistry to functional genetics were applied. To ensure clarity and coherence, this section was divided into subchapters comprising rather experimental questions than reflecting methodical considerations. Despite this approach it was not always possible to address questions raised in one chapter in the subsequent one.
The novel member of the SDR enzyme family from zebrafish named zf3.2 was identified in 2004. Mindnich *et al*. [103] demonstrated a close relationship of zf3.2 to 17β-HSD type 3 and 17β-HSD type 12 and a conserved exon structure of all three genes with only minor differences in the zf3.2 gene. Analysis of expression revealed a ubiquitous expression pattern of zf3.2 in adult tissues and during embryonic development. The authors designated this enzyme to be a putative steroid dehydrogenase, which was further characterized in my diploma thesis. Subcellular localization analyses revealed zf3.2 to be a protein of the endoplasmic reticulum (ER). Several bioinformatic prediction tools identified a transmembrane helix at the N-terminus of zf3.2 and an ER retention motif at the C-terminus suggesting zf3.2 to feature a signal-anchor sequence leading to a type I orientation in the membrane of the ER. In a screen for enzymatic activity using substrates from all classes of steroids and few retinoids, zf3.2 catalyzed solely the conversion of cortisone to an unknown product [115].

3.1 Identification of the reaction product and annotation of zf3.2 as 20β-HSD type 2

Prior to identification of the reaction product, theoretical considerations were carried out to determine possible products. The enzyme zf3.2 catalyzed a $NADPH + H^+$ dependent reduction of cortisone, which would allow for reduction at positions C3, C5, C11, and C20 of the molecule. Including stereoisomers, a total of seven substances were putative products. Unfortunately, C3-hydroxylated isomers were not commercially available. Therefore, only five substances were compared to the unknown reaction product regarding their retention time and mass fragmentation pattern using a LC-MS/MS method. The separation conditions applied resulted in different retention times for the references 5α-pregnanediol and 5β-pregnanediol compared to the product of the enzymatic conversion of cortisone. In addition, cortisol showed a different retention time as well (data not shown). Thus, the enzyme did neither catalyze the reduction of the C4-C5 double bond in cortisone nor the reduction of the carbonyl group at position C11. However, comparison of the reaction product to C20 reduced steroids, namely 20α-hydroxycortisone (4-pregnen-17α,20α,21-triol-3,11-dione) and 20β-hydroxycortisone (4-pregnen-17α,20β,21-triol-3,11-dione), revealed that the reaction product eluted at a retention time equivalent to that of 20β-hydroxycortisone (Figure 3.1). Moreover, the fragmentation pattern of 20β-hydroxycortisone was identical with the pattern obtained from the unknown product (Figure 3.1). These results demonstrated that the novel enzyme catalyzes a reduction reaction at position C20 on the steroid backbone of cortisone leading to 20β-hydroxycortisone. Accordingly, zf3.2 was annotated 20β-HSD. As this enzyme did not show homology to earlier characterized carbonyl reductase-like 20β-HSDs (20β-HSD/CR), the affix type 2 was added to the enzyme's name.

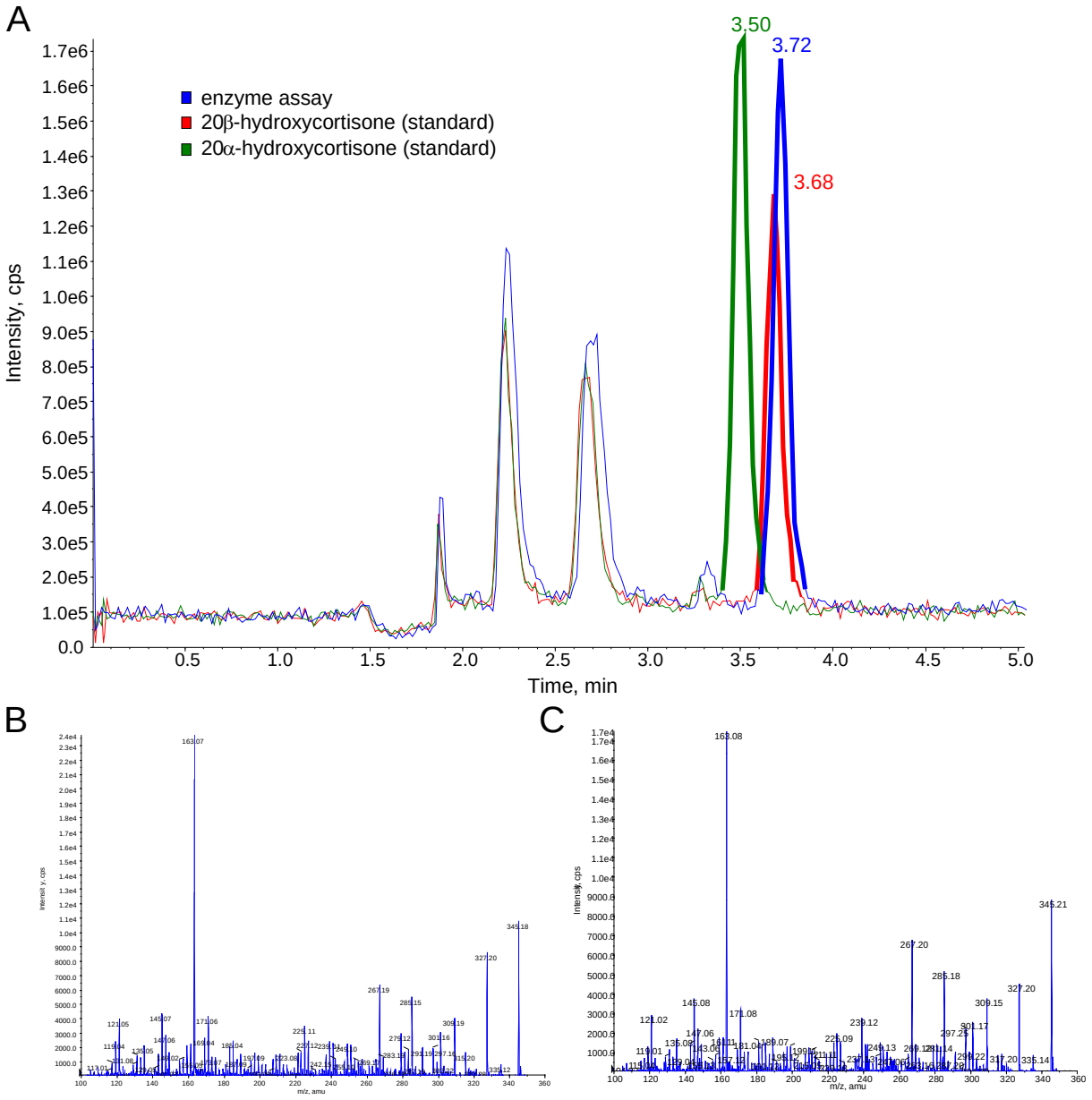

Figure 3.1: The reaction product of zf3.2 is 20β-hydroxycortisone. Using cortisone as substrate the product was identified by LC-MS/MS as 20β-hydroxycortisone upon identical retention time and mass fragmentation pattern with a standard substance. (A) Total ion chromatograms of the product (blue) derived from the enzymatic conversion of cortisone, compared to reference steroids 20β-hydroxycortisone (red) and 20α-hydroxycortisone (green). (B) MS/MS spectrum of enzyme product peak at retention time 3.72 min. (C) MS/MS spectrum of 20β-hydroxycortisone peak at retention time 3.68 min. cps, counts per second.

3.2 Biochemical characterization of zebrafish 20β-HSD type 2 and its orthologs from other species

Although the close relationship of zebrafish 20β-HSD type 2 to 17β-HSD types 3 and 12 led to its identification [103], this fact also entailed difficulties on identification of orthologs from other species based alone on sequence similarity searches. Therefore, careful phylogenetic analyses were necessary to ensure a precise assignment of each candidate sequence to one of the enzyme families. Several searches for candidate sequences of zebrafish 20β-HSD type 2 orthologs in other species conducted in 2008 resulted in a set of six 20β-HSD type 2 candidates from teleost fish (rainbow trout, tilapia, and

guppy), frog, and two mammals (cow, and sheep) (Figure 3.2). Despite thorough investigation of databases, no orthologs in human or rodents could be found. The separation of the 20β-HSD type 2 group from 17β-HSD type 3 and type 12 groups was supported by high bootstrap values. The tilapia sequence clustering with zebrafish 20β-HSD type 2 was earlier annotated as 17β-HSD type 12 [107]. However, analysis of amino acid similarity revealed higher similarity to zebrafish 20β-HSD type 2 (57 %) than to zebrafish 17β-HSD type 12a and b (42 % and 43 %, respectively), indicating that tilapia 17β-HSD type 12 might belong functionally to the group of 20β-HSD type 2 enzymes.

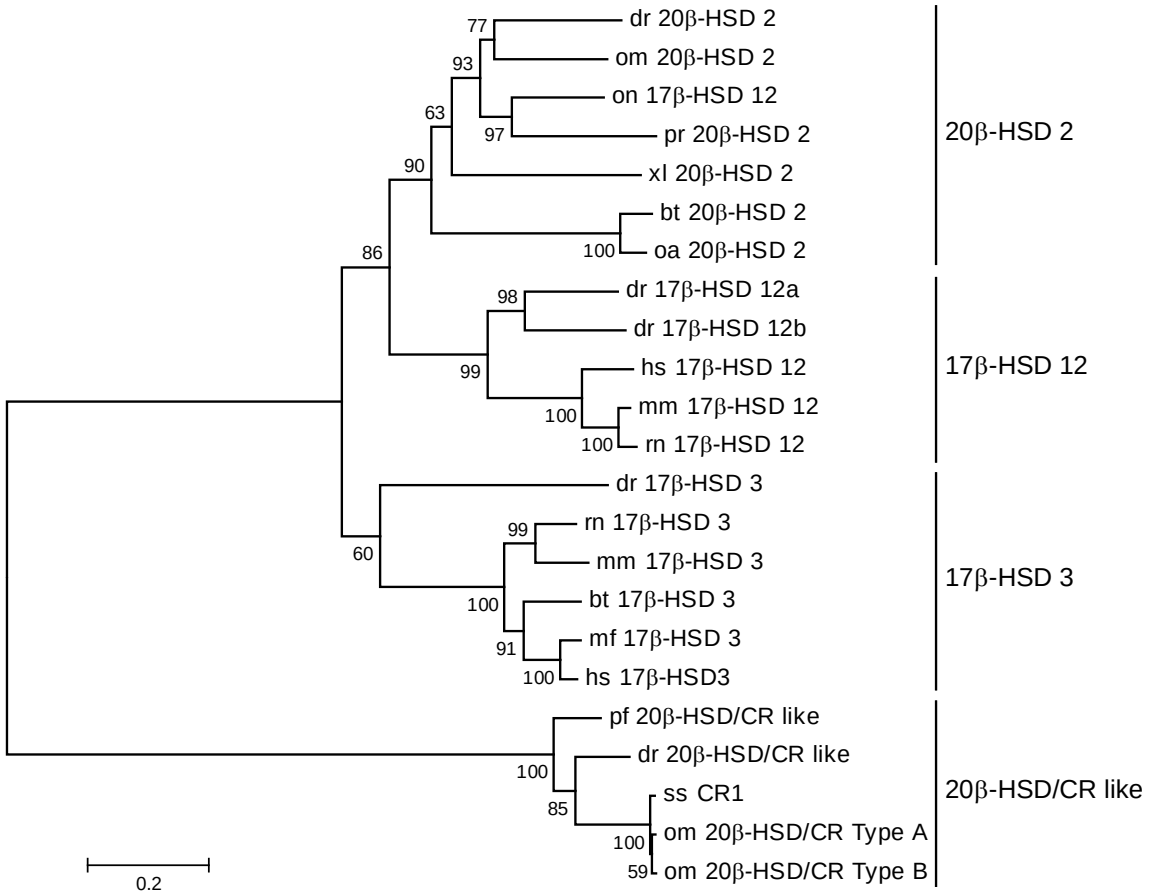

Figure 3.2: Phylogenetic analysis identifies putative zebrafish 20β-HSD type 2 orthologs from other species. 20β-HSD type 2 enzymes show high similarity to 17β-HSD type 3 and type 12 enzymes, while 20β-HSD/carbonylreductases cluster together in a separate group. The tree was calculated by means of Neighbor-Joining with bootstrap values out of 1000 pseudoreplicates, given in percent at each dichotomy. Species abbreviations: bt, *Bos taurus*; dr, *Danio rerio*; hs, *Homo sapies*; mf, *Macaca fascicularis*; mm, *Mus musculus*; oa, *Ovis aries*; om, *Oncorhynchus mykiss*; on, *Oreochromis niloticus*; pf, *Pelteobagrus fulvidraco*; pr, *Poecilia reticulata*; rn, *Rattus norvecigus*; ss, *Salmo salar*; xl, *Xenopus laevis*.

Teleost candidate sequences were cloned from plasmids and mammalian candidate sequences were cloned from cDNA, while the frog candidate was not available and therefore excluded from further functional analysis. All obtained open reading frames were subcloned into modified pcDNA-DEST plasmids resulting in N-terminal and C-terminal myc-tagged constructs. Analyses of subcellular localization detected all candidate proteins in the endoplasmic reticulum. Figure 3.3 depicts the representative result for zebrafish 20β-HSD type 2, while Pearson's coefficients of colocalization with the ER are shown for all candidates. The N- or C-terminal position of the myc tag had no influence on the distribution of the candidate enzyme, with the only exception of the sheep candidate. In this case, the correlation coefficient of colocalization with the ER using a C-terminal tag was significantly lower compared to the N-terminal tag.

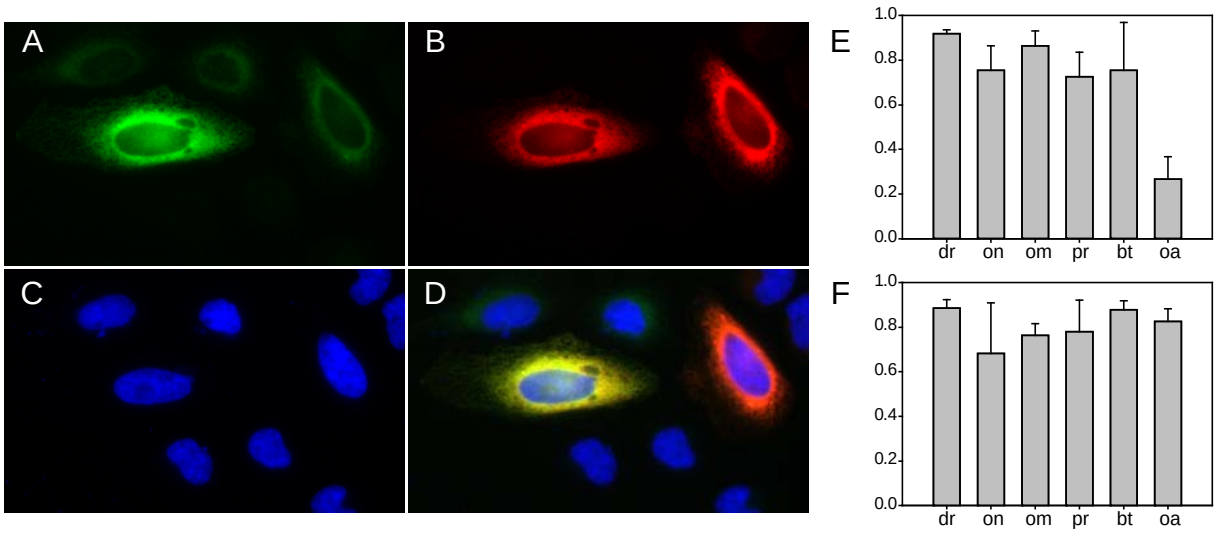

Figure 3.3: Analyses of subcellular localization find all 20β-HSD type 2 enzymes in the endoplasmic reticulum. (A-D) These panels depict the result for zebrafish 20β-HSD type 2. (A) Detection of 20β-HSD type 2 with anti-myc FITC-labeled antibody. (B) Counterstaining of the endoplasmic reticulum with DsRed. (C) Counterstaining of the nuclei with Hoechst 33342. (D) Overlay of fluorescence patterns from panels A-C. (E) Pearson's correlation coefficients for colocalization of C-terminal tagged 20β-HSD type 2 enzymes with the ER. (F) Pearson's correlation coefficients for colocalization of N-terminal tagged 20β-HSD type 2 enzymes with the ER. Species abbreviations in (E) and (F): dr, *Danio rerio*; on, *Oreochromis niloticus*; om, *Oncorhynchus mykiss*; pr, *Poecilia reticulata*; bt, *Bos taurus*; oa, *Ovis aries*.

To investigate whether the orthologs from other species were able to catalyze the same reaction as zebrafish 20β-HSD type 2, enzyme activity assays using transiently transfected HEK293 cells were performed. All orthologous enzymes, except the cow protein, catalyzed the reduction of cortisone to 20β-hydroxycortisone (data not shown). The cow protein was totally enzymatically inactive in the applied assay conditions. Prior to further enzymatic characterization, the pH optimum was determined for zebrafish 20β-HSD type 2 activity. This enzyme was found to display highest cortisone conversion in a pH range of 7.0 to 8.5 (data not shown). Subsequent determination of kinetic parameters at pH 7.3 revealed that zebrafish 20β-HSD type 2 showed the lowest K_M and highest v_{max} value towards cortisone compared to the other teleost orthologs (Table 3.1).The low catalytic activities of sheep and guppy 20β-HSD type 2 did not allow for evaluation of kinetic parameters.

Table 3.1: Kinetic constants of 20β-HSDs type 2.

20β-HSD type 2	apparent K_M (μM)	apparent v_{max} (nmol min^{-1} mg^{-1} total protein)	v_{max}/K_M
guppy	n.d.	n.d.	n.d.
rainbow trout	0.454 ± 0.112	0.007 ± 0.001	0.015
sheep	n.d.	n.d.	n.d.
tilapia	0.214 ± 0.032	0.011 ± 0.001	0.051
zebrafish	0.142 ± 0.037	0.064 ± 0.006	0.451

Parameters for teleost 20β-HSD type 2 were determined at 28 °C. n.d., not determined due to low activity.

Although zebrafish 20β-HSD type 2 catalyzed cortisone reduction efficiently after recombinant expression in mammalian cells, a method for verification of the same activity in zebrafish embryos was developed. Therefore, embryo homogenates were incubated with cortisone in the presence and absence of cofactor NADPH + H^+. Formation of 20β-hydroxycortisone was observed in homogenates incubated with cortisone and cofactor, while no product was detected in control assays without cofactor (Table 3.2). These experiments clearly indicate endogenous 20β-HSD type 2 activity in zebrafish.

Table 3.2: Conversion of cortisone to 20β-hydroxycortisone in zebrafish embryo homogenates.

stage	20β-hydroxycortisone formation (% conversion)	
	+ NADPH + H^+	- NADPH + H^+
24 hpf	31.5 ± 1.2	0
48 hpf	48.9 ± 4.3	0
72 hpf	42.8 ± 5.3	0

Homogenates were prepared from 20 embryos and incubated for 4 h at 28 °C.

3.3 Expression analyses of zebrafish 20β-HSD type 2

Although the expression pattern of zebrafish 20β-HSD type 2 in embryonic development and in adult tissues of both sexes was already a part of an earlier work [103], an attempt to expand this knowledge was made by including more developmental stages and additional tissues into the expression analyses. Instead of sensitive qPCR, RT-PCR was chosen due to tissue sample limitations. RT-PCR analyses found 20β-HSD type 2 to be expressed in every adult tissue analyzed with strongest signals in liver, kidney, gonads, intestine, and gills (Figure 3.4). Only minor differences in expression level between the sexes were observed. 20β-HSD type 2 was expressed also throughout the whole embryonic development. Its mRNA was already detectable as early as in the 1 cell stage, indicating a maternal supply of 20β-HSD type 2 mRNA to the zygote. After onset of embryonic transcription (between 512 and 1000 cell stage), the amount of 20β-HSD type 2 mRNA increased until tailbud stage, decreased during the onset of somitogenesis, and remained on a constant level after 24 hpf.

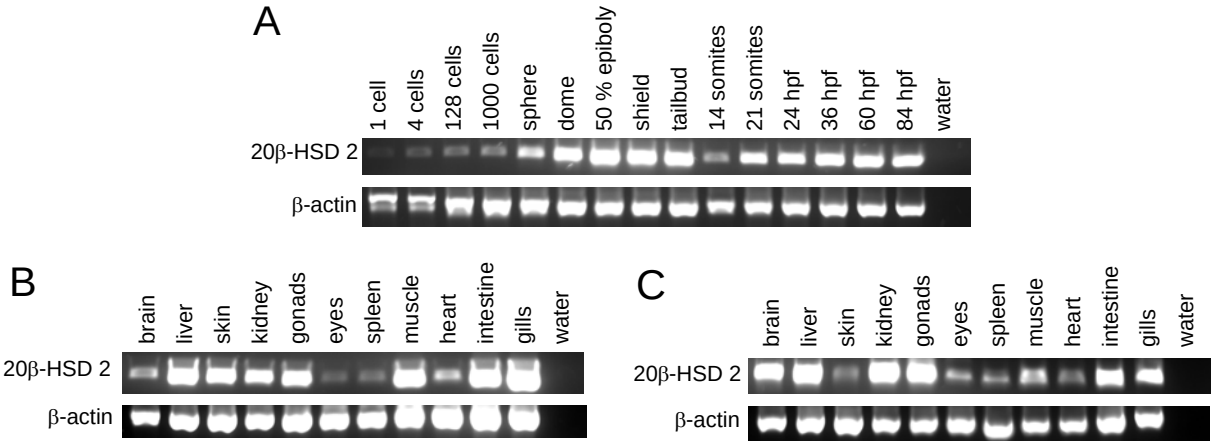

Figure 3.4: Expression pattern of zebrafish 20β-HSD type 2 is ubiquitous in adult tissues and starts at 1 cell stage in embryonic development. Gel photographs show the observed distribution of RT-PCR signals for 20β-HSD type 2 and β-actin, which was included for normalization. (A) Zebrafish development. (B) Adult female tissues. (C) Adult male tissues. hpf, hours post fertilization.

For analysis of the spatial expression pattern of 20β-HSD type 2 during embryonic development, whole mount *in situ* hybridization was performed. Zebrafish embryos at the 3 somites stage displayed widespread expression of 20β-HSD type 2 with no spatial restriction (data not shown). In later stages a broad distribution of 20β-HSD type 2 expression was observed, displaying a distinct pattern with stronger signals in certain tissues. For precise determination of tissues expressing 20β-HSD type 2, the embryos were sectioned transversally and each section carefully analyzed for 20β-HSD type 2 signals. In 30 hpf embryos, expression was detected in brain, eye, lens, intestine, liver, and pronephric ducts (Figure 3.5 B, B1-B3). In the brain, signals were more intensive where ventricles ended and different parts of the brain adjoined to each other. 20β-HSD type 2 expression in 48 hpf embryos was additionally observed in the inner ear, heart, pharynx, pharyngeal arches, and the pectoral fins. In this

stage, staining of the pronephric ducts was more intensive in the posterior parts of the organ (Figure 3.5 D3). 3 dpf larvae displayed staining in brain, eye, lens, inner ear, pharyngeal arches, pharynx, intestine, liver, and pronephric ducts. Intestinal cells showed stronger 20β-HSD type 2 expression in the apical pole of the cells (Figure 3.5 F2 and F3). The pronephric ducts displayed weaker staining at this stage, but the signal intensity increased in posterior direction. In addition to the tissues with 20β-HSD type 2 expression in 3 dpf larvae, signals were detected in pancreas and neuromasts in 4 dpf larvae. At this stage, the staining of the intestine was stronger in the caudal region than in the anterior part of the organ. Pharyngeal arches develop into gills, while neuromasts are small sensory patches along the side of the fish developing into the lateral line. 20β-HSD type 2 showed strong expression in the brain in all stages analyzed displaying no restriction to certain parts. However, starting with 48 hpf expression of 20β-HSD type 2 in the brain was restricted to the grey matter containing neuron cell bodies, while no expression was observed in myelinated nerve fibers, the white matter (Figure 3.5 D1, F1, and H1). Certain tissues showed invariably no 20β-HSD type 2 expression, e.g., somitic muscle or notochord.

3.4 Steroid-dependent regulation of 20β-HSD type 2

3.4.1 Influence of cortisol on zebrafish 20β-HSD type 2

To determine if 20β-HSD type 2 expression is regulated by cortisol, zebrafish embryos were treated with different concentrations of cortisol ranging from 10 mg/l to 100 mg/l. During cortisol treatment, zebrafish embryos were constantly monitored for viability and developmental changes. Zebrafish embryos treated with 10 mg/l cortisol exhibited no phenotypical changes compared to control embryos. However, with increasing cortisol concentrations, the mortality rate increased as well as phenotypical changes of surviving fish embryos occurred. These fish larvae showed developmental abnormalities manifesting at 48 hpf and intensifying until 72 hpf. Beside alterations in size and shape of the yolk sac and yolk sac extension, altered somitogenesis leading to kinked or truncated tails and pericardial edema were observed. Some specimens additionally showed blood pooling in the yolk sac extension. These morphological alterations have already been described as linked to cortisol [44]. While wild-type zebrafish embryos hatch between 48 hpf and 72 hpf, cortisol treated embryos showed delayed hatching. Embryos treated with 100 mg/l cortisol did not hatch until 72 hpf (data not shown).
The effect of cortisol on 20β-HSD type 2 expression was analyzed on mRNA level by qPCR and on enzymatic activity level by activity assays. Expression analysis by qPCR revealed a strong up-regulation of 20β-HSD type 2 upon cortisol treatment in all stages (Figure 3.6). In 24 hpf embryos, a two- to eight-fold induction was detected, while in 48 hpf embryos the transcript of 20β-HSD type 2 was induced up to 18-fold after treatment with 100 mg/l cortisol. The up-regulation remained four- to six-fold in 72 hpf larvae. In the cortisol concentration range used no dosage dependency of 20β-HSD type 2 up-regulation was observed.
Strikingly, the enzymatic activity of 20β-HSD type 2 was negatively correlated with the mRNA level (Figure 3.6). Starting with 25 mg/l cortisol in all developmental stages analyzed, a marked decrease in cortisone conversion was observed. The reduction of 20β-HSD type 2 activity was not as pronounced in 10 mg/l treated fish embryos. This discrepancy of cortisol-induced reduction of 20β-HSD type 2 activity despite strong up-regulation on mRNA level will be the focus of chapters 3.5 and 3.6.

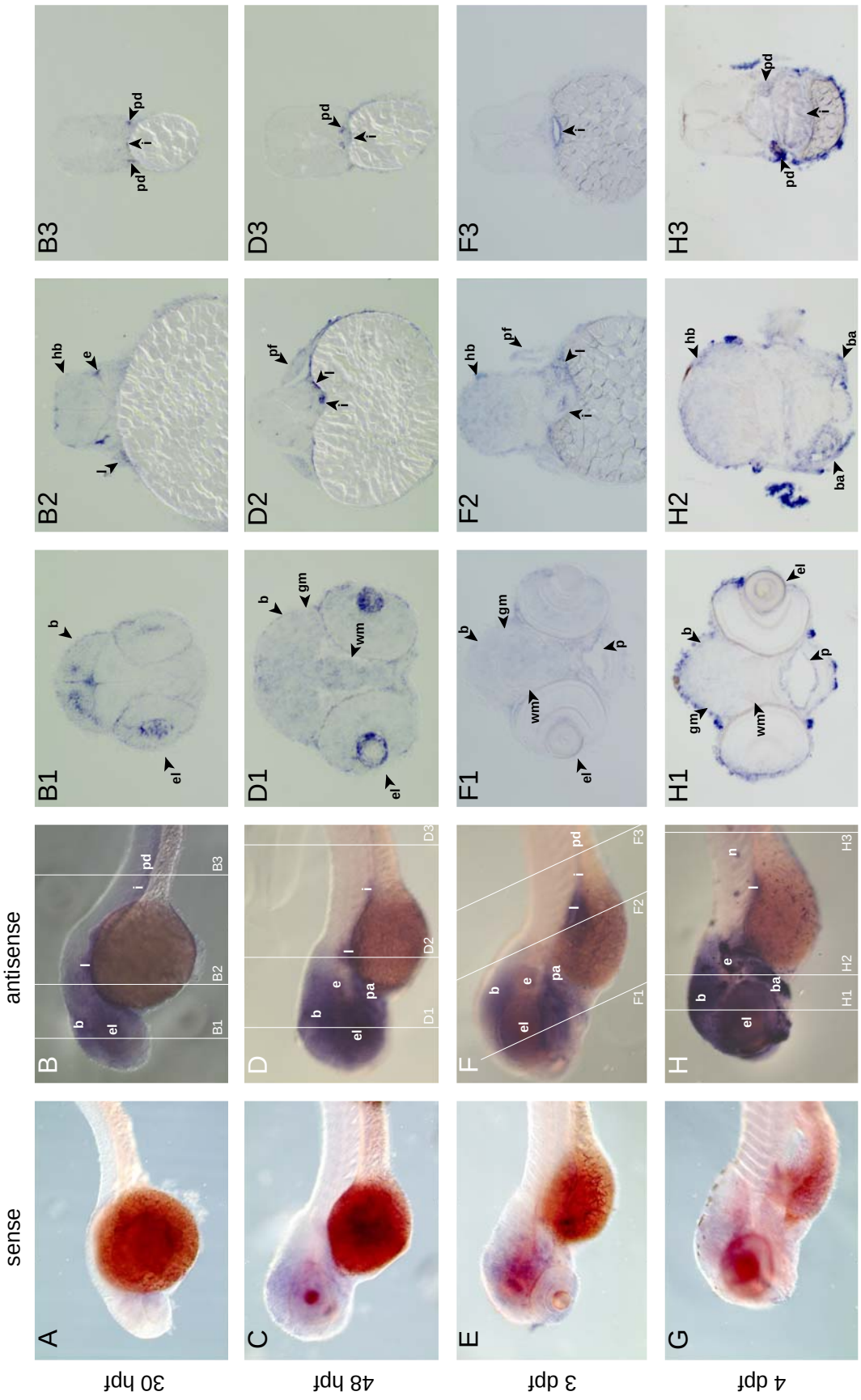

Figure 3.5: Whole mount *in situ* hybridization show distinct expression of 20β-HSD type 2 during zebrafish development.
For detailed legend refer to page 51.

Figure 3.5 (see page 50): Whole mount *in situ* hybridization show distinct expression of 20β-HSD type 2 during zebrafish development. In 30 hpf embryos (B and B1-B3), expression is observed in brain, eye, ear, intestine, liver, and pronephric ducts. In 48 hpf (D and D1-D3) and 3 dpf larvae (F and F1-F3), signals are detected in all parts of brain, eye, intestine, liver, pronephric ducts, and branchial arches. 4 dpf larvae (H and H1-H3) show expression in brain, eye, ear, pharyngeal arches, intestine, liver, pronephric ducts, and neuromasts. Specific hybridization is indicated by blue color. Control hybridizations with sense probe are shown for all stages (30 hpf (A), 48 hpf (C), 3 dpf (E), and 4 dpf (G)). Locations of transversal sections in each stage are indicated by white lines in panels B, D, F, and H, and labeled accordingly. Abbreviations: hpf, hours post fertilization; dpf, days post fertilization; b, brain; ba, branchial arches; e, ear; el, eye and lens; gm, grey matter; hb, hindbrain; i, intestine; l, liver; n, neuromasts; p, pharynx; pa, pharyngeal arches; pd, pronephric ducts; pf, pectoral fin; wm, white matter. Magnification: 5x for A-H, 10x for B1-B3, D1-D3, F1-F3, and H1-H3.

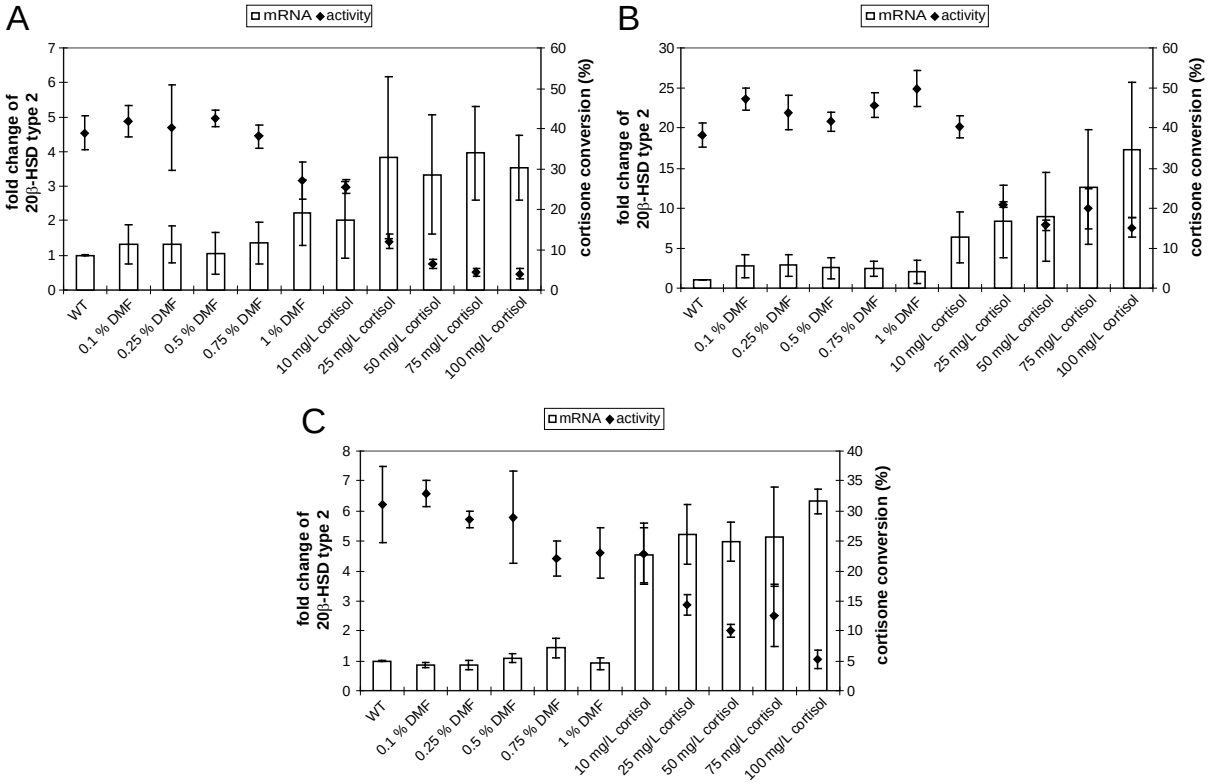

Figure 3.6: Cortisol treatment induces 20β-HSD type 2 expression, but leads to a decrease in enzymatic activity. In each panel, the treatment regimen is shown on the x-axis, while the fold change of 20β-HSD type 2 mRNA amount is shown on the primary y-axis and the cortisone conversion is displayed on the secondary y-axis. 0.1 % DMF is the vehicle control for 10 mg/l cortisol, 0.25 % DMF for 25 mg/l cortisol, and so on. Results for 24 hpf embryos (A), 48 hpf embryos (B) and 72 hpf larvae (C) are shown. Fold changes were calculated after normalization to β-actin and compared to untreated fish embryos (WT). For determination of enzymatic activity, equal numbers of embryos were used.

To determine if cortisol did not only increase the amount of 20β-HSD type 2 mRNA but also influence the spatial expression in embryos, whole mount *in situ* hybridizations were performed. For this purpose, zebrafish embryos were treated with 10 mg/l cortisol and fixed for *in situ* hybridizations at 30 hpf, 48 hpf, 3 dpf, and 4 dpf. Untreated and DMF treated fish embryos showed 20β-HSD type 2 expression in the same tissues as described in detail in the previous chapter. Also, cortisol treated embryos showed no differences in spatial expression of 20β-HSD type 2, but markedly increased signals (Figure 3.7).

Figure 3.7: Whole mount *in situ* hybridization of cortisol treated zebrafish embryos show intensified signals of 20β-HSD type 2 expression in all stages. Control hybridizations for all stages are shown in the first row, followed by antisense hybridization of wild-type fish embryos in the second row. The third row displays 0.1 % DMF treated fish embryos, while the specimens in the fourth row were treated with 10 mg/l cortisol. For each stage and condition a picture showing the anterior and posterior part of the fish embryo is displayed. hpf, hours post fertilization; dpf, days post fertilization. Magnification: 5x.

The impact of cortisol treatment in early zebrafish development was analyzed by short-term exposure of embryos to 50 mg/l cortisol. Embryos were treated with cortisol until 24 hpf and kept afterwards in plain embryo water until 72 hpf. As observed in the long-term exposure, the mortality increased in the cortisol treated group compared to controls until 24 hpf. However, despite the application of cortisol in a concentration that was found to induce morphological abnormalities, the short-term exposed embryos did not develop the above described phenotype at 48 hpf. Additionally, the hatching behavior was not changed compared to untreated controls (data not shown).
Quantification of 20β-HSD type 2 mRNA in short-term cortisol exposed embryos revealed in 24 hpf embryos a two-fold induction of the transcript (Figure 3.8 A), which was slightly lower than in the long-term cortisol challenge experiment (Figure 3.6 A). Regarding the enzymatic activity of 20β-HSD type 2, a similar reduction was observed as before. 48 hpf embryos (24 hours post cortisol treatment) displayed a strong up-regulation of 20β-HSD type 2 transcript (approximately eight-fold) and the enzymatic activity was fully restored and slightly higher than in control embryos. In 72 hpf embryos (48 hours post cortisol treatment), the amount of 20β-HSD type 2 transcript decreased to normal level, while the enzymatic activity was still slightly elevated (Figure 3.8).

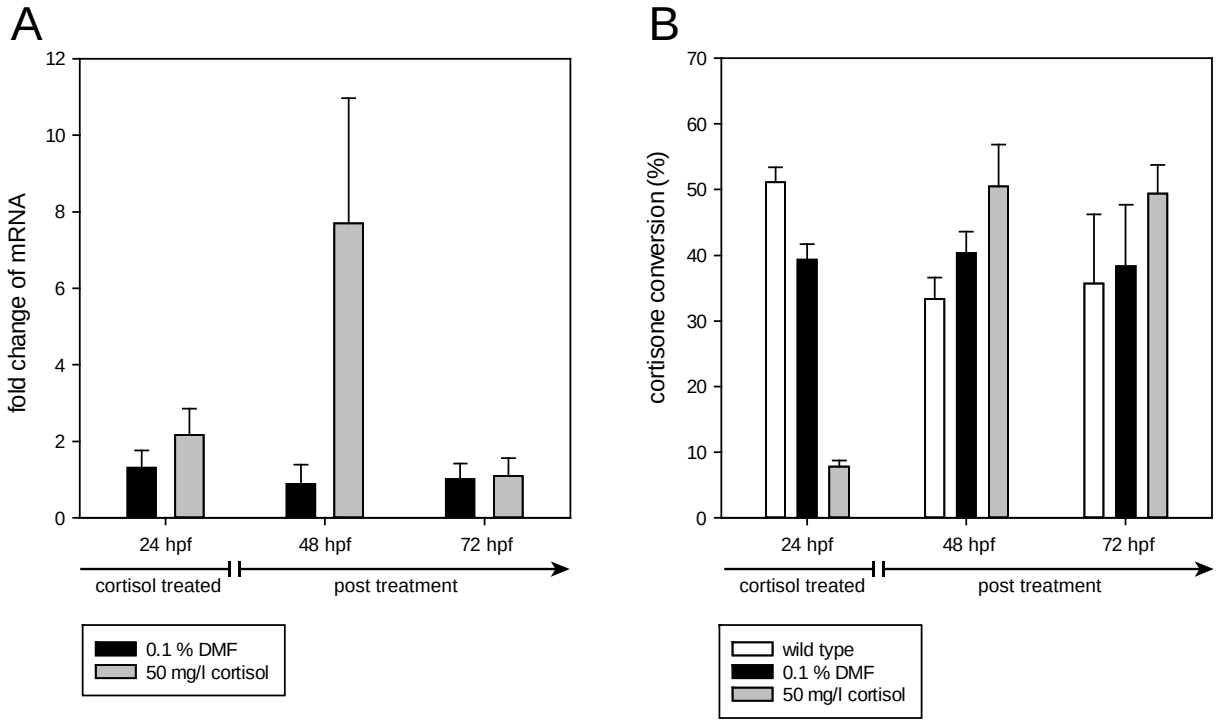

Figure 3.8: Short-term exposure of zebrafish embryos to cortisol results in up-regulation of 20β-HSD type 2 expression in 24 hpf and 48 hpf embryos, while 20β-HSD type 2 activity decreases in 24 hpf embryos, but increases in 48 hpf embryos. Zebrafish embryos were treated until 24 hpf with 50 mg/l cortisol and afterwards kept in cortisol-free embryo water. (A) Fold change of 20β-HSD type 2 mRNA expression was calculated after normalization to β-actin and compared to untreated fish embryos. (B) 20β-HSD type 2 activity was assessed by analyzing the conversion of cortisone to 20β-hydroxycortisone in each treatment group. hpf, hours post fertilization.

3.4.2 Effects of other steroids on 20β-HSD type 2 expression

Since cortisol was found to induce 20β-HSD type 2 expression markedly, the effects of compounds from other steroidal classes on the regulation of 20β-HSD type 2 expression were elucidated. The class of corticosteroids was represented by corticosterone and progesterone, while for androgens and estrogens the respective active steroid hormones were chosen, namely 11-ketotestosterone and estradiol, respectively. According to the cortisol challenge experiments, corticosterone was applied at concentrations of 10 mg/l and 25 mg/l. However, for progesterone, 11-ketotestosterone, and estradiol the concentrations had to be reduced, because these steroids are not as soluble in water as corticosterone or cortisol. During the experiments, embryos were constantly monitored for viability and developmental abnormalities.

Corticosterone treated fish embryos showed no morphological abnormalities in all stages, displayed no increased mortality, and showed similar behavior in response to touching stimuli as wild-type fish embryos (data not shown). Treatment with 10 mg/l corticosterone yielded a two- to three-fold induction of 20β-HSD type 2 expression in all stages analyzed, while 25 mg/l resulted in two- to five-fold up-regulation with its maximum in 72 hpf fish larvae (Figure 3.9).

Fish embryos treated with progesterone showed no developmental changes at 24 hpf, but moved less in their chorions compared to control embryos. At 48 hpf, no increased mortality was observed, although the zebrafish embryos displayed slightly enlarged heart cavities, less pigmentation, delayed hatching, and slower movement upon a touching stimulus. The delayed hatching was even more prominent at 72 hpf accompanied with a significantly increased mortality rate. Most embryos showed enlarged heart cavities with blood pools, yolk deformations, and responded after a touching stimulus only with tremor instead of swimming away (data not shown). Despite these phenotypical observations, progesterone was found to have no significant influence on 20β-HSD type 2 expression (Figure 3.9).

Not only progesterone treatment induced developmental abnormalities, but also estradiol application to zebrafish embryos. While embryos treated with 1 mg/l estradiol developed and behaved like control embryos, specimen treated with 5 mg/l estradiol showed severe malformations already at 24 hpf. The embryos had significantly smaller brains and eyes and were not totally lucent, but appeared ‘milky’ in the head region. At 48 hpf, the phenotype intensified and was characterized by yolk deformations (the yolk sac extension was thick and short), altered somitogenesis resulting in kinked tails, pericardial lesions, reduced pigmentation, and significantly smaller brains, which were partially not lucent. In general, embryos treated with 5 mg/l estradiol showed a delayed development. At 72 hpf the embryos had hardly further developed from 48 hpf and appeared totally deformed. Additionally, they displayed very weak pigmentation, large pericardial edema, and a thick and shortened yolk sac extension. Embryos did not hatch and showed no reaction to touching stimuli, although the heart beat demonstrated viability (data not shown). The severe phenotypical changes were accompanied by only slight induction of 20β-HSD type 2 expression in 24 hpf embryos. However, in older embryos the transcript amount was found to be reduced compared to control embryos (Figure 3.9).

Treatment of zebrafish embryos with the active androgen 11-ketotestosterone entailed no morphological changes in all stages. Treated embryos only hatched earlier and swam faster after touching stimulus than control embryos (data not shown). The hormone induced no significant changes in 20β-HSD type 2 expression (Figure 3.9).

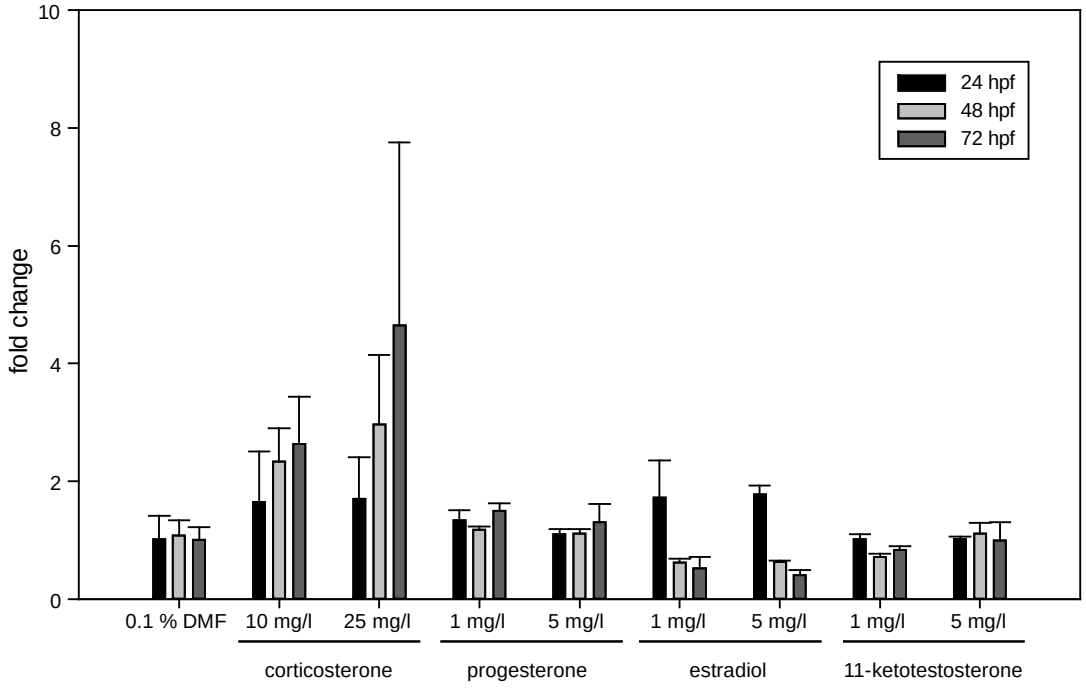

Figure 3.9: Analysis of regulation of 20β-HSD type 2 expression after treatment with different steroids shows induction by corticosterone. Fold changes of 20β-HSD type 2 mRNA amounts were calculated after normalization to β-actin (or rpl8 in case of estradiol) and compared to untreated fish embryos. Steroids used for treatment were corticosterone, progesterone, estradiol, and 11-ketotestosterone. The concentrations applied are given on the x-axis. Controls with 0.1 % DMF were run separately for each experiment. hpf, hours post fertilization.

3.5 Analysis of 20β-HSD type 2 inhibition by cortisol

Cortisol treatment of zebrafish embryos resulted in the observation of a strong up-regulation of 20β-HSD type 2 on mRNA level accompanied with a marked decrease in enzymatic activity. Short-term exposure to cortisol yielded up-regulation of mRNA and activity reduction in the presence of cortisol, but restored enzymatic activity 24 hours after cortisol removal from the medium (see chapter 3.4.1). These results indicated rather an inhibited enzyme than differences between regulation of mRNA and protein (and the activity of the protein). Therefore, inhibition analyses were carried out with 20β-HSD type 2 recombinantly expressed in HEK293 cells. Initial experiments demonstrated that 20β-HSD type 2 is neither inhibited by its substrate cortisone nor its product 20β-hydroxycortisone (data not shown). However, when cortisol was added to the reaction in final concentrations of 1 µM or 2 µM, an inhibition of 20β-HSD type 2 was observed. Lineweaver-Burk analysis revealed that addition of cortisol left v_{max} of 20β-HSD type 2 unchanged, while its K_M value was increased with increasing concentration of cortisol (Table 3.3, Figure 3.10). This result demonstrated that cortisol acts as competitive inhibitor of 20β-HSD type 2 with a K_I of 1.2 µM.

Table 3.3: Kinetic constants of zebrafish 20β-HSD type 2 with and without inhibition by cortisol.

additive	apparent K_M (µM)	apparent v_{max} (nmol min^{-1} mg^{-1} total protein)
none	0.128 ± 0.009	0.023 ± 0.001
1 µM cortisol	0.284 ± 0.047	0.025 ± 0.002
2 µM cortisol	0.357 ± 0.090	0.024 ± 0.003

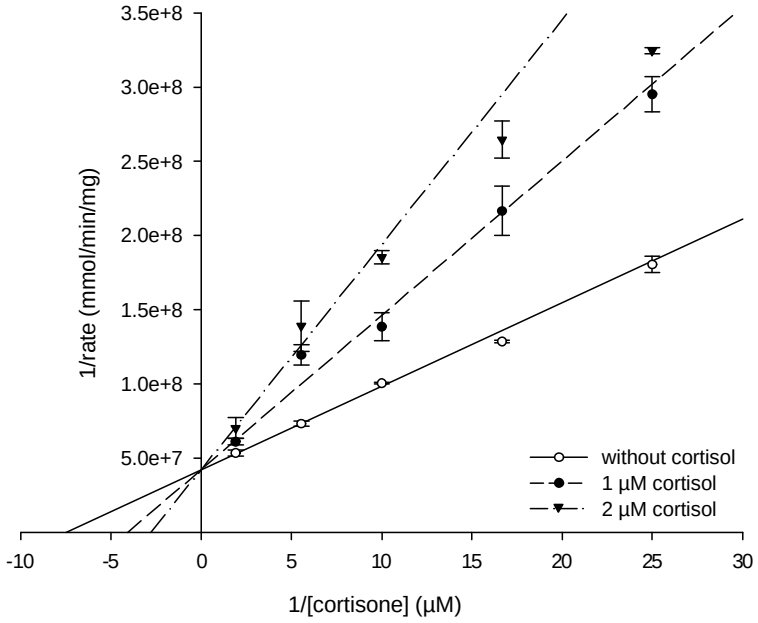

Figure 3.10: Kinetic analysis in presence of cortisol reveals that cortisol acts as competitive inhibitor of 20β-HSD type 2. Lineweaver-Burk analysis of kinetic data in the presence of 1 µM and 2 µM cortisol demonstrated an unchanged v_{max} value but an increased K_M value indicating competitive inhibition. Data were corrected for background of transiently transfected HEK293 cells.

3.6 Development of a polyclonal antibody against zebrafish 20β-HSD type 2

The results of cortisol treated fish embryos showed a striking discrepancy between 20β-HSD type 2 mRNA levels and activity and raised the question how the protein level itself was influenced by cortisol. For this purpose, a specific antibody recognizing zebrafish 20β-HSD type 2 was needed. The design of the antigen (a peptide), the production of this peptide and the immunization of three rabbits for production of polyclonal 20β-HSD type 2 antibodies was carried out by Pineda Antikörper Service, Berlin.

3.6.1 Design of a peptide used for immunization

A polyclonal antibody against zebrafish 20β-HSD type 2 could have been produced by immunizing rabbits with either purified 20β-HSD type 2 or a peptide derived from the protein. Zebrafish 20β-HSD type 2 is an integral membrane protein of the endoplasmic reticulum. Thus, it was not attempted to purify the protein, since the probability to obtain pure 20β-HSD type 2 for immunization was estimated to be low. Instead, a suitable peptide was chosen as antigen. To this end, thorough epitope analysis of the 20β-HSD type 2 sequence was performed by Pineda Antikörper Service. Since it is of importance that the epitope is located on the surface and not hidden in the core of the protein, a surface profile regarding hydrophobicity and accessibility was first generated. Predictions of potential sites for glycosylation and phosphorylation were also taken into account. Additionally, the sequence of 20β-HSD type 2 was searched for regions containing many charged amino acid residues, which are known to be responsible for a high binding strength between antigen and antibody (avidity). Taking all these predictions together, Pineda Antikörper Service proposed four potential peptides for immunization. However, analyses of cross-reactivity excluded three peptides, because they showed high identity with zebrafish 17β-HSD type 3, type 12a, and type 12b (Table 3.4). Thus, only the peptide zf-4 of zebrafish 20β-HSD type 2 was chosen for production of polyclonal antibodies in rabbits.

Table 3.4: Maximum identity of peptide sequence with candidate protein.

peptide	20β-HSD type 2	17β-HSD type 3	17β-HSD type 12a	17β-HSD type 12b
zf-1	100 %	66 %	72 %	78 %
zf-2	100 %	47 %	42 %	47 %
zf-3	100 %	30 %	35 %	35 %
zf-4	100 %	0 %	21 %	11 %

Prior to immunization, Pineda Antikörper Service provided pre-immune sera derived from six rabbits. These sera were evaluated in Western Blot analysis including protein samples from zebrafish embryos and HEK293 cells expressing zebrafish 20β-HSD type 2 (data not shown). The results were used to choose three animals showing only little unspecific signals especially in the range of 30-50 kDa (the estimated molecular weight of 20β-HSD type 2 is 37 kDa). The peptide zf-4 was synthesized and coupled to keyhole limpet haemocyanin (KLH) as carrier. Pineda Antikörper Service followed their standard protocol for immunization and provided immune sera starting with day 61 of the immunization protocol for testing in the desired application. If the results in the desired application were not satisfying, Pineda Antikörper Service elongated the immunization protocol with repeated boosts on request. For zebrafish 20β-HSD type 2 polyclonal antibody, immune sera were collected at day 61, 90, 120, 150 and 180, and the animals were finally bled at day 200. At this stage, the determination of the best suited antiserum had proceeded, and some immune sera were chosen for affinity purification. To this end, Pineda Antikörper Service used the antigen for extraction of the monospecific IgG fraction from immune sera from all animals at immunization days 120 and 150.

3.6.2 Determination of the antiserum with best antigen recognition

To find the antiserum that produces best signals in the desired application (Western Blot), zebrafish 20β-HSD type 2 was recombinantly expressed in *E. coli*. In this expression system, 20β-HSD type 2 was fused to glutathione S-transferase (GST) increasing the theoretical molecular weight to ~ 63 kDa but allowing for detection with a GST antibody as control. Although the enzyme showed no activity after bacterial expression (data not shown), it was expressed in high amounts and was therefore a suitable starting material for characterization of immune sera.
E. coli lysates were fractionated into soluble and insoluble proteins. In SDS-PAGE, protein samples with and without GST-20β-HSD type 2 were separated on 8 % gels. Pre-immune sera, immune sera, and blocked immune sera from each animal were used for detection. All immune sera were diluted 1:1000 and in case of blocked immune sera pre-adsorbed with 20 µg/ml peptide zf-4. In blocked immune sera, the polyclonal antibody against zebrafish 20β-HSD type 2 is saturated with its antigen zf-4 peptide and therefore does not bind to its antigen on the membrane.
Despite usage of old protein samples resulting in poor protein resolution, the results in Figure 3.11 show that the immune sera derived from all three rabbits at day 150 specifically recognized zebrafish 20β-HSD type 2 overexpressed in *E. coli*. The control Western Blot using anti-GST antibody showed that GST-20β-HSD type 2 appeared at ~ 45 kDa and therefore lower than the expected ~ 63 kDa. Pre-immune sera from all animals contained already antibodies recognizing different endogenous *E. coli* proteins. However, immune sera (day 150) from all rabbits gave specific signals for 20β-HSD type 2. Specificity was proven by blocking solely these bands after addition of the antigen zf-4. Although all immune sera recognized 20β-HSD type 2, differences between the animals could be observed. Rabbit #1 and #2 gave signals with higher intensity than rabbit #3, which was reflected in an elongated exposition time of the blot for rabbit #3. For further development of the polyclonal antibody against zebrafish 20β-HSD type 2, rabbit #2 was chosen, since the serum of this animal displayed most intense signals.

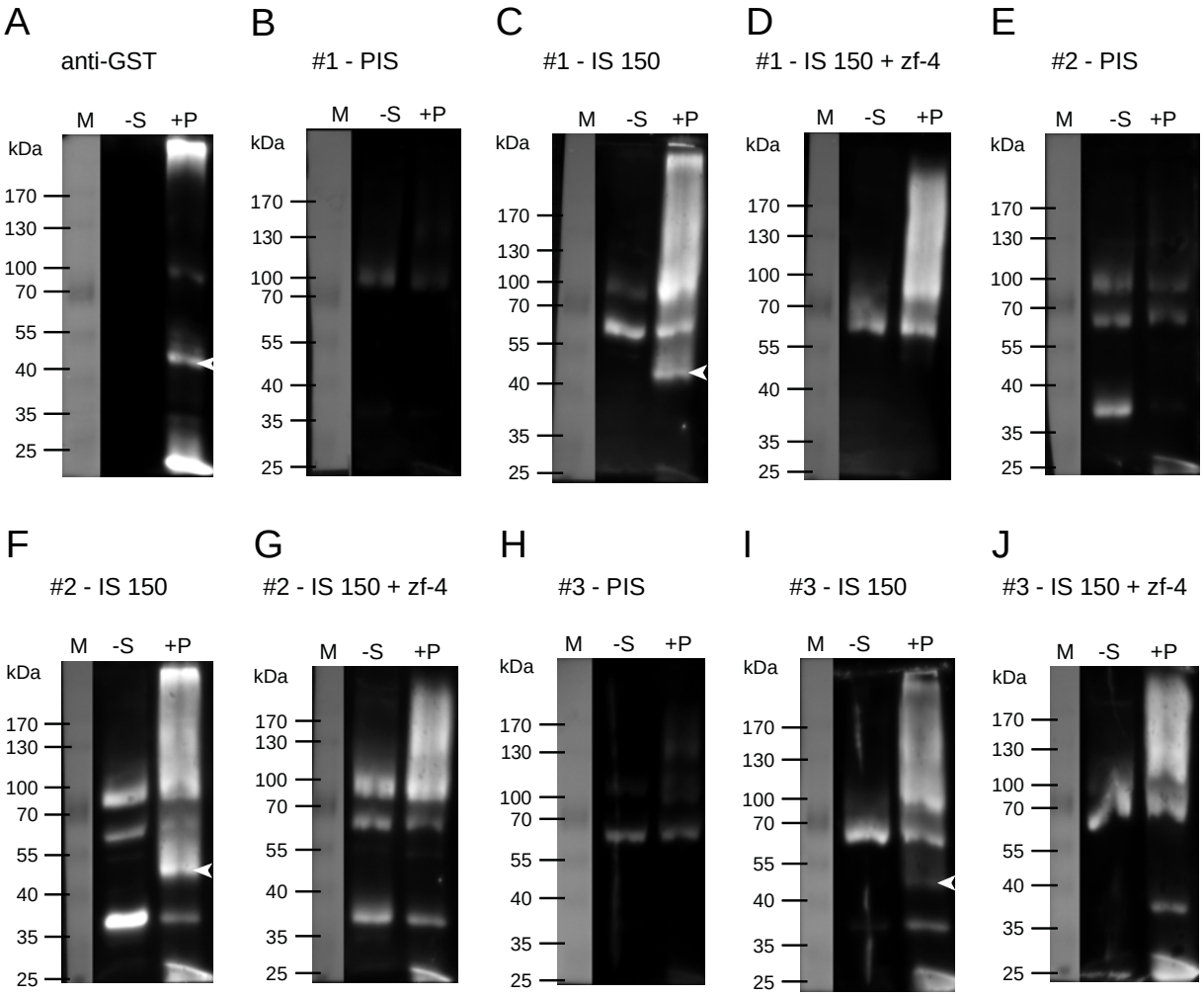

Figure 3.11: Western Blot analysis reveals that polyclonal antibodies from three rabbits recognize zebrafish 20β-HSD type 2 expressed in *E. coli*. 5 µg of each fraction were separated on 8 % SDS gels alongside molecular weight marker. Western Blots were developed using chemiluminescence and the signals detected with Fusion FX7 applying different exposition times (2.5 min for A and H-J; 1 min for B-G). The signals for 20β-HSD type 2 are marked by white arrowheads. Western Blot using anti-GST antibody as positive control (A), sera from rabbit #1 (B-D), rabbit #2 (E-G), and rabbit #3 (H-J) are shown. Abbreviations: PIS, pre-immune serum; IS 150, immune serum from day 150; IS 150 + zf-4, immune serum from day 150 blocked with 20 µg/ml zf-4 peptide; M, molecular weight marker; -S, not induced soluble proteins; +P, induced insoluble proteins.

3.6.3 Optimization of Western Blot procedures using rabbit #2 immune serum

The next step of optimization of Western Blot conditions with the polyclonal antibody produced in rabbit #2 against zebrafish 20β-HSD type 2 was to determine if the antibody recognizes 20β-HSD type 2 expressed in a mammalian system, namely HEK293 cells. HEK293 cells were transiently transfected with zebrafish 20β-HSD type 2 and zebrafish 11β-HSD type 2 as negative control. Both enzymes were expressed as fusion proteins with a myc tag, which was used in Western Blots to verify the expression. First experiments were carried out with total cell lysates and unpurified immune serum and resulted in detection of specific, but weak signals (data not shown). To increase signal intensity, it was decided to switch to affinity purified immune serum and to enrich 20β-HSD type 2 in cell lysates by fractionation using differential centrifugation. The two-step centrifugation protocol (first 700 x g followed by 55000 x g) proved sufficient for enrichment of 20β-HSD type 2 in the 700 x g pellet (data not shown).

Pineda Antikörper Service recommended using the affinity purified serum in a dilution of 1:10, but this dilution was found to cause a lot of unspecific background. Therefore, a dilution series was performed to determine the optimal concentration of the affinity purified serum from day 150. Using the 700 x g pellet of cells transfected with 20β-HSD type 2 and 11β-HSD type 2 as negative control, the dilution series revealed good 20β-HSD type 2 detection with the purified antibody diluted 1:150. Additionally, detection of unspecific bands decreased and the background signals were reduced (Figure 3.12). Despite a theoretical molecular mass of approximately 41 kDa, the apparent protein size was found to be significantly smaller than 40 kDa. This discrepancy was also observed using a myc antibody (data not shown).

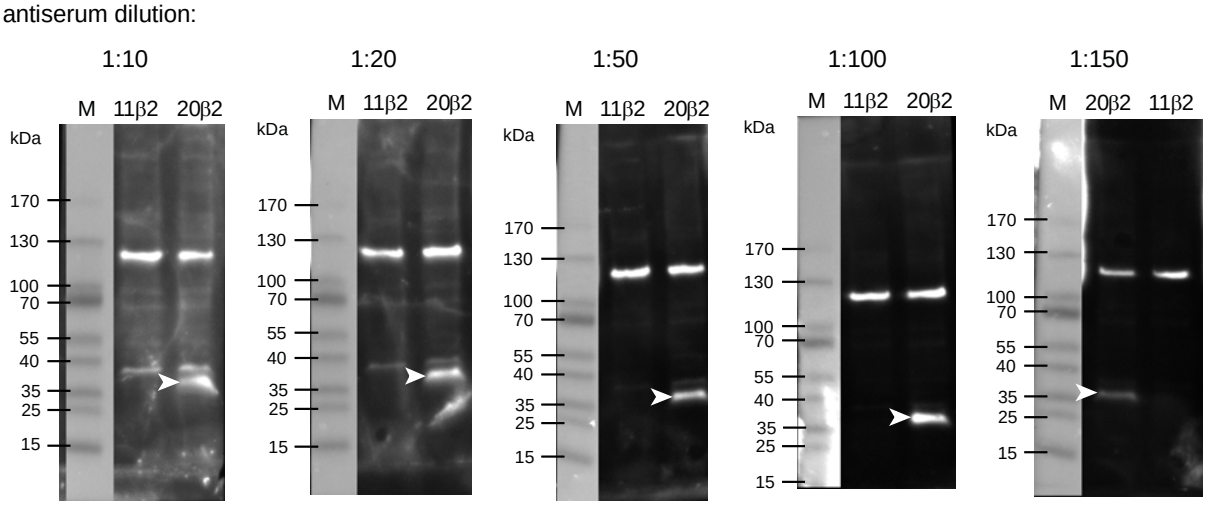

Figure 3.12: Western Blot experiments for optimization of affinity purified serum dilution demonstrate good detection and low background with a dilution of 1:150. 15 µg protein of the 700 x g pellets were separated on 4-15 % gels alongside molecular weight marker. Western Blots were developed using chemiluminescence and the signals detected with Fusion FX7 (exposition time 10 min). The signals for 20β-HSD type 2 are marked by white arrowheads. Affinity purified immune serum from day 150 from rabbit #2 was used in different dilutions as indicated. Abbreviations: M, molecular weight marker, 11β2, 11β-HSD type 2 in HEK293 cells; 20β2, 20β-HSD type 2 in HEK293 cells.

For discrimination of unspecific from specific signals two approaches were available. Firstly, a sample containing the desired protein was compared to a similar sample without the protein of interest. With recombinant expression systems, this goal can be easily achieved. In *E. coli*, induced samples were compared to samples taken prior to induction of expression, while in cell culture target and non-target constructs were transfected (see Figure 3.11 and Figure 3.12). The second approach for discrimination of specific from unspecific signals was to pre-absorb the antiserum with its antigen, so called 'blocking' of the antibody. With successful blocking, proteins carrying an antigenic part were not detected anymore and easily identified when compared to unblocked controls. This approach was found to be effective when non-purified immune sera were used (see Figure 3.11).

The final goal of the development of a polyclonal antibody against zebrafish 20β-HSD type 2 was to detect 20β-HSD type 2 in zebrafish embryo lysates. Since zebrafish lysates without 20β-HSD type 2 could not be generated, the only approach to discriminate specific from unspecific signals was to use blocked immune serum. In initial experiments with samples derived from cell culture, the affinity purified serum from day 150 from rabbit #2 was blocked with 20 µg/ml peptide zf-4, the concentration recommended by Pineda Antikörper Service. Unfortunately, blocking affinity purified immune serum with this peptide concentration resulted in chemiluminescence signals all over the membrane (data not shown). This was probably due to unspecific precipitation of peptide-antibody complexes on the membrane. Neither optimization of the washing protocol, nor addition of bovine serum albumin or ovalbumin to the antibody solution, nor addition of detergent to the antibody solution improved the results. Therefore, a titration experiment was performed to determine the optimal concentration of zf-4 peptide for blocking. The results demonstrated that 10 µg/ml and 1 µg/ml peptide zf-4 still led to precipitate on the membrane, while 100 ng/ml led to a faint signal of 20β-HSD type 2 (Figure 3.13).

The intensity of 20β-HSD type 2 signal was almost comparable to unblocked serum at a concentration of 10 ng/ml peptide. Since Figure 3.13 is showing only a part of all concentrations tested, it was decided to perform further blocking experiments with 250 ng/ml peptide zf-4.

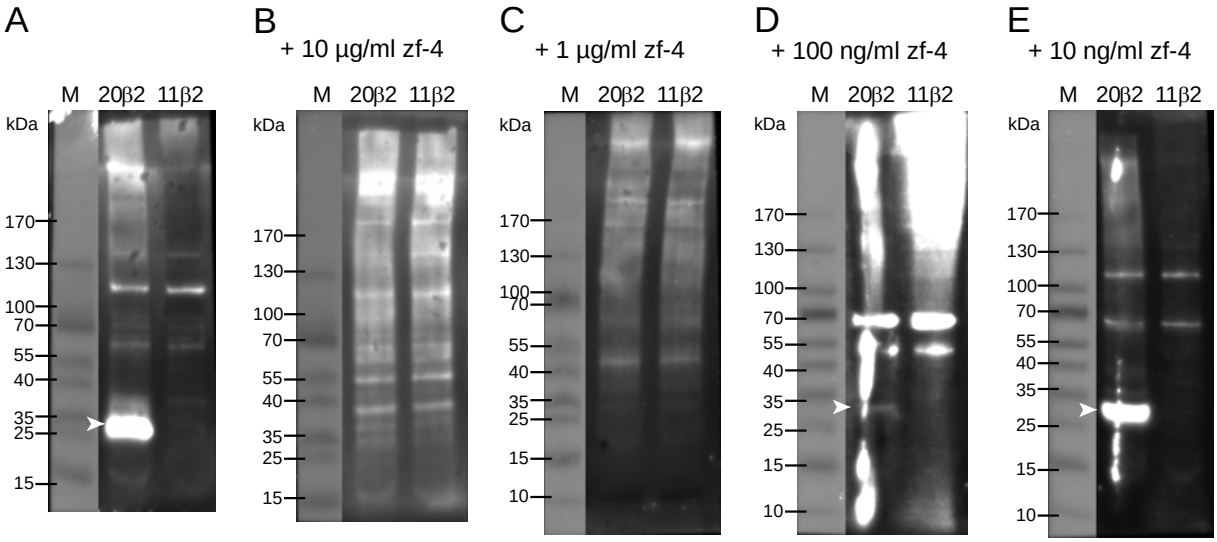

Figure 3.13: Western Blot analysis for determining optimal zf-4 peptide concentration for blocking of affinity purified immune serum show efficient blocking and low precipitation between 1 µg/ml and 100 ng/ml. 5 µg protein of the 700 x g pellet were separated on 4-15 % gels alongside molecular weight marker. Western Blots were developed using chemiluminescence and the signals detected with Fusion FX7 (exposition time 45 min). The signals for 20β-HSD type 2 are marked by white arrowheads. Affinity purified serum from day 150 from rabbit #2 was used at a dilution of 1:150. Concentration of zf-4 peptide used for blocking varied: (A) without zf-4, (B) with 10 µg/ml zf-4, (C) with 1 µg/ml zf-4, (D) with 100 ng/ml zf-4, and (E) with 10 ng/ml zf-4. Abbreviations: M, molecular weight marker, 11β2, 11β-HSD type 2 in HEK293 cells; 20β2, 20β-HSD type 2 in HEK293 cells.

3.6.4 Detection of 20β-HSD type 2 in zebrafish embryo samples

The previous chapter has shown that the polyclonal antibody against zebrafish 20β-HSD type 2 recognized the enzyme after recombinant expression in HEK293 cells. The optimized Western Blotting protocol was then applied to samples derived from zebrafish larvae. For this approach, 3 dpf larvae were chosen for comparing wild-type larvae to cortisol treated fish larvae (50 mg/l cortisol for 72 hours). The larvae were homogenized and fractionated using the two-step protocol (first centrifugation at 700 x g followed by centrifugation at 55000 x g), which had been found to be sufficient for 20β-HSD type 2 enrichment after expression in HEK293 cells. While the accumulation of 20β-HSD type 2 in the desired fraction after recombinant expression could be easily controlled by myc antibody, this approach was not applicable to zebrafish larvae fractions. Therefore, the enrichment of 20β-HSD type 2 was controlled using enzyme activity assays.
Most of 20β-HSD type 2 activity was found in the 55000 x g pellet (P2), followed by the 700 x g pellet (P1) (data not shown). In the supernatant only marginal activity could be detected, reflecting the insoluble characteristics of 20β-HSD type 2. Thus, all obtained fractions were separated by SDS-PAGE alongside positive and negative controls derived from cell culture. The functionality of the Western Blot was demonstrated by a 20β-HSD type 2 signal after expression in HEK293 cells (white arrowhead in Figure 3.14 A), that was blocked using zf-4 pre-absorbed antiserum (Figure 3.14 B). Furthermore, specific signals for 20β-HSD type 2 in zebrafish fractions pellet 1 and pellet 2 were detected, where the signals obtained in pellet 2 were more intense matching the observation of higher activity in enzymatic assays (red arrowheads in Figure 3.14 A). These signals were totally blocked by using zf-4 pre-absorbed immune serum (Figure 3.14 B). Additionally, potential degradation products in the range of 10-15 kDa were entirely competed with zf-4 peptide. Although zebrafish 20β-HSD

type 2 was estimated to have a molecular weight of approximately 36.9 kDa, the apparent protein size was found to be slightly smaller, as already observed in the above described experiments.

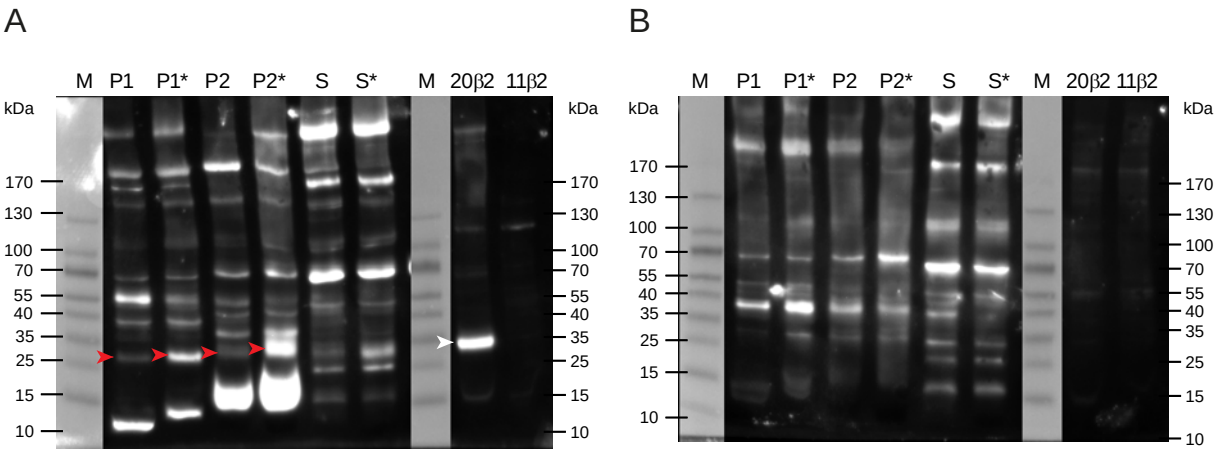

Figure 3.14: Western Blot analysis detects 20β-HSD type 2 in 3 dpf zebrafish larvae in the fractions containing insoluble proteins. 15 µg protein of each fraction derived from zebrafish larvae were separated on 4-15 % gels alongside molecular weight marker and 2.5 µg of the 700 x g pellet derived from cell culture. Western Blots were developed using chemiluminescence and the signals detected with Fusion FX7 (exposition time 45 min). The signal for recombinantly expressed 20β-HSD type 2 is marked by a white arrowhead, while the signals for 20β-HSD type 2 in zebrafish fractions are highlighted with red arrowheads. (A) Affinity purified serum from day 150 from rabbit #2 was used at a dilution of 1:150. (B) Serum was diluted as in (A) and 0.25 µg/ml zf-4 peptide was added. Abbreviations: M, molecular weight marker; P1, 700 x g pellet; P2, 55000 x g pellet; S, supernatant; *, fractions derived from fish larvae treated with 50 mg/l cortisol; 20β2, 20β-HSD type 2 in HEK293 cells; 11β2, 11β-HSD type 2 in HEK293 cells.

3.6.5 Quantification of 20β-HSD type 2 in cortisol treated zebrafish larvae

The amount of 20β-HSD type 2 in cortisol treated zebrafish larvae was determined only in 3 dpf larvae due to sample limitations, as one sample consisted of at least 200 larvae. For the same reason, only representative cortisol concentrations were chosen, namely 10 mg/l, 50 mg/l, and 100 mg/l cortisol. Larvae were homogenized and fractionated using the two-step protocol, and each collected fraction was assessed for 20β-HSD type 2 activity.

As observed previously, most of the 20β-HSD type 2 activity was enriched in the 55000 x g pellet (P2). The 700 x g pellet (P1) contained less 20β-HSD type 2, and in the soluble fraction only minor 20β-HSD type 2 activity was observed (Figure 3.15 A). While the activity of 20β-HSD type 2 in DMF (vehicle) treated larvae was comparable to that in wild-types, the enzymatic activity was significantly increased in all fractions of cortisol treated larvae. Both pellet fractions were separated independently alongside positive and negative controls derived from cell culture by SDS-PAGE. Specificity of the antibody was demonstrated by a 20β-HSD type 2 signal after expression in HEK293 cells (white arrowhead in Figure 3.15 B and C), that was completely blocked using zf-4 pre-absorbed immune serum (data not shown). In all zebrafish samples signals for 20β-HSD type 2 were detected (red arrowhead in Figure 3.15 B and C). The signals in pellet 2 were stronger than those in pellet 1 reflecting the observation of the activity assay.

Relative quantification of 20β-HSD type 2 signals in both fractions illustrated what could be already observed on the Western Blot itself. In the 700 x g fraction (P1) a linear correlation of 20β-HSD type 2 amount and cortisol concentration was detected (Figure 3.15 D). However, in the 55000 x g pellet (P2) the relative abundance of 20β-HSD type 2 in 100 mg/l cortisol treated fish larvae was comparable to that of 10 mg/l cortisol. This observation was not due to increased degradation (Figure 3.15 E).

In general, cortisol treatment of zebrafish larvae increased the amount of 20β-HSD type 2 protein.

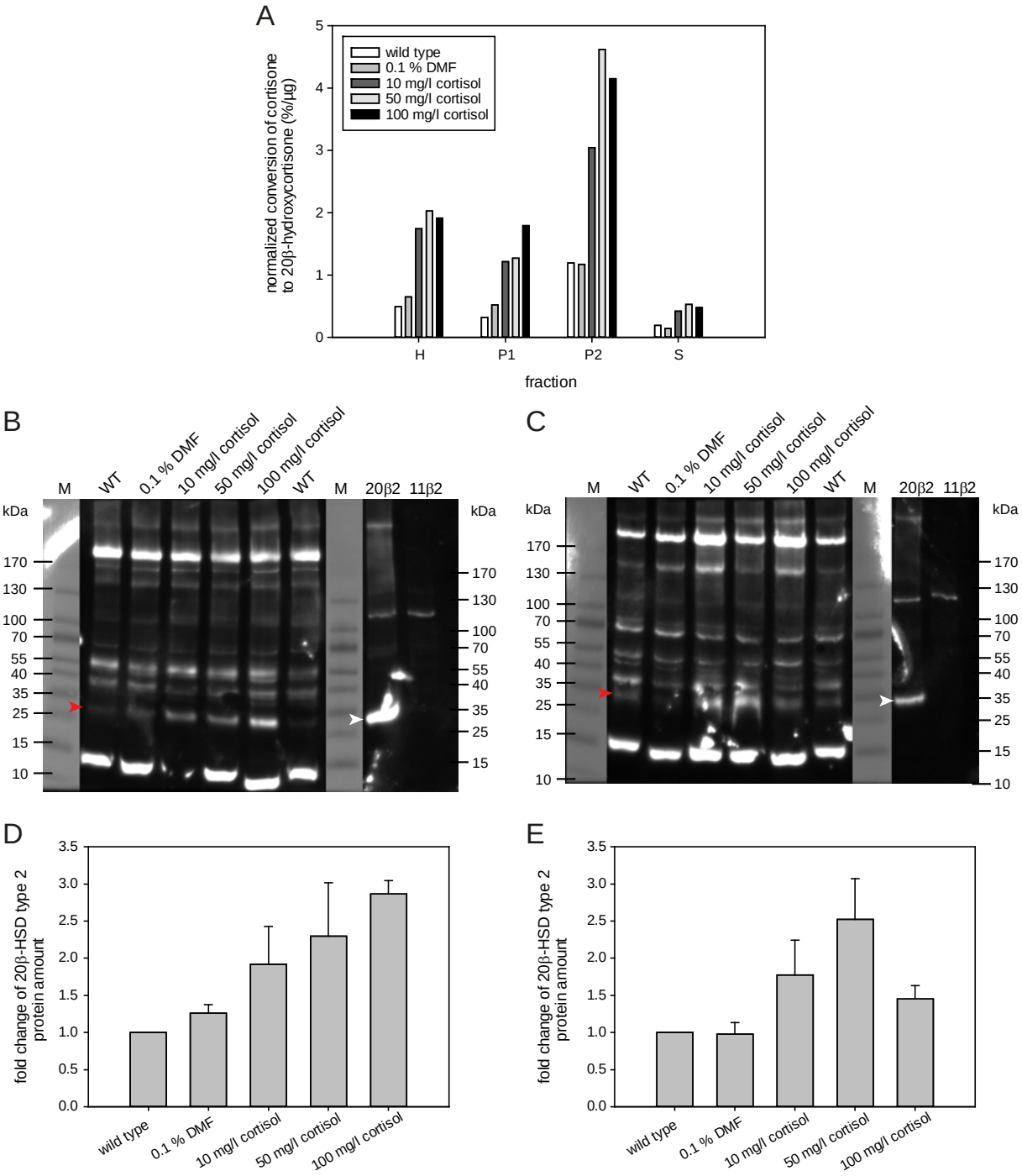

Figure 3.15: Western Blot analyses and subsequent relative quantification reveal increased amount of 20β-HSD type 2 upon cortisol treatment in 3 dpf zebrafish larvae. (A) Determination of 20β-HSD type 2 activity in fractions derived from 3 dpf larvae. Conversion of cortisone was normalized to input protein amount. Abbreviations: H, homogenate prior to fractionation; P1, 700 x g pellet; P2, 55000 x g pellet; S, supernatant. (B), (C) 15 µg protein of each fraction (P1 in (B), and P2 in (C)) derived from zebrafish larvae were separated on 4-15 % gels alongside molecular weight marker and 2.5 µg of the 700 x g pellet derived from cell culture (20β-HSD type 2 and 11β-HSD type 2). Western Blots were developed using chemiluminescence and the signals detected with Fusion FX7 (exposition time 45 min). The signal for recombinantly expressed 20β-HSD type 2 is marked by a white arrowhead, while the signals from 20β-HSD type 2 in zebrafish fractions are highlighted with red arrowheads. Affinity purified serum from day 150 from rabbit #2 was used at a dilution of 1:150. Representative results are shown. Abbreviations: M, molecular weight marker; WT, wild-type; 20β2, 20β-HSD type 2 in HEK293 cells; 11β2, 11β-HSD type 2 in HEK293 cells. (D), (E) Fold changes of 20β-HSD type 2 in treated fish fractions (Pellet 1 in (D), Pellet 2 in (E)) compared to wild-type samples were determined by relative quantification using Bio-1D software. Mean values from three independent experiments are shown.

3.7 Morpholino-induced knock-down of 20β-HSD type 2 in zebrafish embryos

Morpholino antisense oligos are analogs of nucleic acids consisting of morpholine rings instead of deoxyribose or ribose rings which are linked through phosphorodiamidate groups instead of phosphates. This structure renders morpholinos stable oligos that are not degraded in a biological system. Morpholinos bind to complementary sequences of RNA and can thereby inhibit splicing of mRNA precursors or translation of mRNA [116, 117]. Since the analysis of 20β-HSD type 2 expression in early zebrafish development revealed a maternal supply of its mRNA to the zygote (see chapter 3.3), a splicing morpholino was designed. This morpholino would exert its action after onset of embryonic transcription (between 512 and 1000 cells) thereby avoiding potentially lethal effects of a translation blocking morpholino, whose action would arise directly after injection. The 20β-HSD type 2 morpholino was designed to target the donor splice site of exon 2 (Figure 3.16 A). Morpholino-induced mis-splicing would lead to a 20β-HSD type 2 transcript shortened by exon 2, which after translation would result in a 20β-HSD type 2 enzyme lacking the TGx_3GxG motif of the cofactor binding site. The loss of this motif was intended to render the enzyme totally inactive.
Initially, morpholinos were injected at different concentrations to ensure sufficient knock-down, which was evaluated on mRNA level. In RT-PCR using primers binding in the first and fourth exon, wild-type 20β-HSD type 2 yielded a PCR fragment of 343 bp, while the mis-spliced PCR product was only 269 bp in size. First injections using 125 µM and 250 µM morpholino resulted hardly in formation of the shorter PCR product (data not shown). Therefore, 375 µM and 500 µM morpholino were injected. Upon injection of 375 µM morpholino, the wild-type PCR fragment visibly decreased giving rise to considerable amounts of the shorter mis-spliced product. The amount of the mis-spliced product could even be increased by injection of 500 µM morpholino (Figure 3.16 B). Both PCR products were cloned and sequenced for verification of accurate morpholino action. As expected, the mis-spliced PCR product was lacking exon 2.
The knock-down on mRNA level appeared to be approximately 30 % at both 375 µM and 500 µM. Additionally, the efficiency of morpholino-induced knock-down was assessed by determining 20β-HSD type 2 activity in morphant fish larvae. These experiments revealed that injection of 500 µM morpholino did not further reduce 20β-HSD type 2 activity compared to 375 µM injected zebrafish embryos (Figure 3.16 C). On 20β-HSD type 2 activity level, the knock-down was approximately 80 % at both concentrations. Thus, for further experiments 375 µM morpholino was chosen to reduce the possibility of toxic effects of the morpholino itself on zebrafish development.

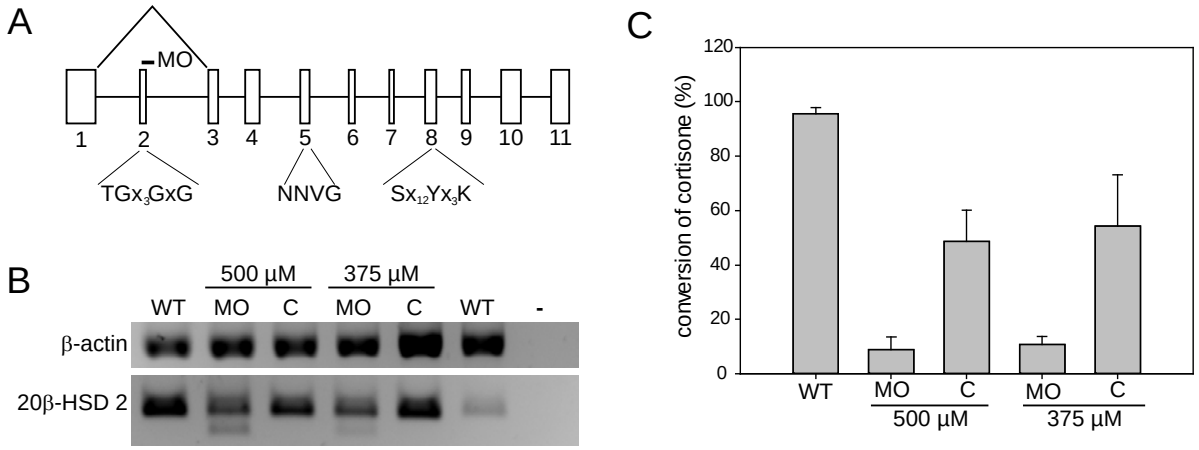

Figure 3.16: Analysis of knock-down efficiency of 20β-HSD type 2 splicing morpholino at 48 hpf on mRNA and enzymatic activity level shows significant reduction of 20β-HSD type 2 activity. (A) In the genomic structure of zebrafish 20β-HSD type 2, exons are indicated by boxes and numbered. Below, important SDR motifs are denoted in single letter code. 'x' denotes any amino acid and when present the subsequent number indicates the number of x residues. The splice site targeted by the morpholino is indicated by a dash. Morpholino-induced mis-splicing is illustrated by the triangle above the genomic structure. Exons are in scale, whereas the space between exons does not reflect the respective intron size. (B) Analysis of morpholino efficiency on mRNA level by RT-PCR using primers binding in the first and fourth exon demonstrates mis-splicing in morpholino-injected fish. The smaller PCR product does not occur in control morpholino-injected fish embryos. The respective morpholino concentration is denoted. β-actin controls were included for normalization. (C) Knock-down efficiency on enzymatic activity was assessed by analyzing conversion of cortisone to 20β-hydroxycortisone in morpholino- and control morpholino-injected fish embryos. The respective morpholino concentration used is denoted. MO, 20β-HSD type 2 morpholino; C, control morpholino; WT, wild-type.

Despite the knock-down of 20β-HSD type 2, morphants showed no developmental abnormalities under normal culturing conditions. Since cortisol was found to induce 20β-HSD type 2 expression, it was self-evident to challenge morphants with cortisol, thereby mimicking stress. For this purpose, the cortisol concentration to be chosen had to fulfill two criteria: firstly, the amount of cortisol should be sufficient to robustly induce 20β-HSD type 2 expression, but secondly, the cortisol concentration should not be too high causing developmental abnormalities in wild-type fish embryos. The application of 10 mg/l cortisol met both criteria as described in chapter 3.4.1 and was therefore chosen for treatment of morphant embryos. The efficiency of 20β-HSD type 2 knock-down in cortisol treated morphants and control embryos was determined by RT-PCR at 24 hpf, 48 hpf, and 72 hpf. As expected, cortisol treatment enhanced the expression of 20β-HSD type 2, but in morpholino-injected embryos also the amount of the mis-spliced PCR product increased (data not shown). Likewise to previous observations of cortisol treated zebrafish embryos, developmental abnormalities manifested with 48 hpf (Figure 3.17 A). Cortisol challenged morphants displayed alterations of size and shape of both yolk sac and yolk sac extension, altered somitogenesis, and kinked or shortened tails. The phenotypes could be categorized into a 'mild' and a 'severe' form, where the severe form showed strongly truncated tails. The described developmental abnormalities persisted until 72 hpf, but at this stage additionally strong pericardial edema were observed (Figure 3.17 B). The distribution of phenotypes in cortisol treated 20β-HSD type 2 morphants is denoted in Table 3.5.

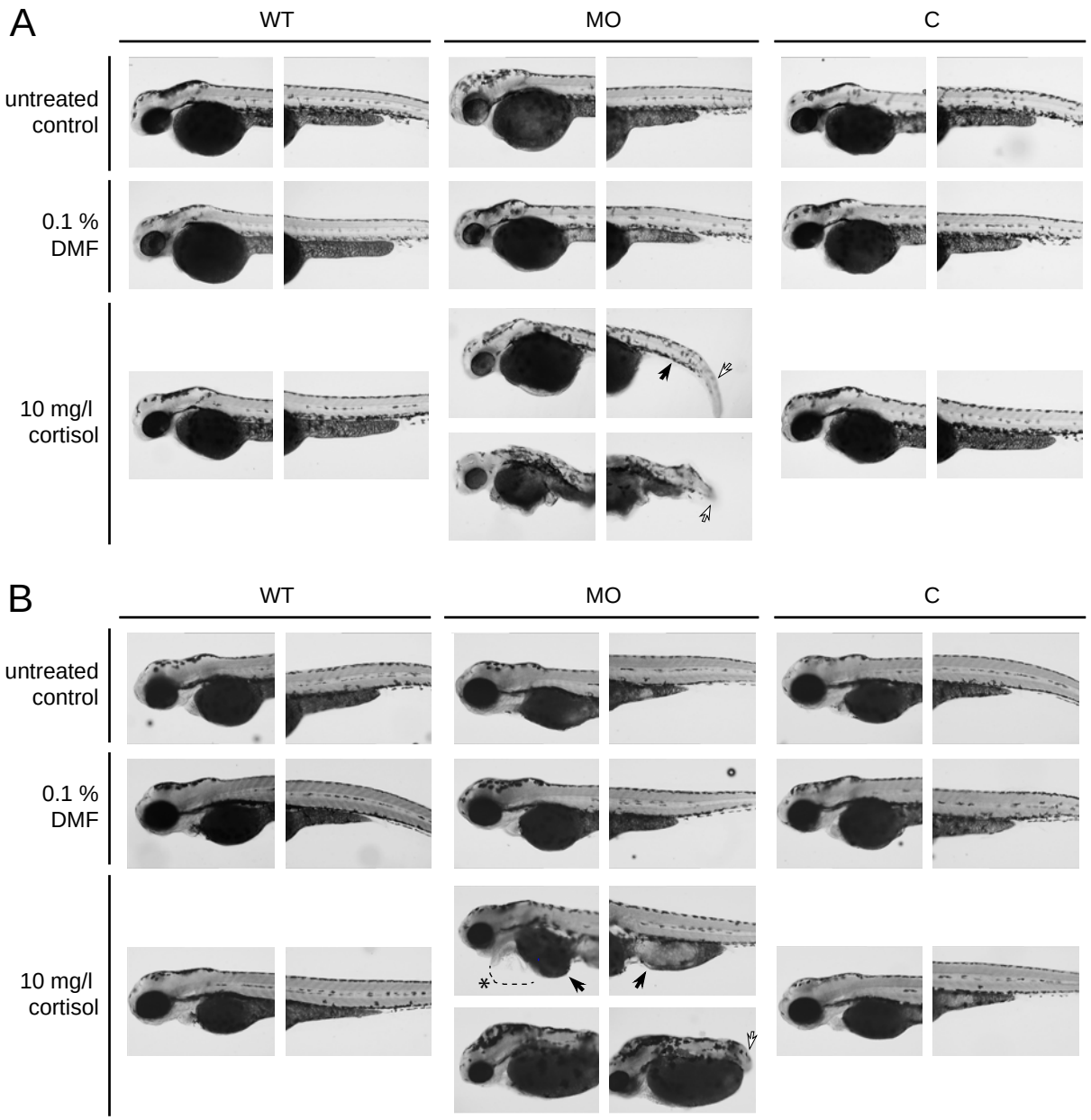

Figure 3.17: 20β-HSD type 2 morphants display developmental abnormalities upon cortisol treatment. Animals are presented in lateral view, anterior to the left. The treatment regimen is shown in rows: the top row depicts untreated control animals, the middle row shows 0.1 % DMF (vehicle) treated specimens, and the third row displays fish embryos treated with 10 mg/l cortisol. Wild-type embryos are shown in the first column, 20β-HSD type 2 morphants (MO) in the second column, and control morpholino (C) injected fish embryos in the third column. For cortisol treated 20β-HSD type 2 morphants, representative specimens for the 'mild' and the 'severe' phenotype are shown. (A) Embryos at 48 hpf. (B) Embryos at 72 hpf. Black arrows point to yolk deformations, white arrows to altered somitogenesis resulting in kinked or truncated tails, and the asterisk denotes pericardial edema. MO, 20β-HSD type 2 morpholino; C, control morpholino; WT, wild-type. Magnification 5x.

Table 3.5: Distribution of phenotypes in 20β-HSD type 2 morphant zebrafish larvae.

48 hpf

	treatment											
	untreated control				0.1 % DMF				10 mg/l cortisol			
	none (%)	mild (%)	severe (%)	n	none (%)	mild (%)	severe (%)	n	none (%)	mild (%)	severe (%)	n
WT	100 ± 0	0 ± 0	0 ± 0	135	100 ± 0	0 ± 0	0 ± 0	179	100 ± 0	0 ± 0	0 ± 0	153
MO	100 ± 0	0 ± 0	0 ± 0	87	99 ± 2	1 ± 1	1 ± 1	91	52 ± 21	33 ± 19	16 ± 5	104
C	99 ± 2	1 ± 2	0 ± 0	85	100 ± 0	0 ± 0	0 ± 0	114	96 ± 5	5 ± 5	0 ± 0	111

72 hpf

	treatment											
	untreated control				0.1 % DMF				10 mg/l cortisol			
	none (%)	mild (%)	severe (%)	n	none (%)	mild (%)	severe (%)	n	none (%)	mild (%)	severe (%)	n
WT	100 ± 0	0 ± 0	0 ± 0	146	100 ± 0	0 ± 0	0 ± 0	188	98 ± 3	2 ± 3	0 ± 0	160
MO	91 ± 11	4 ± 4	4 ± 7	83	94 ± 7	5 ± 7	1 ± 1	88	37 ± 20	44 ± 12	19 ± 7	101
C	99 ± 2	1 ± 2	0 ± 0	77	95 ± 7	5 ± 7	0 ± 0	102	86 ± 12	14 ± 12	0 ± 0	110

Abbreviations: C, control morpholino injected fish (375 µM); MO, 20β-HSD type 2 morpholino injected fish (375 µM); WT, wild-type fish; n, number of larvae. Data were pooled from four experiments and expressed as means with standard deviations.

3.8 Influence of physical stress on 20β-HSD type 2 expression

Previous experiments have shown that 20β-HSD type 2 expression is strongly stimulated by cortisol treatment of zebrafish embryos. To determine if 20β-HSD type 2 is also up-regulated upon a stressor regimen independent of artificial cortisol treatment, 5 dpf zebrafish larvae were challenged with a physical stress composed of swirling the larvae vigorously for 30 sec. This stressor was found to be sufficient to increase cortisol levels already 5 min post stress in 97 hpf zebrafish larvae. By this age, the stress axis is fully functional [42]. Thus, 5 dpf zebrafish larvae were chosen for the stress challenge to ensure proper stress perception and transduction. To assess time-dependent changes of expression levels of the genes of interest, samples were taken at different time points after the stress and compared to unstressed control larvae.

Target genes for quantification by qPCR were chosen according to literature on hypothalamus-pituitary-interrenal axis (HPI axis) in zebrafish [42, 49]. The genes of interest covered central positions in the HPI axis and were quantified to ensure accurate stress perception and transduction. The first transmitter after perceiving the stressor in the hypothalamus, corticotropin releasing hormone (*Crh*), was included as well as the ACTH receptor on the surface of interrenal cells, melanocortin 2 receptor (*Mc2r*). Two genes responsible for cortisol biosynthesis were chosen: steroid acute regulatory protein (*Star*) mediating cholesterol transport and 11β-hydroxylase (*Cyp11b2*) catalyzing the final step of cortisol formation. 11β-HSD type 2 is responsible for the first inactivation step of cortisol to cortisone and its gene was included into quantification (for further characterization of 11β-HSD type 2 in zebrafish, refer to chapter 3.11) alongside 20β-HSD type 2 (*Hsd20b2*). qPCR pre-experiments revealed problems with normalization to one reference gene (e.g., β-actin) only, because β-actin showed small changes (data not shown). To ensure accurate normalization, the geometric mean of three reference genes was chosen (BestKeeper tool developed by Pfaffl [120]) instead of normalization to only one reference gene.

In stressed zebrafish larvae *Crh* was slightly increased after the stressor and remained on this level for 60 min (Figure 3.18 A). The expression of *Mc2r* undulated in the first 10 min after the stressor, before

increasing until 30 min and then decreasing to the mRNA level in unstressed fish. *Mc2r* displayed a high variability between different pools of larvae. The transcript of *Star* increased 1.7-fold until 20 min post stress and remained on this level throughout the experiment (Figure 3.18 B). *Cyp11b2* showed highest inter-individual variability in the expression levels after the stressor. Some samples revealed strong up-regulation of *Cyp11b2* shortly after the stressor, while others displayed a marked decrease. This observation averaged in no significant changes until 60 min post stress. The mRNA of 11β-HSD type 2 increased steadily after the stressor to 1.5-fold induction compared to unstressed fish. 20β-HSD type 2 was 1.6-fold induced already 5 min post stress. Its mRNA levels increased until 60 min to 2.2-fold induction (Figure 3.18 C). With the exception of *Mc2r*, all target genes did not decrease to unstressed levels throughout the experiment.
In addition to quantification of 20β-HSD type 2 mRNA, the activity of this enzyme was elucidated in stressed zebrafish larvae. This analysis revealed no significant changes of stressed fish to unstressed controls (Figure 3.18 D). Only in fish larvae 60 min after perceiving the stressor a minor decrease in 20β-HSD type 2 activity could be observed.

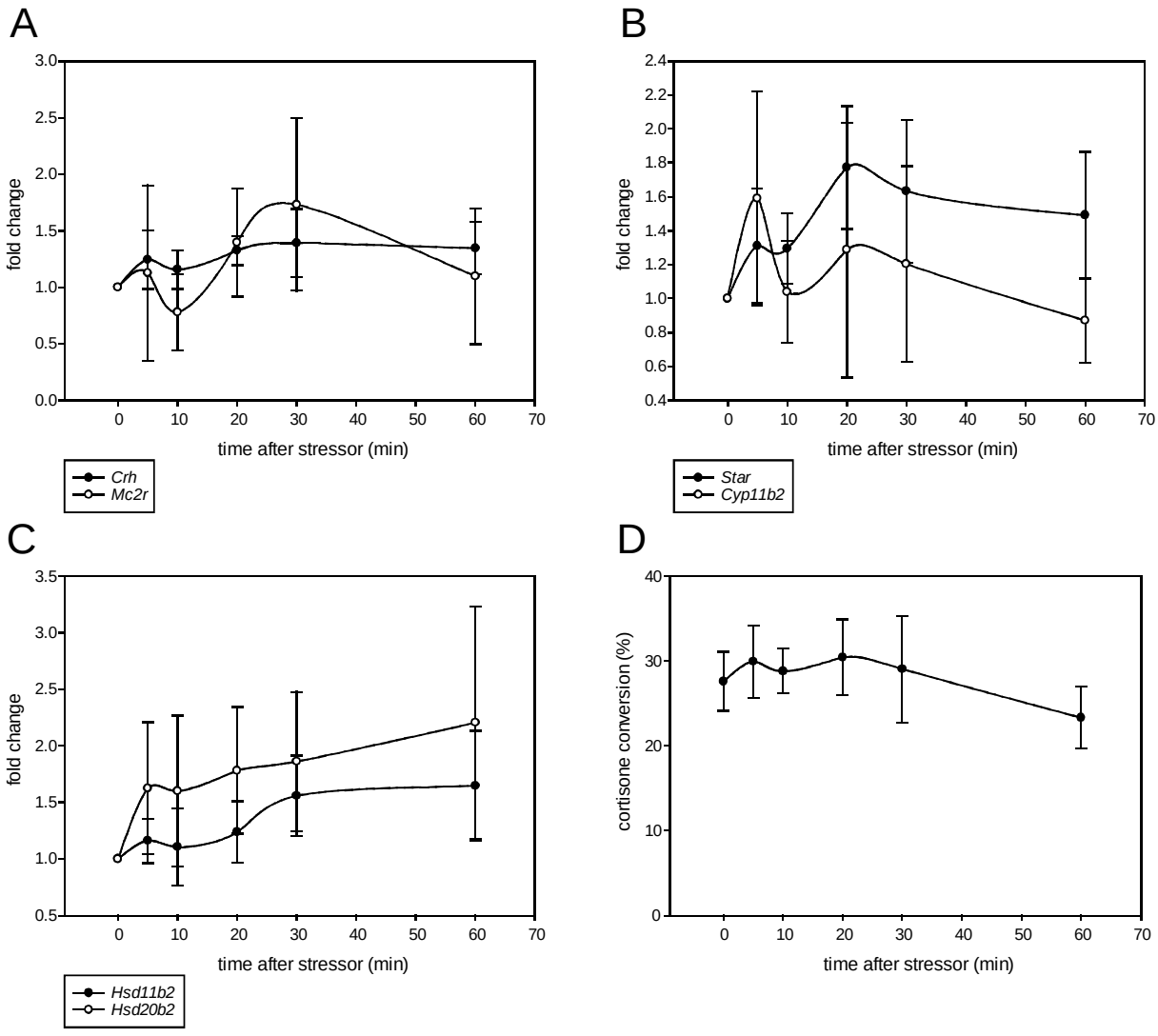

Figure 3.18: Challenging of 5 dpf zebrafish larvae with physical stressor result in up-regulation of most HPI axis genes alongside up-regulation of 11β-HSD type 2 and 20β-HSD type 2. Zebrafish larvae were subjected to 30 sec swirling stress and sampled at the indicated time points. Fold changes of target genes from six biological replicates were calculated after normalization to the geometric mean of three reference genes and compared to unstressed fish. (A) qPCR results for *Crh* and *Mc2r*. (B) qPCR results for *Star* and *Cyp11b2*. (C) qPCR results for *Hsd11b2* and *Hsd20b2*. (D) 20β-HSD type 2 activity was assessed by analyzing conversion of cortisone to 20β-hydroxycortisone.

3.9 Analysis of receptor activation by 20β-hydroxycortisone

To elucidate whether the reaction product of 20β-HSD type 2, 20β-hydroxycortisone, played a physiological role by binding and activating receptors, reporter gene experiments were performed. Zebrafish glucocorticoid receptor α isoform (GRα) and mineralocorticoid receptor (MR) being known targets for C21 steroids were taken into account. The expression plasmid coding for zebrafish GRα (pCS2+_zfGRα) was a kind gift of M. Schaaf [25]. Cloning of the respective construct for zebrafish MR was tried in our lab but proved virtually impossible. Therefore, the coding sequence was synthesized by GeneScript and the resulting plasmid used for subcloning by GeneArt to produce an expression plasmid coding for zebrafish MR (pCS2+_zfMR). Each receptor plasmid was cotransfected with a plasmid containing a luciferase gene driven by the MMTV promoter, which comprises several glucocorticoid response elements. For normalization of transfection, the plasmid pGL4.74[*hRluc*/TK] was transfected alongside the other plasmids. The cell line COS-1 was used for reporter gene experiments, because these cells lack an endogenous GR and are therefore frequently used in reporter gene assays [25]. To ensure comparability, COS-1 cells were used for MR experiments as well, although these cells express endogenous MR (data not shown).
Dose-response curves were determined for each receptor independently with five steroidal ligands, namely cortisol, cortisone, 20β-hydroxycortisone, 11-dehydrocorticosterone, and aldosterone. Cortisol is known to activate GRα and MR [20, 25, 26] and was included for normalization and as positive control demonstrating functionality of the assay. Since the physiological ligand for teleost MR is not yet definitively determined [31], aldosterone and 11-dehydrocorticosterone were added to the experiment. The latter steroid is discussed to act as mineralocorticoid in teleost fish [27, 34].
Of all five steroids analyzed, only cortisol activated zebrafish GRα (Figure 3.19 A) showing an EC_{50} value of 1.9 nM (Table 3.6). Cortisone, an inactive glucocorticoid, showed an EC_{50} value of 104.7 nM. All other steroids induced no significant luciferase expression, which is reflected in theoretical EC_{50} values with high standard errors and low R^2 coefficients. The results for MR showed that cortisol, 11-dehydrocorticosterone, and aldosterone stimulated the receptor-induced reporter expression (Figure 3.19 B), while cortisone and 20β-hydroxycortisone slightly stimulated activation only at high concentrations. Application of 20β-hydroxycortisone in concentrations below 10 nM resulted in a decrease of luciferase expression relative to the background, while with higher concentrations of 20β-hydroxycortisone an increase of luciferase expression above the background was observed (Figure 3.19 B).

Table 3.6: EC_{50} values of different steroidal ligands for zebrafish GRα and MR.

zebrafish GRα		
ligand	EC_{50} (nM)	R^2
cortisol	1.9 ± 2.0	0.8033
cortisone	104.7 ± 1.2	0.9868
20β-hydroxycortisone	24.4 ± 133.9	0.0804
11-dehydrocorticosterone	5.7 ± 105.2	0.0817
aldosterone	$2.1e^{-4}$ ± ∞	0.1838
zebrafish MR		
ligand	EC_{50} (nM)	R^2
cortisol	0.3 ± 1.8	0.8930
cortisone	0.8 ± 5.6	0.3687
20β-hydroxycortisone	35.2 ± 2.0	0.8260
11-dehydrocorticosterone	5.8 ± 1.5	0.9216
aldosterone	0.5 ± 2.3	0.7540

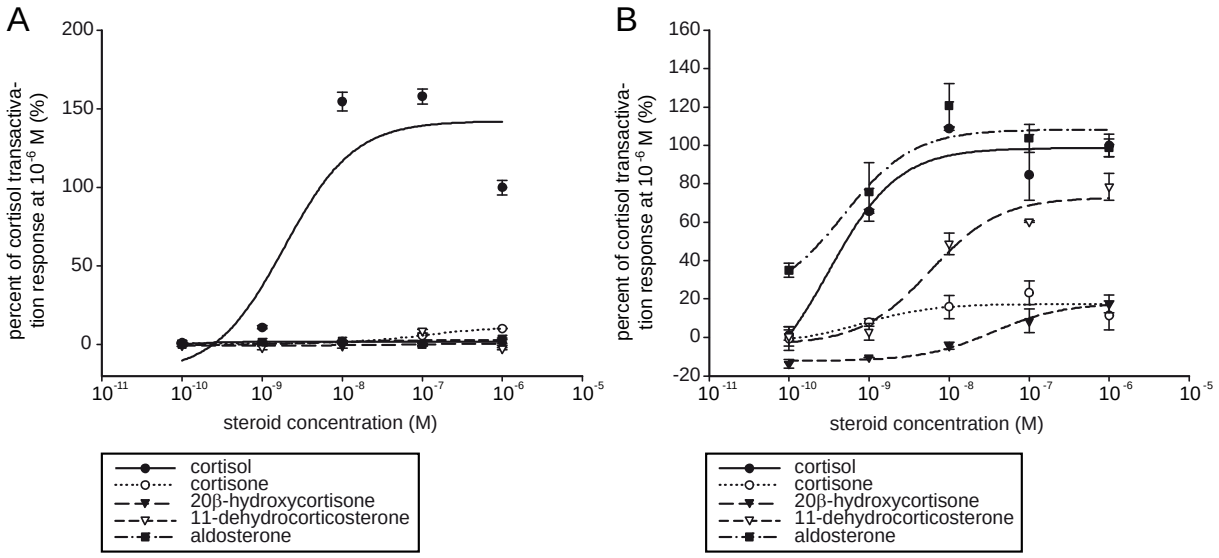

Figure 3.19: 20β-hydroxycortisone is not a physiological ligand for neither zebrafish GRα nor MR. Analysis of reporter gene activation mediated by zebrafish GRα (A) and zebrafish MR (B) using five different steroidal ligands: cortisol, cortisone, 20β-hydroxycortisone, 11-dehydrocorticosterone, and aldosterone. Firefly luciferase values were normalized to renilla luciferase, corrected for background of methanol treated cells, and related to the ratio luciferase/renilla of cortisol at the highest concentration.

3.10 Investigation of glucocorticoids in fish holding water

During the work on this thesis, several hypotheses regarding the physiological role of 20β-HSD type 2 were proposed. According to one of them, 20β-hydroxycortisone was suggested to be an excreted glucocorticoid and therefore released into fish holding water. Initial experiments focused on extraction of unconjugated glucocorticoids from adult fish holding water. Analysis of these extracts detected cortisol, cortisone, 20β-hydroxycortisone, and 20α-hydroxycortisone (data not shown). The amount of 20β-hydroxycortisone was close to the amount of cortisol or even higher. Sex specific differences were not observed (data not shown). The promising outcome of these initial experiments resulted in development of an extraction method according to Payne *et al*. [123] allowing for the separation of conjugated from unconjugated steroids. This goal was achieved by differential elution, and conjugated steroids were further separated in glucuronidated and sulfated steroids and hydrolyzed by enzymatic digestion prior to analysis by LC-MS/MS.

Generally, in all steroid fractions derived from fish holding water four different glucocorticoids were detected with 20β-hydroxycortisone as the most abundant steroid (Figure 3.20 A-C). In the free steroid fractions, also ample amounts of cortisol, cortisone, and 20α-hydroxycortisone were found. In both glucuronidated and sulfated steroid fractions, the amount of 20β-hydroxycortisone was an order of magnitude higher than the amount of all other glucocorticoids. Significant sex-specific differences were not observed, although male zebrafish seemed to excrete slightly more 20β-hydroxycortisone than females. Controls using water without fish demonstrated no steroid contamination. Steroid extraction from fish holding water subjected to the same extraction protocol but without addition of β-glucuronidase and sulfatase showed only minor carry-over of free steroids.

To ensure that the extraction and hydrolyzation protocol is working as intended, water samples containing two different reference steroids were subjected to the extraction protocol. Cortisol-21-glucuronide and cortisone-21-sulfate were chosen as references. Both references displayed contamination with free cortisol, cortisone, and both isomers of 20-reduced cortisone. Nevertheless, most cortisol-21-glucuronide was hydrolyzed by β-glucuronidase, and most cortisone-21-sulfate was digested by sulfatase, demonstrating functionality of both enzymes (Figure 3.20 A-C).

For determination if the LC-MS/MS method was able to measure conjugated steroids, steroids of one fish holding water sample were extracted and divided into conjugated and free steroids. The conjugated steroids were not enzymatically hydrolyzed but analyzed in comparison to free steroids.

LC-MS/MS analysis revealed lower amounts of glucocorticoids in the conjugated fraction compared to the free steroid fraction (Figure 3.20 D). This result demonstrated that the vast amount of conjugated 20β-hydroxycortisone was not detected without enzymatic hydrolysis. Although controls using reference substances showed functionality of both enzymes in this extraction protocol, another control experiment with a double β-glucuronidase digestion was carried out to assess the amount of left-over glucuronidated steroids in the sulfated steroids fraction (Figure 3.20 E). The results showed that the first β-glucuronidase digestion hydrolyzed glucuronidated steroids for the most part, while in the second β-glucuronidase digestion only a small amount (approximately 6 %) of glucocorticoids was additionally released. This result demonstrated that the amount of sulfated steroids extracted from fish water might be slightly overrated due to left-over glucuronidated steroids in this fraction.

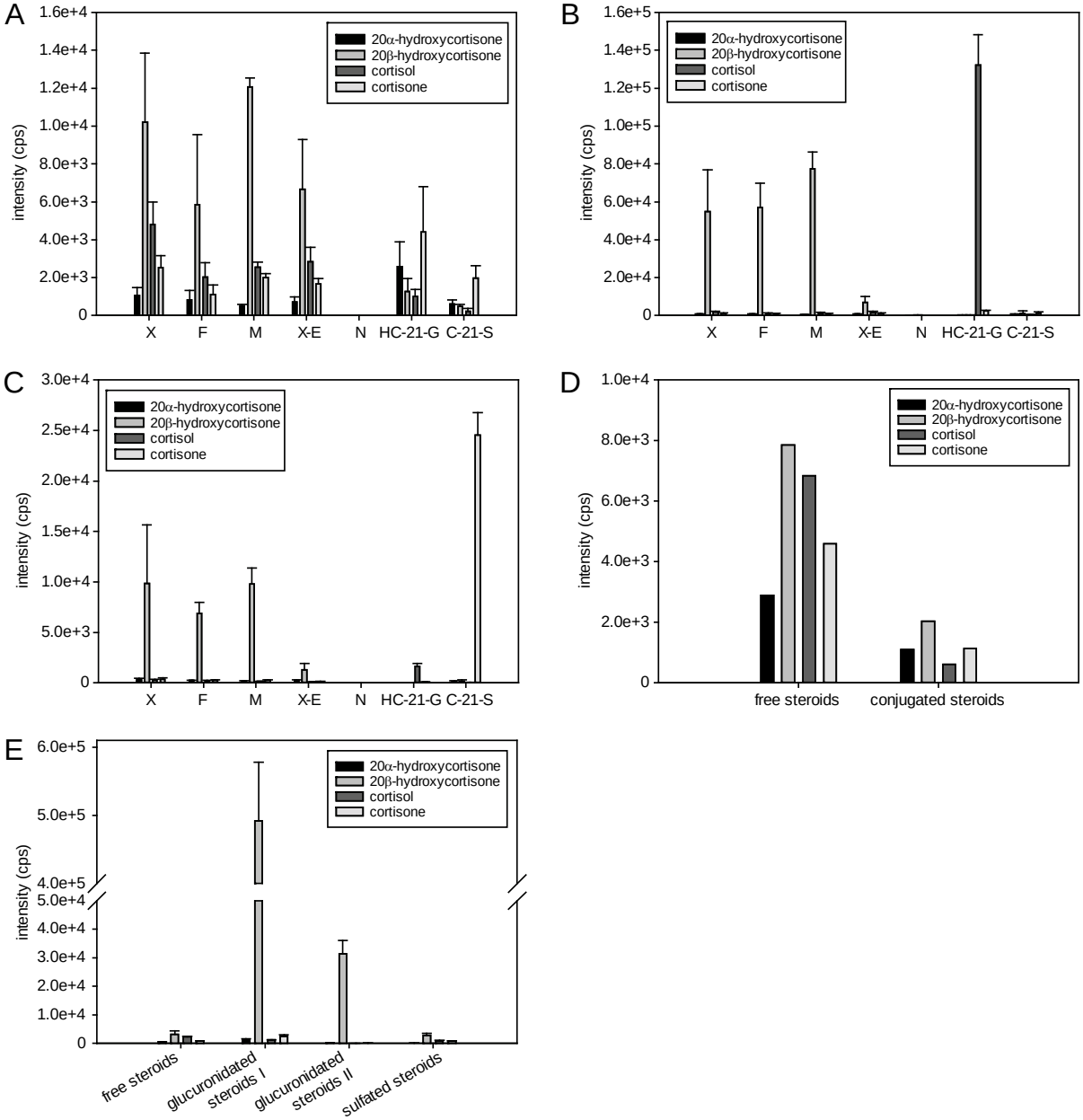

Figure 3.20: 20β-hydroxycortisone is the most abundant steroid in unconjugated and conjugated steroid fractions extracted from adult zebrafish holding water. After extraction and hydrolysis of steroid conjugates, four glucocorticoids were determined by LC-MS/MS for each fraction separately: (A) unconjugated steroids; (B) glucuronidated steroids; (C) sulfated steroids. Panel (D) depicts the comparison of a sample containing unconjugated steroids to a sample with conjugated, but not enzymatically hydrolyzed steroids. The results of double β-glucuronidase digestion are shown in panel (E). Sample abbreviations are as follows: X, mixed gender group; F, all female group; M, all male group; X-E, mixed gender group, without addition of digestive enzymes;

N, control without fish; HC-21-G, reference steroid cortisol-21-glucuronide; C-21-S, reference steroid cortisone-21-sulfate; cps, counts per second.

3.11 Consideration of zebrafish 11β-HSDs

Zebrafish 20β-HSD type 2 was found to catalyze the conversion of cortisone to 20β-hydroxycortisone indicating an involvement in glucocorticoid metabolism. To further elucidate the exact role of the enzyme, it was self-evident to investigate other enzymes accepting cortisone as substrate and also enzymes producing cortisone. These enzymes belong to the family of 11β-HSDs, a family nonuniformly characterized in teleost fish: 11β-HSD type 2 enzymes are described in detail, as these enzymes are responsible for the conversion of cortisol to cortisone and 11-hydroxytestosterone to 11-ketotestosterone, thereby being involved in regulation of stress and reproduction, respectively [111, 112]. 11β-HSD type 1 is annotated in some fish species and supposed to catalyze the conversion of cortisone to cortisol [113, 124]. However, in zebrafish and few other fish species, an enzyme with 11β-HSD type 1 functionality has not yet been found, and its function is thought to be fulfilled by its ancestor 11β-HSD type 3 in zebrafish [113].
Concerning zebrafish 11β-HSD type 2 and 11β-HSD type 3, no data on functional analyses were available in the literature. At the outset of the characterization of zebrafish 11β-HSDs, it was therefore assumed that 11β-HSD type 2 catalyzes the oxidation of cortisol to cortisone and 11β-HSD type 3 the reverse reaction activating cortisone to cortisol. The characterization of zebrafish 11β-HSDs focused on expression analyses during embryonic development, in adult tissues and their expression in dependency of cortisol. Additionally, biochemical parameters were to be determined and compared to 20β-HSD type 2. By analyzing enzymatic activities of all three enzymes, their interplay in glucocorticoid metabolism was to be elucidated.

3.11.1 Expression analysis of 11β-HSDs

The expression pattern of 11β-HSD type 2 and 11β-HSD type 3 during embryonic development and in adult tissues was determined by RT-PCR in comparison to that of 20β-HSD type 2. The results showed that both 11β-HSD type 2 and type 3 were ubiquitously expressed in adult tissues of both sexes with weaker signals for 11β-HSD type 2 in brain, eyes, and spleen (Figure 3.21). 11β-HSD type 3 showed weaker signals only in brain of both male and female fish. During embryonic development, 11β-HSD type 3 displayed a constant level of expression, while 11β-HSD type 2 was expressed with nearly the same pattern as 20β-HSD type 2. Transcripts of both 11β-HSD type 2 and 11β-HSD type 3 were maternally supplied to the zygote as demonstrated by signals obtained already in the 1 cell stage.

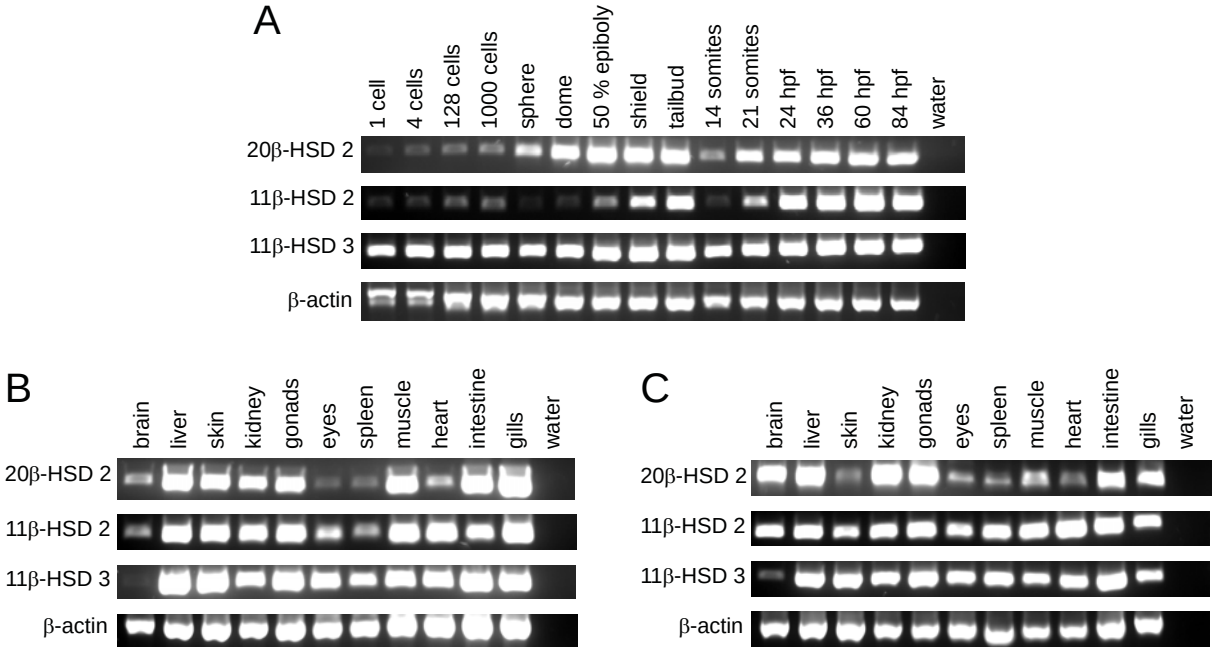

Figure 3.21: Analysis of expression pattern of zebrafish 20β-HSD type 2, 11β-HSD type 2, and 11β-HSD type 3 reveals similar expression of 20β-HSD type 2 and 11β-HSD type 2. Gel photographs show the observed distribution of RT-PCR signals for 20β-HSD type 2, 11β-HSD type 2, 11β-HSD type 3, and β-actin, which was included for normalization. (A) Embryonic development. (B) Adult female tissues. (C) Adult male tissues. hpf, hours post fertilization.

To analyze the influence of cortisol on 11β-HSD type 2 and 11β-HSD type 3, their expression was analyzed in cortisol treated zebrafish embryos by qPCR and compared to the results obtained for 20β-HSD type 2 under these conditions. While 20β-HSD type 2 was up-regulated two- to eight-fold in 24 hpf embryos, 11β-HSD type 2 was moderately up-regulated in a range of 1.5- to two-fold induction. 11β-HSD type 3 was not affected by the treatment even with high cortisol concentrations (Figure 3.22 A). In 48 hpf embryos, 20β-HSD type 2 displayed a prominent induction of up to 18-fold, while 11β-HSD type 2 was up-regulated two- to four-fold. Again, cortisol treatment had no influence on 11β-HSD type 3 expression in this stage (Figure 3.22 B). The up-regulation of zebrafish 20β-HSD type 2 remained four- to six-fold in 72 hpf fish embryos and was accompanied by an up-regulation of 11β-HSD type 2 in the range of two- to four-fold induction. However, the degree of up-regulation of 11β-HSD type 2 was negatively correlated with the cortisol concentration used for the treatment. 11β-HSD type 3 showed a slight down-regulation in 72 hpf cortisol treated embryos at higher cortisol concentrations (Figure 3.22 C).

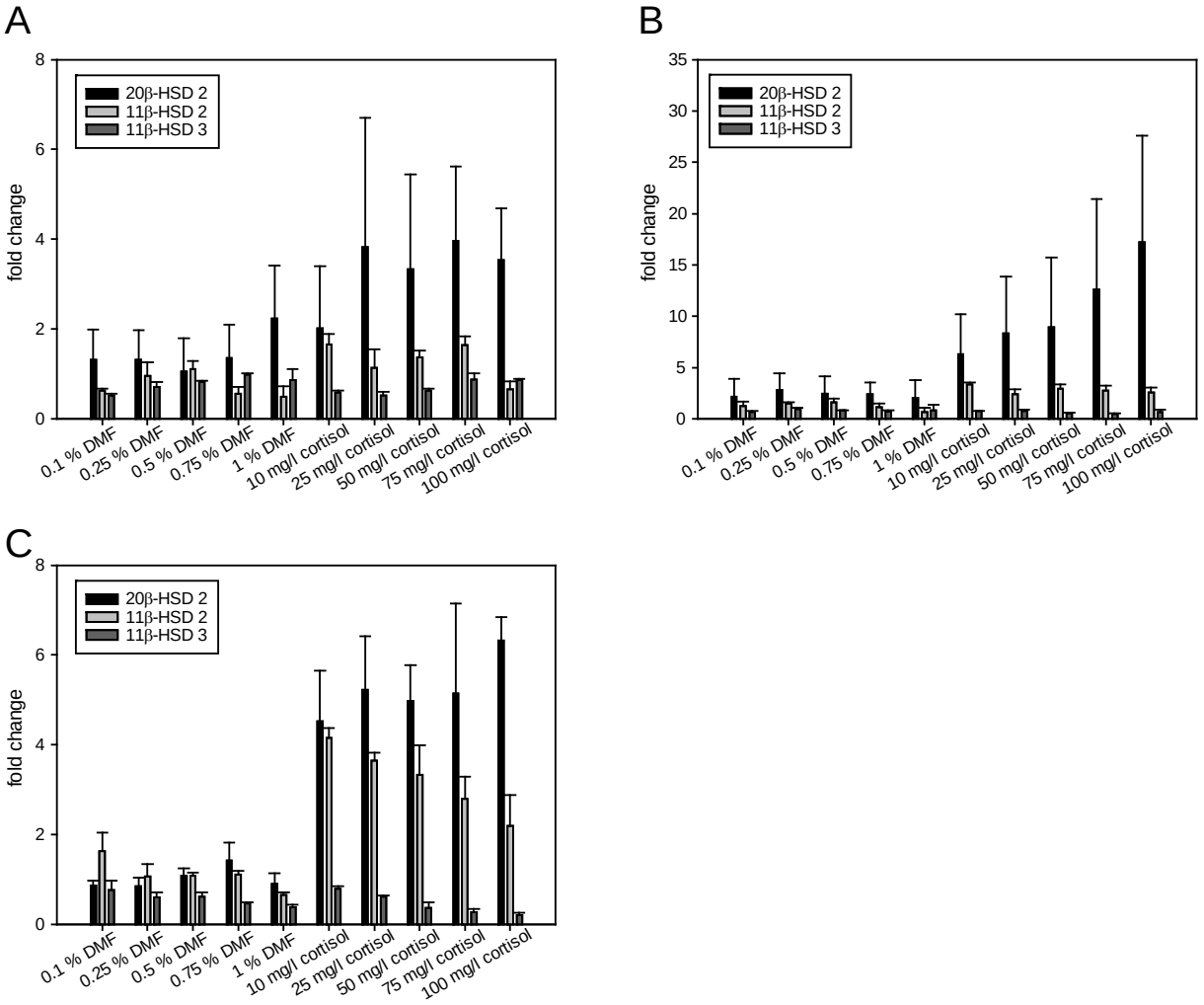

Figure 3.22: Cortisol treatment induces expression of both 20β-HSD type 2 and 11β-HSD type 2, while the expression level of 11β-HSD type 3 is not affected or slightly down-regulated. In each panel, the treatment regimen is shown on the x-axis. Fold changes for 20β-HSD type 2, 11β-HSD type 2, and 11β-HSD type 3 were calculated after normalization to β-actin and compared to untreated fish embryos. 0.1 % DMF is the vehicle control for 10 mg/l cortisol, 0.25 % DMF for 25 mg/l cortisol, and so on. Results for 24 hpf embryos (A), 48 hpf embryos (B), and 72 hpf larvae (C) are shown.

For determination whether cortisol induces the observed effects also after short-time exposure, both 11β-HSD transcripts were quantified in shortly cortisol-treated zebrafish embryos and compared to the results for 20β-HSD type 2. At 24 hpf, both 20β-HSD type 2 and 11β-HSD type 2 revealed a two-fold induction of their transcripts (Figure 3.23). 24 hours post treatment, induction of both genes was even higher in 48 hpf fish embryos with eight-fold induction of 20β-HSD type 2 and 2.5-fold induction of 11β-HSD type 2. Both genes decreased to normal levels at the age of 72 hpf being 48 hours after the cortisol challenge. 11β-HSD type 3 showed no significant expression changes at all throughout the experiment.

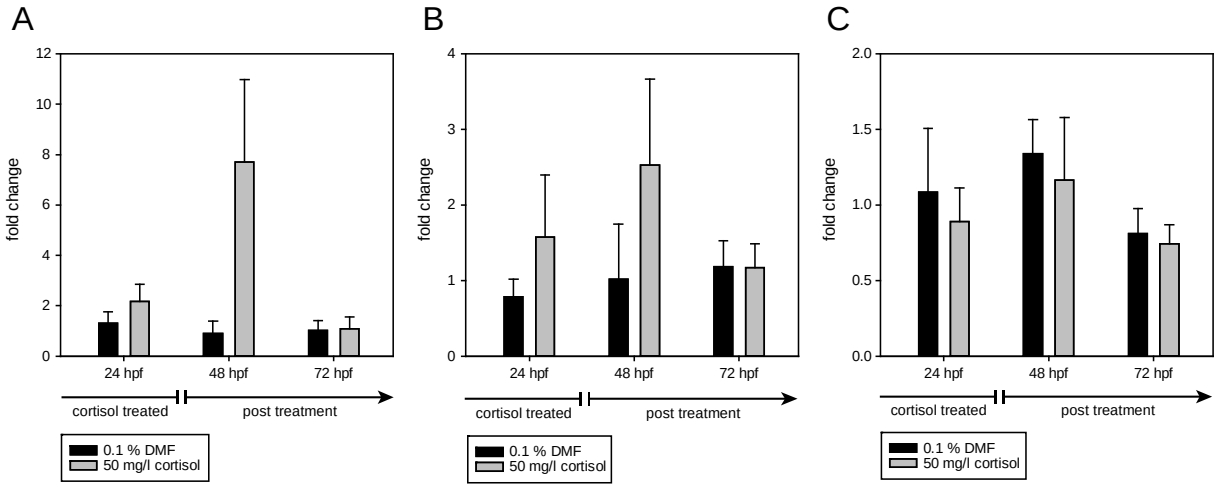

Figure 3.23: Short-term exposure of zebrafish embryos to cortisol results in up-regulation of both 20β-HSD type 2 and 11β-HSD type 2 in 24 hpf and 48 hpf embryos, while 11β-HSD type 3 is not affected. Zebrafish embryos were treated until 24 hpf with 50 mg/l cortisol and afterwards kept in cortisol-free embryo water. Fold changes of gene expression were calculated after normalization to β-actin and compared to untreated fish embryos for (A) 20β-HSD type 2, (B) 11β-HSD type 2, and (C) 11β-HSD type 3.

3.11.2 Biochemical characterization of zebrafish 11β-HSDs

The coding sequences for both 11β-HSD type 2 and 11β-HSD type 3 of zebrafish had been cloned into pcDNA4/*myc*-His B vector by F. Haller. This vector allowed for expression of the enzymes in mammalian systems and produced a fusion protein with a combined myc-his tag at the C-terminus of the protein. Analysis of subcellular localization revealed that both 11β-HSDs localized in the endoplasmic reticulum (data not shown). Pearson's coefficients of colocalization with the ER were 0.76 ± 0.11 for 11β-HSD type 2 and 0.88 ± 0.04 for 11β-HSD type 3, respectively.

In the next step, the catalytic activity of both 11β-HSDs was assessed. Zebrafish 11β-HSD type 2 catalyzed the conversion of cortisol to cortisone using the cofactor NAD^+ with a K_M of 0.189 ± 0.03 µM and a v_{max} of 0.008 ± 0.0005 nmol min^{-1} mg^{-1}. These values were in a similar range than those obtained for zebrafish 20β-HSD type 2 (see Table 3.1).

Zebrafish 11β-HSD type 3 did not catalyze the expected reduction of cortisone to cortisol irrespective of different cofactors that were added to the reaction ($NADH + H^+$ or $NADPH + H^+$). This observation raised the question whether the 11β-HSD type 3 enzyme characterized here is the only potential candidate for the catalysis of the reduction of cortisone to cortisol. In consequence, several databases were searched for fish 11β-HSD type 3 and 11β-HSD type 1 orthologs and the retrieved sequences were analyzed for their relationship using phylogeny. For characterization of the phylogenetic environment, 11β-HSD type 2, 17β-HSD type 2, and 20β-HSD type 2 sequences were included.

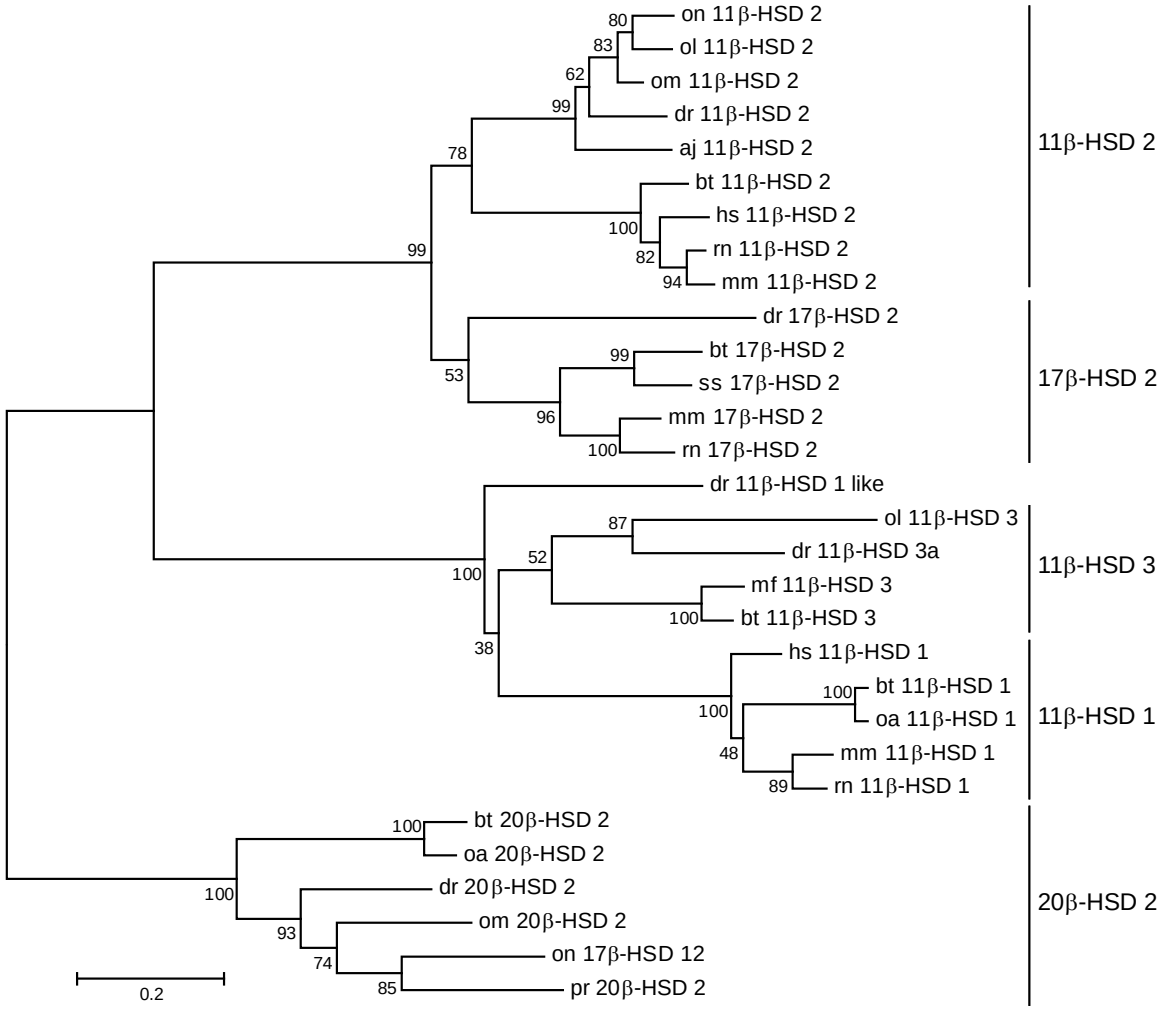

Figure 3.24: Phylogenetic analysis characterizes the related families of 11β-HSD type 2 and 11β-HSD type 3 and identifies an 11β-HSD type 1 like enzyme potentially catalyzing the cortisone-cortisol conversion. 11β-HSD type 2 enzymes cluster together with closely related 17β-HSD type 2 enzymes, while 11β-HSD type 1 and 11β-HSD type 3 enzymes form a separate group. 20β-HSD type 2 enzymes were used as outgroup for this tree. The tree was calculated by means of Neighbor-Joining with bootstrap values of 1000 pseudoreplicates, given in percent at each dichotomy. Species abbreviations: aj, *Anguilla japonica*; bt, *Bos taurus*; dr, *Danio rerio*; hs, *Homo sapiens*; mf, *Macaca fascicularis*; mm, *Mus musculus*; oa, *Ovis aries*; ol, *Oryzias latipes*; om, *Oncorhynchus mykiss*; on, *Oreochromis niloticus*; pr, *Poecilia reticulata*; rn, *Rattus norvegicus*; ss, *Sus scrofa*.

The phylogenetic analysis showed that zebrafish 11β-HSD type 2 clustered in the group of 11β-HSD type 2 enzymes from other species, which was closely related to 17β-HSD type 2 enzymes (Figure 3.24). A second large group was formed by 11β-HSD type 1 and 11β-HSD type 3 enzymes. The 11β-HSD type 3 characterized in this thesis can be found as 11β-HSD type 3a in the tree, as the sequence is annotated like this in some databases. Additionally, a zebrafish enzyme called 11β-HSD type 1 like was found to group in proximity to the 11β-HSD type 1 and type 3 cluster. This sequence is in some databases referred to as 11β-HSD type 3b as it might have originated from a teleost specific genome duplication event. Thus, the 11β-HSD type 1 like sequence constituted a potential candidate for the cortisone-cortisol conversion in zebrafish. However, the question of which enzyme (if any) is really responsible for cortisol formation from cortisol was not further pursued.

3.11.3 Concerted action of 11β-HSD type 2 and 20β-HSD type 2

To determine whether 11β-HSD type 2 and 20β-HSD type 2 can act together in the same pathway in cortisol metabolism (see Figure 4.2), it was attempted to analyze the 20β-hydroxycortisone formation after addition of cortisol and the required cofactors to zebrafish embryo homogenates. To this end, twenty 3 dpf larvae per reaction were homogenized and incubated with cortisol, NAD^+, and $NADPH + H^+$ overnight at 28 °C. Controls for the single reactions of 20β-HSD type 2 (addition of cortisone and $NADPH + H^+$) and 11β-HSD type 2 (addition of cortisol and NAD^+) were included as well as controls without cofactor addition. All obtained samples were analyzed by LC-MS/MS to ensure good sensitivity and separation of 20β-hydroxycortisone and 20α-hydroxycortisone. The single reactions of both enzymes revealed approximately 50 % conversion for 20β-HSD type 2 and 35 % for 11β-HSD type 2. However, in the sample incubated with cortisol, NAD^+, and $NADPH + H^+$ no 20β-hydroxycortisone formation above background levels could be detected, though cortisone was formed (data not shown). This effect was first accredited to the inhibition potential of cortisol towards 20β-HSD type 2 and the experiment was modified by decreasing the cortisol input and increasing the input of zebrafish embryo homogenate. Both approaches proved not successful (data not shown).
Since $NADPH + H^+$ is generally considered to be less stable than NAD^+ [125], the reason for the lack of 20β-hydroxycortisone formation by zebrafish homogenates incubated with cortisol and the required cofactors might have been the degradation of $NADPH + H^+$. Therefore, a sequential set-up of the experiment was designed: the zebrafish embryo homogenate was incubated overnight with cortisol and NAD^+ to allow for the 11β-HSD type 2 reaction. Subsequently, $NADPH + H^+$ was added to the reaction to start 20β-HSD type 2 conversion and incubated for another 8 hours prior to steroid extraction and analysis by LC-MS/MS. Controls for the single reactions of 11β-HSD type 2 and 20β-HSD type 2 as well as controls without the respective cofactors were included and incubated overnight and the following day. Additionally, a control for the 20β-HSD type 2 reaction over day using freshly prepared homogenates was included to determine if 20β-HSD type 2 was degraded during an overnight incubation.
The results (Figure 3.25) showed that again both enzymes catalyzed the expected conversion in their single reactions after an overnight and over day incubation. 11β-HSD type 2 converted approximately 60 % of cortisol to cortisone, while 20β-HSD type 2 produced roughly 80 % 20β-hydroxycortisone. Compared to the formation of approximately 55 % 20β-hydroxycortisone from cortisone by 20β-HSD type 2 after over day incubation alone, this result demonstrated that the enzyme 20β-HSD type 2 is not significantly degraded during long incubation times. In the samples derived from the sequential set-up, formation of cortisone and 20β-hydroxycortisone considerably above background level was detected. This result indicated that 11β-HSD type 2 and 20β-HSD type 2 acted concertedly for the formation of 20β-hydroxycortisone from cortisol via cortisone.

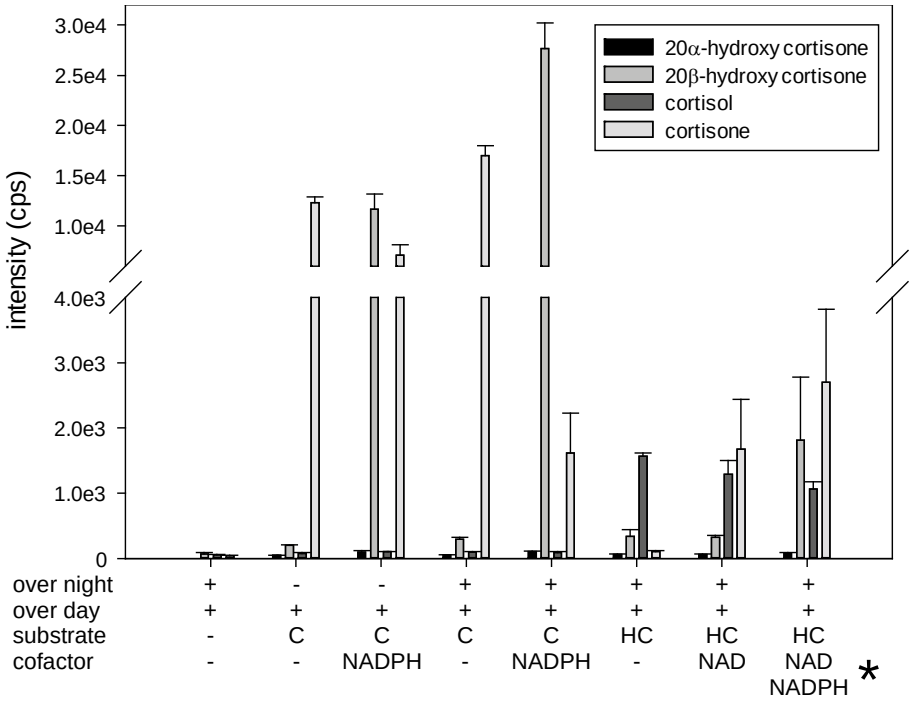

Figure 3.25: Formation of 20β-hydroxycortisone from cortisol can be detected using sequential set-up and demonstrates concerted action of 11β-HSD type 2 and 20β-HSD type 2. Homogenates of 3 dpf zebrafish embryos were incubated for the indicated time (overnight and/or over day) with the denoted substrate and cofactor. Detection of steroids was performed by LC-MS/MS analysis. The asterisk indicates sequential addition of cofactors (NAD^+ overnight followed by addition of $NADPH + H^+$ over day). Abbreviations: C, cortisone; HC, cortisol; NAD, NAD^+; NADPH, $NADPH + H^+$; cps, counts per second.

4 Discussion

The goal of this work was to perform a functional characterization of the orphan SDR enzyme zf3.2 from zebrafish, to assign a physiological function to it, and to annotate the enzyme accordingly. An important milestone to achieve this goal was the identification of the reaction product that was formed by zf3.2 using cortisone as substrate and NADPH + H^+ as cofactor. The SDR enzyme was found to catalyze the reduction of cortisone at position C20 yielding 4-pregnen-17,20β,21-triol-3,11-dione, a steroid that was named 20β-hydroxycortisone (Figure 4.1). This discovery resulted in annotation of zf3.2 as zebrafish 20β-HSD.

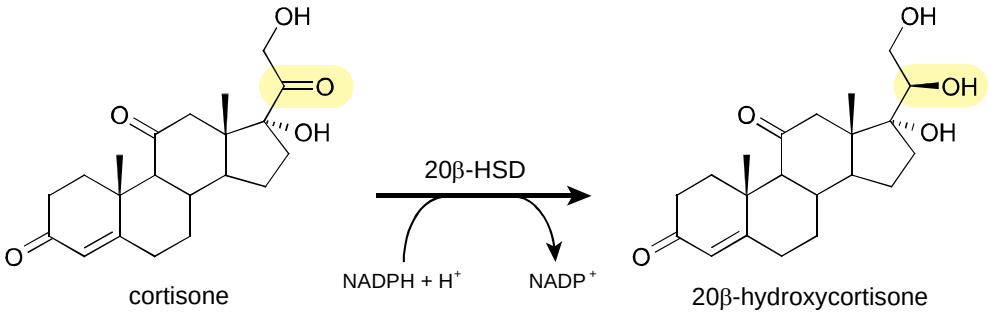

Figure 4.1: Zebrafish 20β-HSD catalyzes the reduction of cortisone to 20β-hydroxycortisone in the presence of cofactor NADPH + H^+.

To demonstrate that this enzyme is not unique to zebrafish and to search for a potential human ortholog, *in silico* searches using Hidden-Markov-Models were performed and returned putative orthologs from many fish species, frog, and two mammals. Surprisingly, no promising candidate sequences were found in rodents or human. The close relationship of 20β-HSDs to enzymes of the 17β-HSD type 3 and 17β-HSD type 12 families complicated the assignment of candidate sequences to either of the three families. Showing approximately 40 % sequence identity, the similarity between all three groups is higher than generally observed for convergently evolved SDR enzymes (approximately 15-30 % sequence identity [79]). Since the ancestor of 17β-HSD type 3 was found to be 17β-HSD type 12 [104], it is most likely that the family of 20β-HSDs evolved from the same ancestral SDR. Thus, sequence homology of an unknown sequence to one of the three families is not sufficient to ensure accurate annotation. Therefore, a thorough phylogenetic analysis is necessary; however, only functional validation can ascertain a correct classification.

To substantiate the annotation of the novel SDR family of 20β-HSD enzymes, it was attempted to include as many 20β-HSD candidate sequences as possible into functional characterization. Among the sequences, the candidate from tilapia had been already annotated as 17β-HSD type 12 by Zhou *et al.* [107], although the authors observed that this sequence clustered in phylogenetic analysis between 17β-HSD type 12 and 17β-HSD type 3. Additionally, after overexpression of the protein Zhou *et al.* detected no activity with the steroidal substrates testosterone, androstenedione, estradiol, and estrone and therefore suggested tilapia 17β-HSD type 12 to belong to a yet unidentified type of SDR [107]. The biochemical characterization of this enzyme performed here supports this suggestion and showed clearly that tilapia 17β-HSD type 12 belongs to the new family of 20β-HSD enzymes. All other fish orthologs as well as the candidate derived from sheep were found to catalyze the same reaction as the zebrafish enzyme. The ortholog from cow was inactive in the assay conditions used here. The characteristics of both mammalian 20β-HSD enzymes are discussed in more detail in chapter 4.3.

The novel 20β-HSDs showed a wide distance in phylogenetic analysis to carbonyl reductase-like 20β-HSD enzymes (20β-HSD/CR) and shared only few identical amino acid residues (approximately 5-10 %), although both enzyme groups belong to the SDR superfamily. Both enzyme families differed

also in substrate specificity and tissue distribution (which is discussed in depth in chapter 4.2). Therefore, it was suggested to name 20β-HSD/CR-like enzymes 20β-HSD type 1, and to separate the novel 20β-HSDs characterized in this thesis by adding the affix type 2 [126]. This approach was in accordance to the nomenclature of other HSD family members, which have been named in the order of their discovery [97]. The SDR nomenclature initiative [75] assigned the acronym SDR12C55 to the gene of zebrafish 20β-HSD type 2 [126].
After elucidation of the reaction product of zebrafish 20β-HSD type 2 and the identification of orthologs in other species (though mostly fish), three hypotheses regarding the biological function of the novel enzyme were proposed. The first hypothesis suggested an involvement of 20β-HSD type 2 concertedly with 11β-HSD type 2 in cortisol catabolism based on the fact that cortisol is inactivated by 11β-HSD type 2 to cortisone [56], which is the substrate for 20β-HSD type 2. The second hypothesis proposed 20β-HSD type 2 to be involved in the biosynthesis of pheromones or 20β-hydroxycortisone to act as a pheromone. Fish commonly use pheromones to mediate a variety of reproductive and non-reproductive functions influencing their behavior [50], and certainly not all molecules functioning as pheromonal cues are known up to now. Another important process involving C21 steroids in fish physiology is the induction of oocyte maturation by the maturation-inducing hormone stimulating the breakdown of the germinal vesicle, chromosome condensation, and formation of the first polar body [127]. The third hypothesis proposed an involvement of 20β-HSD type 2 in the biosynthesis of the maturation-inducing hormone, since this hormone shares structural features with 20β-hydroxycortisone and is synthesized (in some fish species) by enzymes of the 20β-HSD/CR like family.

4.1 Involvement of 20β-HSD type 2 in cortisol catabolism – the identification of a novel pathway

Like in mammals, cortisol functions as major stress hormone in teleostean fish. Stressors are perceived in the hypothalamus via input from the nervous system and then transmitted along hormone cascades of the hypothalamus-pituitary-interrenal axis (HPI axis) for immediate activation [13, 14]. Stimulated interrenal cells enclosed in the head kidney synthesize and release cortisol to the circulation [18]. *De novo* biosynthesis of cortisol starts with the transport of cholesterol into the mitochondria followed by side chain cleavage and 17α-hydroxylation. Further steps include 3β-hydroxysteroid dehydrogenation, 21-hydroxylation, and 11-hydroxylation [20]. When released to the circulation, cortisol contributes to a general activation of the organism and preparation of the appropriate stress response [20]. Additionally, the hormone is responsible for the regulation of the intermediary metabolism [128], ionic and osmotic homeostasis [40], as well as immune functions, growth, and behavior [6, 20]. Beside its role in stress response, cortisol was also found to be important for the circadian cell cycle rhythm [46] and to play a role in embryonic development, though the precise function is not unraveled yet [13, 42].
Cortisol mediates its effects via binding to the glucocorticoid receptor, which subsequently translocate to the nucleus and regulate transcription of target genes [20, 25]. Afterwards, metabolic clearance comes into action, with the first inactivating step of cortisol being oxidized to cortisone catalyzed by 11β-HSD type 2 [56, 124]. Further reactions of catabolism include reductases, oxidoreductases, and hydroxylases yielding a broad spectrum of glucocorticoids that can be excreted [20]. As described briefly in the previous chapter, it was hypothesized for the novel 20β-HSD type 2 together with 11β-HSD type 2 to play a role in cortisol catabolism (Figure 4.2). The reaction product 20β-hydroxycortisone might be subsequently conjugated with glucuronic acid and/or sulfates generating a water soluble excretion product. Therefore, 11β-HSD type 2 and 20β-HSD type 2 might represent an effective mechanism for stress reduction. According to the situation in humans, where 11β-HSD type 1 is responsible for tissue specific, local production of cortisol from cortisone [96], it was assumed that the fish ortholog 11β-HSD type 3 resumes this function in teleostean fish (Figure 4.2). The varied experimental evidence obtained in this work support this hypothesis strongly and is discussed in the following chapters.

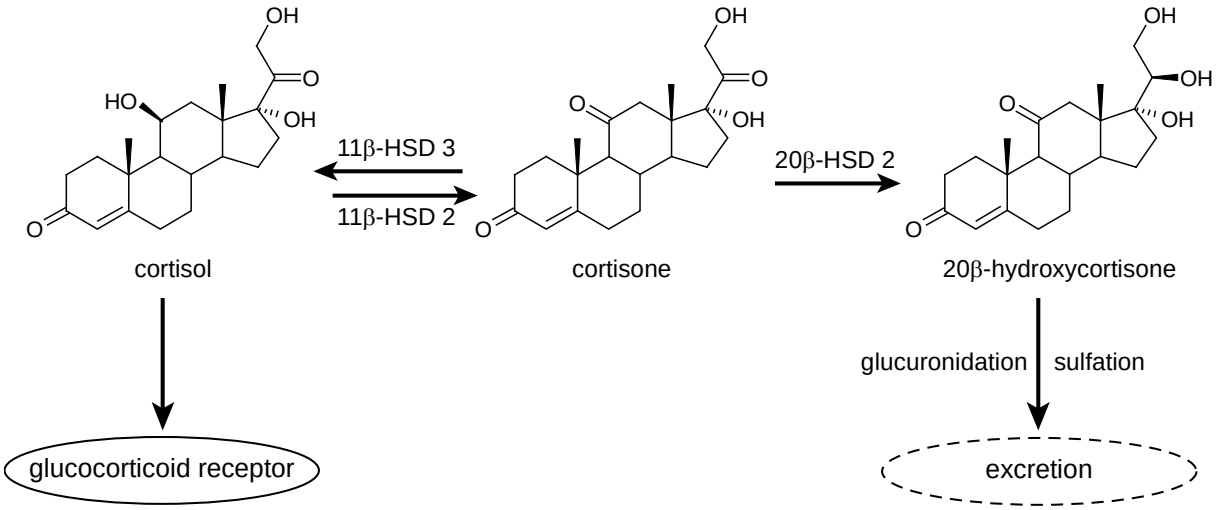

Figure 4.2: Hypothetical pathway for cortisol inactivation and excretion in zebrafish. 11β-HSD type 2 and 20β-HSD type 2 are hypothesized to act together in cortisol inactivation. The reaction product of 20β-HSD type 2, 20β-hydroxycortisone, could be glucuronidated and/or sulfated and subsequently excreted. 11β-HSD type 3 is assumed to form cortisol from cortisone, thereby enhancing glucocorticoid action.

4.1.1 First clue: cell biology, kinetic parameters, and expression of 20β-HSD type 2

Steady-state kinetic analyses demonstrated a low K_M value for zebrafish 20β-HSD type 2 towards cortisone and a K_M value in a similar dimension for 11β-HSD type 2 towards cortisol. Both values lay in the range of physiological steroid concentrations and are comparable to corresponding kinetic parameters of 17β-HSD type 1 from zebrafish and human [94], thereby highlighting physiological significance of both catalyzed reactions. The obtained kinetic parameters of 11β-HSD type 2 and 20β-HSD type 2 indicate an efficient conversion of cortisol to cortisone to 20β-hydroxycortisone, thus reducing the amount of cortisol able to activate the glucocorticoid receptor. Additionally, 20β-HSD type 2 can be considered to be responsible for reducing cortisone amounts available for reconversion to cortisol by 11β-HSD type 3.

Regarding subcellular localization, both 11β-HSD type 2 and 20β-HSD type 2 were found to localize in the endoplasmic reticulum. This close spatial proximity in the same compartment might hint to a concerted action, facilitating steroid transport between the two enzymes and thereby ensuring a rapid conversion. Beside this speculation, localization in the endoplasmic reticulum is common among 17β-HSD enzymes from different families [93]. The two families of 17β-HSD type 3 and 17β-HSD type 12, closely related to 20β-HSD type 2, have been found to localize in this compartment as well [104, 129]. The subcellular localization of human 11β-HSD type 2 is not conclusively analyzed, as experimental evidence demonstrated either endoplasmic [30], cytoplasmic or nuclear localization [28]. Since the large molecule GFP as tag to analyze subcellular localizations of recombinant proteins has the potential to mask localization signals [130], the significantly smaller myc tag has been used here. Nevertheless, for each candidate protein the tag was placed N-terminally and C-terminally to rule out any influences on localization by the tag. Generally, the position of the myc tag had no influence on the subcellular localization, which is reflected in similar correlation coefficients for colocalization with the compartment marker molecules. Only 20β-HSD type 2 from sheep fused to a C-terminal myc tag showed a significantly lower correlation coefficient. This discrepancy was probably due to a different level of expression for the sheep 20β-HSD type 2.

The expression of 20β-HSD type 2, 11β-HSD type 2, and 11β-HSD type 3 was analyzed in detail by RT-PCR in adult zebrafish tissues and during the development of zebrafish embryos. In adults, all three enzymes were ubiquitously expressed, although 20β-HSD type 2 and 11β-HSD type 2 showed stronger signals in liver, kidney, intestine, and gills. Since these tissues are associated with steroid excretion [55], the expression pattern underlines an involvement of 11β-HSD type 2 and 20β-HSD

type 2 in cortisol catabolism and excretion. Some minor differences in expression of both enzymes between the sexes were observed, but these differences were not sufficiently prominent to warrant a sex-specific function of both enzymes.

Expression analysis by RT-PCR revealed an undulating expression for 20β-HSD type 2 during zebrafish development with increasing signals until tailbud stage, a decrease during somitogenesis followed by stable expression after 24 hpf. 11β-HSD type 2 displayed a remarkably similar pattern during the development, while 11β-HSD type 3 showed no differences in expression level. The observation of expression of all three enzymes already in the zygote demonstrates maternal supply of the respective transcripts to the embryo, underlining the importance of these mRNAs for early embryonic development. After onset of embryonic transcription, signals for 11β-HSD type 2 and 20β-HSD type 2 grow more intense, indicating embryonic transcription of the respective genes. Alsop & Vijayan [42] have quantified cortisol in zebrafish embryos and showed maternal supply of the hormone to the zygote. Cortisol concentrations decreased until hatch, which indicate catabolic processes. The concerted action of 11β-HSD type 2 and 20β-HSD type 2 might be responsible for the decrease of cortisol levels to protect the developing embryo from excess cortisol.

Valuable insights into spatial 20β-HSD type 2 expression during embryogenesis were obtained by whole mount *in situ* hybridization analysis. Generally, a similar expression pattern as for adults determined by RT-PCR was observed, but the restriction of 20β-HSD type 2 expression to certain tissues already in 30 hpf embryos was striking. Strong signals were obtained in pronephric ducts, digestion associated tissues, and neuronal tissues. The restriction of 20β-HSD type 2 expression to the grey matter of the brain fits to the theory of a protective mechanism that involves both 11β-HSD type 2 and 20β-HSD type 2, since cortisol action takes place in the cell body and not in the myelinated nerve fibers. As soon as the gills start to develop (first as pharyngeal arches in 48 hpf, then as branchial arches in 4 dpf larvae), strong signals of 20β-HSD type 2 expression could be detected in this tissue. Apparently, the gills are another location for steroid catabolism in zebrafish larvae beside pronephric ducts and the digestive tract. In rainbow trout, it has been demonstrated that steroids can be excreted via three routes: from the digestive system via bile, from the kidney via urine, and from the gills via diffusion [55].

Noteworthy is the similarity of the spatial expression pattern obtained for 20β-HSD type 2 compared to published data for the zebrafish glucocorticoid receptor isoform α (GRα). By means of RT-PCR, GRα was detected in brain, eye, gills, heart, intestine, kidney, liver, muscle, ovary, and spleen [38]. Furthermore, GRα mRNA was also found in these tissues by whole mount *in situ* hybridization analysis of developing embryos [25, 131], displaying a strikingly similar pattern to that of 20β-HSD type 2. Expression data for 11β-HSD type 2 is limited; some studies have analyzed its expression by RT-PCR [38, 42], but only one study analyzed the expression by whole mount *in situ* hybridization [132]. Signals for 11β-HSD type 2 were detected in the head mesenchyme, heart, otic vesicle, pancreas, pharyngeal arches, pharynx, and the retina of zebrafish embryos of the AB/Tuebingen strain, which is slightly different from the strain AB/EK used here. These strain differences might be the reason for slightly different spatial expression pattern of 11β-HSD type 2 compared to 20β-HSD type 2 and GRα. Nevertheless, a similar expression pattern of 20β-HSD type 2, 11β-HSD type 2, and GRα would strongly underline an involvement of both enzymes in cortisol metabolism, thereby protecting glucocorticoid target tissues from an excess of cortisol and allowing for fast inactivation and removal of cortisol. Since a direct comparison of expression patterns by whole mount *in situ* hybridization is missing up to now, conclusive validation of a concerted action of 20β-HSD type 2 and 11β-HSD type 2 based alone on expression data is not yet possible. Thus, whole mount *in situ* hybridization for all three genes in parallel or dual-color *in situ* hybridization assays using the same zebrafish strain would be advisable.

4.1.2 Mimicking stress: cortisol and its implications on 20β-HSD type 2

The results obtained after cortisol treatment of zebrafish embryos were fundamental for the elucidation of the biological function of 20β-HSD type 2, but they also raised additional questions. Initially, zebrafish embryos were treated with different cortisol concentrations for a long time (between 3 hpf and 72 hpf). Quantification of 20β-HSD type 2 and 11β-HSD type 2 transcripts showed an up-regulation of both genes in cortisol treated zebrafish embryos, while 11β-HSD type 3 was not affected or slightly down-regulated. These observations emphasized the hypothesis regarding the role of all three enzymes in cortisol metabolism. Both 11β-HSD type 2 and 20β-HSD type 2 were induced by cortisol, mediating efficient inactivation of the potent hormone, while the putative cortisol-synthesizing enzyme 11β-HSD type 3 was not regulated or slightly decreased. Although no promoter analyses were performed, it is likely that the regulation of these genes is glucocorticoid receptor dependent.

Spatial expression analysis of 20β-HSD type 2 in cortisol treated zebrafish embryos by whole mount *in situ* hybridization revealed no differences compared to untreated embryos. However, the intensity of specific staining increased, indicating stronger expression upon cortisol treatment as already quantified by qPCR.

Cortisol treatment, especially with concentrations exceeding 10 mg/l, entailed developmental changes, that were first observed at 48 hpf, but in some cases intensified until 72 hpf. Similar results were obtained by Hillegass *et al.* [44], who also observed no phenotypical alterations with concentrations below 10 mg/l. The authors addicted the impact of high cortisol concentrations on somitogenesis, organ development, and tissue architecture to a dysregulation of several matrix metalloproteinases [44, 45], which are responsible for remodeling of the extracellular matrix that occurs during tissue development.

While 20β-HSD type 2 expression was strongly induced by cortisol treatment, the significant decrease of the enzymatic activity was surprising. This discrepancy was in contrast to the expectation that more mRNA also results in more protein and thereby in higher enzymatic activity. However, such deviations have been reported to exist in *Corynebacterium glutamicum* [133], and have also been observed in rats and human lung adenocarcinomas [134, 135]. Other possible explanations might have been translational effects, posttranslational modifications, or inhibitory effects of accumulated substrate or product on the enzyme's activity.

To determine the reason for the marked discrepancy in 20β-HSD type 2 expression and activity, several experiments were performed. At the outset, the influence of a short time exposure of zebrafish embryos to cortisol on 20β-HSD type 2 expression and activity was performed with treatment for 24 hours and cortisol removal after that. In the presence of cortisol at 24 hpf, high mRNA expression was accompanied by a low enzymatic activity, as observed in earlier experiments. 11β-HSD type 2 was also up-regulated as detected before. However, 24 hours after the removal of cortisol (at 48 hpf) the enzymatic activity of 20β-HSD type 2 was fully restored in parallel to high mRNA levels of both 20β-HSD type 2 and 11β-HSD type 2. Despite cortisol removal from the medium, the cortisol concentration in the fish embryo itself was probably still elevated leading to continuous overexpression of both 11β-HSD type 2 and 20β-HSD type 2. Although a cortisol concentration known to induce phenotypical alterations with continuous exposure at 48 hpf was applied (50 mg/l cortisol), the shortly treated zebrafish embryos displayed no abnormalities at 48 hpf. This indicates that cortisol catabolism by 11β-HSD type 2 and 20β-HSD type 2 after cortisol removal from the medium works efficiently to avoid phenotypical changes. On the other hand, it could be that high cortisol concentrations exert their adverse effects first between 24 hpf and 48 hpf. At 72 hpf, being 48 hours after cortisol removal, the transcript amount of 20β-HSD type 2 and 11β-HSD type 2 were comparable to untreated controls, while the enzymatic activity of 20β-HSD type 2 was still slightly elevated. Although the increased mRNA amounts of 11β-HSD type 2 and 20β-HSD type 2 at 48 hpf are putatively necessary to catabolize excess cortisol to regain homeostasis, this process seems to be accomplished at 72 hpf, which is reflected by normal expression of both genes. The restored activity of 20β-HSD type 2 after cortisol withdrawal rather hints to an inhibitory effect of the enzyme in presence of cortisol than to posttranslational modifications or translational effects.

Therefore, inhibition analyses were performed using zebrafish 20β-HSD type 2 recombinantly expressed in HEK293 cells. Initial experiments revealed that 20β-HSD type 2 is neither inhibited by its substrate cortisone nor its product 20β-hydroxycortisone. However, cortisol inhibited zebrafish 20β-HSD type 2 as competitive inhibitor with a K_I of 1.2 µM. These results demonstrated impressively that cortisol causes the discrepancy of 20β-HSD type 2 expression and activity observed in cortisol treated zebrafish embryos. Although the actual concentration of cortisol was not determined in zebrafish larvae, the concentration of cortisol in the fish water was higher than the K_I of 20β-HSD type 2 (Table 4.1). Table 4.1 shows also that the inhibition increased with increasing cortisol concentrations in all stages analyzed.

Table 4.1: Relation of cortisol concentration in fish water and inhibition of zebrafish 20β-HSD type 2 in different stages.

cortisol concentration in fish water (mg/l)	cortisol concentration in fish water (µM)	inhibition of 20β-HSD type 2 (%) 24 hpf	inhibition of 20β-HSD type 2 (%) 48 hpf	inhibition of 20β-HSD type 2 (%) 72 hpf
10	27.6	38.88 ± 3.29	14.91 ± 4.77	30.35 ± 12.77
25	69.0	71.30 ± 3.38	56.00 ± 1.27	56.20 ± 4.29
50	137.9	84.60 ± 2.26	66.84 ± 2.19	69.60 ± 2.71
75	206.9	89.39 ± 1.72	58.01 ± 8.63	61.70 ± 12.70
100	275.9	90.54 ± 2.55	67.95 ± 4.06	84.05 ± 3.68

The inhibition of 20β-HSD type 2 by cortisol could entail severe physiological implications, when a putatively catabolic enzyme is inhibited by the steroid that should be inactivated. However, in these experiments here artificially high cortisol concentrations were used that are unlikely to occur in nature. Additionally, the physiological cortisol concentrations in fish even in stressed situations are in the nanomolar range [42, 43, 48, 136] and therefore far from inhibiting 20β-HSD type 2.

Although the discrepancy between 20β-HSD type 2 mRNA and activity in cortisol treated zebrafish embryos seems to be well explained by cortisol inhibition of the enzyme, a polyclonal antibody was developed to determine the amount of 20β-HSD type 2 protein in fish homogenates. Application of the polyclonal antibody from rabbit #2 in the optimized Western Blot protocol to protein fractions prepared from cortisol-treated zebrafish larvae revealed that the amount of 20β-HSD type 2 increased upon cortisol treatment. This observation was confirmed by relative quantification of signal intensities of 20β-HSD type 2 compared to untreated control samples. Analysis of both insoluble protein fractions, the 700 x g pellet and the 55000 x g pellet, yielded equivalent results. Although these experiments were only performed using 3 dpf zebrafish larvae, they show impressively that the increased mRNA levels of 20β-HSD type 2 induced by cortisol are also translated resulting in increased protein levels compared to untreated controls. Therefore, the expectation that more transcript results in more protein holds true also for 20β-HSD type 2 in cortisol treated zebrafish embryos. The decreased level of 20β-HSD type 2 activity can most probably be ascribed to the inhibitory effect of cortisol (in artificially high concentrations) on the enzyme. This is also underlined by the determination of 20β-HSD type 2 activity during fractionation of zebrafish homogenates as control of the fractionation procedure. The activity of 20β-HSD type 2 per µg total protein in fractions derived from cortisol treated fish was significantly higher than in untreated or DMF treated controls. Although this observation is in contrast to the reduced 20β-HSD type 2 activity as determined without fractionation, it can be explained by the preparation technique necessary for successful Western Blotting. Prior to homogenization and fractionation, zebrafish larvae were thawed in deyolking buffer and the amount of yolk manually reduced. This step seems to decrease cortisol amounts in the fish larvae itself; not indicating that cortisol is solely stored in the yolk, but rather demonstrating a dilution process from the whole fish into the buffer during the preparation. The cortisol concentration seems to be decreased below the K_I of 20β-HSD type 2 restoring its activity in each fraction analyzed.

Despite the artificial inhibition of 20β-HSD type 2 by cortisol it can be stated that cortisol induces 20β-HSD type 2 expression on both transcript and protein level and will probably also lead to increased 20β-HSD type 2 activity in physiological situations. This conclusion further strengthens the hypothesis of 20β-HSD type 2 being involved in cortisol catabolism concertedly with 11β-HSD type 2. Both enzymes therefore are likely to be important in stress reduction.
Analyses of the impact of steroid hormones from other steroidal classes on 20β-HSD type 2 expression were performed to determine if they regulate 20β-HSD type 2 expression mediated by their respective receptors. Unfortunately, no bioinformatic tools allowing for transcription factor binding site prediction in zebrafish promoter sequences were available. Therefore, the observed up-regulation of 20β-HSD type 2 by cortisol can only be speculated to be mediated by the glucocorticoid receptor. However, the observation that corticosterone induced 20β-HSD type 2 expression in a similar range as cortisol underlines the involvement of GRα in 20β-HSD type 2 regulation. Although corticosterone is no hormone naturally occurring in teleostean fish [137], it is almost identical to cortisol lacking only the 17α-hydroxyl group and was found to bind to and activate the teleostean glucocorticoid receptor [20].
Active forms of progestins and androgens had no significant influence on 20β-HSD type 2 expression, indicating that their respective receptors have no binding site in the promoter of 20β-HSD type 2. However, estradiol treatment led to two-fold up-regulation of 20β-HSD type 2 in 24 hpf embryos, while its expression was decreased in older fish embryos. This effect might be due to the severe developmental abnormalities accompanied by treatment with estradiol in the concentrations used here. This is not surprising, as already lower concentrations of 17β-ethinylestradiol, a derivative of estradiol with higher potency [138], resulted in long lasting changes of development and reproduction [139].

4.1.3 20β-HSD type 2 morphants: normally unaffected, but susceptible to stress

Different approaches of gene targeting are powerful tools to analyze gene functions *in vivo* using genetically modified organisms. For most model organisms, beginning with bacteria, yeast, but also plants, vertebrates, and mammals, methods for genetic modifications are available. These methods can either belong to the forward genetics approach (phenotype driven) or to the reverse genetics approach, which is candidate gene driven. Methods for reverse genetic approaches include targeted inactivation (knock-out, loss of function), exchange of genes (knock-in), and targeted mutations yielding an optimized gene (gain of function). Like other model organisms, zebrafish can be used to generate stable transgenic fish expressing the modified gene of interest in subsequent generations [63, 64, 140, 141]. However, since the generation of transgenic zebrafish is time consuming, methods for transient genetic modification especially in zebrafish embryos have been developed. These methods are based on microinjection of nucleic acids (both DNA and RNA are possible) into the embryo leading to transcription and translation of the injected molecules. Optical clarity of the embryo allows for easy monitoring if labeled molecules were used. The drawback of injection of nucleic acids is the naturally occurring degradation, which has been overcome by the development of the morpholino antisense technology [116, 117, 142]. Morpholinos can bind to complementary sequences of RNA and thereby inhibit splicing of mRNA precursors or translation of mRNA [116, 117]. The effects of a morpholino can be best observed in early stages of embryonic development, because every cell division reduces the amount of morpholino per cell.
For the knock-down of zebrafish 20β-HSD type 2 a splicing morpholino was designed, specifically targeting zygotic transcription of the *Hsd20b2* gene. The knock-down of 20β-HSD type 2 was verified on mRNA and activity level and demonstrated a significant decrease in 20β-HSD type 2 activity in morphant fish larvae. However, 20β-HSD type 2 morphants showed no developmental abnormalities under normal culture conditions. Since 20β-HSD type 2 was hypothesized to play a role in cortisol catabolism and was found to be up-regulated upon cortisol treatment, it was self-evident to challenge 20β-HSD type 2 morphants with cortisol, thereby mimicking stress. For challenging, 10 mg/l cortisol was chosen, as this concentration was sufficient for induction of 20β-HSD type 2 expression, but did not visibly harm wild-type zebrafish embryos. In cortisol challenged morphants, phenotypical abnormalities first appeared at 48 hpf and persisted and in some cases intensified until 72 hpf. Cortisol

challenged 20β-HSD type 2 morphants that displayed a 'severe' phenotype at 48 hpf were sometimes found to die before getting 72 hours old. The observed developmental changes, characterized by yolk deformation, altered somitogenesis, kinked or truncated tails, and pericardial edema, resembled the 'cortisol phenotype' described earlier by Hillegass *et al.* [44]. This phenotype was also observed in the long-term cortisol challenge experiment performed in this work.
Although the precise role of cortisol in embryonic development of teleost fish is not unraveled yet, the hormone is provided maternally to the zygote of several teleost species ([42], and references therein) indicating its importance in embryonic development [13, 45]. Being a potent hormone, chronic exposure to elevated cortisol concentrations causes severe effects. Teleost fish embryos exposed to excess cortisol show an increased mortality and developmental defects [44, 45, 143]. In adult fish, chronic stress and elevated cortisol concentrations in plasma have impact on growth, reproduction, and immune functions, and lead to increased mortality due to diseases and infections [11, 37, 47, 144]. The phenotypical changes in cortisol challenged 20β-HSD type 2 morphants indicated an impaired cortisol catabolism pathway and a reduced capability to cope with stress. This observation strongly underlines an involvement of zebrafish 20β-HSD type 2 in cortisol catabolism and stress reduction. Additionally, 11β-HSD type 2 and 20β-HSD type 2 might protect developing tissues from an excess of cortisol.
However, not all 20β-HSD type 2 morphants developed abnormalities upon cortisol challenging. This is probably due to egg-to-egg differences in microinjection despite thorough injector calibration. Another parameter difficult to assess is the mortality rate. The knock-down of 20β-HSD type 2 in cortisol challenged fish can be potentially lethal. However, especially in the first 24 hours of zebrafish development it is problematic to determine the exact reason for embryo mortality. Zebrafish embryos perform the first cell divisions even if they were not fertilized [22], but die afterwards. The embryo could also be damaged by the injection procedure or died due to toxic effects of the morpholino.
Since 11β-HSD type 2 and 20β-HSD type 2 are hypothesized to act together in a cortisol catabolism pathway, it would be interesting to analyze the effects of cortisol challenge on a knock-down of 11β-HSD type 2 and compare them to 20β-HSD type 2 morphants. Furthermore, a simultaneous knock-down of both enzymes might provide interesting effects.

4.1.4 Close to physiology: the HPI axis and 20β-HSD type 2

Stressors are perceived in the hypothalamus due to input from the central and peripheral nervous system and subsequently transmitted along the hypothalamus-pituitary-interrenal (HPI) axis in teleost fish [13, 14]. The first hormone secreted by the hypothalamus is corticotropin releasing hormone (CRH) stimulating corticotropic and melanotropic cells of the pituitary [16] to release adrenocorticotropic hormone (ACTH) to the circulation [17]. ACTH binds to the melanocortin 2 receptor on the surface of interrenal cells [15] embedded in the head kidney, thereby inducing the biosynthesis and release of cortisol to the circulation [18]. The *de novo* synthesis of cortisol involves several transport processes and catalytic conversions. Steroidogenic acute regulatory protein (StAR) mediates the transport of cholesterol into mitochondria, where the following enzymatic reactions beginning with the side chain cleavage occur. Afterwards, 17α-hydroxylation, 3β-hydroxysteroid dehydrogenation and 21-hydroxylation yield 11-deoxycortisol, which in the last step is converted to cortisol by 11-hydroxylase (Cyp11b2) [20].
Not every stressor stimulates the same reaction with a similar intensity of stress response. Especially the responses to acute stressors differ from responses to chronic stressors. Acute stressors are derived from challenging situations and are normally short term but induce a strong reaction, e.g., predation or fighting [8]. On the contrary, chronic stressors are less common in nature, but mostly caused by anthropogenic influence on ecosystems like pollution or aquaculture. They evoke a stress response with low intensity that is persisting as long as the stressor is perceived [8]. Beside the classification of acute and chronic stressors, stressors can also be classified by their origin to be either physical and environmental or social and symbolic [8]. For fish, the physical stressors are multifaceted and have been the focus of many studies. Net handling stress [145] and swirling stress [49] are common physical stressors, while crowding or confinement stressors [36, 136] as well as predators [48] are mostly assigned to the category of social stress [8].

While for adult fish many different stressors and reproducible stressing protocols exist in the literature, the situation is quite different for fish larvae. One matter raising problems is the development of the stress axis and the determination of the functionality of the HPI axis. However, the ontogeny of the HPI axis in zebrafish is characterized and the time point at which the larvae react with cortisol synthesis upon a stressor is well determined [13, 15, 42]. These studies therefore provided guidelines for the experimental design of the physical stress assay used in this work.

For elucidation whether 20β-HSD type 2 and 11β-HSD type 2 are up-regulated by stress but independent of artificial cortisol treatment, zebrafish larvae were challenged with a short-time physical stressor. This stressor consisted of swirling for 30 sec and was adapted from Alsop & Vijayan [42], who have shown that the stress axis is fully functional by 97 hpf and that cortisol concentrations are significantly elevated already 5 min after the swirling stress. Here, 5 dpf larvae were subjected to a 30 sec swirling stressor and afterwards several genes from the HPI axis as well as 11β-HSD type 2 and 20β-HSD type 2 were quantified at different time points after the stressor. Most HPI axis genes were up-regulated upon physical stress and did not decrease to unstressed levels, demonstrating an activated HPI axis as well as successful stress transmission. However, these observations deviate slightly from results obtained by subjecting adult zebrafish to a long term, 60 min vortex stressor, where *Mc2r, Star*, and *Cyp11b2* showed highest expression after 20 min, and *Crh* displayed a peak already after 10 min [49]. These discrepancies are most probably caused by differences in stress challenge approaches and RNA sources. Here, 5 dpf larvae were subjected to a short term stressor, while Fuzzen *et al.* applied a long term stressor to adult zebrafish. Furthermore, Fuzzen *et al.* quantified HPI axis genes in head kidney alone, which is contradictory to the approach of quantification of transcripts obtained from whole larvae. Nevertheless, the general outcome of both approaches is comparable and might as well reflect different regulatory processes between larvae and adult zebrafish.

As observed for the other HPI axis genes, the mRNA of the cortisol inactivating enzyme 11β-HSD type 2 was found by Fuzzen *et al.* [49] to increase until 20 min, but after 60 min levels were comparable to unstressed conditions. In 5 dpf larvae subjected to short term stressor, a slight, but steady increase of the 11β-HSD type 2 mRNA was detected. Additionally, 20β-HSD type 2 showed in general the same tendency, but displayed a greater fold change than 11β-HSD type 2. Transcripts of both genes showed no decrease to unstressed levels throughout the experiment, indicating an involvement in biochemical stress reduction by cortisol inactivation and putative excretion even 60 min after the stressor was perceived. In the light of a protective role of 20β-HSD type 2, as assumed and discussed in the previous chapters, this observation is reasonable in view of the fact that excess cortisol concentrations can exert adverse effects on zebrafish development. Both 11β-HSD type 2 and 20β-HSD type 2 remain on higher levels even 60 min post stress to ensure efficient cortisol catabolism, thereby avoiding negative effects of cortisol on the fish's development. It would be interesting, though, to quantify the 20β-HSD type 2 transcript in the experimental set-up used by Fuzzen *et al.* (2010).

Contrary to the expectation, the enzymatic activity of 20β-HSD type 2 was not changed upon swirling stress, although the amount of the transcript increased quickly. Apparently, translation of mRNA into protein might take some time that was not covered in the experimental design. On the other hand, it is also possible that the 20β-HSD type 2 activity is not affected by 30 sec stressor. Different results might be obtained when zebrafish larvae are subjected to a long term swirling stress.

Especially chronic stress or a stressor that is inordinately severe causes the physiological response mechanisms to become detrimental to the fish's health, a state that is called 'maladaption' [6]. Changes in growth, condition, resistance against diseases, behavior, and survival are caused [6]. In this respect, a great importance is attached to the cortisol catabolism pathways, as the amount of cortisol is influenced by the ratio of biosynthesis and catabolism. While many studies have analyzed the impact of stress and cortisol on many aspects of fish physiology [6-8, 11, 20], the aspect of cortisol inactivation and excretion was so far mainly neglected. Only a few studies analyzed the expression of 11β-HSD type 2 as cortisol inactivating enzyme upon stress [10, 42, 49]. The results obtained in this work thus provide an interesting starting point to unravel the biochemical part of stress reduction in fish in more detail.

4.1.5 Excreted glucocorticoids: is 20β-hydroxycortisone among them?

In general, steroids dedicated for excretion have two important characteristics. Firstly, those steroids do not bind to receptors and also do not activate these receptors. Secondly, as steroids are mostly lipophilic compounds, steroids destined for excretion are enzymatically hydrogenated to increase water solubility. The hydrophilicity can be enforced by conjugation of the respective steroid to glucuronic acid or sulfates. Steroid conjugates can then be easily excreted via the urine. However, not all excreted steroids are necessarily conjugated, as in human urine also ample amounts of free steroids can be found [146, 147], given that they have sufficient water solubility.
The above mentioned facts apply to glucocorticoids as well. The results of the characterization of 20β-HSD type 2 obtained up to now substantiate the hypothesis of an involvement of zebrafish 20β-HSD type 2 in cortisol catabolism. Therefore, experiments elucidating whether 20β-hydroxycortisone is an excreted glucocorticoid became inevitable. Both mentioned characteristics of excreted steroids (missing affinity to a receptor and conjugation) were assessed for 20β-hydroxycortisone.
For C21 steroids, two different receptors belonging to the nuclear receptor family are known. Upon ligand binding, the receptor translocates to the nucleus and regulates transcription of target genes. In humans and teleost fish, cortisol is the unique ligand with high affinity for the glucocorticoid receptor (GR) [20, 25, 26]. Strikingly, the affinity of cortisol to the mineralocorticoid receptor (MR) is higher than the affinity of the native MR ligand in humans, aldosterone [26]. Since cortisol is more abundant in circulation than aldosterone, permanent MR activation by cortisol is averted by expression of the cortisol-inactivating enzyme 11β-HSD type 2 in mineralocorticoid sensitive tissues [28, 29]. The native ligand of MR in teleost fish is not yet unraveled, as fish lack the capability of aldosterone biosynthesis [31]. Nonetheless, recent studies provided evidence that 11-dehydrocorticosterone might be the ligand for teleostean MR [27, 34].
These two receptors known to bind C21 steroids in teleost fish were taken into account to assess the ability of 20β-hydroxycortisone to bind and activate a receptor in steroid signaling. Cortisol as known ligand for both receptors was used as positive control of the reporter gene experiments and for normalization of obtained data. The results for zebrafish GRα reinforced the highly affine binding of cortisol published earlier (EC_{50} value of approximately 10 nM [25]), but demonstrated additionally that no other steroidal ligand tested here, including 20β-hydroxycortisone, was able to activate reporter gene expression mediated by this receptor. As expected from literature, zebrafish MR displayed a broader ligand spectrum than GRα being activated by aldosterone, cortisol, and 11-dehydrocorticosterone. This confirms 11-dehydrocorticosterone putatively being the native ligand of zebrafish MR, as suggested earlier [27, 34]. Although aldosterone does not occur in teleost fish, it was found to be the ligand for MR displaying highest affinity. For precise EC_{50} assessment, usage of even lower aldosterone concentrations is advisable, as 0.1 nM aldosterone already resulted in approximately 40 % reporter gene activation. Cortisone and 20β-hydroxycortisone induced MR dependent reporter gene expression only to a negligible extent at high concentrations far above physiological steroid levels. These results showed plainly that 20β-hydroxycortisone does not bind and activate neither GR nor MR and has probably no role in steroid signaling pathways.
Since 20β-hydroxycortisone was found not to be involved in steroid signaling mediated by GR or MR, it was elucidated if this steroid is conjugated with glucuronic acid or sulfates and excreted by adult zebrafish. In humans, cortisol is primarily inactivated by 11β-HSD type 2 catalyzing the oxidation to cortisone [56]. Subsequent catabolic steps include the reduction of the C4-C5 double bond resulting in dihydro-derivatives and reductions of carbonyl groups at C3 and C20. These products are afterwards either glucuronidated to increase water solubility or excreted without conjugation. A variety of glucocorticoids have been detected in human urine underlining complex catabolic pathways of cortisol [148, 149] (Figure 4.3). For teleost fish, it is generally considered that cortisol catabolism and excretion proceed along the same pathways [20], but excretion of glucocorticoids have been the focus of only few publications [55, 57, 58]. Vermeirssen & Scott [55] demonstrated that steroids can be excreted via three different routes in adult rainbow trout. Glucuronidated steroids are mostly released via the bile; sulfated steroids are predominantly excreted with urine, while free steroids are easily removed via diffusion from the gills. In bile of rainbow trout, manifold glucocorticoid moieties were

found after enzymatic hydrolysis: tetrahydrocortisone, tetrahydrocortisol, cortisone, cortisol, 20β-cortolone, and 5β-dihydrocortisone [57, 58] (Figure 4.3).

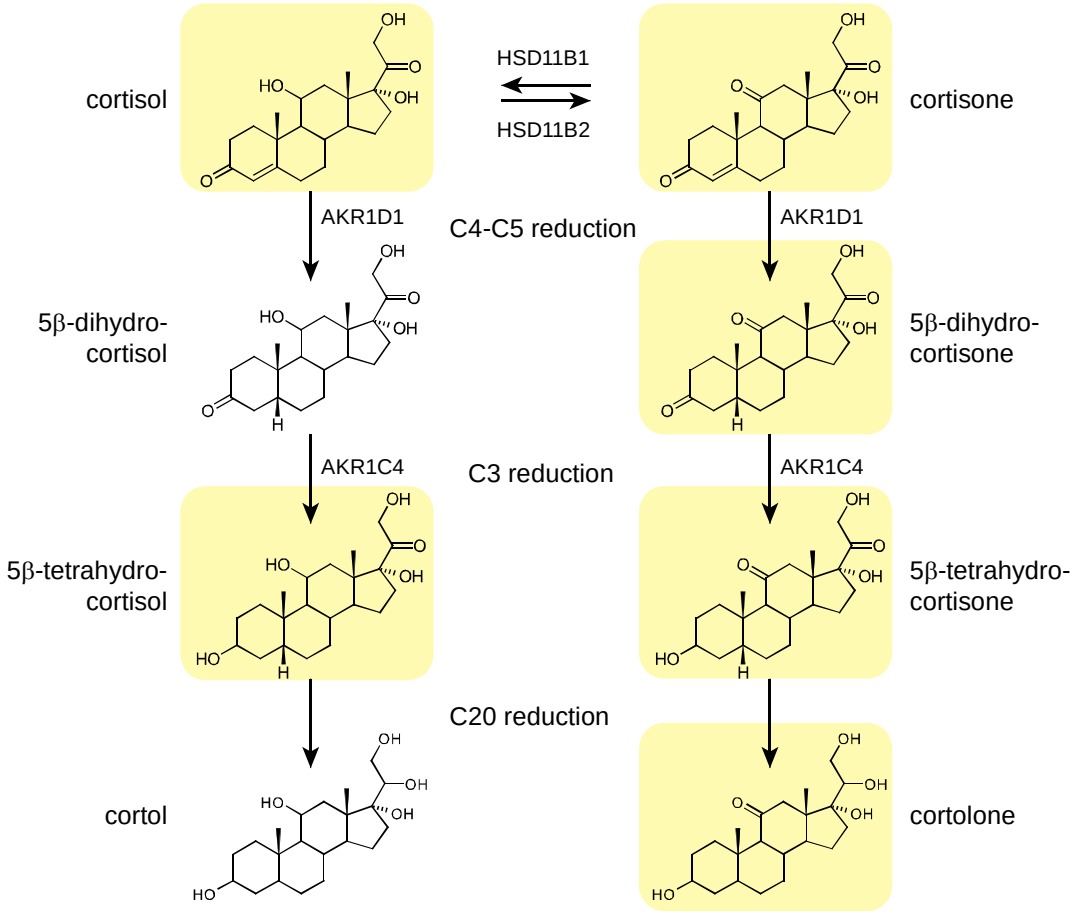

Figure 4.3: Excerpt of human cortisol catabolism pathway and comparison to teleost fish. The responsible enzymes are denoted as known for the human pathway. Reduction at positions C3 and C20 can occur leading to α- and β-isomers and are therefore not specified. Metabolites found to be excreted in rainbow trout are highlighted in yellow.

The method for steroid extraction and separation of conjugated from unconjugated steroids from zebrafish holding water was adapted from Payne *et al.* [123]. In the LC-MS/MS method applied, four glucocorticoids were analyzed, namely cortisol, cortisone, 20β-hydroxycortisone, and 20α-hydroxycortisone. Among these, 20β-hydroxycortisone was found to be the most abundant steroid in both conjugated and unconjugated fractions. The amount of steroids measured in the unconjugated fraction can be considered to equal the amount of steroids in the fish, as they represent passive 'leakage' from the gills that is driven by the concentration gradient [51]. However, the high amount of 20β-hydroxycortisone especially in glucuronidated and sulfated fractions indicate that this steroid is predominantly conjugated and most probably dedicated for excretion. This observation might suggest a putative excretion pathway parallel and independent to that described in Figure 4.3. Instead of reduction of the C4-C5 double bond with subsequent reductions of carbonyl groups at C3 and C20, a shorter pathway for cortisol catabolism and excretion might exist. This pathway only involves 11β-HSD type 2, 20β-HSD type 2, glucuronosyltransferase, and sulfatase. The other known excretion products (e.g., tetrahydro- and dihydro-derivatives of both cortisol and cortisone) were not included in the LC-MS/MS analysis here. Thus, it is not possible to directly evaluate which pathway might be preferentially used in zebrafish.
In rainbow trout, steroids were found to be excreted via gills, bile, and urine [55]. Noteworthy, 20β-HSD type 2 was strongly expressed in tissues related with excretion, as discussed in chapter 4.1.1. Similar results were obtained in zebrafish embryos and larvae, indicating the importance of this pathway already in embryonic development. Therefore, it was attempted to extract glucocorticoids

from embryo water, which would have allowed for answering some interesting questions: do zebrafish embryos excrete 20β-hydroxycortisone, and if so, is there a difference comparing wild-type embryos to 20β-HSD type 2 morphants? Unfortunately, the method that was perfect for steroids derived from adult fish holding water proved to be not sensitive enough to analyze glucocorticoids derived from embryo water. Good results were obtained when steroids were extracted from water of approximately 400 embryos (data not shown). These results at least demonstrated that already zebrafish embryos released 20β-hydroxycortisone to their medium. However, usage of 400 embryos to obtain good results rendered this method not applicable to morphants.
20β-HSD type 2 was not only identified in zebrafish, but was also found and biochemically characterized in other teleost fish. Thus, the postulated short pathway of cortisol excretion might be a general feature of teleost fish that has escaped attention of those few researchers elucidating cortisol catabolism up to now.
Whether 20β-hydroxycortisone, both free and conjugated, is passively released or rather actively excreted from the fish, remains a matter of speculation. As mentioned above, the amount of free steroids in water can be most probably addicted to passive diffusion processes according to concentration gradients and might therefore be correlated to the steroid concentrations in plasma of different fish species [51, 55, 150]. In contrast, conjugated steroids, both glucuronidated and sulfated, are considered to be derived from active excretion processes in teleost fish [51, 55, 150]. Certainly, transport proteins are responsible for such active processes, but their nature is not unraveled yet in teleost fish. In humans, several transporters are known to facilitate active excretion of conjugated and unconjugated steroids in kidney. While Trauner *et al.* [151] designated OATP1 (a member of the organic anion-transporting polypeptide family) a multispecific transport system for a variety of substrates, it was later considered to be the main efflux route for conjugated steroids in kidney [152]. Beside OATP1, two members of subgroups of the ATP-binding cassette superfamily are also involved in the transport of steroids, both conjugated and unconjugated, from the kidney to the urine, namely ABCG2 [153] and MDR1/P [152]. Whether teleost orthologs of one of these proteins or other, so far unknown transport proteins are responsible for excretion of conjugated 20β-hydroxycortisone in teleost fish remains elusive up to now.

4.1.6 Evidence for a concerted action of 11β-HSD type 2 and 20β-HSD type 2

The characterization of zebrafish 11β-HSD type 2 revealed a striking similarity to 20β-HSD type 2. The kinetic parameters of both enzymes were in a similar range, and both were localized in the same subcellular compartment, the endoplasmic reticulum. Additionally, the expression pattern of both genes in embryonic development and in adult zebrafish tissues was fairly comparable. Moreover, both genes were found to be up-regulated upon artificial stress induced by cortisol treatment as well as by physical stress caused by swirling. Although this evidence might be considered to suffice for a hypothesis of both enzymes acting together in the same pathway, a better argument would be to clearly demonstrate concerted enzymatic action.
To this end, cortisol was added to zebrafish larvae homogenate together with both cofactors NAD^+ and $NADPH + H^+$ required by 11β-HSD type 2 and 20β-HSD type 2, respectively. While cortisone was produced in this reaction as expected, unfortunately no 20β-hydroxycortisone formation above background levels was detected. Nevertheless, controls for the single reactions of both enzymes assured functionality of the experimental conditions. After experimental exclusion of the inhibitory effect of cortisol on 20β-HSD type 2 as reason for the lack of 20β-hydroxycortisone formation, the stability of the cofactor $NADPH + H^+$ was considered. Apparently, a large amount of $NADPH + H^+$ was degraded overnight in the complex mixture of zebrafish homogenate or was probably used for all kinds of other reduction reactions. Indeed, $NADPH + H^+$ was described to be less stable than $NADH + H^+$ in the same buffer conditions [125].
Taking the stability of $NADPH + H^+$ into account, a sequential set-up was designed that allowed for 11β-HSD type 2 reaction first followed by subsequent addition of $NADPH + H^+$ for 20β-HSD type 2 conversion. This approach demonstrated 20β-hydroxycortisone formation far above background levels and provided evidence for a concerted action of 11β-HSD type 2 and 20β-HSD type 2 in cortisol catabolism.

Despite being coherent, this result was only obtained *in vitro* and is thus not comparable to results obtained from animal model experiments. Significant evidence for a concerted action of 11β-HSD type 2 and 20β-HSD type 2 could be obtained with tracer experiments, therefore exposing zebrafish to labeled cortisol and subsequent detection of labeled 20β-hydroxycortisone. Since zebrafish are too small for injection of labeled steroids, a possible application method would be to dilute labeled cortisol into the fish water and examine possible excretion products in the water.

4.1.7 Mysterious enzyme: has 11β-HSD type 3 any function in fish?

The family of 11β-HSDs is nonuniformly characterized in teleost fish. Especially comparisons to mammalian findings and analyses regarding the evolution of this enzyme family have raised questions that are not answered to date due to the apparent lack of functional studies on teleost 11β-HSDs.
Human 11β-HSDs play a crucial role in controlling glucocorticoid and mineralocorticoid hormone action [28]. 11β-HSD type 1 catalyzes the conversion of cortisone to cortisol and is therefore a tissue specific modulator of glucocorticoid response enhancing the action of GR *in vivo* [96, 154]. In contrast, 11β-HSD type 2 is involved in cortisol to cortisone conversion and confers thereby aldosterone specificity in mineralocorticoid target tissues [26]. Mutations in the 11β-HSD type 2 gene cause a cortisol induced activation of MR leading to hypertension, hypokalemia, and decreased aldosterone concentrations in the circulation [100].
In teleost fish, 11β-HSD type 2 is considered to play a similar role as in humans, but the enzyme is additionally involved in the formation of the active androgen 11-ketotestosterone [124]. 11β-HSD type 2 is expressed in a variety of tissues with stronger signals in gills, kidney, and testis [112], underlining its importance in both cortisol inactivation and androgen formation. The conversion of cortisol to cortisone was confirmed for 11β-HSD type 2 from Japanese eel [112] and rainbow trout [111], while the enzyme from trout was also shown to catalyze 11-ketotestosterone formation from 11-hydroxytestosterone [111]. Concerning 11β-HSD type 1 in fish, the situation gets even more complex, as 11β-HSD type 1 and 11β-HSD type 3 are considered to be paralogs; but 11β-HSD type 3 might also be the ancestor of 11β-HSD type 1 [113, 114]. 11β-HSD type 1 enzymes were annotated in some fish species but remained elusive in others (including zebrafish), where the 11β-HSD type 3 enzymes were found and suggested to fulfill 11β-HSD type 1 functions [113]. However, no study has been published up to date confirming any catalytic function of either 11β-HSD type 1 or 11β-HSD type 3 from teleost fish.
With this background, 11β-HSDs from zebrafish were characterized in this work, assuming that 11β-HSD type 2 catalyzes the cortisol to cortisone oxidation and 11β-HSD type 3 catalyzes the reverse reaction, thereby being the paralog of human 11β-HSD type 1. It turned out that 11β-HSD type 2 matched to the hypothesis, as was discussed in detail in the previous chapters. The expression pattern and the cortisol-dependent regulation of 11β-HSD type 3 were in line with the hypothesis as well: when cortisol was externally provided, 11β-HSD type 3 expression was not affected or slightly down-regulated, as additional cortisol synthesis would not be necessary. However, the finding that 11β-HSD type 3 did not catalyze the reduction of cortisone to cortisol was surprising and unexpected. Subsequent phylogenetic analysis revealed a closely related candidate for this conversion: 11β-HSD type 3b (also annotated as 11β-HSD type 1 like), which occurred probably due to a teleost specific genome duplication event [155, 156]. Interestingly, the cortisone to cortisol reaction could be observed in zebrafish homogenates, but this reaction could not be attributed to neither 11β-HSD type 3a nor 11β-HSD type 3b after recombinant expression of both enzymes (personal communication with Prof. Dr. Alex Odermatt at the Congress of Steroid Research, Chicago, USA, March 29, 2011).
The intriguing results for 11β-HSD type 3 obtained here and also in Prof. Dr. Odermatts group add to the confusion about the role of 11β-HSD type 3 and/or type 1 enzymes in fish. Although Baker [114] speculated that 11β-HSD type 3 catalyzes the reverse reactions of 11β-HSD type 2 and therefore has "an important role in fish physiology", the findings discussed above seem to contradict his statement at least in part. The substrate for zebrafish 11β-HSD type 3 was not unraveled up to now and hence, the physiological function of this enzyme remains elusive.

4.2 20β-HSD type 2 and reproduction – an unlikely relation

Beside their involvement in glucocorticoid and mineralocorticoid signaling, C21 steroids fulfill additional functions in fish physiology. Therefore it might have been possible for zebrafish 20β-HSD type 2 to be involved in the biosynthesis of pheromones or the reaction product, 20β-hydroxycortisone, might act as pheromone. The third hypothesis proposed a role for 20β-HSD type 2 in the biosynthesis of the maturation-inducing hormone, which is a C21 steroid sharing structural similarities with 20β-hydroxycortisone.

Oocyte maturation occurs prior to ovulation and is required for a successful fertilization [127, 157]. The process of meiotic maturation includes breakdown of the germinal vesicle, chromosome condensation, and the assembly of the first polar body. Many hormones of the hypothalamus-pituitary-gonad axis act subsequently to ensure proper oocyte maturation. The pituitary releases gonadotropin (GTH), which stimulates ovarian follicular cells to synthesize the maturation-inducing hormone (MIH). Upon MIH release, this hormone binds to a receptor that induces the aforementioned processes mediated by the maturation-inducing factor(s), being cdc2 kinase and cyclin B (for reviews on this topic and the downstream processes refer to [127, 157]). The MIH is a C21 steroid, and in most teleost fish species examined to date 17α,20β-dihydroxy-4-pregnen-3-one (17α,20β-DP) was found to be the most effective MIH [157]. 17α,20β-DP is synthesized from 17α-hydroxyprogesterone catalyzed by an enzyme termed carbonyl reductase like 20β-HSD (20β-HSD/CR like) that shares a striking similarity to mammalian carbonyl reductase 1 (CR1) [158], although the impact for this observation is not yet unraveled [127]. 20β-HSD/CR like enzymes were cloned from the ovaries of rainbow trout, tilapia, and zebrafish [159-161], and the conversion of 17α-hydroxyprogesterone to 17α,20β-DP was confirmed for the trout and tilapia enzymes [159, 160]. 20β-HSD/CR like enzymes were found to have a broader substrate spectrum converting progestins, androgens, xenobiotics, and prostaglandins beside 17α-hydroxyprogesterone [159, 160].

Although 20β-HSD/CR like is considered to be the key enzyme in MIH synthesis, its expression is not restricted to the gonads, but was also found in almost every tissue analyzed with strong signals in gills, kidney, and brain in different fish species [158-161]. In fish with a long reproductive cycle, 20β-HSD/CR like showed a positive correlation with phases of the ovarian cycle, showing higher expression in vitellogenesis and migratory nucleus stage [158, 162]. In addition, a direct stimulatory effect of gonadotropin on 20β-HSD/CR like expression in gonads was demonstrated, while the extragonadal expressed 20β-HSD/CR like was not influenced [158, 160]. However, zebrafish seem to represent an exception, as zebrafish 20β-HSD/CR like was not influenced by gonadotropin treatment and maturation functions without significant changes in 20β-HSD/CR like expression [161].

While the role of 20β-HSD/CR like enzymes in oocyte maturation in teleost fish is well understood, some aspects remain unclear up to now. Firstly, the widespread expression pattern observed in several fish species was not explained so far. Secondly, the broad substrate spectrum still awaits a physiological clarification, and thirdly, the function of 20β-HSD/CR like in male fish, especially in testis, is not addressed until now, though it was speculated to be involved in testis maturation during sexual maturation [160].

The novel 20β-HSD type 2 enzymes characterized in this work are set apart from the described 20β-HSD/CR like enzymes due to their cortisone converting ability. Even though both families belong to the short-chain dehydrogenase/reductase superfamily, they are only distantly related and share nothing more than the conserved motifs of the SDR family. Nevertheless, the reaction product of 20β-HSD type 2, 20β-hydroxycortisone, and the MIH, 17α,20β-DP, resemble each other, but they differ in two important positions (Figure 4.4). 17α,20β-DP is more hydrophobic lacking the carbonyl group at position C11 and a hydroxyl group at C21. Especially the carbonyl group at C11 in 20β-hydroxycortisone would probably diminish if not totally avert a binding of 20β-hydroxycortisone to the MIH receptor. Moreover, the pathways for the biosynthesis of 17α,20β-DP are well characterized rendering a conversion of 20β-hydroxycortisone to the MIH 17α,20β-DP unlikely.

The expression pattern of 20β-HSD/CR like in developing fish was so far not analyzed, impeding a direct comparison to 20β-HSD type 2. Taking the role of 20β-HSD/CR like in oocyte maturation into

account, an expression prior to sexual maturation of the fish appears improbable. If 20β-HSD type 2 would be involved in the biosynthesis of the MIH, the gene would not be expressed early in embryonic development. Another intriguing observation is the cortisol dependent stimulation of 20β-HSD type 2 expression. Unfortunately, the direct influence of cortisol on teleost 20β-HSD/CR like enzymes has not been studied to date. Moreover, the effects of stress and cortisol on fish reproduction are not elucidated to the molecular level until now, though being an important topic also for aquaculture. Stress can harm reproduction by interference with sex steroids [20, 163]. However, this effect is depending on the time point of stress in life cycle, the severity and the duration of the stress and can range from acceleration of ovulation to total inhibition of reproduction [7].
In the light of the depicted differences of 20β-HSD type 2 and 20β-HSD/CR like, a role for either 20β-HSD type 2 or 20β-hydroxycortisone in oocyte maturation seems unlikely.

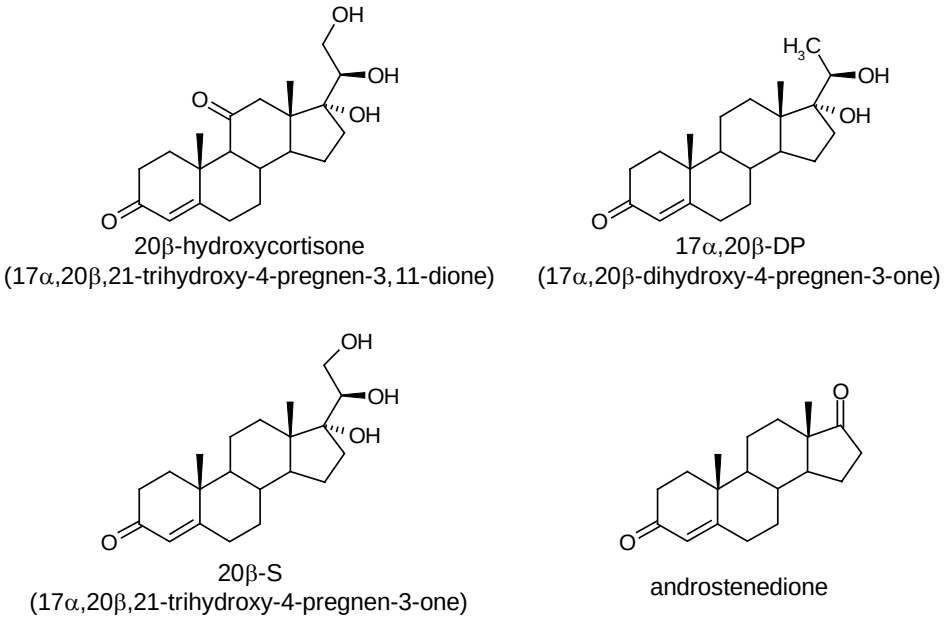

Figure 4.4: Chemical structures of maturation-inducing hormone, common fish sex pheromones, and 20β-hydroxycortisone. 17α,20β-DP has a dual role acting both as MIH and as pheromone. 20β-S and androstenedione, a C19 steroid, are sex pheromones.

Another important function of C21 steroids in fish is their action as pheromones. Pheromones are defined as substances (or mixture of substances) released by an individual and eliciting an adaptive, specific, and species-specific response in other individuals, that does neither need experience nor learning [50]. Fish commonly use pheromones to regulate a variety of functions, e.g., anti-predation and alarm cues, non-reproductive aggregation like kin recognition in hierarchies or formation of schools, and reproductive stimulations [50]. Pheromones that are characterized regarding release, olfactory detection and behavioral response belong to either gonadal steroids, prostaglandins, or bile acids [50]. Naturally, different fish species have diverse rates and discrete patterns of pheromonal release [51], but some congruencies have been observed.
The cichlid *Haplochromis burtoni* detects a variety of conjugated C18, C19, and C21 steroids acting via specific receptor mechanisms. Males and females display an equal sensitivity. No response was observed with unconjugated steroids and prostaglandins [164]. Both sexes of roach *Rutilus rutilus* detect unconjugated and glucuronidated 17α,20β-dihydroxy-4-pregnen-3-one (17α,20β-DP). Females additionally released unconjugated and glucuronidated androstenedione, which can be detected by males [165]. The goldfish *Carassius auratus* releases manifold unconjugated and conjugated C18, C19, and C21 steroids, but the most important pheromonal cues released by females are sulfated forms of 17α,20β-DP, 17α,20β,21-trihydroxy-4-pregnen-3-one (20β-S), and androstenedione. Here, 17α,20β-DP plays a dual role being both the priming hormone for gonadotropin release and the MIH [166]. As observed for goldfish, in eurasian ruffe (*Gymnocephalus cernuus*) the trihydroxylated

progestin 20β-S was shown to stimulate oocyte maturation and pheromone release, but was not the pheromone itself, as the steroid induced no electro-olfactogram response [167]. In zebrafish, the glucuronidated 17α,20β-DP among other steroids produced by males induced ovulation of female fish. Ovulation was also induced by mere male holding water, but the effect was abolished after β-glucuronidase treatment, underlining the importance of conjugation [168-170].

The two major pheromones 17α,20β-DP and 20β-S have a similar structure as 20β-hydroxycortisone, but lack the carbonyl group at position C11 (Figure 4.4). It can be speculated that this carbonyl group could be removed by 11β-hydroxylases, characterized in fish [128, 171], but there is no evidence that these enzymes play additional roles beside their functions in cortisol and 11-ketotestosterone synthesis. As mentioned above, the carbonyl group at C11 of 20β-hydroxycortisone might impede successful receptor binding and activation. Unfortunately, neither the receptors mediating pheromone responses nor the enzymes synthesizing pheromones are characterized to date. Therefore, receptor binding studies of 20β-hydroxycortisone and comparison of biochemical parameters or expression pattern of 20β-HSD type 2 was precluded.

The early expression of 20β-HSD type 2 in embryonic development far before sexual maturation renders a hypothesis involving the enzyme in sex pheromone biosynthesis very unlikely. Sexual maturation occurs in zebrafish at a length of 17-19 mm [66] (approximately week 12-16). The gene is also expressed ubiquitously and displays no restriction to the gonads, as would be expected for an enzyme producing a gonadal pheromone. Gonadal pheromones are commonly glucuronidated steroids (sulfated in case of goldfish) and 20β-hydroxycortisone was found in the fish holding water in conjugated form with both glucuronic acid and sulfates. However, if 20β-hydroxycortisone conjugates act as sex pheromones, a difference in conjugated 20β-hydroxycortisone amounts should have been observed between the sexes, which was not the case. Thus, a role for 20β-HSD type 2 in pheromone synthesis or for 20β-hydroxycortisone being a sex pheromone appears to be rather unlikely.

4.3 20β-HSD type 2 in mammals – prospects for the future

4.3.1 Constraints of bioinformatic analysis

Zebrafish 20β-HSD type 2 was identified by its close relationship and high similarity to enzymes from the 17β-HSD type 3 and type 12 families [103]. Further BLAST searches in genomes from other species and phylogenetic analyses identified 20β-HSD type 2 orthologs in other species, being mostly teleost fish, but also frog and two mammals. Strikingly, no candidate sequences were found in rodents or humans. At the end of my experimental work (early in 2012), additional *in silico* searches for mammalian candidate sequences in databases were conducted. In the meantime, many genomes from other species have been sequenced, and the search therefore yielded many candidate sequences from diverse species ranging from insects to mammals. However, these new candidates never clustered together with 20β-HSD type 2 enzymes in phylogenetic analysis but were mostly orthologs of 17β-HSD type 12. The physiological role of 17β-HSD type 12 was controversially discussed suggesting an involvement in both estradiol and fatty acid metabolism [93], but recent evidence demonstrated that 17β-HSD type 12 is required for fatty acid synthesis and is crucial for mouse organogenesis [172]. The identification of orthologs in virtually every species sequenced to date underlines an involvement of 17β-HSD type 12 in lipid metabolism, though characterization of enzymatic conversion with lipid substrates has not yet been published.
To exclude the vast amount of 17β-HSD type 12 candidate sequences that were obtained using a BLAST approach against the nucleotide collection of all species, a more restricted approach was performed. All up to now characterized 20β-HSD type 2 sequences were searched against the human reference database and the obtained hits were then included in a new phylogenetic analysis (Figure 4.5). Most candidates are members of the SDR family, but clustered in different clades than 17β-HSD type 3, 17β-HSD type 12, and 20β-HSD type 2. The single exception was human hydroxysteroid dehydrogenase-like 1 (HSDL1) clustering between 20β-HSD type 2 and 17β-HSD type 12. However, HSDL1 being the ortholog of zebrafish 20β-HSD type 2 can be ruled out, since HSDL1 showed an exchange of the crucial tyrosine in the active center (Sx_{12}FSxxK instead of Sx_{12}YSxxK) rendering the enzyme totally inactive towards a variety of substrates [173].
In silico analyses allow for quick identification of closely related orthologs, homologs or paralogs, and are therefore a valuable tool in molecular biology. The algorithms are based on sequence similarities and identities and are also used to annotate unknown sequences and even whole genomes without further molecular characterization. However, this approach affects the query of a human 20β-HSD type 2 ortholog adversely, because only related sequences can be returned – with the input of a SDR sequence, only SDR sequences can be expected. Since no promising candidate for a human 20β-HSD type 2 ortholog was identified by similarity searches *in silico*, it appears likely that a candidate with 20β-HSD activity does not belong to the SDR family. Several enzymes known to be involved in mammalian glucocorticoid catabolism were found to belong to the aldo-keto reductase family (AKR) [174] (Figure 4.9). Perhaps this large family comprises the human 20β-HSD type 2 enzyme.
For identification of the human 20β-HSD type 2 ortholog bioinformatics appears not to be the most promising tool. Since many studies have detected 20β-reduced isomers of corticosteroids in human urine [148, 149, 175], it is generally accepted that a 20β-HSD is existing in humans. However, a laborious but maybe successful approach for identification would include screening a human cDNA library for the respective enzymatic activity, assuming a similar reaction compared to zebrafish 20β-HSD type 2.

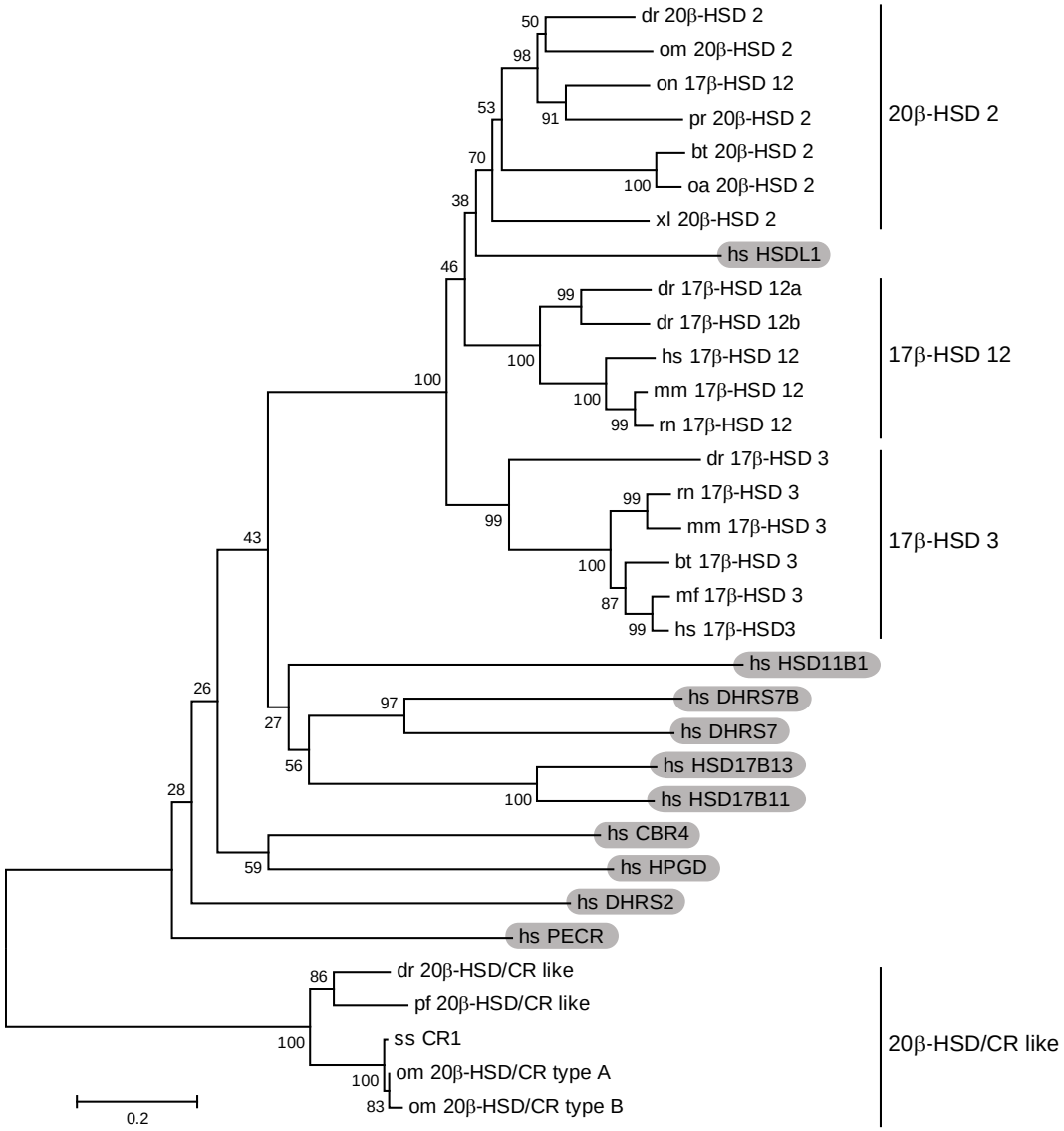

Figure 4.5: Phylogenetic analysis show closest human orthologs of 20β-HSD type 2 enzymes. 17β-HSD type 12 and 17β-HSD type 3 enzymes were included to characterize the environment of 20β-HSD type 2. Teleost 20β-HSD/CR like enzymes were used as outgroup. Human candidate sequences were highlighted in grey. The tree was calculated by means of Neighbor-Joining with bootstrap values out of 1000 pseudoreplicates, given in percent at each dichotomy. Species abbreviations: bt, *Bos taurus*; dr, *Danio rerio*; hs, *Homo sapiens*; mf, *Macaca fascicularis*; mm, *Mus musculus*; oa, *Ovis aries*; om, *Oncorhynchus mykiss*; on, *Oreochromis niloticus*; pf, *Pelteobagrus fulvidraco*; pr, *Poecilia reticulata*; rn, *Rattus norvegicus*; ss, *Salmo salar*; xl, *Xenopus laevis*. Abbreviations for human candidate enzymes: CBR, carbonyl reductase; DHRS, dehydrogenase/reductase member; HSD, hydroxysteroid dehydrogenase; HPGD, hydroxyprostaglandin dehydrogenase-15; PECR, peroxisomal trans-2-enoyl CoA reductase.

4.3.2 Cow 20β-HSD type 2: a special case

Although the 20β-HSD type 2 enzyme from sheep was able to catalyze the NADPH + H^+ dependent 20β-hydroxycortisone formation (though only weakly), its closest homolog, 20β-HSD type 2 from cow, was enzymatically inactive in the assay conditions used. A reason for this lack of activity was not revealed by careful sequence analysis (Figure 4.6), as all important SDR motifs were present and well conserved between the species. Additionally, all SDR motifs showed the appropriate distance between them [79]. In cooperation with Dr. Rebekka Mindnich (University of Pennsylvania, Philadelphia, USA), the cow sequence was analyzed in more detail using molecular modeling to identify potential amino acids as candidates for site-directed mutation.

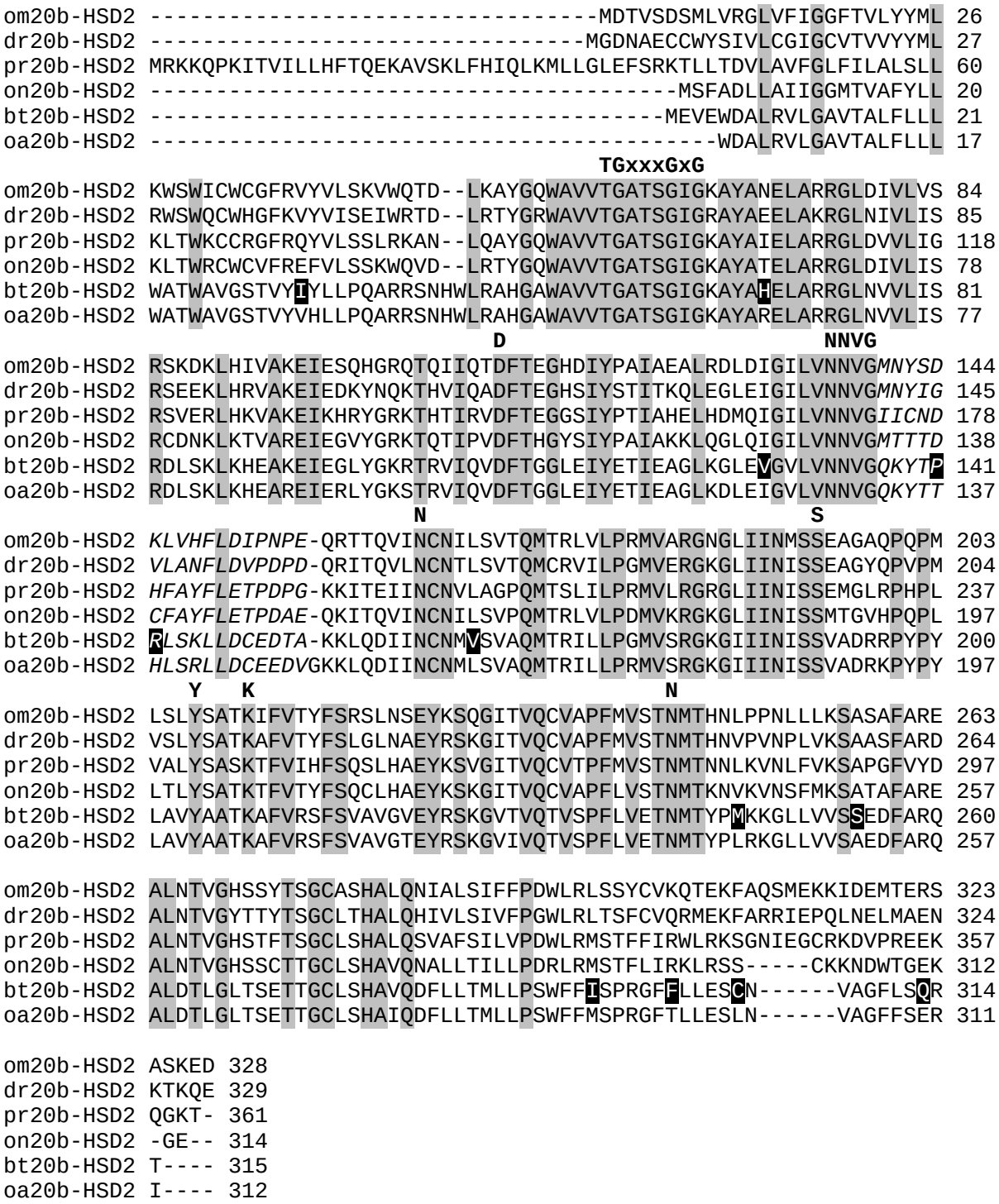

Figure 4.6: Sequence comparison of all 20β-HSD type 2 enzymes shows conservation of typical SDR motifs. SDR motifs are depicted in bold above the alignment, and residues conserved in all species are shaded in grey. The loop region is highlighted by italics. Amino acids as candidates for mutation in *Bos taurus* sequence are shown in white letters on black background. Amino acids are in single letter code. Species abbreviations: bt, *Bos taurus*; dr, *Danio rerio*; om, *Oncorhynchus mykiss*; on, *Oreochromis niloticus*; oa, *Ovis aries*; pr, *Poecilia reticulata*.

Despite an identity score of 90 %, several amino acids were found to be significantly different to the sheep protein (Figure 4.6) and therefore closely inspected in an overlay of both sheep and cow 20β-HSD type 2 models. Both models were fitted to the crystal structure of murine 11β-HSD type 1 and afterwards superimposed. The superimposed models were used to evaluate the impact of significantly different amino acids on the conformation and activity of cow 20β-HSD type 2. The N-

and C-termini of both sequences were not included into the model, and therefore no conclusion can be drawn for the candidate residues I 33, I 294, F 300, C 305, and Q 313. H 68 was considered to be no good candidate as this residue points outward in the model, and V 128 was also excluded despite high conservation of isoleucine at this position in the other sequences. The candidates P 141 and R 142 are located in the loop region complicating possible conclusions, as this region is highly unstructured and difficult to predict. V 165 is located in the dimerization interface, but this amino acid is even smaller than leucine and still hydrophobic, rendering V 165 an unlikely candidate. Dimerization is essential for functionality of SDR enzymes [84, 176, 177]. M 245 was considered to be a good candidate together with P 141 and R 142, since these residues can form a hydrophobic zipper that may be crucial to correctly position the NNVG motif (Figure 4.7). The NNVG motif has an important role in stabilization of the central β-sheet and thereby for the cofactor binding and the enzyme's activity [76, 80]. Methionine is slightly bulkier than the conserved valine and leucine. However, the overlay of both sheep and cow models displayed an exact match of the NNVG motif (Figure 4.7), but this observation can also be caused by the modeling of both candidates on the same crystal structure, that does not necessarily reflect the real situation in both cow and sheep 20β-HSD type 2. The last candidate, S 254, was also not considered to cause problems, as S 254 overlaps in the models with sheep A 251.

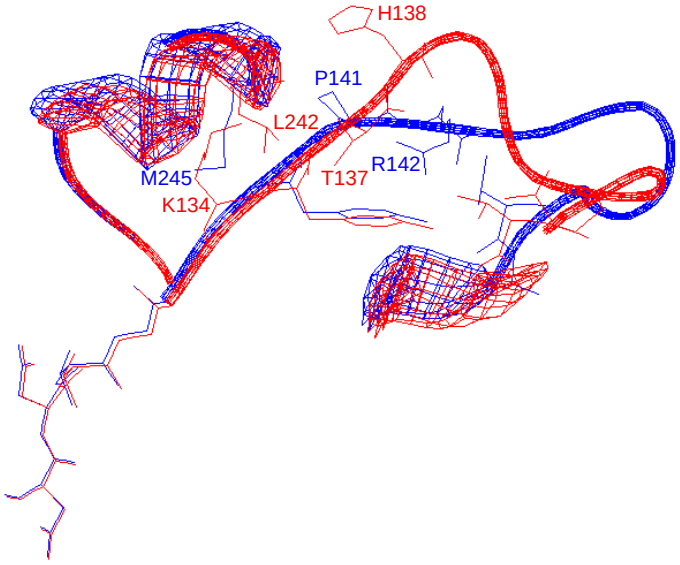

Figure 4.7: Comparison of the loop region and adjacent amino acids of sheep and cow 20β-HSD type 2. Sheep 20β-HSD type 2 is shown in red, while the cow model is depicted in blue. Rendered secondary structures are shown together with amino acid residues. Residues dedicated for mutation in cow 20β-HSD type 2 are labeled together with their sheep counterparts. The NNVG motif is displayed at the bottom left of the model and not rendered with secondary structures.

In the light of these analyses, it was suggested to mutate M 245, P 141, and R 142 in cow 20β-HSD type 2. Thus, enzymes with single mutations M245L and P141T/R142H were generated together with an enzyme containing all three mutations (M245L/P141T/R142H). However, analysis of the enzymatic activity of all three mutants revealed no reduction of cortisone to 20β-hydroxycortisone, indicating that the respective amino acids were not responsible for the lack of enzymatic activity. To narrow the search for the responsible amino acid (or stretch of sequence) down, construction of chimeric enzymes out of sheep and cow 20β-HSD type 2 might prove helpful. This approach has been successful in restoring the activity of zebrafish 17β-HSD type 2 [105].
Despite this thorough *in silico* attempt to elucidate the lack of cow 20β-HSD type 2 activity towards cortisone, a reason could not be unveiled. Since both sheep and cow 20β-HSD type 2 clustered in phylogenetic analysis slightly apart from fish 20β-HSDs type 2, it may also be possible that they differ in substrate or cofactor requirements. The observation that sheep 20β-HSD type 2 was able to catalyze the 20β-hydroxycortisone formation, but only to a low extent, indicates that cortisone might not be the preferred substrate of the enzyme. Further evolutionary considerations with regard to this topic are discussed in chapter 4.3.4.

4.3.3 20β-hydroxycortisone in humans: a metabolite fallen into oblivion

In silico analysis using searches based on Hidden Markov Models failed to identify a human ortholog of 20β-HSD type 2, but it is generally accepted that 20β- and 20α-reductions of different corticosteroids can occur in humans. Many studies have detected both α- and β-isomers of cortols and cortolones in human urine [148, 149, 175], and the existence of a 20β-HSD enzyme is postulated [148] but not evidenced. Since bioinformatic approaches and pathway analyses gave no hint regarding a human 20β-HSD type 2 candidate, the reaction product, 20β-hydroxycortisone, was searched for in human urine (Figure 4.8).

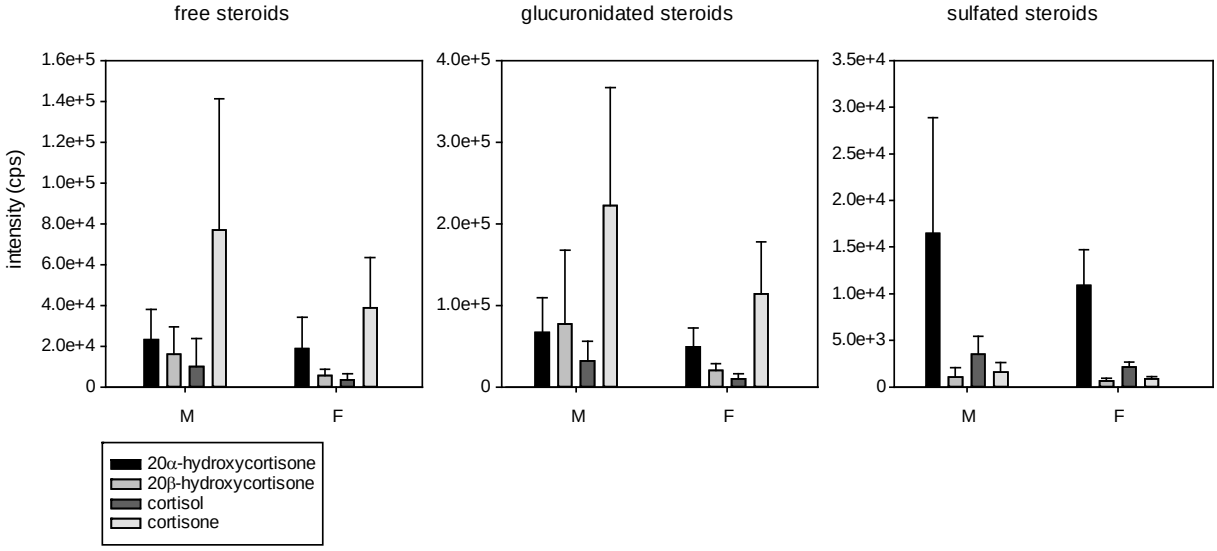

Figure 4.8: Analysis of glucocorticoids extracted from human urine samples reveals 20β-hydroxycortisone to be an excreted steroid. First-morning urine samples were collected from three healthy males and three healthy females aged between 25-32 years. 25 ml each in three replicates were extracted according to the extraction protocol developed for fish water and the obtained fractions were analyzed by LC-MS/MS. Abbreviations: cps, counts per second; F, female; M, male.

The obtained pattern of glucocorticoid excretion in human urine deviated from that observed in zebrafish. Generally, the amount of excreted glucocorticoids is higher in male than in female fractions, which is in accordance to a previous study [178]. 20α-hydroxycortisone and cortisone were found to be the most abundant steroids among the four glucocorticoids analyzed in all fractions, but 20β-hydroxycortisone was also detectable in vast amounts especially in the glucuronidated steroid fraction. This result demonstrates clearly that 20β-hydroxycortisone (and the α-isomer as well) is an excreted glucocorticoid not only in fish, but also in humans. However, as other known excreted glucocorticoids were not included in the LC-MS/MS method, a conclusion regarding the relative importance of the novel metabolites compared to the already known products can not be drawn.
In-depth literature research revealed that the potential for formation of both 20α- and 20β-hydroxycortisone in human liver and uterine fibroblasts has been known since the 1960ies [179, 180]. In the 1980ies, both isomers were detected in human urine and the excretion rates for the unconjugated isomers determined (20α-hydroxycortisone 5.7 µmol/mol creatinine, 20β-hydroxycortisone 1.3 µmol/mol creatinine) [181, 182]. The authors showed that both metabolites had a circadian rhythm in urine similar to cortisol, and that the 20α-isomers of hydroxycortisol and hydroxycortisone were predominant over the respective 20β-forms [181]. Despite the knowledge of these metabolites in human urine and their sources (liver, kidney, adrenal cortex), the role in human physiology remained unclear [181, 182] and was up to now not elucidated. The obvious idea of these metabolites being excretion products was not published until now, although being evidenced by conjugation and detection of large amounts in urine in the aforementioned publications.

Strikingly, 20β-hydroxycortisone and its α-isomer virtually vanished from literature after 1987. One study was published in 1992 demonstrating 20β-hydroxycortisone formation from cortisol in human liver fractions [183], but this study added no vital information about the biological function. The same holds true for two other studies reporting method development including 20α-/20β-hydroxycortisone, but demonstrating no application of these methods to human material [184, 185]. The sinking to oblivion of 20α-/20β-hydroxycortisone might have been enhanced by the fact that no enzyme(s) producing these metabolites have been identified and characterized in humans up to now. Interestingly, an enzyme catalyzing the cortisone to 20β-hydroxycortisone conversion as discovered in this thesis in different teleost fish was long known to exist in bacteria [186]. The cortisone reductase was well characterized in *Clostridium scindens* in the late 1980ies and was found to produce preferably 20α-reduced steroids. *C. scindens* cortisone reductase (also termed 20α-HSD) displayed a high specific activity for cortisone, was less reactive with cortisol, and favored $NADH + H^+$ over $NADPH + H^+$ for catalysis of reduction at position C20 [187, 188]. Although *C. scindens* is a member of the normal human intestinal flora and might be responsible for 20α-HSD activity therein [188], it is unfeasible to addict the high amount of 20-reduced corticosteroids in human urine to symbiotic bacteria from the intestinal flora.

Although 20β-hydroxycortisone has been undoubtedly detected in humane urine and is formed by human tissues, the metabolite was not incorporated in either standard literature or into pathway databases (e.g., KEGG PATHWAY database). Certainly, the lack of an enzyme producing 20β-hydroxycortisone is jointly responsible for this state.

As long as a 20β-HSD or 20α-HSD remain elusive in humans, the source of 20α- and 20β-hydroxycortisone in human urine can only be a matter of speculation. Most likely (and similar to 20β-HSD type 2 from zebrafish), the α- and β-isomers of 20-hydroxycortisone and 20-hydroxycortisol are generated using cortisone and cortisol, respectively, as substrates (Figure 4.9). It is possible that only one enzyme exists, which accepts both cortisol and cortisone as substrate, but it is also likely to think of two (or more) distinct enzymes, since zebrafish 20β-HSD type 2 for example only converts cortisone and not cortisol, and produces exclusively 20β-hydroxycortisone and not the α-isomer [126]. Since all other steroids denoted in Figure 4.9 were detected in humane urine [148], it is also possible that 20-hydroxycortisol and 20-hydroxycortisone can be further reduced at positions C5 and C3 via the denoted aldo-keto reductases AKR1D1 and AKR1C4 yielding cortols and cortolones. Obviously, not all steps and enzymes of the human glucocorticoid catabolism are known and extensively characterized, so that the pathway of cortisol catabolism and excretion might not be as clear and unidirectional as implicated in Figure 4.9.

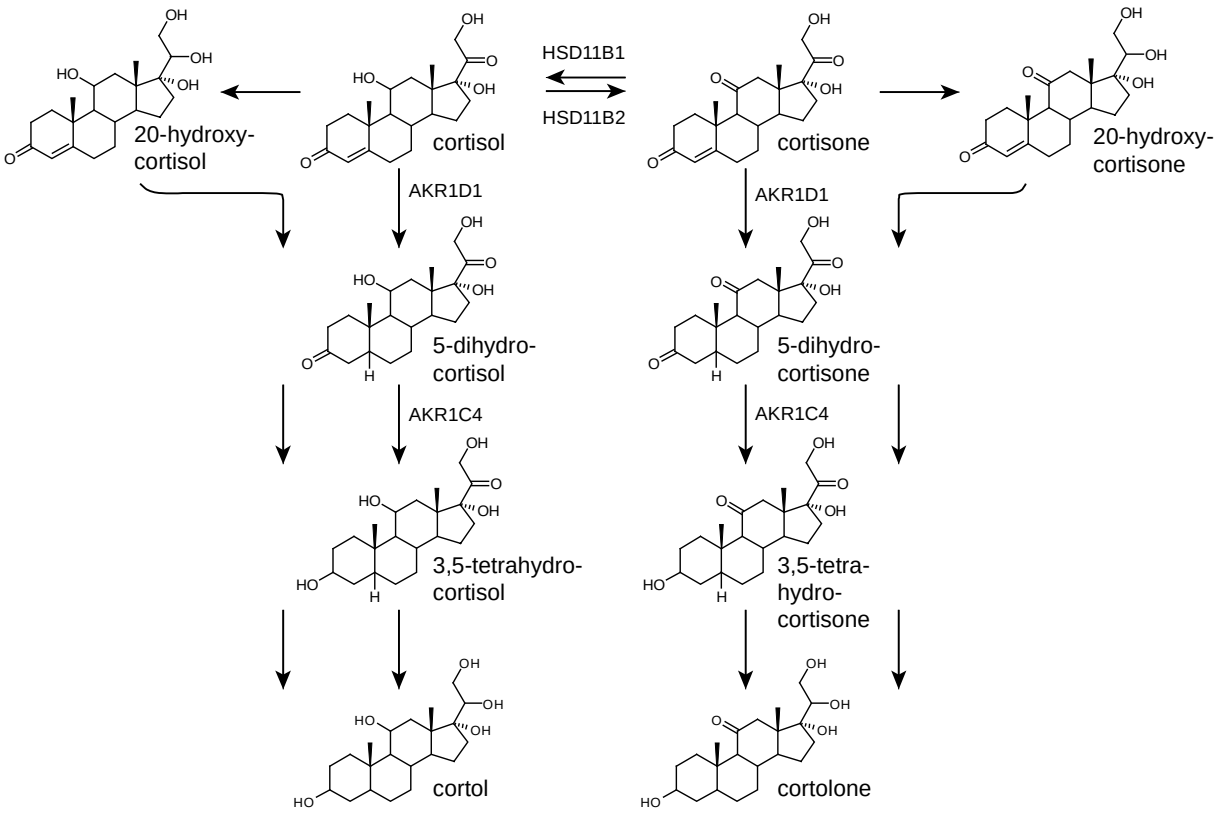

Figure 4.9: Postulated 20α- and 20β-HSDs in human cortisol catabolism. The responsible enzymes are denoted so far known for humans. Reductions at C3, C5, and C20 can occur yielding both α- and β-isomers and are therefore not specified. To some extent, 20-hydroxycortisol and 20-hydroxycortisone might be converted to cortol and cortolone, respectively. All shown metabolites were detected in human urine (this work and [148, 149, 181]).

4.3.4 Evolutionary considerations

The glucocorticoid catabolism pathways of teleost fish and humans, though both not definitely analyzed, share some similarities but also differ from each other. Some metabolites have been found to be excreted by both fish and human, and the enzymes responsible for their formation are mostly unknown in both species. However, there is also a striking difference: zebrafish 11β-HSD type 2 and 20β-HSD type 2 showed a widespread expression during embryonic development as well as in adult tissues, indicating cortisol catabolism to take place in many different tissues. Mammalian 11β-HSD type 2 was found to be ubiquitously expressed in early development of rodents, but later on and especially in adult tissues displayed a strongly tissue-specific expression pattern [95, 189]. This discrepancy might reflect the evolution of different catabolic processes for glucocorticoids, which is in line with the hypothesis that 20β-HSD type 2 enzymes evolved early alongside the ancestor of 17β-HSD type 3 and type 12 but were lost during evolution of higher vertebrates. More likely, vertebrate 20β-HSD type 2 enzymes have lost their cortisone converting ability gradually. This might be speculated from the fact that the sheep enzyme was found slightly active while its close relative from cow was unable to catalyze the same reaction. The loss of 20β-HSD type 2 activity released the enzymes of evolutionary selection pressure and allowed for varied mutations and changes. The inactive HSDL1 might be the evolutionary remainder of 20β-HSD type 2 in humans, since the group of HSD like enzymes is closely related to 17β-HSD type 3, 17β-HSD type 12, and 20β-HSD type 2.
However, the apparent lack of 20β-HSD type 2 orthologs in rodents and human but the discovery of 20β-hydroxycortisone in human urine [181, 182] indicate that a different enzyme might have gained the function of cortisone reduction at C20, but is not similar to zebrafish 20β-HSD type 2. This enzyme probably is a member of the AKR family.

The expression pattern of human 11β-HSD type 2 and many studies analyzing glucocorticoid catabolism implied the evolution of a tissue-restricted pathway for glucocorticoid catabolism in mammals. The primary inactivation of cortisol by 11β-HSD type 2 takes place in kidney and liver [190, 191], and these tissues were found to be the major site for production of excreted glucocorticoids [178, 179, 192]. Steroids dedicated for excretion are either conjugated or released in free form predominantly via the urine. Fish have additional possibilities to excrete steroids (e.g., through gills and bile). The widespread expression of zebrafish 11β-HSD type 2 and 20β-HSD type 2 demonstrates that cortisol inactivation can putatively occur in many different tissues in fish. This situation can mirror the adaptation to an aquatic environment allowing for fast and easy steroid excretion, while terrestrial vertebrates have developed a liver and kidney-restricted cortisol catabolism pathway.

5 Bibliography

[1] S.A.E. Geurts, S. Sonnentag, Recovery as an explanatory mechanism in the relation between acute stress reactions and chronic health impairment, Scandinavian journal of work, environment & health 32 (2006) 482-492.
[2] A. Steptoe, M. Kivimaki, Stress and cardiovascular disease, Nature reviews. Cardiology advance online publication (2012).
[3] M.B. Danhof-Pont, T. van Veen, F.G. Zitman, Biomarkers in burnout: a systematic review, Journal of psychosomatic research 70 (2011) 505-524.
[4] M. Cutolo, F. Buttgereit, R.H. Straub, Regulation of glucocorticoids by the central nervous system, Clinical and experimental rheumatology 29 (2011) S-19-22.
[5] H. Seyle, The evolution of the stress concept, American scientist 61 (1973) 692-699.
[6] B.A. Barton, Stress in fishes: a diversity of responses with particular reference to changes in circulating corticosteroids, Integrative and comparative biology 42(3) (2002) 517-525.
[7] C.B. Schreck, Stress and fish reproduction: the roles of allostasis and hormesis, General and comparative endocrinology 165 (2010) 549-556.
[8] L. Tort, Stress and immune modulation in fish, Developmental and comparative immunology 35 (2011) 2366-2375.
[9] N. Aluru, M.M. Vijayan, Stress transcriptomics in fish: a role for genomic cortisol signaling, General and comparative endocrinology 164 (2009) 142-150.
[10] M.L.M. Fuzzen, N.J. Bernier, G. van der Kraak, Differential effects of 17β-estradiol and 11-ketotestosterone on the endocrine stress response in zebrafish (Danio rerio), General and comparative endocrinology 170(2) (2010) 365-373.
[11] C.B. Schreck, W. Contreras-Sanchez, M.S. Fitzpatrick, Effects of stress on fish reproduction, gamete quality, and progeny, Aquaculture 197(1-4) (2001) 3-24.
[12] C. Chai, Y.-W. Liu, W.-K. Chan, Ff1b is required for the development of steroidogenic component of the zebrafish interrenal organ, Developmental biology 260 (2003) 226-244.
[13] D. Alsop, M.M. Vijayan, Molecular programming of the corticosteroid stress axis during zebrafish development, Comparative biochemistry and physiology. Part A, Molecular & integrative physiology 153 (2009) 49-54.
[14] R. Linda, Visceral sensory inputs to the endocrine hypothalamus, Frontiers in neuroendocrinology 28(1) (2007) 50-60.
[15] S.L. Alderman, N.J. Bernier, Ontogeny of the corticotropin-releasing factor system in zebrafish, General and comparative endocrinology 164 (2009) 61-69.
[16] M. Olivereau, J. Olivereau, Localization of CRF-like immunoreactivity in the brain and pituitary of teleost fish, Peptides 9(1) (1988) 13-21.
[17] J.R. Metz, J.J.M. Peters, G. Flik, Molecular biology and physiology of the melanocortin system in fish: a review, General and comparative endocrinology 148(2) (2006) 150-162.
[18] D. Alsop, M. Vijayan, The zebrafish stress axis: molecular fallout from the teleost-specific genome duplication event, General and comparative endocrinology 161 (2009) 62-66.
[19] W.L. Miller, H.S. Bose, Early steps in steroidogenesis: intracellular cholesterol trafficking, Journal of lipid research 52 (2011) 2111-2135.
[20] T.P. Mommsen, M.M. Vijayan, T.W. Moon, Cortisol in teleosts: dynamics, mechanisms of action, and metabolic regulation, Reviews of fish biology and fisheries 9 (1999) 211-268.
[21] A.J. Stouthart, E.C. Lucassen, F.J. van Strien, P.H. Balm, R.A. Lock, S.E. Wendelaar Bonga, Stress responsiveness of the pituitary-interrenal axis during early life stages of common carp (Cyprinus carpio), Journal of endocrinology 157 (1998) 127-137.
[22] C.B. Kimmel, W.W. Ballard, S.R. Kimmel, B. Ullmann, T.F. Schilling, Stages of embryonic development of the zebrafish, Developmental dynamics 203 (1995) 253-310.
[23] N.J. McKenna, B.W. O'Malley, Minireview: nuclear receptor coactivators - an update, Endocrinology 143 (2002) 2461-2465.

[24] H. Gronemeyer, J.-A. Gustafsson, V. Laudet, Principles for modulation of the nuclear receptor subfamily, Nature reviews. Drug discovery 3 (2004) 950-964.
[25] M.J. Schaaf, D. Champagne, I.H.C. van Laanen, D.C.W.A. van Wijk, A.H. Meijer, O.C. Meijer, H.P. Spaink, M.K. Richardson, Discovery of a functional glucocorticoid receptor beta-isoform in zebrafish, Endocrinology 149 (2008) 1591-1599.
[26] J.W. Funder, Glucocorticoid and mineralocorticoid receptors: biology and clinical relevance, Annual review of medicine 48 (1997) 231-240.
[27] A. Sturm, N. Bury, L. Dengreville, J. Fagart, G. Flouriot, M.E. Rafestin-Oblin, P. Prunet, 11-Deoxycorticosterone is a potent agonist of the rainbow trout (Oncorhynchus mykiss) mineralocorticoid receptor, Endocrinology 146(1) (2005) 47-55.
[28] I. Bujalska, M. Shimojo, A. Howie, P.M. Stewart, Human 11beta-hydroxysteroid dehydrogenase: studies on the stably transfected isoforms and localization of the type 2 isozyme within renal tissue, Steroids 62 (1997) 77-82.
[29] M. Shimojo, Immunodetection of 11beta-hydroxysteroid dehydrogenase type 2 in human mineralocorticoid target tissues: evidence for nuclear localization, Endocrinology 138 (1997) 1305-1311.
[30] A. Odermatt, P. Arnold, F.J. Frey, The intracellular localization of the mineralocorticoid receptor is regulated by 11beta-hydroxysteroid dehydrogenase type 2, Journal of biological chemistry 276 (2001) 28484-28492.
[31] J.-Q. Jiang, G. Young, T. Kobayashi, Y. Nagahama, Eel (Anguilla japonica) testis 11beta-hydroxylase gene is expressed in interrenal tissue and its product lacks aldosterone synthesizing activity, Molecular and cellular endocrinology 146(1-2) (1998) 207-211.
[32] H.A. Bern, S.S. Madsen, A selective survey of the endocrine system of the rainbow trout (Oncorhynchus mykiss) with emphasis on the hormonal regulation of ion balance, Aquaculture 100 (1992) 237-262.
[33] S.D. McCormick, A. Regish, M.F. O'Dea, J.M. Shrimpton, Are we missing a mineralocorticoid in teleost fish? Effects of cortisol, deoxycorticosterone and aldosterone on osmoregulation, gill Na+,K+-ATPase activity and isoform mRNA levels in Atlantic salmon, General and comparative endocrinology 157(1) (2008) 35-40.
[34] J.B. Pippal, C.M.I. Cheung, Y.-Z. Yao, F.E. Brennan, P.J. Fuller, Characterization of the zebrafish (Danio rerio) mineralocorticoid receptor, Molecular and cellular endocrinology 332(1-2) (2011) 58-66.
[35] P. Thomas, Rapid steroid hormone actions initiated at the cell surface and the receptors that mediate them with an emphasis on recent progress in fish models, General and Comparative Endocrinology 175 (2012) 367-383.
[36] M.M. Vijayan, C. Pereira, E.G. Grau, G.K. Iwama, Metabolic responses associated with confinement stress in tilapia: the role of cortisol, Comparative biochemistry and physiology. Part C, Pharmacology, toxicology and endocrinology 116 (1997) 89-95.
[37] A.D. Pickering, T.G. Pottinger, Stress responses and disease resistance in salmonid fish: effects of chronic elevation of plasma cortisol, Fish physiology and biochemistry 7 (1989) 253-258.
[38] C.-H. Lin, I.-L. Tsai, C.-H. Su, D.-Y. Tseng, P.-P. Hwang, Reverse effect of mammalian hypocalcemic cortisol in fish: cortisol stimulates Ca2+ uptake via glucocorticoid receptor-mediated vitamin D3 metabolism, PloS one 6 (2011) 1-13.
[39] A. McGuire, N. Aluru, A. Takemura, R. Weil, J.M. Wilson, M.M. Vijayan, Hyperosmotic shock adaptation by cortisol involves upregulation of branchial osmotic stress transcription factor 1 gene expression in Mozambique tilapia, General and comparative endocrinology 165 (2010) 321-329.
[40] S.D. McCormick, Endocrine control of osmoregulation in teleost fish, American zoologist 41(4) (2001) 781-794.
[41] S. Pikulkaew, F. Benato, A. Celeghin, C. Zucal, T. Skobo, L. Colombo, L. Dalla Valle, The knockdown of maternal glucocorticoid receptor mRNA alters embryo development in zebrafish, Developmental dynamics 240 (2011) 874-889.
[42] D. Alsop, M.M. Vijayan, Development of the corticosteroid stress axis and receptor expression in zebrafish, American journal of physiology. Regulatory, integrative and comparative physiology 294 (2008) 711-719.
[43] M. Li, D.P. Bureau, W.A. King, J.F. Leatherland, The actions of in ovo cortisol on egg fertility, embryo development and the expression of growth-related genes in rainbow trout embryos,

and the growth performance of juveniles, Molecular reproduction and development 77 (2010) 922-931.
[44] J.M. Hillegass, C.M. Villano, K.R. Cooper, L.A. White, Matrix metalloproteinase-13 is required for zebra fish (Danio rerio) development and is a target for glucocorticoids, Toxicological sciences 100 (2007) 168-179.
[45] J.M. Hillegass, C.M. Villano, K.R. Cooper, L.A. White, Glucocorticoids alter craniofacial development and increase expression and activity of matrix metalloproteinases in developing zebrafish (Danio rerio), Toxicological sciences 102 (2008) 413-424.
[46] T. Dickmeis, K. Lahiri, G. Nica, D. Vallone, C. Santoriello, C.J. Neumann, M. Hammerschmidt, N.S. Foulkes, Glucocorticoids play a key role in circadian cell cycle rhythms, PLoS biology 5 (2007) e78.
[47] A.D. Pickering, Rainbow trout husbandry: management of the stress response, Aquaculture 100(1-3) (1992) 125-139.
[48] L. Barcellos, F. Ritter, L. Kreutz, R. Quevedo, L. Dasilva, A. Bedin, J. Finco, L. Cericato, Whole-body cortisol increases after direct and visual contact with a predator in zebrafish, Danio rerio, Aquaculture 272 (2007) 774-778.
[49] M.L.M. Fuzzen, G. van der Kraak, N.J. Bernier, Stirring up new ideas about the regulation of the hypothalamic-pituitary-interrenal axis in zebrafish (Danio rerio), Zebrafish 7(4) (2010) 349-358.
[50] P.W. Sorensen, N.E. Stacey, Brief review of fish pheromones and discussion of their possible uses in the control of non-indigenous teleost fishes, New Zealand Journal of marine and freshwater research 38 (2004) 399-417.
[51] A.P. Scott, T. Ellis, Measurement of fish steroids in water - a review, General and comparative endocrinology 153 (2007) 392-400.
[52] T. Ellis, J.D. James, C. Stewart, A.P. Scott, A non-invasive stress assay based upon measurement of free cortisol released into the water by rainbow trout, Journal of fish biology 65 (2004) 1233-1252.
[53] C.E. Kidd, M.R. Kidd, H.A. Hofmann, Measuring multiple hormones from a single water sample using enzyme immunoassays, General and comparative endocrinology 165 (2010) 277-285.
[54] F.Z. Stanczyk, J.S. Lee, R.J. Santen, Standardization of steroid hormone assays: why, how, and when?, Cancer epidemiology, biomarkers & prevention 16 (2007) 1713-1719.
[55] E.L.M. Vermeirssen, A.P. Scott, Excretion of free and conjugated steroids in rainbow trout (Oncorhynchus mykiss): evidence for branchial excretion of the maturation-inducing steroid, 17,20beta-dihydroxy-4-pregnen-3-one, General and comparative endocrinology 101 (1996) 180-194.
[56] C.R.W. Edwards, R. Benediktsson, R.S. Lindsay, J.R. Seckl, 11beta-Hydroxysteroid dehydrogenases: key enzymes in determining tissue-specific glucocorticoid effects, Steroids 61 (1996) 263-269.
[57] T.G. Pottinger, T.A. Moran, P.A. Cranwell, The biliary accumulation of corticosteroids in rainbow trout, Oncorhynchus mykiss, during acute and chronic stress, Fish physiology and biochemistry 10 (1992) 55-66.
[58] B. Truscott, Steroid metabolism in fish. Identification of steroid moieties of hydrolyzable conjugates of cortisol in the bile of trout Salmo gairdnerii, General and comparative endocrinology 38 (1979) 196-206.
[59] M. Westerfield, The Zebrafish Book. A guide for the laboratory use of zebrafish (Danio rerio), University of Oregon Press, Eugene, 2000.
[60] H. Segner, Zebrafish (Danio rerio) as a model organism for investigating endocrine disruption, Comparative biochemistry and physiology. Part C, Toxicology and pharmacology 149 (2009) 187-195.
[61] G.J. Lieschke, P.D. Currie, Animal models of human disease: zebrafish swim into view, Nature reviews. Genetics 8 (2007) 353-367.
[62] M.J.M. Schaaf, A. Chatzopoulou, H.P. Spaink, The zebrafish as a model system for glucocorticoid receptor research, Comparative biochemistry and physiology. Part A, Molecular & integrative physiology 153 (2009) 75-82.
[63] I. Skromne, V.E. Prince, Current perspectives in zebrafish reverse genetics: moving forward, Developmental dynamics 237 (2008) 861-882.

[64] M.A. Pickart, S. Sivasubbu, A.L. Nielsen, S. Shriram, R.A. King, S.C. Ekker, Functional genomics tools for the analysis of zebrafish pigment, Pigment cell & melanoma research 17 (2004) 461-470.
[65] A.J. Udvadia, E. Linney, Windows into development: historic, current, and future perspectives on transgenic zebrafish, Developmental biology 256 (2003) 1-17.
[66] D.M. Parichy, M.R. Elizondo, M.G. Mills, T.N. Gordon, R.E. Engeszer, Normal table of postembryonic zebrafish development: staging by externally visible anatomy of the living fish, Developmental dynamics 238 (2009) 2975-3015.
[67] Y. Bradford, T. Conlin, N. Dunn, D. Fashena, K. Frazer, D. Howe, J. Knight, P. Mani, R. Martin, S. Moxon, H. Paddock, C. Pich, S. Ramachandran, B. Ruef, L. Ruzicka, H. Bauer Schaper, K. Schaper, X. Shao, A. Singer, J. Sprague, B. Sprunger, C. van Slyke, M. Westerfield, ZFIN: enhancements and updates to the zebrafish model organism database, Nucleic acid research 39 (2011) D822-D829.
[68] W. Driever, Z. Rangini, Characterization of a cell line derived from zebrafish (Brachydanio rerio) embryos, In vitro cellular & developmental biology - Animal 29A (1993) 749-754.
[69] W. Norton, L. Bally-Cuif, Adult zebrafish as a model organism for behavioural genetics, BMC neuroscience 11 (2010) 90.
[70] D.J. Grunwald, J.S. Eisen, Headwaters of the zebrafish - emergence of a new model vertebrate, Nature reviews. Genetics 3 (2002) 717-724.
[71] E.R. Busby, G.J. Roch, N.M. Sherwood, Endocrinology of zebrafish: a small fish with a large gene pool, Elsevier, 2010.
[72] R. Mindnich, J. Adamski, Zebrafish 17beta-hydroxysteroid dehydrogenases: an evolutionary perspective, Molecular and cellular endocrinology 301 (2009) 20-26.
[73] J.L. Lyche, R. Nourizadeh-Lillabadi, C. Almaas, B. Stavik, V. Berg, J.U. Skåre, P. Alestrøm, E. Ropstad, Natural mixtures of persistent organic pollutants (POP) increase weight gain, advance puberty, and induce changes in gene expression associated with steroid hormones and obesity in female zebrafish, Journal of toxicology and environmental health. Part A 73 (2010) 1032-1057.
[74] P.J. Schoonheim, A. Chatzopoulou, M.J.M. Schaaf, The zebrafish as an in vivo model system for glucocorticoid resistance, Steroids 75 (2010) 918-925.
[75] B. Persson, Y. Kallberg, J.E. Bray, E. Bruford, S.L. Dellaporta, A.D. Favia, R.G. Duarte, H. Jörnvall, K.L. Kavanagh, N. Kedishvili, M. Kisiela, E. Maser, R. Mindnich, S. Orchard, T.M. Penning, J.M. Thornton, J. Adamski, U. Oppermann, The SDR (short-chain dehydrogenase/reductase and related enzymes) nomenclature initiative, Chemico-biological interactions 178 (2009) 94-98.
[76] Y. Kallberg, U. Oppermann, H. Jornvall, B. Persson, Short-chain dehydrogenases/reductases (SDRs). Coenzyme-based functional assignments in completed genomes, European journal of biochemistry 269 (2002) 4409-4417.
[77] U.C. Oppermann, C. Filling, H. Jörnvall, Forms and functions of human SDR enzymes, Chemico-biological interactions 130-132 (2001) 699-705.
[78] Y. Kallberg, U. Oppermann, H. Jörnvall, B. Persson, Short-chain dehydrogenase/reductase (SDR) relationships: a large family with eight clusters common to human, animal, and plant genomes, Protein science 11 (2002) 636-641.
[79] U. Oppermann, C. Filling, M. Hult, N. Shafqat, X. Wu, M. Lindh, J. Shafqat, E. Nordling, Y. Kallberg, B. Persson, H. Jörnvall, Short-chain dehydrogenases/reductases (SDR): the 2002 update, Chemico-biological interactions 143-144 (2003) 247-253.
[80] C. Filling, K.D. Berndt, J. Benach, S. Knapp, T. Prozorovski, E. Nordling, R. Ladenstein, H. Jörnvall, U. Oppermann, Critical residues for structure and catalysis in short-chain dehydrogenases/reductases, Journal of biological chemistry 277 (2002) 25677-25684.
[81] J.M. Jez, T.M. Penning, The aldo-keto reductase (AKR) superfamily: an update, Chemico-biological interactions 130-132 (2001) 499-525.
[82] J. Benach, S. Atrian, R. Ladenstein, R. Gonzàlez-Duarte, Genesis of Drosophila ADH: the shaping of the enzymatic activity from a SDR ancestor, Chemico-biological interactions 130-132 (2001) 405-415.
[83] F. Hoffmann, E. Maser, Carbonyl reductases and pluripotent hydroxysteroid dehydrogenases of the short-chain dehydrogenase/reductase superfamily, Drug metabolism reviews 39 (2007) 87-144.

[84] X. Wu, P. Lukacik, K.L. Kavanagh, U. Oppermann, SDR-type human hydroxysteroid dehydrogenases involved in steroid hormone activation, Molecular and cellular endocrinology 265-266 (2007) 71-76.
[85] T.M. Penning, Hydroxysteroid dehydrogenases and pre-receptor regulation of steroid hormone action, Human reproduction update 9 (2003) 193-205.
[86] T.M. Penning, Molecular endocrinology of hydroxysteroid dehydrogenases, Endocrine reviews 18 (1997) 281-305.
[87] S. Nobel, L. Abrahmsen, U. Oppermann, Metabolic conversion as a pre-receptor control mechanism for lipophilic hormones, European journal of biochemistry 268 (2001) 4113-4125.
[88] H. Peltoketo, V. Luu-The, J. Simard, J. Adamski, 17beta-hydroxysteroid dehydrogenase (HSD)/17-ketosteroid reductase (KSR) family; nomenclature and main characteristics of the 17HSD/KSR enzymes, Journal of molecular endocrinology 23 (1999) 1-11.
[89] R. Mindnich, G. Möller, J. Adamski, The role of 17beta-hydroxysteroid dehydrogenases, Molecular and cellular endocrinology 218 (2004) 7-20.
[90] D.P. Sherbet, M. Papari-Zareei, N. Khan, K.K. Sharma, A. Brandmaier, S. Rambally, A. Chattopadhyay, S. Andersson, A.K. Agarwal, R.J. Auchus, Cofactors, redox state, and directional preferences of hydroxysteroid dehydrogenases, Molecular and cellular endocrinology 265-266 (2007) 83-88.
[91] F. Labrie, V. Luu-The, S.-X. Lin, C. Labrie, J. Simard, R. Breton, A. Bélanger, The key role of 17beta-hydroxysteroid dehydrogenases in sex steroid biology, Steroids 62 (1997) 148-158.
[92] G. Moeller, J. Adamski, Multifunctionality of human 17beta-hydroxysteroid dehydrogenases, Molecular and cellular endocrinology 248 (2006) 47-55.
[93] G. Moeller, J. Adamski, Integrated view on 17beta-hydroxysteroid dehydrogenases, Molecular and cellular endocrinology 301 (2009) 7-19.
[94] F. Haller, E. Moman, R.W. Hartmann, J. Adamski, R. Mindnich, Molecular framework of steroid/retinoid discrimination in 17β-hydroxysteroid dehydrogenase type 1 and photoreceptor-associated retinol dehydrogenase, Journal of molecular biology 399 (2010) 255-267.
[95] M.W. Voice, J.R. Seckl, C.R.W. Edwards, K.E. Chapman, 11beta-Hydroxysteroid dehydrogenase type 1 expression in 2S FAZA hepatoma cells is hormonally regulated: a model system for the study of hepatic glucocorticoid metabolism, Biochemical journal 317 (1996) 621-625.
[96] J.W. Tomlinson, E.A. Walker, I.J. Bujalska, N. Draper, G.G. Lavery, M.S. Cooper, M. Hewison, P.M. Stewart, 11beta-hydroxysteroid dehydrogenase type 1: a tissue-specific regulator of glucocorticoid response, Endocrine reviews 25 (2004) 831-866.
[97] M. Meier, G. Möller, J. Adamski, Perspectives in understanding the role of human 17beta-hydroxysteroid dehydrogenases in health and disease, Annals of the New York academy of sciences 1155 (2009) 15-24.
[98] N.M. Morton, Obesity and corticosteroids: 11beta-hydroxysteroid type 1 as a cause and therapeutic target in metabolic disease, Molecular and cellular endocrinology 316 (2010) 154-164.
[99] U. Oppermann, Type 1 11beta-hydroxysteroid dehydrogenase as universal drug target in metabolic diseases?, Endocrine, metabolic & immune disorders drug targets 6 (2006) 259-269.
[100] A.G. Atanasov, I.D. Ignatova, L.G. Nashev, B. Dick, P. Ferrari, F.J. Frey, A. Odermatt, Impaired protein stability of 11beta-hydroxysteroid dehydrogenase type 2: a novel mechanism of apparent mineralocorticoid excess, Journal of the american society of nephrology 18 (2007) 1262-1270.
[101] I.J. Bujalska, L.L. Gathercole, J.W. Tomlinson, C. Darimont, J. Ermolieff, A.N. Fanjul, P.A. Rejto, P.M. Stewart, A novel selective 11beta-hydroxysteroid dehydrogenase type 1 inhibitor prevents human adipogenesis, Journal of endocrinology 197 (2008) 297-307.
[102] R. Mindnich, J. Adamski, Functional aspects of 17beta-hydroxysteroid dehydrogenase 1 determined by comparison to a closely related retinol dehydrogenase, Journal of steroid biochemistry and molecular biology 104 (2007) 334-339.
[103] R. Mindnich, D. Deluca, J. Adamski, Identification and characterization of 17beta-hydroxysteroid dehydrogenases in the zebrafish, Danio rerio, Molecular and cellular endocrinology 215 (2004) 19-30.
[104] R. Mindnich, F. Haller, F. Halbach, G. Moeller, M. Hrabé de Angelis, J. Adamski, Androgen metabolism via 17beta-hydroxysteroid dehydrogenase type 3 in mammalian and non-mammalian

vertebrates: comparison of the human and the zebrafish enzyme, Journal of molecular endocrinology 35 (2005) 305-316.
[105] R. Mindnich, M. Hrabé de Angelis, J. Adamski, Functional genome analysis indicates loss of 17beta-hydroxysteroid dehydrogenase type 2 enzyme in the zebrafish, Journal of steroid biochemistry and molecular biology 103 (2007) 35-43.
[106] Y. Kazeto, S. Ijiri, H. Matsubara, S. Adachi, K. Yamauchi, Cloning of 17beta-hydroxysteroid dehydrogenase-I cDNAs from Japanese eel ovary, Biochemical and biophysical research communications 279 (2000) 451-456.
[107] L.Y. Zhou, D.S. Wang, B. Senthilkumaran, M. Yoshikuni, Y. Shibata, T. Kobayashi, C.C. Sudhakumari, Y. Nagahama, Cloning, expression and characterization of three types of 17beta-hydroxysteroid dehydrogenases from the Nile tilapia, Oreochromis niloticus, Journal of molecular endocrinology 35 (2005) 103-116.
[108] L.F.C. Castro, M.J. Rocha, A. Lobo-da-Cunha, C. Batista-Pinto, A. Machado, E. Rocha, The 17beta-hydroxysteroid dehydrogenase 4: gender-specific and seasonal gene expression in the liver of brown trout (Salmo trutta f. fario), Comparative biochemistry and physiology. Part B, Biochemistry & molecular biology 153 (2009) 157-164.
[109] Y. Ozaki, M. Higuchi, C. Miura, S. Yamaguchi, Y. Tozawa, T. Miura, Roles of 11beta-hydroxysteroid dehydrogenase in fish spermatogenesis, Endocrinology 147 (2006) 5139-5146.
[110] M.K. Rasheeda, H. Kagawa, R. Kirubagaran, A. Dutta-Gupta, B. Senthilkumaran, Cloning, expression and enzyme activity analysis of testicular 11beta-hydroxysteroid dehydrogenase during seasonal cycle and after hCG induction in air-breathing catfish Clarias gariepinus, Journal of steroid biochemistry and molecular biology 120 (2010) 1-10.
[111] M. Kusakabe, 11beta-Hydroxysteroid dehydrogenase complementary deoxyribonucleic acid in rainbow trout: cloning, sites of expression, and seasonal changes in gonads, Endocrinology 144 (2003) 2534-2545.
[112] J.Q. Jiang, D.S. Wang, B. Senthilkumaran, T. Kobayashi, H.K. Kobayashi, A. Yamaguchi, W. Ge, G. Young, Y. Nagahama, Isolation, characterization and expression of 11beta-hydroxysteroid dehydrogenase type 2 cDNAs from the testes of Japanese eel (Anguilla japonica) and Nile tilapia (Oreochromis niloticus), Journal of molecular endocrinology 31 (2003) 305-315.
[113] M.E. Baker, Evolutionary analysis of 11beta-hydroxysteroid dehydrogenase-type 1, -type 2, -type 3 and 17beta-hydroxysteroid dehydrogenase-type 2 in fish, FEBS Letters 574 (2004) 167-170.
[114] M.E. Baker, Evolution of 11beta-hydroxysteroid dehydrogenase-type 1 and 11beta-hydroxysteroid dehydrogenase-type 3, FEBS letters 584 (2010) 2279-2284.
[115] J. Tokarz, Neue Short-Chain Dehydrogenasen/Reduktasen aus Zebrafisch - Identifizierung und funkionelle Charakterisierung, AV Akademikerverlag GmbH & Co. KG, Saarbrücken, Deutschland, 2011.
[116] P.A. Morcos, Achieving targeted and quantifiable alteration of mRNA splicing with Morpholino oligos, Biochemical and biophysical research communications 358 (2007) 521-527.
[117] J.D. Moulton, Y.-L. Yan, Using Morpholinos to control gene expression, Current protocols in molecular biology / edited by Frederick M. Ausubel ... [et al.] Chapter 26 (2008) Unit 26.28.
[118] S. Rozen, H. Skaletzky, Primer3 on the WWW for general users and for biologist programmers, Methods in molecular biology 132(3) (1999) 365-368.
[119] M.W. Pfaffl, A new mathematical model for relative quantification in real-time RT-PCR, Nucleic acids research 29 (2001) e45.
[120] M.W. Pfaffl, A. Tichopad, C. Prgomet, T.P. Neuvians, Determination of stable housekeeping genes, differentially regulated target genes and sample integrity: BestKeeper-Excel-based tool using pair-wise correlations, Biotechnology letters 26 (2004) 509-515.
[121] T.A. Hall, BioEdit: a user-friendly biological sequence alignment editor and analysis program for Windows 95/98/NT, Nucleic acids symposium series 41 (1999) 95-98.
[122] K. Tamura, J. Dudley, M. Nei, S. Kumar, MEGA4: Molecular Evolutionary Genetics Analysis (MEGA) software version 4.0, Molecular biology and evolution 24 (2007) 1596-1599.
[123] D.W. Payne, W.D. Holtzclaw, E.Y. Adashi, A convenient, unified scheme for the differential extraction of conjugated and unconjugated serum C19 steroids on Sep-Pak C18-cartridges, Journal of steroid biochemistry 33 (1989) 289-295.

[124] M.E. Baker, 11beta-hydroxysteroid dehydrogenase-type 2 evolved from an ancestral 17beta-hydroxysteroid dehydrogenase-type 2, Biochemical and biophysical research communications 399(2) (2010) 215-220.
[125] J.T. Wu, L.H. Wu, J.A. Knight, Stability of NADPH: effect of various factors on the kinetics of degradation, Clinical chemistry 32 (1986) 314-319.
[126] J. Tokarz, R. Mindnich, W. Norton, G. Möller, M. Hrabé de Angelis, J. Adamski, Discovery of a novel enzyme mediating glucocorticoid catabolism in fish: 20beta-hydroxysteroid dehydrogenase type 2, Molecular and cellular endocrinology 349 (2012) 202-213.
[127] Y. Nagahama, M. Yamashita, Regulation of oocyte maturation in fish, Development, growth and differentiation 50 Suppl 1 (2008) S195-219.
[128] M.M. Vijayan, J.S. Ballantyne, J.F. Leatherland, Cortisol-induced changes in some aspects of the intermediary metabolism of Salvelinus fontinalis, General and comparative endocrinology 82 (1991) 476-486.
[129] Y.-A. Moon, J.D. Horton, Identification of two mammalian reductases involved in the two-carbon fatty acyl elongation cascade, Journal of biological chemistry 278 (2003) 7335-7343.
[130] K.M. Wagstaff, D.A. Jans, Intramolecular masking of nuclear localization signals: analysis of importin binding using a novel AlphaScreen-based method, Analytical biochemistry 348 (2006) 49-56.
[131] S. Bertrand, B. Thisse, R. Tavares, L. Sachs, A. Chaumot, P.-L. Bardet, H. Escrivà, M. Duffraisse, O. Marchand, R. Safi, C. Thisse, V. Laudet, Unexpected novel relational links uncovered by extensive developmental profiling of nuclear receptor expression, PLoS genetics 3 (2007) e188.
[132] B. Thisse, C. Thisse, Fast release clones: a high throughput expression analysis, ZFIN direct data submission (http://zfin.org), 2004.
[133] C. Glanemann, A. Loos, N. Gorret, L.B. Willis, X.M. O'Brien, P.A. Lessard, A.J. Sinskey, Disparity between changes in mRNA abundance and enzyme activity in Corynebacterium glutamicum: implications for DNA microarray analysis, Applied microbiology and biotechnology 61 (2003) 61-68.
[134] F. Abruzzese, M. Greco, E. Perlino, S. Doonan, E. Marra, Lack of correlation between mRNA expression and enzymatic activity of the aspartate aminotransferase isoenzymes in various tissues of the rat, FEBS letters 366 (1995) 170-172.
[135] G. Chen, Discordant protein and mRNA expression in lung adenocarcinomas, Molecular and cellular proteomics 1 (2002) 304-313.
[136] J. Ramsay, G. Feist, Z. Varga, M. Westerfield, M. Kent, C. Schreck, Whole-body cortisol is an indicator of crowding stress in adult zebrafish, Danio rerio, Aquaculture 258 (2006) 565-574.
[137] P.H.M. Balm, J.D.G. Lambert, S.E. Wendelaar Bonga, Corticosteroid biosynthesis in the interrenal cells of the teleost fish, Oreochromis mossambicus, General and comparative endocrinology 76 (1989) 53-62.
[138] K.L. Thorpe, R.I. Cummings, T.H. Hutchinson, M. Scholze, G. Brighty, J.P. Sumpter, C.R. Tyler, Relative potencies and combination effects of steroidal estrogens in fish, Environmental science and technology 37 (2003) 1142-1149.
[139] F. Brion, C.R. Tyler, X. Palazzi, B. Laillet, J.M. Porcher, J. Garric, P. Flammarion, Impacts of 17beta-estradiol, including environmentally relevant concentrations, on reproduction after exposure during embryo-larval-, juvenile- and adult-life stages in zebrafish (Danio rerio), Aquatic toxicology 68(3) (2004) 193-217.
[140] U.J. Pyati, A.E. Webb, D. Kimelman, Transgenic zebrafish reveal stage-specific roles for Bmp signaling in ventral and posterior mesoderm development, Development 132 (2005) 2333-2343.
[141] H. Chen, J. Hu, J. Yang, Y. Wang, H. Xu, Q. Jiang, Y. Gong, Y. Gu, H. Song, Generation of a fluorescent transgenic zebrafish for detection of environmental estrogens, Aquatic toxicology 96 (2010) 53-61.
[142] B.W. Draper, P.A. Morcos, C.B. Kimmel, Inhibition of zebrafish fgf8 pre-mRNA splicing with morpholino oligos: a quantifiable method for gene knockdown, Genesis 30 (2001) 154 -156.
[143] M.I. McCormick, I.V. Nechaev, Influence of cortisol on developmental rhythms during embryogenesis in a tropical damselfish, Journal of experimental zoology 293(5) (2002) 456-466.
[144] A.G. Maule, R.A. Tripp, S.L. Kaattari, C.B. Schreck, Stress alters immune function and disease resistance in chinook salmon (Oncorhynchus tshawytscha), Journal of endocrinology 120 (1989) 135-142.

[145] J.M. Ramsay, G.W. Feist, Z.M. Varga, M. Westerfield, M.L. Kent, C.B. Schreck, Whole-body cortisol response of zebrafish to acute net handling stress, Aquaculture 297 (2009) 157-162.
[146] M.V. Mericq, G.B. Cutler, High fluid intake increases urine free cortisol excretion in normal subjects, Journal of clinical endocrinology and metabolism 83 (1998) 682-684.
[147] O.A. Sharef, J. Feely, P.V. Kavanagh, K.R. Scott, S.C. Sharma, An HPLC method for the determination of the free cortisol/cortisone ratio in human urine, Biomedical chromatography 21 (2007) 1201-1206.
[148] H.-J. Cho, J.D. Kim, W.-Y. Lee, B.C. Chung, M.H. Choi, Quantitative metabolic profiling of 21 endogenous corticosteroids in urine by liquid chromatography-triple quadrupole-mass spectrometry, Analytica chimica acta 632 (2009) 101-108.
[149] W.K. Jerjes, N.F. Taylor, T.J. Peters, S. Wessely, A.J. Cleare, Urinary cortisol and cortisol metabolite excretion in chronic fatigue syndrome, Psychosomatic medicine 68 (2006) 578-582.
[150] K. Hirschenhauser, A.V.M. Canário, A.F.H. Ros, M. Taborsky, R.F. Oliveira, Social context may affect urinary excretion of 11-ketotestosterone in African cichlids, Behaviour 145 (2008) 1367-1388.
[151] M. Trauner, J.L. Boyer, Bile salt transporters: molecular characterization, function, and regulation, Physiological reviews 83 (2003) 633-671.
[152] V. Launay-Vacher, H. Izzedine, S. Karie, J.S. Hulot, A. Baumelou, G. Deray, Renal tubular drug transporters, Nephron physiology 103 (2006) 97-106.
[153] M. Suzuki, H. Suzuki, Y. Sugimoto, Y. Sugiyama, ABCG2 transports sulfated conjugates of steroids and xenobiotics, Journal of biological chemistry 278 (2003) 22644-22649.
[154] J.R. Seckl, B.R. Walker, Minireview: 11beta-hydroxysteroid dehydrogenase type 1 - a tissue-specific amplifier of glucocorticoid action, Endocrinology 142 (2001) 1371-1376.
[155] A. Christoffels, E.G.L. Koh, J.-M. Chia, S. Brenner, S. Aparicio, B. Venkatesh, Fugu genome analysis provides evidence for a whole-genome duplication early during the evolution of ray-finned fishes, Molecular biology and evolution 21 (2004) 1146-1151.
[156] P.W. Holland, Gene duplication: past, present and future, Seminars in cell & developmental biology 10 (1999) 541-547.
[157] Y. Nagahama, 17alpha,20beta-Dihydroxy-4-pregnen-3-one, a maturation-inducing hormone in fish oocytes: mechanisms of synthesis and action, Steroids 62 (1997) 190-196.
[158] G. Sreenivasulu, B. Senthilkumaran, New evidences for the involvement of 20beta-hydroxysteroid dehydrogenase in final oocyte maturation of air-breathing catfish, General and comparative endocrinology 163 (2009) 259-269.
[159] G. Guan, M. Tanaka, T. Todo, G. Young, M. Yoshikuni, Y. Nagahama, Cloning and expression of two carbonyl reductase-like 20beta-hydroxysteroid dehydrogenase cDNAs in ovarian follicles of rainbow trout (Oncorhynchus mykiss), Biochemical and biophysical research communications 255 (1999) 123-128.
[160] B. Senthilkumaran, C.-C. Sudhakumari, X.-T. Chang, T. Kobayashi, Y. Oba, G. Guan, Y. Yoshiura, M. Yoshikuni, Y. Nagahama, Ovarian carbonyl reductase-like 20beta-hydroxysteroid dehydrogenase shows distinct surge in messenger RNA expression during natural and gonadotropin-induced meiotic maturation in Nile tilapia, Biology of reproduction 67 (2002) 1080-1086.
[161] Y. Wang, W. Ge, Cloning of zebrafish ovarian carbonyl reductase-like 20 beta-hydroxysteroid dehydrogenase and characterization of its spatial and temporal expression, General and comparative endocrinology 127 (2002) 209-216.
[162] Y. Kazeto, S. Adachi, K. Yamauchi, 20beta-Hydroxysteroid dehydrogenase of the Japanese eel ovary: its cellular localization and changes in the enzymatic activity during sexual maturation, General and comparative endocrinology 122 (2001) 109-115.
[163] S. Milla, N. Wang, S.N.M. Mandiki, P. Kestemont, Corticosteroids: friends or foes of teleost reproduction?, Comparative biochemistry and physiology. Part A, Molecular and integrative physiology 153 (2009) 242-251.
[164] T.B. Cole, N.E. Stacey, Olfactory responses to steroids in an African mouth-brooding cichlid, Haplochromis burtoni (Günther), Journal of fish biology 68 (2006) 661-680.
[165] N. Lower, A.P. Scott, A. Moore, Release of sex steroids into the water by roach, Journal of fish biology 64 (2004) 16-33.

[166] A.P. Scott, P.W. Sorensen, Time course of release of pheromonally active gonadal steroids and their conjugates by ovulatory goldfish, General and comparative endocrinology 96 (1994) 309-323.
[167] P.W. Sorensen, C.A. Murphy, K. Loomis, P. Maniak, P. Thomas, Evidence that 4-pregnen-17,20beta,21-triol-3-one functions as a maturation-inducing hormone and pheromonal precursor in the percid fish, Gymnocephalus cernuus, General and comparative endocrinology 139 (2004) 1-11.
[168] R. van den Hurk, W.G. Schoonen, G.A. van Zoelen, J.G. Lambert, The biosynthesis of steroid glucuronides in the testis of the zebrafish, Brachydanio rerio, and their pheromonal function as ovulation inducers, General and comparative endocrinology 68 (1987) 179-188.
[169] J.G.D. Lambert, R. van den Hurk, W.G.E.J. Schoonen, J.W. Resink, P.G.W.J. van Oordt, Gonadal steroidogenesis and the possible role of steroid glucuronides as sex pheromones in two species of teleosts, Fish physiology and biochemistry 2 (1986) 101-107.
[170] R. van den Hurk, J.W. Resink, Male reproductive system as sex pheromone producer in teleost fish, Journal of experimental zoology 261 (1992) 204-213.
[171] W.-L. Zhang, L.-Y. Zhou, B. Senthilkumaran, B.-F. Huang, C.C. Sudhakumari, T. Kobayashi, Y. Nagahama, D.-S. Wang, Molecular cloning of two isoforms of 11beta-hydroxylase and their expressions in the Nile tilapia, Oreochromis niloticus, General and comparative endocrinology 165 (2010) 34-41.
[172] P. Rantakari, H. Lagerbohm, M. Kaimainen, J.-P. Suomela, L. Strauss, K. Sainio, P. Pakarinen, M. Poutanen, Hydroxysteroid 17beta-dehydrogenase 12 is essential for mouse organogenesis and embryonic survival, Endocrinology 151 (2010) 1893-1901.
[173] M. Meier, J. Tokarz, F. Haller, R. Mindnich, J. Adamski, Human and zebrafish hydroxysteroid dehydrogenase like 1 (HSDL1) proteins are inactive enzymes but conserved among species, Chemico-biological interactions 178 (2009) 197-205.
[174] L. Di Costanzo, J.E. Drury, T.M. Penning, D.W. Christianson, Crystal structure of human liver Delta4-3-ketosteroid 5beta-reductase (AKR1D1) and implications for substrate binding and catalysis, Journal of biological chemistry 283 (2008) 16830-16839.
[175] W. Shamim, M. Yousufuddin, A. Bakhai, A.J. Coats, J.W. Honour, Gender differences in the urinary excretion rates of cortisol and androgen metabolites, Annals of clinical biochemistry 37 (2000) 770-774.
[176] C. Grimm, E. Maser, E. Möbus, G. Klebe, K. Reuter, R. Ficner, The crystal structure of 3alpha-hydroxysteroid dehydrogenase/carbonyl reductase from Comamonas testosteroni shows a novel oligomerization pattern within the short chain dehydrogenase/reductase family, Journal of biological chemistry 275 (2000) 41333-41339.
[177] M.-L. Lu, Y.-W. Huang, S.-X. Lin, Purification, reconstitution, and steady-state kinetics of the trans-membrane 17beta-hydroxysteroid dehydrogenase 2, Journal of biological chemistry 277 (2002) 22123-22130.
[178] R. Andrew, D.I. Phillips, B.W. Walker, Obesity and gender influence cortisol secretion and metabolism in man, Journal of clinical endocrinology and metabolism 83 (1998) 1806-1809.
[179] R.A. Meigs, L.L. Engel, The metabolism of adrenocortical steroids by human tissues, Endocrinology 69 (1961) 152-162.
[180] L.L. Engel, L.J. Langer, Biochemistry of steroid hormones, Annual reviews biochemistry 30 (1961) 499-524.
[181] B. Eisenschmid, P. Heilmann, W. Oelkers, R. Rejaibi, M. Schöneshöfer, 20-Dihydroisomers of cortisol and cortisone in human urine: excretion rates under different physiological conditions, Journal of clinical chemistry and clinical biochemistry 25 (1987) 345-349.
[182] M. Schöneshöfer, A. Kage, B. Eisenschmid, P. Heilmann, T. Dhar, B. Weber, Automated liquid chromatographic determination of the 20-dihydro isomers of cortisol and cortisone in human urine, Journal of chromatography 380 (1986) 267-274.
[183] S.M. Abel, J.L. Maggs, D.J. Back, B.K. Park, Cortisol metabolism by human liver in vitro - I. Metabolite identification and inter-individual variability, Journal of steroid biochemistry and molecular biology 43 (1992) 713-719.
[184] H.M. Dodds, D.J. Maguire, R.H. Mortimer, R.S. Addison, G.R. Cannell, High performance liquid chromatographic separation of cortisol, cortisone, and their 20–reduced metabolites in perfusion media, Journal of liquid chromatography 18 (1995) 1809-1820.

[185] H.M. Dodds, P.J. Taylor, G.R. Cannell, S.M. Pond, A high-performance liquid chromatography-electrospray-tandem mass spectrometry analysis of cortisol and metabolites in placental perfusate, Analytical biochemistry 247 (1997) 342-347.
[186] W. Gibb, J. Jeffery, Steric, chiral and conformational aspects of the 3-hydroxy- and 20-hydroxysteroid dehydrogenase activities of cortisone reductase preparations, Biochimica et biophysica acta 268 (1972) 13-20.
[187] A.E. Krafft, P.B. Hylemon, Purification and characterization of a novel form of 20alpha-hydroxysteroid dehydrogenase from Clostridium scindens, Journal of bacteriology 171 (1989) 2925-2932.
[188] A.E. Krafft, J. Winter, V.D. Bokkenheuser, P.B. Hylemon, Cofactor requirements of steroid-17-20-desmolase and 20alpha-hydroxysteroid dehydrogenase activities in cell extracts of Clostridium scindens, Journal of steroid biochemistry 28 (1987) 49-54.
[189] R.W. Brown, R. Diaz, A.C. Robson, Y.V. Kotelevtsev, J.J. Mullins, M.H. Kaufman, J.R. Seckl, The ontogeny of 11beta-hydroxysteroid dehydrogenase type 2 and mineralocorticoid receptor gene expression reveal intricate control of glucocorticoid action in development, Endocrinology 137 (1996) 794-797.
[190] N. Draper, P.M. Stewart, 11beta-Hydroxysteroid dehydrogenase and the pre-receptor regulation of corticosteroid hormone action, Journal of endocrinology 186 (2005) 251-271.
[191] M. Palermo, C.H. Shackleton, F. Mantero, P.M. Stewart, Urinary free cortisone and the assessment of 11beta-hydroxysteroid dehydrogenase activity in man, Clinical endocrinology 45 (1996) 605-611.
[192] R.E. Peterson, Adrenocortical steroid metabolism and adrenal cortical function in liver disease, Journal of Clinical Investigation 39 (1960) 320-331.

6 Appendix

6.1 Publications and presentations

6.1.1 Scientific presentations

Endocrine Society Meeting ENDO2012, June 23-26, **2012**, Houston, USA
Tokarz, J, Norton W, Möller G, Hrabé de Angelis M, Adamski J: *Short pathway for cortisol catabolism and stress reduction in zebrafish*. (Poster presentation)

Congress of Steroid Research, March 27-29, **2011**, Chicago, USA
Tokarz J, Mindnich R, Norton W, Schieweg M, Adamski J: *A novel 20beta-hydroxysteroid dehydrogenase from zebrafish is important in glucocorticoid catabolism.* (Short oral communication)

Congress of Steroid Research, March 27-29, **2011**, Chicago, USA
Tokarz, J, Mindnich R, Norton W, Schieweg M, Adamski J: *A novel 20beta-hydroxysteroid dehydrogenase is important for glucocorticoid catabolism*. (Poster presentation)

Congress of Steroid Research, March 27-29, **2011**, Chicago, USA
Tokarz J, Lenz T, Dieks H, Möller G, Kroll F, Sefkow M, Dreger M, Köster H, Adamski J: *Capture-Compound Mass Spectrometry: Searching for novel cortisol-binding proteins as potential drug targets.* (Poster presentation)

Endocrine Society Meeting ENDO2010, June 19-22, **2010**, San Diego, USA
Tokarz J, Mindnich R, Adamski J: *Novel 20beta-Hydroxysteroid dehydrogenase of zebrafish plays a role in glucocorticoid catabolism*. (Poster presentation)

Workshop on pre-receptor steroid metabolism as target for pharmacological treatment, May 26-28, **2008**, Grainau, Germany
Tokarz J, Mindnich R, Adamski J: C*haracterization of novel SDRs of zebrafish*. (Poster presentation)

6.1.2 Scientific papers

Tokarz J, Norton W, Möller G, Hrabé de Angelis M, Adamski J: *Zebrafish 20beta-hydroxysteroid dehydrogenase type 2 is important for glucocorticoid catabolism in stress response*. Submitted

Tokarz J, Mindnich R, Norton W, Möller G, Hrabé de Angelis M, Adamski J: *Discovery of a novel enzyme mediating glucocorticoid catabolism in fish: 20beta-Hydroxysteroid dehydrogenase type 2.* Molecular and cellular endocrinology, **2012**, volume 349, issue 2, pages 202-213

Tarrant AM, Reitzel AM, Blomquist CH, Haller F, **Tokarz J**, Adamski J: *Steroid metabolism in cnidarians: insights from Nematostella vectensis*. Molecular and cellular endocrinology, **2009**, volume 301, issue 1-2, pages 27-36

Meier M, **Tokarz J**, Haller F, Mindnich R, Adamski J: *Human and zebrafish hydroxysteroid dehydrogenase like 1 (HSDL1) proteins are inactive enzymes but conserved among species*. Chemico-biological interactions, **2009**, volume 178, issue 1-3, pages 197-205

6.1.3 Books

Tokarz J: *Neue Short-Chain Dehydrogenasen/Reduktasen aus Zebrafisch. Identifizierung und funktionelle Charakterisierung.* AV Akademikerverlag, Saarbrücken, **2011**, ISBN 978-3-639-38451-2

6.2 Primers

6.2.1 Vector primers

Name	Internal Number	Sequence (5' → 3')	Direction	T_m (°C)
T7_for	1732	AATACGACTCACTATAGGG	for	53
SP6	1744	AGCTATTTAGGTGACACTATAG	rev	57
pDONR201_fwd	1640	TCGCGTTAACGCTAGCATGGATCTC	for	67
pDONR201_rev	1641	GTAACATCAGAGATTTTGAGACAC	rev	60
pDNR-LIB_seq_for	1913	AGTCAGTGAGCGAGGAAGC	for	58
pDNR-LIB_seq_rev	1914	CCAAACGAATGGTCTAGAAAG	rev	43

6.2.2 Gene internal sequencing primers

Gene (Species)	Name	Internal Number	Sequence (5' → 3')	Direction	T_m (°C)
Hsd20b2	zf3.2_seq_int1	1773	GTTGCACCAGTTACAACAGC	rev	58
(Danio rerio)	zf3.2_seq_int2	1774	GCTACACAACATACACAAGC	for	56
Hsd20b2 *(Poecilia reticulata)*	pr3.2_seq_int1	1915	TGAAATGGGTCTCCGTCC	for	56
Hsd20b2	om3.2_seq_int1	1936	CGCATGGTTGCAAGAGGG	for	58
(Oncorhyn-chus mykiss)	om3.2_seq_int2_ rev	1953	GCTGACCAGTACAATGTCC	rev	57
Hsd20b2	bt3.2_seq_int_1	2031	GTTCAGACCTCTCCGGGCGAGC	for	70
(Bos taurus)	bt3.2_seq_int_2	2032	AACAAATATGACCTATCCCATG	for	57
Hsd20b2	oa3.2_int1_for	2049	GGCATCATCATCAACATATCTT CAGTAGC	for	68
(Ovis aries)	oa3.2_int1_rev	2050	GCTACTGAAGATATGTTGATGA TGATGCC	rev	68

6.2.3 Cloning primers

Gene (Species)	Name	Internal Number	Sequence (5' → 3')	Direction	T_m (°C)
Hsd20b2 *(Danio rerio)*	zf3.2_A_for	1718	GGGGACAAGTTTGTACAAAAAAGCAGGCTTCGAAGGAGATAGAACCATGGGAGACAATGCAGAGTGCTGC	for	88
	zf3.2_K_rev	1719	GGGGACCACTTTGTTACAAGAAAGCTGGGTTTCATTCCTGTTTGGTTTTGTTCTCC	rev	85
	zf3.2_L_rev	1720	GGGGACCACTTTGTACAAGAAAGCTGGGTGTTCCTGTTTGGTTTTGTTCTCC	rev	85
Hsd20b2 *(Poecilia reticulata)*	pr3.2_A_for	1920	GGGGACAAGTTTGTACAAAAAAGCAGGCTTCGAAGGAGATAGAACCATGAGAAAGAAGCAACCTAAAATCACG	for	86
	pr3.2_K_rev	1921	GGGGACCACTTTGTACAAGAAAGCTGGGTTTTATGTTTTTCCCTGTTTCTCTTCC	rev	84
	pr3.2_L_rev	1922	GGGGACCACTTTGTACAAGAAAGCTGGGTGTGTTTTTCCCTGTTTCTCTTCC	rev	85
Hsd20b2 *(Oncorhynchus mykiss)*	om3.2_A_for	1950	GGGGACAAGTTTGTACAAAAAAGCAGGCTTCGAAGGAGATAGAACCATGGATACTGTATCAGACTCGATGCTTG	for	87
	om3.2_K_rev	1951	GGGGACCACTTTGTACAAGAAAGCTGGGTTTTAGTCCTCTTTGCTCGCAGAACGTTC	rev	87
	om3.2_L_rev	1952	GGGGACCACTTTGTACAAGAAAGCTGGGTGGTCCTCTTTGCTCGCAGAACGTTC	rev	88
Hsd20b2 *(Bos taurus)*	bt3.2_A2_for	2015	GGGACAAGTTTGTACAAAAAAGCAGGCTTCGAAGGAGATAGAACCATGGAGGTGGAGTGGGATGCACTGAGAG	for	89
	bt3.2_K_rev	2011	GGGGACCACTTTGTACAAGAAAGCTGGGTTTCAAGTTCTTTGAGAAAGGAATCCTGC	rev	85
	bt3.2_L_rev	2012	GGGGACCACTTTGTACAAGAAAGCTGGGTGAGTTCTTTGAGAAAGGAATCCTGC	rev	86
Hsd20b2 *(Ovis aries)*	oa3.2_A2_for	2048	GGGGACAAGTTTGTACAAAAAAGCAGGCTTCGAAGGAGATAGAACCATGTGGGACGCGCTGAGAGTGCTGGG	for	90
	oa3.2_K_rev	2094	GGGGACCACTTTGTACAAGAAAGCTGGGTTTCAAATTCTTTCAGAAAAGAATCCTGC	rev	84
	oa3.2_L_rev	2095	GGGGACCACTTTGTACAAGAAAGCTGGGTGAATTCTTTCAGAAAAGAATCCTGC	rev	84
Hsd20b2 *(Oreochromis niloticus)*	on3.2_A_for	2053	GGGGACAAGTTTGTACAAAAAAGCAGGCTTCGAAGGAGATAGAACCATGTCATTTGCTGACCTACTGGCCATC	for	88
	on3.2_K_ref	2054	GGGGACCACTTTGTACAAGAAAGCTGGGTTCTACTCCCCCTTTTCACCGGTCCAATCG	rev	89
	on3.2_L_rev	2055	GGGGACCACTTTGTACAAGAAAGCTGGGTGCTCCCCCTTTTCACCGGTCCAATCG	rev	89

6.2.4 Site-directed mutagenesis primers

Gene (Species)	Name	Internal Number	Sequence (5' → 3')	Direction	T_m (°C)
Hsd20b2	bt32_mut-PR_for	2153	GGGCCAAAAATATACAACCCA CTTGAGTAAACTGC	for	73
(Bos taurus)	bt32_mut_PR_rev	2154	GCAGTTTACTCAACTGGGTTGT ATATTTTTGGCCC	rev	73
Hsd20b2	bt32_mut_M_for	2155	CAAATATGACCTATCCCCTGAA AAAGGGACTGCTC	for	74
(Bos taurus)	bt32_mut_M_rev	2156	GAGCAGTCCCTTTTTCAGGGGA TAGGTCATATTTG	rev	74

6.2.5 RT-PCR primers

Only genes from zebrafish (*Danio rerio*) were analyzed.

Gene	Name	Internal Number	Sequence (5' → 3')	Direction	T_m (°C)
Beta-actin	zf-actin-for	36580	CTGGTTGTTGACAACGGATCCG	for	59
	zf-actin-rev	36581	CAGACTCATCGTACTCCTGCTT GC	rev	57
Hsd20b2	zf-pHSD3.2-for1	37423	AGACAATGCAGAGTGCTGCTG CTGG	for	57
	zf-pHSD3.2-rev1	37424	GCCCTCTGTGAAGTCTGCCTG	rev	56
Hsd11b2	zfHSD11B2_233_for	2215	TGCTGCTGGCTGTACTTCAC	for	60
	zfHSD11B2_759_rev	2220	TGGAAGAGCTCCTTGGTCTC	rev	60
Hsd11b3	zfHSD11B3_420_for	2221	CAGCACACACGATGGCTACT	for	60
	zfHSD11B3_680_rev	2224	GGGAACCAATCCCTGAAGAG	rev	60

6.2.6 Primers for qPCR

Only genes from zebrafish (*Danio rerio*) were amplified and quantified.

Gene	Name	Internal Number	Sequence (5' → 3')	Direction	T_m (°C)
Beta-actin	zf_b-actin_363_for	1968	AAGGCCAACAGGGAAAAGAT	for	56
	zf_b-actin_363_rev	1969	GTGGTACGACCGGAGGCATAC	rev	56
Hsd20b2	zf3.2_684_for	2188	AATGGTTGAAAGGGGGAAAG	for	56
	zf3.2_684_ref	2189	TTATGGGTCATGTTCGTGGA	rev	56
Hsd11b2	zfHSD11B2_769_for	2219	GGGGGTCAAAGTTTCCACTA	for	58
	zfHSD11B2_769_rev	2220	TGGAAGAGCTCCTTGGTCTC	rev	60
Hsd11b3	zfHSD11B3_420_for	2221	CAGCACACACGATGGCTACT	for	60
	zfHSD11B3_420_rev	2222	TCTGAAGCCCTCCAAAGAAA	rev	56
Rpl8	zf_rpl8_110_for	2290	CCCCTTTCGCTTCCTCTTT	for	57
	zf_rpl8_100_rev	2291	GTCCTTCACGATTCCCTTGA	rev	58
Cyp11b2	zf_cyp11b2_1402_for	2304	ATGAAGTGGCGCAGGATTT	for	55
	zf_cyp11b2_1402_rev	2305	CTCCACAGCCGAAATGAAG	rev	57
Star	zf_star_339_for	2312	AACAAGGGCAAGAAGCTCTG	for	58
	zf_star_339_rev	2313	CCCCCATTTGTTCCATGTTA	rev	56
Mc2r	zf_mc2r_574_for	2316	TTCAGCATCCTCGCCATAG	for	57
	zf_mc2r_574_rev	2317	TCAGGAGCAGAGCTGTGAAG	rev	60

Gene	Name	Internal Number	Sequence (5' → 3')	Direction	T_m (°C)
Crh	zf_crf_571_for	2326	TCTGTTGGAGGGGAAAGTTG	for	58
	zf_crf_571_rev	2327	ATTTTGCGGTTGCTGTGAG	rev	55
Ef1a	zf_ef1a_676_for	2412	CAAGGAAGTCAGCGCATACA	for	58
	zf_ef1a_676_rev	2413	GCATCAAGGGCATCAAGAAG	rev	58

6.3 Expression constructs

Gene (Species)	additional name	Vector	Dedication
Hsd20b2 *(Bos taurus)*	bt3.2_C-Myc	pDEST-530	expression in mammalian cells
	bt3.2_N-Myc	pcDNA3myc/DEST	expression in mammalian cells
Hsd20b2 *(Bos taurus)* M245L	bt3.2_M*_C-Myc	pDEST-530	expression in mammalian cells
	bt3.2_M*_N-Myc	pcDNA3myc/DEST	expression in mammalian cells
Hsd20b2 *(Bos taurus)* P141T/R142H	bt3.2_PR*_C-Myc	pDEST-530	expression in mammalian cells
	bt3.2_PR*_N-Myc	pcDNA3myc/DEST	expression in mammalian cells
Hsd20b2 *(Bos taurus)* P141T/R142H/M245L	bt3.2_PR*M*_C-Myc	pDEST-530	expression in mammalian cells
	bt3.2_PR*M*_N-Myc	pcDNA3myc/DEST	expression in mammalian cells
Hsd20b2 *(Ovis aries)*	oa3.2_C-Myc	pDEST-530	expression in mammalian cells
	oa3.2_N-Myc	pcDNA3myc/DEST	expression in mammalian cells
Hsd20b2 *(Oncorhynchus mykiss)*	om3.2_C-Myc	pDEST-530	expression in mammalian cells
	om3.2_N-Myc	pcDNA3myc/DEST	expression in mammalian cells
Hsd17b12 *(Oreochromis niloticus)*	on3.2_C-Myc	pDEST-530	expression in mammalian cells
	on3.2_N-Myc	pcDNA3myc/DEST	expression in mammalian cells
Hsd20b2 *(Poecilia reticulata)*	pr3.2_C-Myc	pDEST-530	expression in mammalian cells
	pr3.2_N-Myc	pcDNA3myc/DEST	expression in mammalian cells
Hsd20b2 *(Danio rerio)*	zf3.2_C-Myc	pDEST-530	expression in mammalian cells
	zf3.2_N-GST	pDEST-15	expression in *E. coli*
	zf3.2_N-Myc	pcDNA3myc/DEST	expression in mammalian cells
	zf3.2_pBSK+	pBluescript SK+	*in vitro* transcription

6.4 Sequences for phylogenetic analyses

Name	Species	Accession Number (NCBI)	origin
aj 11β-HSD type 2	*Anguilla japonica*	BAC67576	protein
bt 11β-HSD type 2	*Bos taurus*	DAA20013	protein
bt 11β-HSD type 1	*Bos taurus*	AAN40687	protein
bt 11β-HSD type 3	*Bos taurus*	AAS68530	protein
bt 17β-HSD type 2	*Bos taurus*	NP_001069194	protein
bt 17β-HSD type 3	*Bos taurus*	AAI09701	protein
bt 20β-HSD type 2	*Bos taurus*	AAI12590	protein
dr 11β-HSD type 1 like	*Danio rerio*	XM_002660963	nucleotide
dr 11β-HSD type 2	*Danio rerio*	NM_212720	nucleotide
dr 11β-HSD type 3 a	*Danio rerio*	NM_200323	nucleotide
dr 17β-HSD type 12 a	*Danio rerio*	AAS58452	protein
dr 17β-HSD type 12 b	*Danio rerio*	AAS58450	protein
dr 17β-HSD type 2	*Danio rerio*	NP_001035278	protein
dr 17β-HSD type 3	*Danio rerio*	AAS58451	protein
dr 20β-HSD type 2	*Danio rerio*	CAM14225	protein
dr 20β-HSD/CR like	*Danio rerio*	AAG23178	protein
hs 11β-HSD type 1	*Homo sapiens*	NP_005516	protein
hs 11β-HSD type 2	*Homo sapiens*	NP_000187	protein
hs 17β-HSD type 11	*Homo sapiens*	NM_016245	nucleotide
hs 17β-HSD type 12	*Homo sapiens*	NP_057226	protein
hs 17β-HSD type 13	*Homo sapiens*	NM_178135	nucleotide
hs 17β-HSD type 3	*Homo sapiens*	NP_000188	protein
hs CBR4	*Homo sapiens*	NM_032783	nucleotide
hs DHRS2	*Homo sapiens*	NM_182908	nucleotide
hs DHRS7	*Homo sapiens*	NM_016029	nucleotide
hs DHRS7B	*Homo sapiens*	NM_015510	nucleotide
hs HPGD	*Homo sapiens*	NM_000860	nucleotide
hs HSDL1	*Homo sapiens*	NM_031463	nucleotide
hs PECR	*Homo sapiens*	NM_018441	nucleotide
mf 11β-HSD type 3	*Macaca fascicularis*	AAS68529	protein
mf 17β-HSD type 3	*Macaca fascicularis*	AAY84568	protein
mm 11β-HSD type 1	*Mus musculus*	NP_001038216	protein
mm 11β-HSD type 2	*Mus musculus*	NP_032315	protein
mm 17β-HSD type 12	*Mus musculus*	CAM27609	protein
mm 17β-HSD type 2	*Mus musculus*	AAH12682	protein
mm 17β-HSD type 3	*Mus musculus*	AAB06793	protein
oa 11β-HSD type 1	*Ovis aries*	NP_001009395	protein
oa 20β-HSD type 2	*Ovis aries*	EE748178	EST
ol 11β-HSD type 2	*Oryzias latipes*	ABK59971	protein
ol 11β-HSD type 3	*Oryzias latipes*	NP_001098261	protein
om 11β-HSD type 2	*Oncorhynchus mykiss*	NP_001117690	protein
om 20β-HSD type 2	*Oncorhynchus mykiss*	BX911053	EST
om 20β-HSD/CR like type a	*Oncorhynchus mykiss*	NP_001118068	protein
om 20β-HSD/CR like type b	*Oncorhynchus mykiss*	NP_001117727	protein
on 11β-HSD type 2	*Oreochromis niloticus*	AAO42610	protein
on 17β-HSD type 12	*Oreochromis niloticus*	AAV74183	protein
pf 20β-HSD/CR like	*Pelteobagrus fulvidraco*	ACK38263	protein

Name	Species	Accession Number (NCBI)	origin
pr 20β-HSD type 2	*Poecilia reticulata*	ES381104	EST
rn 11β-HSD type 1	*Rattus norvegicus*	NP_058776	protein
rn 11β-HSD type 2	*Rattus norvegicus*	AAA87007	protein
rn 17β-HSD type 12	*Rattus norvegicus*	AAH61543	protein
rn 17β-HSD type 2	*Rattus norvegicus*	EDL92656	protein
rn 17β-HSD type 3	*Rattus norvegicus*	O54939	protein
ss 17β-HSD type 2	*Sus scrofa*	NP_001161121	protein
ss CR1	*Salmo salar*	ACI67351	protein
xl 20β-HSD type 2	*Xenopus laevis*	NP_001086077	protein

Acknowledgements

Ohne die Unterstützung einer Vielzahl von Menschen wäre diese Dissertation nicht das geworden, was sie jetzt ist. Mein besonderer Dank gebührt meinem Doktorvater Prof. Dr. Jerzy Adamski, nicht nur für die Bereitstellung des Themas, sondern auch für den unerschütterlichen Glauben an das Projekt und an mich sowie für seine unnachahmliche Art, mich zu motivieren. Bedanken möchte ich mich auch für die diversen Möglichkeiten, meine Arbeit international zu präsentieren, und seine Fähigkeit, mir den Rücken frei zu halten, wenn es absolut erforderlich war.
Herzlich bedanken möchte ich mich bei Dr. Gabriele Möller: Für ihr ständiges Interesse an den Ergebnissen, ihre kontinuierlichen, weiterführenden Ideen, ihre fundierten Ratschläge, um aus Sackgassen herauszufinden, und nicht zuletzt für das immer gründliche und konstruktive Korrekturlesen diverser Veröffentlichungen. Bei Dr. Cornelia Prehn und Dr. Ferdinand Haller möchte ich mich bedanken für unschätzbare Hilfe bei Fragen rund um HPLC (anfangs) und Massenspektrometrie (später). Dr. Ferdinand Haller und Dr. Marc Meier, meinen anfänglichen Weggefährten, gebührt außerdem Dank für die Starthilfe und die gute Stimmung auf der gegenüberliegenden Bench. Darüber hinaus möchte ich mich auch bedanken bei Susanne Weber für intensive Diskussionen über alles Mögliche, und auch dafür, dass sie für absolut jede Frage und jedes Problem offen war. Unschätzbare Hilfe habe ich erhalten von unseren technischen Angestellten, die immer dann eingesprungen sind, wenn Not am Mann war. Marion Schieweg, Gabriele Zieglmeier, Maria Kugler, Bianca Schmick und (früher) Kerstin Schwerdtner und Tamara Halex möchte ich meinen herzlichen Dank aussprechen. Danken möchte ich auch diversen Studentinnen für ihre Mithilfe an widerspenstigen Projekten und die Erfahrungen, die ich durch diese Betreuungen machen durfte: Andrea Kneuttinger, Katharina Franke, Beate Solfrank und Juliane Hundt.
Bei Dr. Rebekka Mindnich möchte ich mich ebenfalls bedanken: Sie hat das ganze Projekt ins Rollen gebracht, trotz der Distanz ihre Faszination daran erhalten und wichtige Ideen beigesteuert. Danke auch dafür, dass sie für nicht-wissenschaftliche Fragen immer ein offenes Ohr hatte.
Besonderer Dank gebührt Dr. William Norton, Dr. Laure Bally-Cuif und Dr. Prisca Chapouton. Vor allem Will möchte ich dafür danken, dass er mir geduldig die Arbeit mit den Fischen näher gebracht hat, ein kompetenter Ansprechpartner für alle Fisch-Fragen war und mir die ihnen eigene Schönheit der Zebrafische vor Augen geführt hat. Dr. Laure Bally-Cuif und Dr. Prisca Chapouton danke ich für die Bereitstellung von adulten Zebrafischen. Bei Heike Grunewald und Yvonne Riedel möchte ich mich für die immer gute Pflege meiner Fische bedanken.
Eine Reihe von Wissenschaftlern weltweit haben mir unkompliziert Plasmide zur Verfügung gestellt. Dafür möchte ich mich bei Dr. Johannes Glöckner (Universität Tübingen, Deutschland), Dr. Margarete Hoffmann (Max-Planck-Institut für Entwicklungsbiologie, Tübingen, Deutschland), Dr. Diane Esquerré (Institut Nationale de la Recherche Agronomique, Jouy en Josas, Frankreich), Dr. Linyan Zhou (National Institute for Basic Biology, Okazaki, Japan) und Dr. Marcel Schaaf (Universität Leiden, Niederlande) bedanken.
Viele weitere Wegbegleiter sind nicht namentlich genannt: Post-Docs, Doktoranden, Auszubildende, Praktikanten. Trotzdem gilt mein Dank auch ihnen, für Anregungen, Diskussionen, Lernbereitschaft und bohrende Fragen.